JOINT INSTITUTE FOR NUCLEAR RESEARCH
FRANK LABARATORY OF NEUTRON PHYSICS

ANNUAL REPORT 2008

DUBNA

CONTENTS

PREFACE

We would like to offer the readers the report on the scientific activity of the Frank Laboratory of Neutron Physics for 2008. The first part presents a brief review of the experimental and theoretical results achieved in the main scientific directions – condensed matter physics, neutron nuclear physics and applied research. The second part includes the reports on the modernization of the IBR-2 pulsed reactor and realization of the IREN project. The third part is concerned with the development and creation of elements of neutron spectrometers for condensed matter investigations. The fourth part presents the experimental reports that cover the main scientific directions in greater detail. The list of publications for 2008 completes the report.

During 2008 the works on the modernization of ***IBR-2*** were mainly focused on:

- Dismantling of all replaced equipment of the IBR-2;
- Installation of new equipment of the IBR-2M reactor;
- Manufacturing of new equipment for IBR-2M;
- Complex of cryogenic moderators (CM) of IBR-2M;
- Building and construction activities.

The IREN Project. The main tasks of the Frank Laboratory of Neutron Physics and the Laboratory of High Energy Physics in 2008 were the completion of installation, testing and commissioning of the equipment of the first stage of the LUE-200 accelerator. By June, 2008 work on the installation of the equipment in the accelerator halls was completed. Starting at the end of June, 2008 work to transport the beam and to train various systems of the accelerator was in progress. On June 17, 2008 an electron beam with the specified parameters was obtained at the exit of the electron source whereupon work to adjust the klystron and the modulator of the first accelerating section began.

On December 15, 2008 the accelerated electron beam with a pulse current of 300-400 mA at a frequency of up to 5 Hz was transported to the prototype target. Neutrons produced were detected by a gas proportional neutron counter placed at a distance of 11 m from the target on the floor of the target hall.

In spite of the IBR-2 reactor shutdown the activities of the Department of Condensed Matter Research and the Department of Spectrometers Complex were focused both on modernization of the spectrometers and scientific research in allied centers in Russia and abroad.

In 2008 a start has been made on the manufacturing of the head part of the mirror vacuum neutron guide within the framework of the realization of the project for construction of the DN-6 diffractometer for neutron diffraction studies of microsamples (beam 6b of IBR-2M).

For the GRAINS reflectometer to be installed on beam 10 of IBR-2M the manufacturing of the head part consisting of a two-beam splitting system encased in a vacuum housing has started. Section design is realized. The collimation system of the reflectometer, which comprises a massive support for housing the setup units is under construction.

The technical design of a mirror vacuum neutron guide for the DIN-2PI spectrometer has been completed and work to prepare an installation site for the neutron guide has been carried out. The work on the mirror vacuum neutron guide is conducted in cooperation with PNPI RAS (Gatchina).

The device for measuring low-temperature magnetoresistance at low temperatures has been constructed. The device is intended for prompt analysis of La1-xSrxMnO3 manganites, which are ferromagnetics with a “bad metal” behaviour.

The crystal and magnetic structures of the Pb2-xBaxFe2O5 solid solution series with $x \approx 1$ have been studied using x-ray and neutron powder diffraction, electron microscopy and Mössbauer spectroscopy. These compounds belong to the type of anion-deficient perovskites, which are of peculiar interest due to the coexistence of magnetic and ferroelectric properties.

The studies of high pressure effects on the crystal and magnetic structures of complex magnetic transition metal oxides continued. The experiments with hexagonal frustrated manganite YMnO3 exhibiting multiferroic properties have revealed that the diffuse magnetic scattering gets significantly stronger and the ordered magnetic moments are drastically suppressed with increasing pressure at low temperatures.

Within the framework of the Helmholtz Association (Germany)-RFBR Joint Research Groups (HRJRG) project «Study of structural aspects of biocompatible ferrofluids by scattering methods: stabilization, properties control and applications» small-angle neutron scattering experiments using the contrast variation method have been carried out with a number of water-based magnetic fluids from various manufacturers including the Centre of Fundamental and Advanced Technical Research (Timisoara Branch of RAS, Romania), Pierre&Marie Curie University (Paris, France), Institute of Experimental Physics of SAS (Kosice, Slovak Republic). Also, in the framework of the study of the mobility of brain cancer cells incorporating magnetic nanoparticles a search for a proper source of magnetic nanoparticles has been conducted among water-based magnetic fluids with sterical stabilization on the basis of double coating of magnetite with various surfactants including citric (CA+CA), oleic (OA+OA), myristic (MA+MA) and lauric (LA+LA) acids. The LA+LA stabilized magnetic fluid was demonstrated to be the most preferable source of magnetic nanoparticles. From the viewpoint of structural peculiarities the given fluid has the least aggregation

rate, which explains higher absorption of magnetic nanoparticles by the cancer cells in the given case and might also be the reason of their lowest cytotoxicity for the cells.

Within the framework of the study of the coexistence of ferromagnetism (FM) and superconductivity (S) in thin multilayers, data treatment and interpretation of the results obtained for a three-layer system (S)/(FM)/(S), namely, for (Nb)/(Fe)/(Si, Mo) on silicon substrate have been completed. For the first time it has been directly shown that in the three-layer system (S)/(FM)/(S) at the transition of layers to the superconducting state the magnitude of exchange interaction in the ferromagnetic layer decreases.

A new class of polymers produced by regulated synthesis (dendrimers) has been studied. Using small-angle scattering data the spatial distribution of the scattering density for the dendrimer type under study has been obtained. It has been demonstrated that a simple model of dendrimer branch growth fails to explain the anisometry and spatial inhomogeneity of the polymer.

Magnetic elastomers (composite materials consisting of a polymer matrix and highly polydisperse magnetic particles) have been investigated by small-angle neutron scattering and small-angle X-ray scattering. It has been found that the polymer matrix is fragmented and has a nanophase character, and the geometric sizes of nanophase areas depend on the concentration of doped magnetic particles and the strength of the applied magnetic field during the synthesis of material.

The detailed analysis of experimental data on quasi-elastic neutron scattering by water dispersion of nanodiamonds has been performed. A clear slowing down in the diffusion mobility of the molecules of hydration water as compared to that of the bulk water was revealed.

The fluid metamorphogenic (FM) model of seismotectogenesis has been substantiated using the results of neutron and acoustic experiments on mono-crystalline and poly-crystalline quartz samples in the region of polymorphous α-β transition. For the first time, the method of preferred orientation description based on ODF-histograms and ODF-spectra has been used for estimating the expected degree of anisotropy of various physical properties.

A series of studies on the martensitic transformation and fatigue properties of austenitic stainless steels widely used in industry due to their remarkable mechanical, welding and corrosion-resistant characteristics has been completed. Formation mechanisms of the martensitic phase in an initially one-phase (austenitic) material have been determined. It has been shown that in some cases there is a large variance in elastic constants of phases constituting the material, which significantly influences its strength properties.

In 2008 a number of experiments were carried out and some interesting results were obtained in the field of nuclear physics.

Within the framework of preparation and carrying out of the experiment on the direct measurement of neutron-neutron scattering cross section on the YAGUAR reactor (VNIITF, Snezhinsk), the calibrations using noble gases (Ar, He) were carried out, which demonstrated the operational capability of the facility and measuring technique. The obtained values of scattering cross section for the gases coincide with the tabulated values. The first attempt to measure the neutron-neutron scattering showed the presence of high background of thermal neutrons, which exceeds the level of the expected effect by an order of magnitude. Further progress of the project should be connected with the study of this phenomenon and efforts to decrease its influence in the experiment.

Investigations of neutron interaction with nanoparticles were performed. The dependence of angular distribution of neutrons reflected from the surface of diamond nanopowder was measured for various wavelengths of incident neutrons at the angles of incidence of the neutron beam to the surface of 2°, 3° and 4°. As a result of multiple scattering from nanoparticles the neutrons are reflected from the surface with relatively narrow angular distribution, the maximum of which is close to a specular angle. Thus, for cold neutrons with the wavelength λ ranging from 4 Å to 8 Å the quasi-specular albedo in the scattering plane at small angles of incidence (less than 6-9°) is observed. The probability of such albedo may reach 30%.

Theoretical analysis and simulation of possible variants of the experiments to measure neutron lifetime in material traps were performed. Additional detailed calculations of the generation of ultracold neutrons in various moderators for the pulsed reactor TRIGA were carried out and, on this basis, new experiments to measure neutron lifetime in magnetic traps were proposed. New measurements of the generation of ultracold neutrons were performed at the pulsed reactor TRIGA-Mainz in the stationary, pulsed and accumulation modes.

On the beam of the ILL reactor (Grenoble, France) in the framework of the collaboration PNPI (Gatchina) – JINR – Germany – Finland the experiment to observe the rotation of the fissioning nucleus under the action of polarized neutrons (ROT-effect) was carried out. The 239Pu nucleus having spin ½ was chosen as a target. The effect was observed by measuring the angular dependence of the escape of ternary-fission α-particles relative to the rotation axis of the nucleus polarized by incident neutrons. The analysis of the obtained data will be performed in 2009.

In Strasbourg (France) in the framework of the collaboration JINR-France-Germany-Belgium the experiment started to search for correlation of the neutron escape from 252Cf fission fragments with the spins of the fragments. In the experiment the multi-detector facility DEMON to measure neutrons and the ionization chamber CODIS to measure fission fragments are used. The search for

angular correlation between two neutrons emitted from one fragment is in progress. The results of the experiment are expected in 2009.

Within the framework of collaboration with FLNR the treatment of the experimental data obtained in 2006 on the IBR-2 reactor using the “Mini-Fobos” facility to search for the ternary collinear decay continued. A new technique of data treatment was proposed, which implies the determination of charges of the detected fission fragments using the time of electron drift in the Bragg chamber. The obtained results agree with the hypothesis on the existence of exotic modes of fissioning nucleus decay.

In conclusion, it might be well to point out that great interest is being expressed by the JINR Member States in the work in the field of neutron investigations. It is also significant that in the last few years a lot of young people have come to the Laboratory. All these facts confirm that the Laboratory continues to develop successfully and dynamically, carrying out investigations in the interests of the JINR Member States.

A.V.Belushkin

Director

1. SCIENTIFIC RESEARCH

1.1. CONDENSED MATTER PHYSICS

The main objectives of research in the framework of the theme involved the application of neutron scattering techniques for the investigation of the structure and dynamics of condensed matter, obtaining of new data on the microscopic properties of condensed matter, experimental verification of theoretical predictions and models, revealing of new regularities. In view of the IBR-2 reactor shutdown in December, 2006 for the next stage of reconstruction, the tasks of the Department personnel and work plans under the theme in 2007 - 2008 differed noticeably from the traditional program of activities. Namely, the scientific work was transferred to the allied centers in Russia and abroad. Out of fundamental and applied research activities developed by the employees of the FLNP Department of Neutron Investigations of Condensed Matter (NICM), several major scientific directions were chosen and preserved. Work in these directions was conducted in other research centers (first of all in neutron and synchrotron centers) under the existing cooperation agreements. The first stage of the modernization program for the spectrometers at the IBR-2 reactor continued. The work under the theme was carried out by the employees of the FLNP NICM Department structurally organized in the form of sectors (groups) according to the main research directions.

Within the framework of investigations under the theme, the employees of the NICM Department maintained broad cooperation with many scientific organizations in Russia and abroad. The cooperation, as a rule, was documented by joint protocols or agreements. In Russia, particularly active collaboration was with the thematically close organizations, such as RRC KI, PNPI, ISSP RAS, IMP, IC RAS, and others.

The employees of the NICM Department are specialists in performing neutron scattering studies of condensed matter using neutron diffraction from poly- and single crystals, small-angle neutron scattering in systems with large-scale inhomogeneities, inelastic incoherent nuclear and magnetic neutron scattering, reflection and scattering of polarized neutrons at interfaces. A list of main scientific topics investigated using the above-mentioned techniques, includes:

- atomic and magnetic structure of strongly correlated electron systems – complex magnetic oxides**,** multiferroics, etc.;
- structure and phase transitions in model biological membranes;
- large-scale structure of non-crystalline materials: vesicules, polymers, dendrimers, colloidal solutions, magnetic liquids, etc.;
- molecular structure of biological objects;
- properties of surfaces and nanostructures with reduced dimensionality;
- coexistence of magnetism and superconductivity in layered structures;
- melts with dynamic, structural and composition inhomogeneities;
- dynamics of hydrogen-containing groups in organic compounds;
- internal stresses in construction materials and rocks;
- relation of texture and properties of rocks.

I. Scientific results

1.1.1. Atomic and magnetic structure of complex magnetic oxides

The crystal and magnetic structures of the $Pb_{2-x}Ba_xFe_2O_5$ solid solution series with $x \approx 1$ have been studied using x-ray and neutron powder diffraction, electron microscopy and Mössbauer spectroscopy. These compounds belong to the type of anion-deficient perovskites, which are of peculiar interest due to the coexistence of magnetic and ferroelectric properties. Nowadays, materials that simultaneously show ferromagnetism and ferroelectricity are generally called multiferroics. In the diffraction experiments two structural phases (high- and low-temperature) with a phase transition between them at $T_c \approx 540$ K have been revealed. The phases differ in the configuration of two mirror-related chains of FeO_5 trigonal bipyramids, which become ordered below T_c. It follows from the neutron diffraction data that below $T_N = 625$ K $Pb_{1.08}Ba_{0.92}Fe_2O_5$ transforms into an antiferromagnetically (AFM) ordered state with a propagation vector k = [0,½,½] (**Fig. 1**). At the same time the magnetic splitting in Mössbauer spectra occurs only below 520 K. This significant difference in the magnetic ordering temperatures measured by various methods has been explained by a specific spin dynamic behavior resulting from essentially different superexchange interactions between the magnetic moments of Fe atoms in FeO_6 octahedra and in FeO_5 trigonal bipyramids [**1**]. At high temperatures the spin relaxation time appears to be significantly shorter than the ^{57}Fe Mössbauer spectroscopy time scale. The work has been performed in cooperation with the Laboratory of Inorganic Crystal Chemistry (Department of Chemistry, Moscow State University) and the Laboratory for Neutron Scattering (Paul Scherrer Institut, Switzerland).

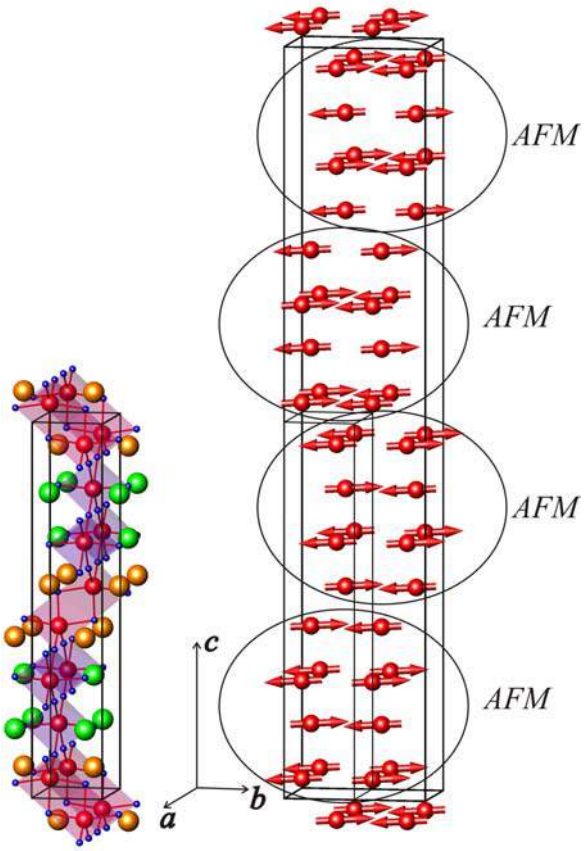

Fig. 1. Illustration of the antiferromagnetic ordering of the magnetic Fe moments for the $Pb_{1.08}Ba_{0.92}Fe_2O_5$ compound (right half of the figure). The unit cell of the crystal structure of the low-temperature form of $Pb_{1.08}Ba_{0.92}Fe_2O_5$ is presented at the left in the same scale (Fe atoms are shown as red balls).

The detailed neutron diffraction study of atomic and magnetic structure of 314-cobaltites $Sr_3YCo_4O_{10.5+\delta}$ (or $Sr_{0.75}R_{0.25}CoO_{2.625+\delta/4}$) wherein A-positions are perfectly ordered, has been completed. The compounds with different oxygen contents (close to optimal, $\delta \approx 0$, and with increased oxygen content, $\delta \approx 0.2$) have been found to have AFM structure of G-type with the moments directed along the c-axis of the tetragonal unit cell [**2**]. Contrary to the earlier studies of similar structures, it has been revealed that Co atoms occupying different positions in a unit cell have different magnitudes of magnetic moments correlating with the oxygen surrounding of the atom. Thus, for the first time a direct relationship between the charge and spin states of Co atoms has been revealed for cobaltites (**Fig. 2**). The work has been performed in cooperation with the Laboratory of Inorganic Crystal Chemistry (Department of Chemistry, Moscow State University) and the Laboratory for Neutron Scattering (Paul Scherrer Institut, Switzerland).

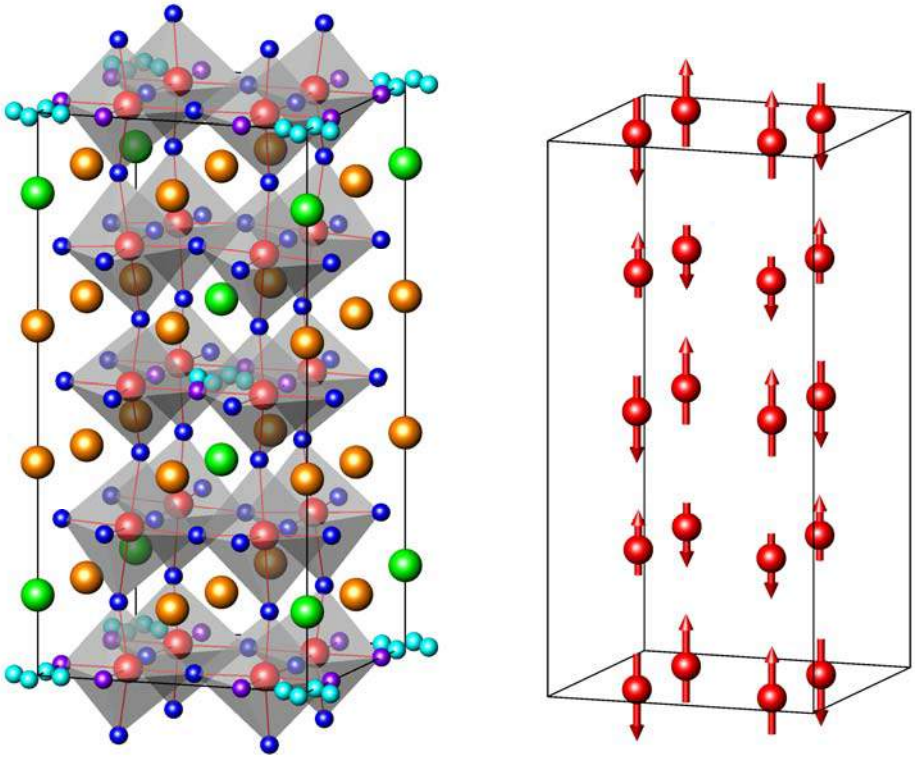

Fig. 2. Crystal (left) and magnetic (right) structures of the $Sr_3YCo_4O_{10.5}$ compound. Big balls are the atoms of Y (green), Sr (golden) and Co (at the centre of oxygen octahedrons) atoms. Oxygen atoms (small balls) occupy filled (dark blue), partially filled (violet) and disordered (light blue) sites. The Co magnetic moment in the layers with the filled oxygen sites ($z \approx 0.25$ and $z \approx 0.75$) is about 1.5 μ_B, whereas in the layers with $z = 0$ and $z = 1/2$ $\mu_{Co} \approx 2.8$ μ_B.

The studies of high pressure effects on the crystal and magnetic structures of complex magnetic transition metal oxides continued. The experiments with hexagonal frustrated manganite $YMnO_3$ exhibiting multiferroic properties have revealed that the diffuse magnetic scattering gets significantly stronger and the ordered magnetic moments are drastically suppressed with increasing pressure at low temperatures (**Fig. 3**). The interpretation of this phenomenon is based on the assumption implying the stabilization of magnetic liquid state with strong spin fluctuations under pressure [**3**].

For the $La_{0.33}Ca_{0.67}MnO_3$ compound studied in the temperature range of 10-300 K and at high pressures of up to 5 GPa, the suppression of the “Wigner-crystal” antiferromagnetic ground state and the stabilization of the C-type AFM state under high pressure have been observed [**4**].

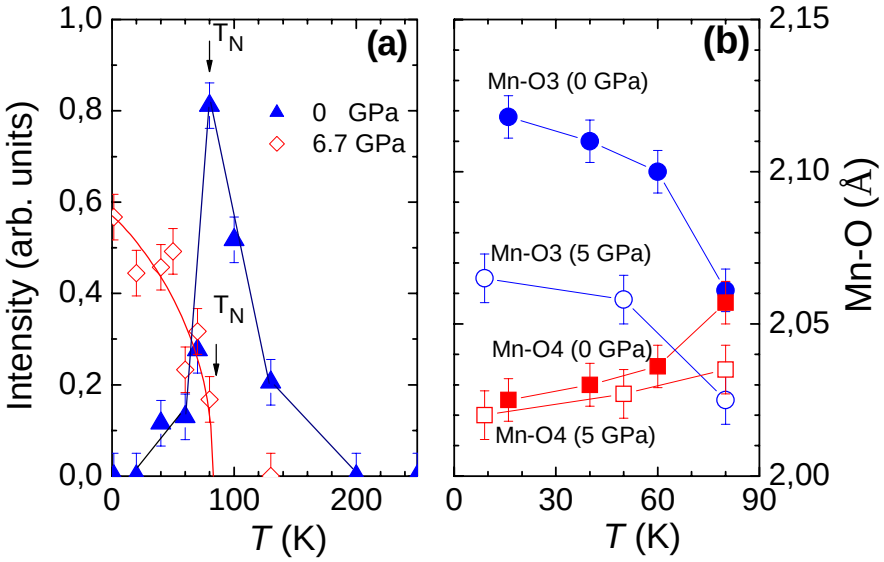

Fig. 3. The temperature dependence of magnetic diffuse scattering in $YMnO_3$ at different pressures (left). The increase in its intensity at high pressures and low temperatures is connected with the formation of spin-liquid state with strong fluctuations due to the symmetrization of the triangular magnetic lattice formed by Mn-O3 and Mn-O4 interatomic bonds (their temperature and pressure dependences are shown at the right).

1.1.2. Investigation of model and biological membranes

For the first time the information on the structural organization of lipid membranes on the basis of phospholipids of *S. Hygroscopicus* actinobacteria has been obtained. A lipid fraction separated from these bacteria forms on quartz substrates a multilayer membrane structure with repeat distance $d_0 = 85.8 \pm 0.5$ Å and $d_0 = 83.5 \pm 0.5$ Å at ambient conditions $T = 20$°C, RH = 97% and $T = 40$°C, RH = 96%, respectively. At the same time, a part of lipids does not enter into the composition of the bilayer and forms liquid micellar phase with the micelle sizes of 54.2 ± 0.2 Å. These results give proof to the liquid crystal structure of the membranes formed by the separated phospholipids of actinobacteria. The liquid crystal structure of such membranes makes it possible to apply X-ray diffraction methods to study the changes in lamellar and lateral structures on cooling the multilayer membranes in excess of aqueous solutions of cryoprotectants. Future investigations into the processes of structural changes on cooling the membranes down to nitrogen temperatures followed by heating will allow more effective selection of cryoprotectants for storage of bacteria.

Neutron diffraction has been applied to study the structural organization of lipid multilayer membranes on the basis of ceramide 6 and mixture of six fatty acids. This composition models the structure of the outermost layer of mammalian skin, the stratum corneum (SC). We used the following acids most commonly occurring in the SC lipid matrix: palmitic acid (C16:0), stearic acid (C18:0), arachic acid (C20:0), behenic acid (C22:0), lignoceric acid (C24:0) and cerotic acid (C26:0) in the molar ratio 1.3/3.3/6.7/41.7/36/6.7. For this composition we determined the effect of cholesterol sulfate on the hydration process and the structure of completely hydrated membranes in the experiments to study the kinetics of membrane swelling in excess of water at 20°C. The example of the measured dependences for the repeat distances of the membranes is shown in **Fig. 4**. It has been found that the membranes based on the mixture of fatty acids have a structure similar to that of the SC model membrane on the basis of palmitic acid. In addition, it has been revealed that the used composition of fatty acids accelerates the membrane hydration time by a factor of 1.5.

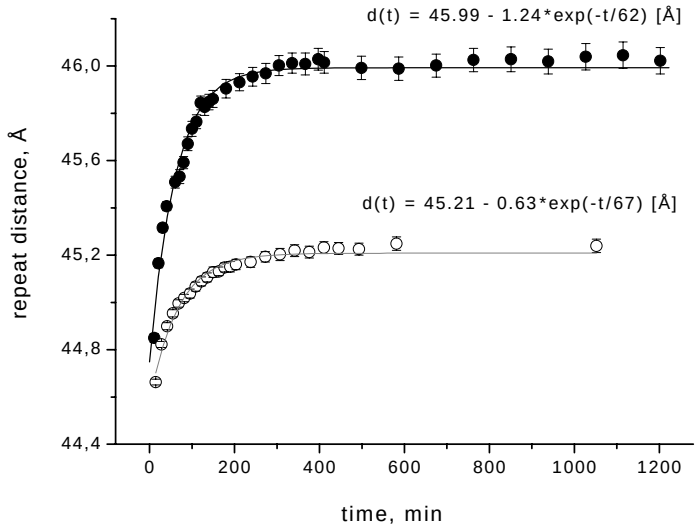

Fig. 4. The time dependence of the repeat distance of membranes on the basis of ceramide 6 and a mixture of six fatty acids with two different component weight ratios during hydration in heavy water at 20°C. Solid lines are drawn in accordance with the exponential time dependence of the repeat distance.

1.1.3. Nanostructured materials

The structure of low-concentrated (volume fraction of magnetic dispersed material of the order of 1%) magnetic fluids (magnetite nanoparticles in decahydronaphtalene) stabilized using saturated monocarboxylic acids of different chain lengths (lauric, myristic, palmitic and stearic acids) has been studied by means of magnetization analysis, electron microscopy and small-angle scattering of non-polarized neutrons (**Fig. 5**) [**5**]. A comparison with the classical magnetic fluid stabilized by unsaturated oleic acid has been carried out. It has been shown that unlike oleic acid, the saturated acids stabilize magnetite nanoparticles of smaller sizes and with lower polydispersity. For the studied saturated acids the mean size values and the polydispersity indices correspond to nearly one size distribution function (**Fig. 5*a***). The effective thickness of a stabilizing shell around magnetite nanoparticles, which correlates with the chain length of the used acid, has been determined on the basis of comparison of small-angle non-polarized neutron scattering curves (**Fig. 5*b***). Thus, it has been concluded that a significant contribution to the stabilization properties of the shell is made by its elasticity, which is approximately the same for saturated acids, but differs greatly from that of the oleic acid. The work has been performed in cooperation with the Centre of Fundamental and Advanced Technical Research (Timisoara Branch of RAS, Romania), the Budapest Neutron Center (Hungary) and the GKSS Research Centre in Geesthacht (Germany).

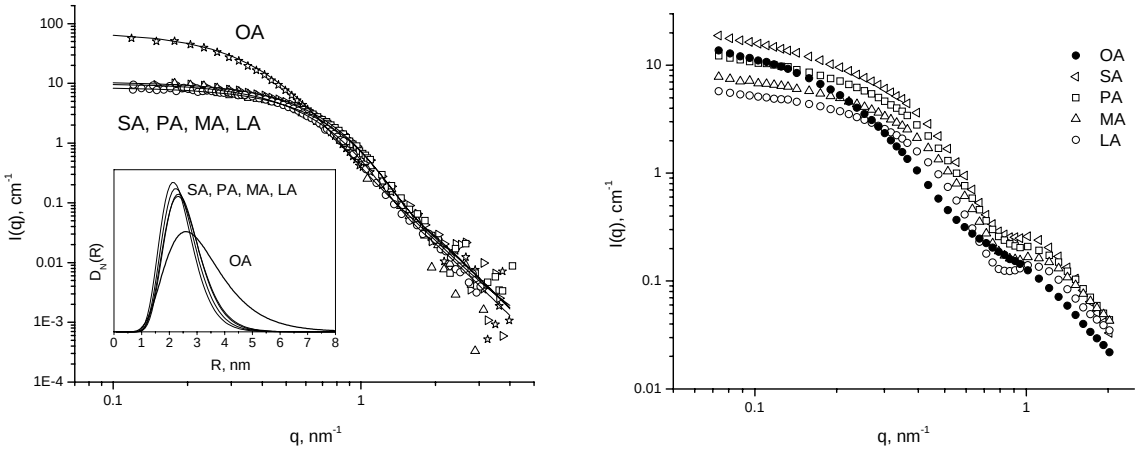

(*a*) **(*b*)**

Fig. 5. Small-angle neutron scattering study of structural differences of non-polar organic magnetic fluids (magnetite nanoparticles in decahydronaphtalene) stabilized by a single layer of monocarboxylic acids of different chain lengths and saturation (oleic (OA), stearic (SA), palmitic (PA), myristic (MA) and lauric (LA) acids). *(a)* Experimental scattering curves for usual (nondeuterated) carrier. Because of small contrast between the carrier and the stabilizing shell, neutrons are scattered only by magnetic nanoparticles. Due to large nuclear contrast, magnetic scattering is insignificant. The inset shows the corresponding particle radius distribution functions. *(b)* Experimental scattering curves for the carrier with 90% of deuterated analogue. The effect of scattering by the shell is visible. For saturated acids (SA, PA, MA, LA) the modulation of scattering depending on the acid, which testifies to the correlation between the shell thickness and the acid chain length can be observed. As may be seen from *(a)*, radius distribution functions for magnetic nanoparticles stabilized by the saturated acids are very close and differ noticeably from that of the unsaturated acid OA.

Within the framework of the Helmholtz Association (Germany)-RFBR Joint Research Groups (HRJRG) project «Study of structural aspects of biocompatible ferrofluids by scattering methods: stabilization, properties control and applications» small-angle neutron scattering experiments using the contrast variation method have been carried out with a number of water-based magnetic fluids from various manufacturers including the Centre of Fundamental and Advanced Technical Research (Timisoara Branch of RAS, Romania), Pierre & Marie Curie University (Paris, France), Institute of Experimental Physics of SAS (Kosice, Slovak Republic). Also, in the framework of the study of the mobility of brain cancer cells incorporating magnetic nanoparticles a proper source of magnetic nanoparticles was searched among water-based magnetic fluids with sterical stabilization on the basis of double coating of magnetite with various surfactants including citric (CA+CA), oleic (OA+OA), myristic (MA+MA) and lauric (LA+LA) acids. The main aspects of the given investigation were the structural characterization of magnetic fluids, their stability in the cancer cell culture, toxicity and absorption by the cells. The structure analysis comprising magnetization, transmission electron microscopy and small-angle neutron scattering experiments showed that a part of magnetite particles in the fluids under study (size ~7 nm, polydispersity 40%) forms stable aggregates with a mean size up to 40 nm depending on the type of the surfactant layer. The magnetic fluids (volume fraction of dispersed magnetite within 1-3 %) were added to the culture medium (Dulbecco modified Eagle medium Glutamax, 10 % fetal calf serum), where brain cancer cell lines G44, G55-T2, G87, G112 (UMC Hamburg Eppendorf) were incubated. The incorporation of nanoparticles into cells was determined via magnetic cell separation, atomic absorption spectroscopy, fluorimetric measurements, as well as Berliner Blue staining. The cytotoxicity of nanoparticles under study was found to be different for various stabilization layers of the surfactants. The LA+LA stabilized magnetic fluid was demonstrated to be

the most preferable source of magnetic nanoparticles. From the viewpoint of structural peculiarities the given fluid has the least aggregation rate (fig.), which explains higher absorption of magnetic nanoparticles by the cancer cells in the given case and might also be the reason of their lowest cytotoxicity for the cells.

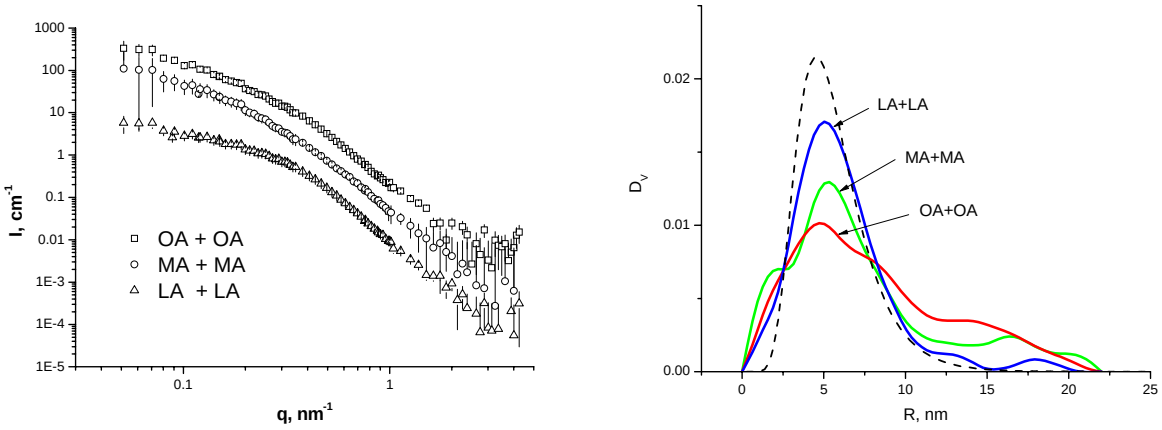

(*a*) (*b*)

Fig. 6. Small-angle neutron scattering by magnetic nanoparticles dispersed in water and stabilized by double layer coating of monocarboxylic acids of different chain lengths and degrees of saturation: oleic (OA+OA), myristic (MA+MA) and lauric (LA+LA) acids *(a)* Experimental scattering curves. *(b)* Obtained volume distribution functions for magnetic particles. The dashed line shows the calculation for separate particles according to the electron microscopy data.

The process of fullerene cluster formation in nitrogen-containing solvent NMP (medium-polar solvent) has been considered within the framework of the nucleation theory by analogy with low-polar solvents [6]. It has been shown that as in the case of low-polar solvents, to explain the stabilization of the cluster size in NMP, the limited growth model describing the formation of an effective stabilizing shell around the clusters should be invoked. The most probable mechanism of the formation of such shell is the appearance of donor-acceptor complexes C_{60}/NMP, which gradually restricts the growth of clusters. We have also considered the reorganization of fullerene clusters on addition of water to the C_{60}/NMP solution which, in particular, manifests itself in a sharp increase in the intensity of small-angle neutron scattering for the sizes of the order of 10 nm. It has been shown that critical changes in the solution that are experimentally observed on addition of water cannot be described by a change in the concentration and thermodynamic characteristics of the system. The work has been performed in cooperation with the Russian Research Center «Kurchatov Institute» (Moscow, Russia), National Taras Shevchenko University of Kyiv, A.A.Chuiko Institute of Surface Chemistry**,** National Academy of Sciences of Ukraine, (Kyiv, Ukraine), M.V.Lomonosov Moscow State University (Moscow, Russia), Research Institute for Solid State Physics and Optics of the Hungarian Academy of Sciences (Budapest, Hungary).

Fe_3O_4-based ferrofluid solutions have been studied using the μSR-spectroscopy method. The experiments have been carried out on a polarized positive muon beam on the synchrotron with the orientation of an external magnetic field in the transverse direction to the orientation of muon spin. The experiments have been conducted in the temperature range from 26 to 300 K. It has been found that the diamagnetic fraction is formed in the ferrofluid in about the same amount as in heavy water, but the muon-spin relaxation rate in the ferrofluid is much higher than in heavy water. A significant shift of the muon-spin precession frequency in the ferrofluid has been observed. It has been shown

that the shift of the muon precession frequency as a function of the external magnetic field is described by the Langevin function typical of paramagnetic magnetization. The mean nanoparticle radius has been estimated (<D> = 12 nm) [**7**].

A new class of polymers produced by regulated synthesis (dendrimers) has been studied in cooperation with the N.S.Enikolopov Institute of Synthetic Polymeric Materials. Using small angle scattering data the spatial distribution of the scattering density for the dendrimer type under study has been obtained (**Fig. 7**). Using the contrast variation method it has been proved that dendrimer molecules in solutions have no closed inner cavities impermeable to a solvent. The partial volume of the dendrimer in solution has been determined. Homogeneous distribution of scattering density has been shown. It has been found that dendrimers of the ninth generation are monodisperse within experimental error. Experimental evidence of homogeneous distribution of the scattering length density inside the dendrimers has been obtained. It has been demonstrated that a simple model of dendrimer branch growth fails to explain the anisometry and spatial inhomogeneity of the polymer [**8**].

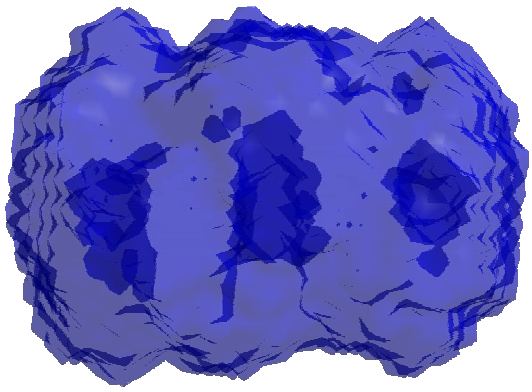

Fig. 7. The spatial distribution of the scattering density for the dendrimer from small-angle scattering data.

Magnetic elastomers (composite materials consisting of a polymer matrix and highly polydisperse magnetic particles) have been investigated by small-angle neutron scattering and small-angle X-ray scattering. It has been found that the polymer matrix is fragmented and has a nanophase character, and the geometric sizes of nanophase areas depend on the concentration of doped magnetic particles and the strength of the applied magnetic field during the synthesis of material.

1.1.4. Physics of thin films

Within the framework of the study of the coexistence of ferromagnetism (FM) and superconductivity (S) in thin multilayers, data treatment and interpretation of the results obtained for a three-layer system (S)/(FM)/(S), namely, for (Nb)/(Fe)/(Si, Mo) on silicon substrate have been completed. The theoretical analysis has shown that due to the proximity effects between (S) and (FM) layers, various scenarios of their interaction are possible: the formation of domain structure, "flowing" of magnetization from (FM) layer to (S) layer, a change in the direct and indirect exchange interactions of (FM) layers. The practical importance of studying these systems is connected with the prospect of development of devices for recording information simultaneously in electric and magnetic channels. The measurements were carried out under a magnetic field of 500 Oe and in the temperature range of 2-60 K. For the first time the reorganization of the domain structure and the decrease in the saturation magnetization in the domains at the transition of Nb(500 Å) layer and [Si(34 Å)/Mo(34 Å)] structure to the superconducting state (**Fig. 8**) have been

simultaneously observed. For the first time it has been directly shown that in the three-layer system (S)/(FM)/(S) at the transition of layers to the superconducting state the magnitude of exchange interaction in the ferromagnetic layer decreases [**9**].

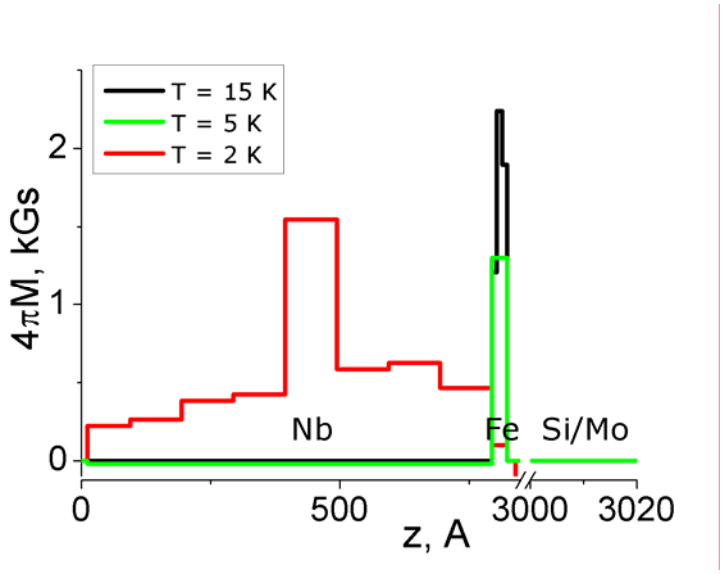

Fig. 8. Magnitization profile in Nb/Fe/[Si/Mo] multilayers at 15, 5 and 2 K in a magnetic field of 500 Oe. With decreasing temperature and at the transition of superconductors (Nb) and (Si/Mo) to the superconducting state, the mean magnetization value decreases in the ferromagnetic Fe layer.

1.1.5. Atomic dynamics

Studies have been performed for isomers of dimethylbutanol $C_6H_{13}OH$ (2,2DM-1B, 3,3DM-1B, 2,3DM-2B and 3,3DM-2B) consisting of globular molecules, which in solid state form orientationally disordered crystalline phases. Calorimetric studies of polymorphism of these compounds have revealed significant differences in the melting temperatures, as well as in the kinetics and number of phase transitions observed during cooling and heating. Simultaneous neutron powder diffraction studies and inelastic incoherent neutron scattering (IINS) investigations have made it possible to identify glassy and crystalline phases, which can coexist at low temperatures [**10**]. The preliminary interpretation of IINS spectra is based on the quantum-chemical calculations of the dynamics of isolated molecules using the B3LYP/6-311G** basis set in the electron density functional theory (DFT). The calculated spectra of density of vibrational states for isolated molecules $G_{cal}(\nu)$ are in qualitative agreement with the experimental spectra $G_{exp}(\nu)$ but do not determine satisfactorily characteristic vibration frequencies of hydrogen bonds [**11**]. Computer simulation of the structure and dynamics of molecular clusters of dimethylbutanol (DMB) isomers has made it possible to determine lengths and characteristic vibration frequencies of hydrogen bonds depending on the number of molecules and the structure of clusters. The comparison of calculated and experimental spectra of density of vibrational states obtained for 2,2DM-1B isomer is presented in **Fig. 9**. The formation of hydrogen bonds results in significant shifts of vibration frequencies of hydroxyl groups OH of isolated molecules. Frequencies of out-of-plane vibrations of hydrogen, γ(C-O-H), increase approximately two times (100%). Frequencies of in-plane δ(C-O-H) mode increase by approximately 30%, whereas frequencies of stretching ν(O-H) mode decrease by approximately 10%. The $G_{cal}(\nu)$ spectra obtained for cyclic tetramers of DMB molecules are sufficient for satisfactory interpretation of vibrational bands observed in the inelastic incoherent neutron scattering (IINS) spectra and infrared (IR) absorption spectra. The average length of

hydrogen bonds for the calculated structures of cyclic tetramers of DMB agrees well with the estimate of hydrogen bond lengths for frequencies of ν(O-H) mode, which were determined from infrared absorption spectra. All computer calculations were carried out in the Poznan Supercomputing and Networking Center.

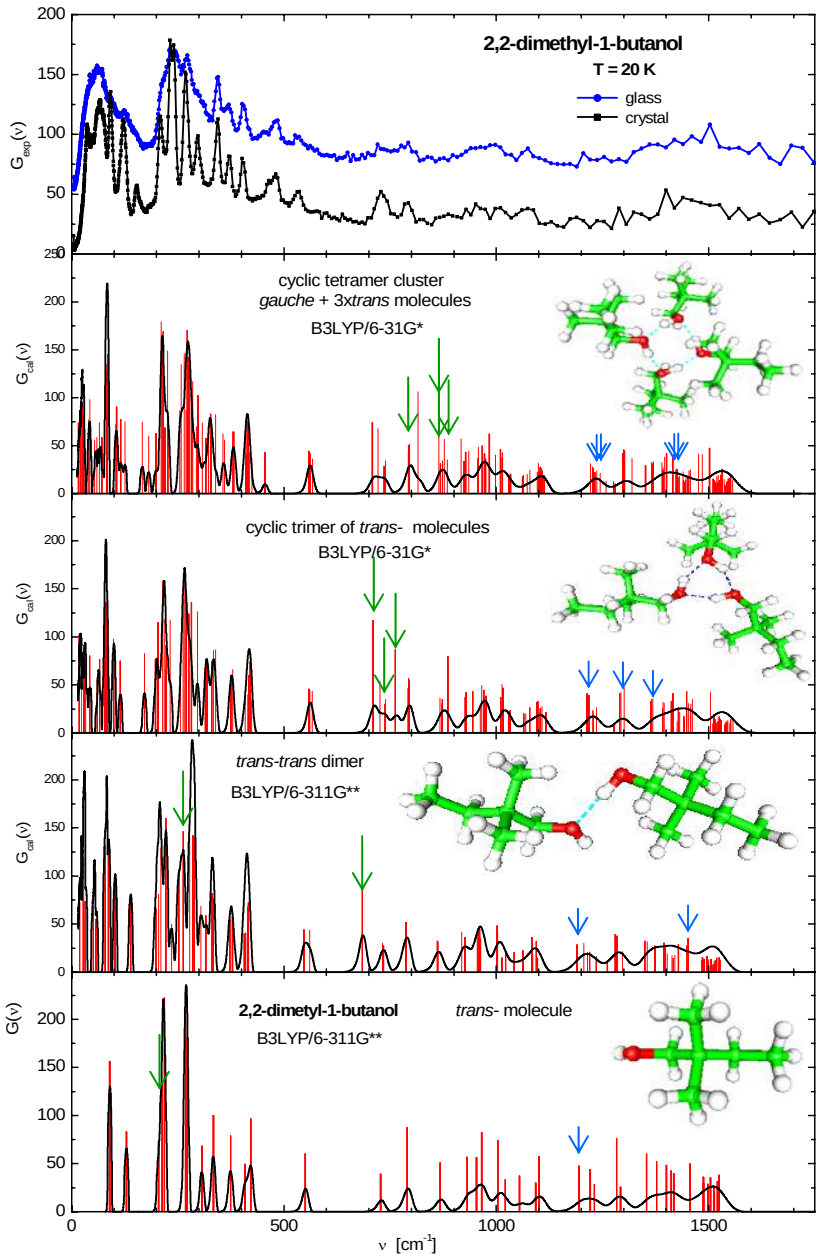

Fig. 9. Example of comparison of experimental and calculated IINS spectra for 2,2-dimethyl-1-butanol.

The detailed analysis of experimental data on quasi-elastic neutron scattering by water dispersion of nanodiamonds (concentration of particles ~ 80 mg/ml, average size of particles ~ 8°nm, temperature of solution ~ 12°C) has been performed. The data analysis was carried out with the use of the model according to which water in the dispersion was assumed to be a two-component system comprising usual water (bulk water) and water immediately adjacent to the surface of nanoparticles and experiencing their influence on its structural-dynamic properties (hereinafter, hydration water). The relative fraction of this water was estimated to be ~ 3 %, which

approximately corresponds to two-three layers of water molecules adjacent to the surface of the nanoparticle. The analysis of diffusion processes in both water components was carried out on the basis of the «stretched exponent» method, which makes it possible to evaluate α-relaxation effects (diffusion processes leading to the distortion of the nearest surrounding of the molecule) in both water components. A clear slowing down in the diffusion mobility of the molecules of hydration water as compared to that of the bulk water was revealed. The intensity of diffusion processes in the hydration water was found to be close to the parameters of the diffusion of supercooled water at a temperature of –(15-20) °C (**Fig. 10**).

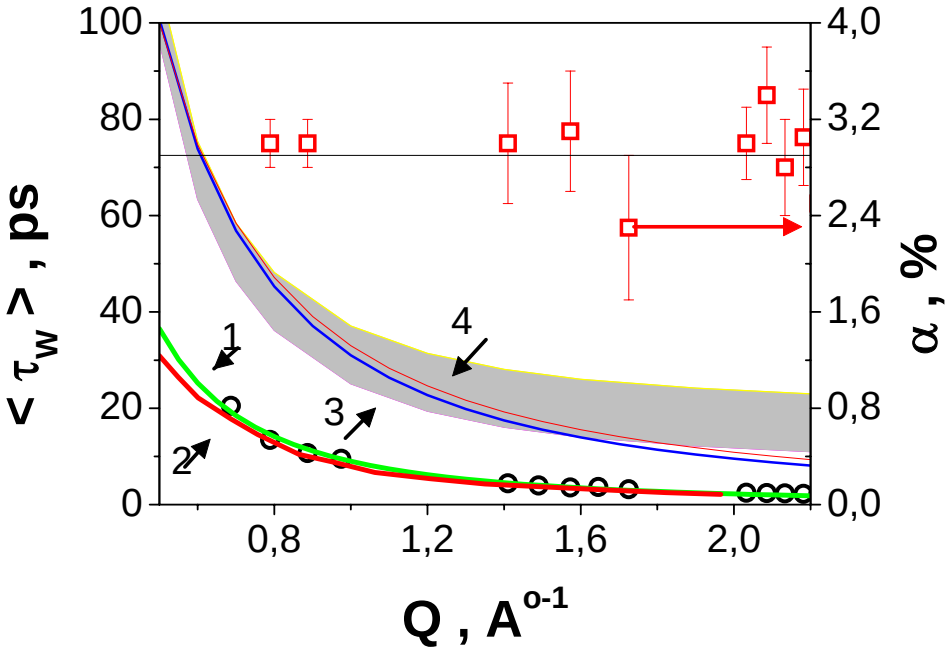

Fig. 10. Dependence of mean α-relaxation time $<\tau_W>$ in bulk and hydration water on neutron wave vector transfer Q. The right ordinate is the relative fraction of hydration water $< \alpha > = (2.9 \pm 0.3)\%$. Curves are denoted by 1 – 4, where 1 – bulk water ($<\tau_W>(Q) = 9.0*Q^{-2.02}$), 2 – MD data for T = 11°C, 3 – hydration water ($<\tau_W>(Q) = 31*Q^{-1.7}$ and $\gamma = 1.7 \pm 0.1$ are obtained in the range 0.5 A^{-1} < Q < 1.4 A^{-1}), 4 – $<\tau_W>$ in the supercooled water, MD data for T = – 20°C.

On the DIN-2PI spectrometer the collective modes in liquid lithium have been studied by the inelastic slow neutron scattering method [**12**]. The measurements were carried out at 500 K ($T_{melt.}$(Li) = 453.7 K). From the experimental spectra the coherent scattering component was extracted and analyzed. We obtained a part of a dispersion curve of collective atomic excitations for lithium melt, which agrees within experimental error with the results of other authors. Figure 11 shows a generalized dispersion curve in rescaled units for liquid alkali metals from the experimental works. It can be seen that the result for lithium is not contradictory to the general picture. The whole set of points forms a single dispersion curve, which supports the conclusion about the microdynamic similarity of liquid alkali metals.

Inelastic neutron scattering spectra for uranium nitride (UN) have been obtained for a temperature range from room temperature up to 1273 K. Uranium nitride is considered as a basic material for creation of a combined fuel for fast neutron reactors, which hold much promise for the development of large-scale nuclear power engineering. Figure 12 presents the functions of phonon density of states of UN for several temperatures, which were determined from the experimental spectra. Uranium nitride exhibits noticeable magnetic scattering, which was not taken into account in the treatment of the experimental spectra, therefore these data are preliminary.

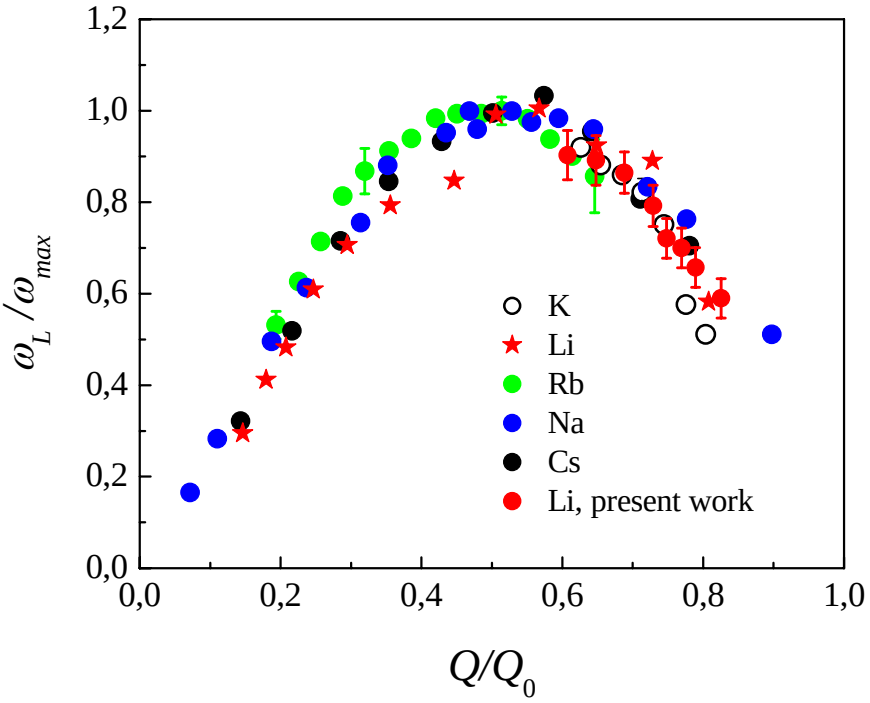

Fig. 11. Generalized dispersion dependence for liquid alkali metals in rescaled units.

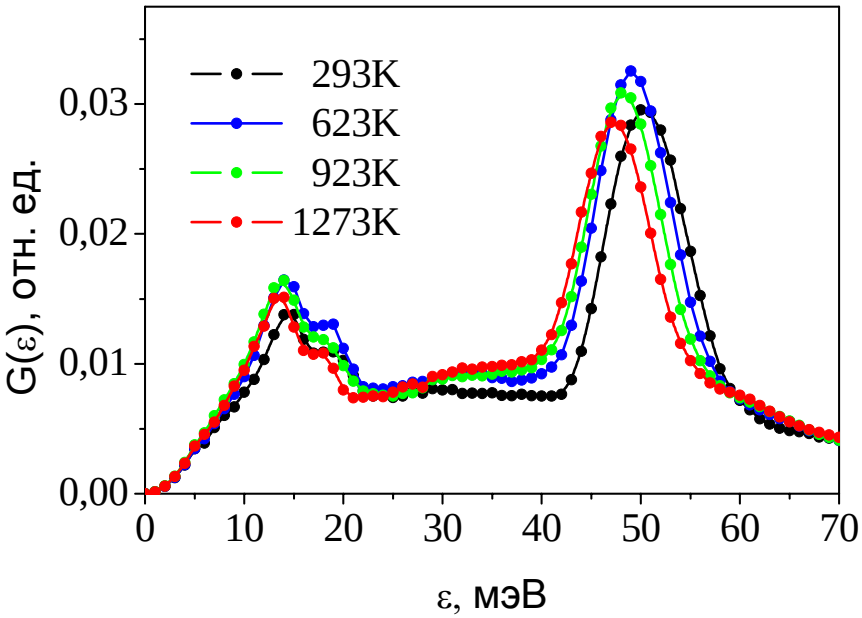

Fig. 12. Functions of phonon density of states of UN at temperatures of 293 – 1273 K. Two regions of vibrations with maxima at energy transfers ε ~ 14 MeV and ~ 50 MeV are observed. The first (acoustic) region corresponds to the vibrations of heavy uranium atoms, the second (optical) one – to that of light nitrogen atoms. With increasing temperature the vibration spectrum softens due to a shift of the optical part to the region of lower energies and the transformation of the acoustic part of the spectrum.

1.1.6. Applied research

Among traditional applied investigations in the Department of Neutron Investigations of Condensed Matter are the experimental studies of internal stresses and texture of rocks and minerals, determination of internal stresses in bulk materials and products, including engineering materials and components of machines and devices. For the most part, these investigations are carried out using neutron diffraction.

The fluid metamorphogenic (FM) model of seismotectogenesis has been substantiated using the results of neutron and acoustic experiments on mono-crystalline and poly-crystalline quartz samples in the region of polymorphous α-β transition. In this model the reason for destructions in the seismic process is an increase in microstress values and decrease in the strength of solids in the course of solid-phase transitions. Model principles are given in the monograph [**13**].

Four types of the crystallographic quartz texture in natural rocks were determined using the quantitative texture analysis. For the first time, the method of preferred orientation description based on orientation distribution function (ODF) histograms and ODF-spectra has been used for estimating the expected degree of anisotropy of various physical properties (**Fig. 13**).

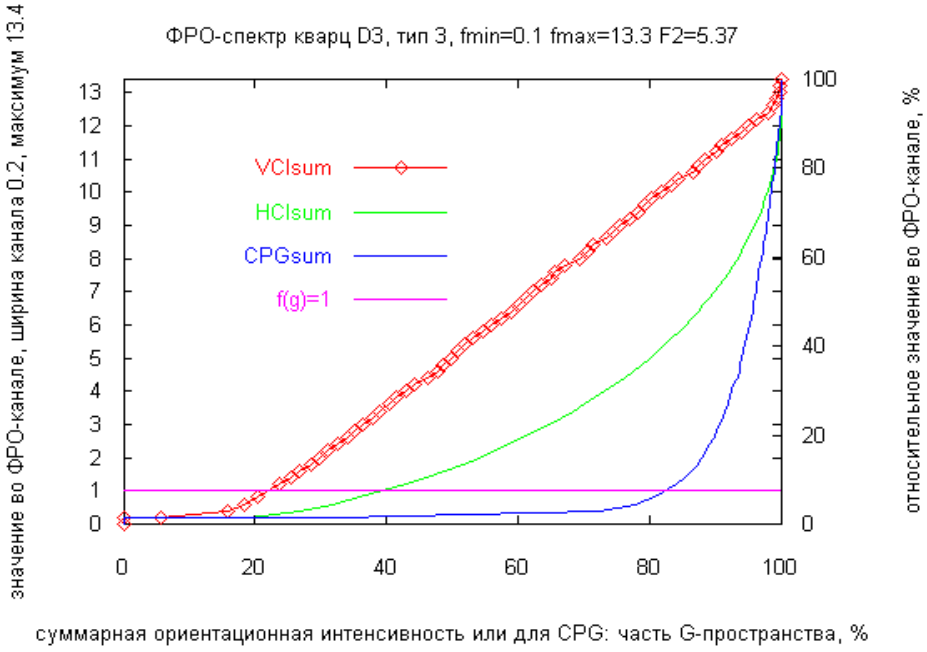

Fig. 13. Example of ODF-spectrum of crystalline quartz.

Complex investigations of biotite gneiss samples using neutron scattering and acoustic methods have been carried out. Some contradictions between the values of the elastic wave velocity found from the quantitative texture analysis data were revealed. The theoretical consideration [**14**] of the interaction of anisotropic (textured) medium with propagating elastic waves made it possible to establish several facts providing an explanation for the above-mentioned contradictions. In particular, it has been shown that in the case of one anisotropy vector one purely transverse wave and two waves with mixed longitudinal-transverse polarization can propagate in a textured medium. When there are two anisotropy vectors, in the general case all waves have mixed longitudinal-transverse polarization. In the general case the triple splitting of the refracted and reflected waves takes place during the reflection from the interface between media with different directions of anisotropy vectors and (or) parameters of anisotropy. In the general case the Snell law for the wave

reflection in anisotropic media does not hold. Longitudinal oscillations take place in various modes propagating with completely different velocities.

A rock type based on anhydride-dolomite minerals ("Zuckerdolomit") has been studied with respect to correlations of intracrystalline residual strain and texture. The rock samples were collected from the Piora Mulde deposit (Central Alps, Switzerland). The experiments were performed using neutron time-of-flight diffraction. The texture of the composite rock (dolomite, anhydride) is characterized by high sample symmetry (orthorhombic). As a rule, internal stresses in dolomite and anhydride have opposite signs corresponding to either compression or tension. Taking into account that the elastic constants for both minerals can differ much depending on the direction in crystal, one should expect the manifestation of a specific geomechanical behaviour of the studied rock determined by the interactions between texture, elasticity and internal stresses. The analysis has showed that the interaction of these factors results in brittle fracture of the rock if the elastic waves propagate in the directions close to foliation planes [**15**].

A series of studies on the martensitic transformation and fatigue properties of austenitic stainless steels widely used in industry due to their remarkable mechanical, welding and corrosion-resistant characteristics has been completed. The experimental simulation of fatigue degradation was performed using tension-compression cyclic loading in the plastic deformation region in the frequency range of 0.1-100 Hz. Regions of characteristic frequencies, which have widely different effects on steel, have been revealed. Formation mechanisms of the martensitic phase in an initially one-phase (austenitic) material have been determined. It has been shown that in some cases there is a large variance (**Fig. 14**) in elastic constants of phases constituting the material, which significantly influences its strength properties.

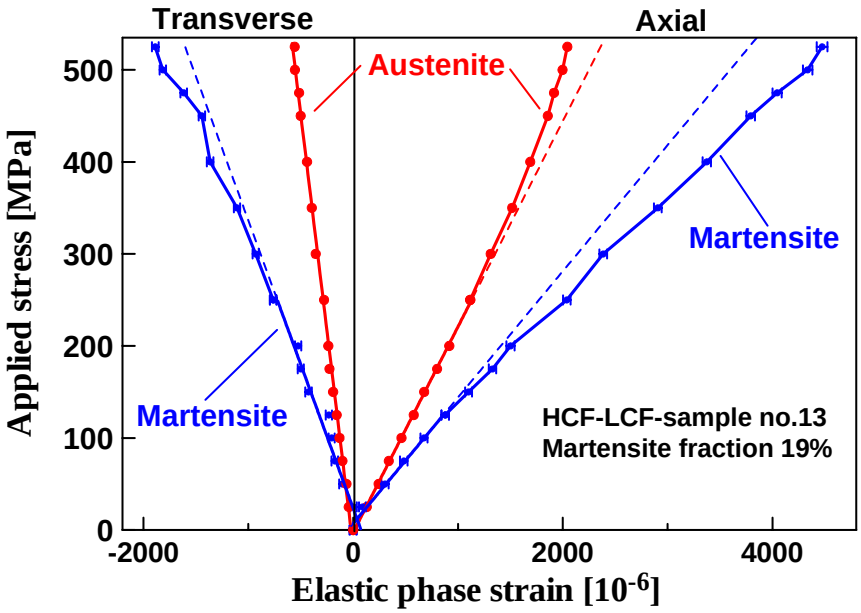

Fig. 14. Strain-stress relations in austenite (initially) stainless steel following high- and low-frequency fatigue loading for axial (right) and tangential (left) components.

II. Instrument developments

A start has been made on the manufacturing of the head part of the mirror vacuum neutron guide within the framework of realization of the project for construction of the DN-6 diffractometer for neutron diffraction studies of microsamples (beam 6b of IBR-2M).

First experiments have been carried out on the reflectometer of the Budapest Neutron Center to explore the possibility to develop next-generation neutron optical mirrors based on a special principle of strengthening of Bragg scattering for a specified value of the wave vector. This approach (developed in [**16**]) to the development of mirrors with high critical angle of total reflection is an alternative to the widely used technique of construction of such mirrors with aperiodic structure by magnetron sputtering. The reflectivity of new mirrors has been studied. The model description of the reflection curves for the systems under investigation has shown good agreement with the experimental data. The work has been performed in cooperation with the Research Institute for Solid State Physics and Optics of the Hungarian Academy of Sciences (Budapest, Hungary) and the MIRROTRON Company (Budapest, Hungary).

In 2008 the project on the new multifunctional reflectometer GRAINS at the IBR-2M reactor was continued. The set-up is intended for studies of various liquid-containing interfaces by means of neutron reflectometry (including polarized neutrons for investigations of interfaces with magnetic nanoparticles). The reflectometer will open up principally new possibilities for investigations in the field of nano-science at the IBR-2M reactor. Additional modes of the GRAINS reflectometer comprise: (1) off-specular scattering and GISANS, which are measured simultaneously in TOF regime with a 2D detector; (2) angular encoding in the horizontal plane, which is provided by a Larmor precession region limited by current sheets in front of the sample; (3) 3D polarimetry in reflection, which is provided by a Larmor precession region around the sample position. The manufacturing of the head part consisting of a two-beam splitting system has started. The collimating system of the reflectometer, which comprises a massive support for housing the setup units (collimating slits, deflecting mirrors) is under construction. A special guide-way allows moving the set-up elements along the beam. The whole construction is enclosed in the vacuum housing, where special entrances are organized for manual access to the elements of the collimating system without dismantling of the housing. The manufacturing of the elements of the collimating system including mirror deflectors (1 m long, supermirror, m=2) for non-polarized and polarized beams has started. The aim of these devices is to deflect the neutron beam towards the sample surface at a given incident angle in non-polarized and polarized modes, respectively. Such deflection makes it possible to regulate the incident angle on the sample surface and also to separate thermal and cold neutrons from fast ones, which pass through the mirrors without reflection, thus avoiding the direct view of the reactor zone and reducing the background. During the year the dismantling of channel 10 and making room for new equipment of the reflectometer was conducted. The work on the project was carried out in the frame of the JINR –BMBF (Germany) Agreement in cooperation with ILL (Grenoble, France), University of Halle, Technical University of Munich (Germany) and Petersburg Nuclear Physics Institute RAS (Gatchina, Russia).

The technical design of a mirror vacuum neutron guide for the DIN-2PI spectrometer has been completed and work to prepare an installation site for the neutron guide has been carried out. The work on the mirror vacuum neutron guide is conducted in cooperation with the user organizations: FLNP JINR and PNPI RAS (Gatchina). The mirror neutron guide being constructed will make it possible to increase the intensity of cold neutrons ($E < 5$ MeV) at the sample position by a factor of 4-6 and at the same time to reduce the sizes of samples under study by a factor of 2-3, which will mean significant improvement in quality of the DIN-2PI spectrometer and the upgrading of its parameters to the level of the best foreign analogues.

The technical design of a mirror vacuum neutron guide for beam 7a of the IBR-2M reactor to be constructed in accordance with the JINR-BMBF (Germany) Agreement has been completed. The realization of this project will make it possible to solve two main problems: increase in thermal neutron flux at the SKAT and EPSILON spectrometers and improvement in signal-to-background ratio for these spectrometers. In addition, within the framework of the project an additional chopper

to vary the used wavelength range (up to 14 Å) is to be installed. The new layout of the spectrometers is shown in **Fig. 15.**

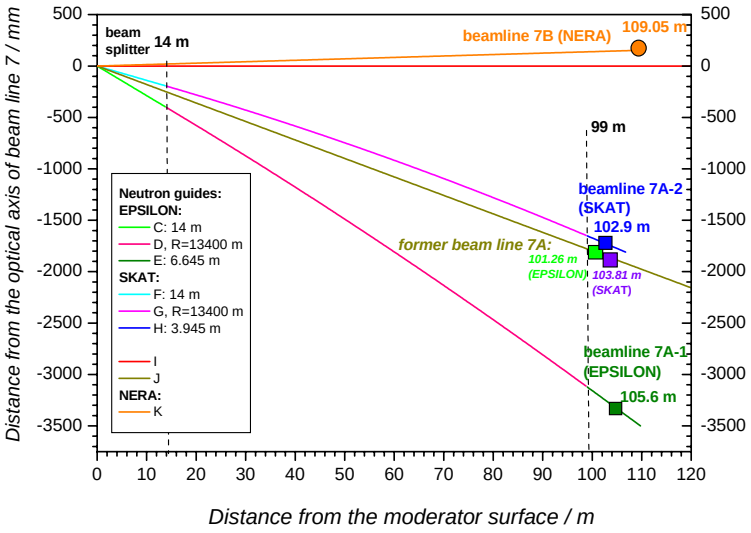

Fig. 15. The layout of neutron beams on channels 7A and 7B (NERA, SKAT, EPSILON spectrometers) with a new neutronguide system. The abscissa is the distance from the moderator surface in meters. The ordinate is the distance from the optical axis of beam line 7 in millimeters. A beam splitter is to be installed in the head part. After the 14-meter mark the beams are formed by separate neutronguides. For beam 7A the former neutronguide for the SKAT and EPSILON spectrometers at the IBR-2 reactor is shown.

The device for measuring low-temperature magnetoresistance at low temperatures has been constructed. The device is intended for prompt analysis of $La_{1-x}Sr_xMnO_3$ manganites, which are ferromagnetics with a “bad metal” behaviour. The manganites are synthesized using the zole-gel technology. Their magnetoresistance has been successfully measured in a magnetic field H_{max} = 1.2 T in the temperature range of 7 – 300 K.

1.1. ФИЗИКА КОНДЕНСИРОВАННЫХ СРЕД

Основные цели исследований по теме состояли в применении методов рассеяния нейтронов для изучения структуры и динамики конденсированных сред, получении новых данных о микроскопических свойствах конденсированных сред, экспериментальной проверке теоретических предсказаний и моделей, обнаружении новых закономерностей. В связи с остановкой в декабре 2006 г. реактора ИБР-2 на проведение очередного этапа реконструкции, задачи коллектива отдела и планы работ по теме в 2008 г. несколько отличались от традиционных. А именно, экспериментальная научная работа была перенесена в родственные центры в России и за рубежом. Из фундаментальных и прикладных направлений, разрабатываемых сотрудниками отдела НИКС ЛНФ, были оставлены несколько основных, работа по которым в других научных центрах, прежде всего нейтронных и синхротронных, была обеспечена существующими соглашениями о сотрудничестве. Продолжался первый этап программы модернизации спектрометров на реакторе ИБР-2. Работа по теме осуществлялась силами сотрудников Отдела нейтронных исследований конденсированных сред (НИКС) ЛНФ, структурно организованного в виде секторов (групп) по основным научным направлениям исследований.

В рамках исследований по теме сотрудники отдела НИКС поддерживали широкие связи со многими научными организациями в России и за рубежом. Как правило, сотрудничество оформлялось совместными протоколами или соглашениями. Особенно активное сотрудничество в России велось с близкими по тематике организациями, такими как РНЦ КИ, ПИЯФ, ИФТТ, ИФМ, ИК РАН и др.

Сотрудники отдела НИКС являются специалистами по проведению нейтронографических исследований конденсированных сред с помощью дифракции нейтронов на поли- и монокристаллах, малоуглового рассеяния нейтронов в веществах с крупномасштабными неоднородностями, неупругого ядерного и магнитного рассеяния нейтронов, отражения и рассеяния поляризованных нейтронов на границах раздела сред. Список основных научных тем, исследования по которым велись в рамках перечисленных методик, включает:

- атомная и магнитная структура сильно-коррелированных электронных систем – сложных магнитных оксидов, мультиферроиков и т.д.;
- структура и фазовые переходы в модельных и биологических мембранах;
- крупномасштабная структура некристаллических материалов: везикул, полимеров, дендримеров, коллоидных растворов, магнитных жидкостей и т.д.;
- надмолекулярная структура биологических объектов;
- свойства поверхности и наноструктур с пониженной размерностью;
- сосуществование магнетизма и сверхпроводимости в многослойных структурах;
- расплавы с динамической, структурной и композиционной неоднородностью;
- динамика водородсодержащих групп в органических соединениях;
- внутренние напряжения в материалах конструкционного назначения и горных породах;
- связь текстуры и свойств горных пород.

I. Научные результаты

1.1.1. Атомная и магнитная структура сложных магнитных оксидов

Атомная и магнитная структура серии твердых растворов $Pb_{2-x}Ba_xFe_2O_5$ с $x \approx 1$ изучена с помощью дифракции нейтронов и рентгеновских лучей, электронной микроскопии и мессбауэровской спектроскопии. Эти составы относятся к типу анион-дефицитных перовскитов, которые интересны сосуществованием магнитных и сегнетоэлектрических свойств. Соединения с такого рода сосуществованием в настоящее время принято называть мультиферроиками. В дифракционных экспериментах обнаружены две структурные фазы (высоко- и низкотемпературная) с переходом между ними при $T_c \approx 540$ K. Фазы различаются конфигурацией двух зеркально-связанных цепочек тригональных FeO_5 бипирамид, которые упорядочиваются ниже T_c. Из нейтронных дифракционных данных следует, что ниже T_N = 625 K в $Pb_{1.08}Ba_{0.92}Fe_2O_5$ возникает антиферромагнитный (AFM) порядок с вектором распространения **k** = [0,½,½] (**рис. 1**). В то же время было обнаружено, что магнитное расщепление мессбауэровских спектров возникает только при температуре ниже 520 K. Столь большая разница в температурах магнитного упорядочения, измеренных разными методами, была объяснена специфическим характером динамики спинов, возникающем вследствие существенно разного сверхобменного взаимодействия между магнитными моментами атомов железа, находящихся в FeO_6 октаэдрах и в FeO_5 тригональных бипирамидах [**1**]. При высоких температурах время релаксации спинов оказывается существенно меньше, чем временная шкала эффекта Мессбауэра для ^{57}Fe. Работа выполнена совместно с Лабораторией неорганической кристаллохимии (Химфак МГУ) и Лабораторией рассеяния нейтронов (PSI, Швейцария).

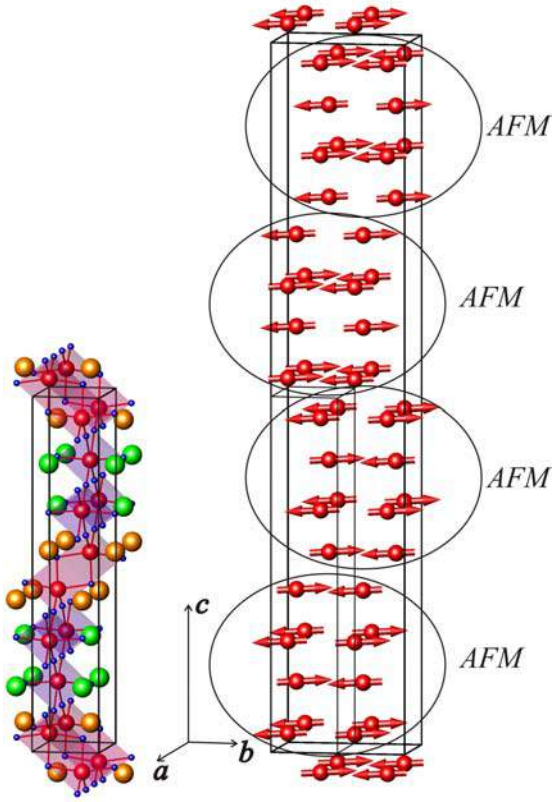

Рис. 1. Иллюстрация антиферромагнитного упорядочения моментов атомов железа в структуре $Pb_{1.08}Ba_{0.92}Fe_2O_5$ (справа). Элементарная ячейка кристаллической структуры низкотемпературной фазы соединения показана слева в той же шкале (атомы Fe изображены красными шарами).

Завершено детальное нейтронное дифракционное исследование атомной и магнитной структуры 314-кобальтитов $Sr_3YCo_4O_{10.5+\delta}$ (или $Sr_{0.75}R_{0.25}CoO_{2.625+\delta/4}$), в которых A-позиции являются идеально упорядоченными. В составах с разным содержанием кислорода (близким к оптимальному, $\delta \approx 0$ и увеличенным, $\delta \approx 0.26$) установлен G-тип AFM структуры, с моментами, направленными вдоль *c*-оси тетрагональной ячейки [**2**]. В отличие от ранних исследований подобных структур было найдено, что атомы Co, находящиеся в различных позициях элементарной ячейки, имеют различную величину магнитного момента, которая коррелирует с кислородным окружением атома. Таким образом, впервые для кобальтитов установлена прямая связь между зарядовым и спиновым состояниями атомов Co (**рис. 2**). Работа выполнена совместно с Лабораторией неорганической кристаллохимии (Химфак МГУ) и Лабораторией рассеяния нейтронов (PSI, Швейцария).

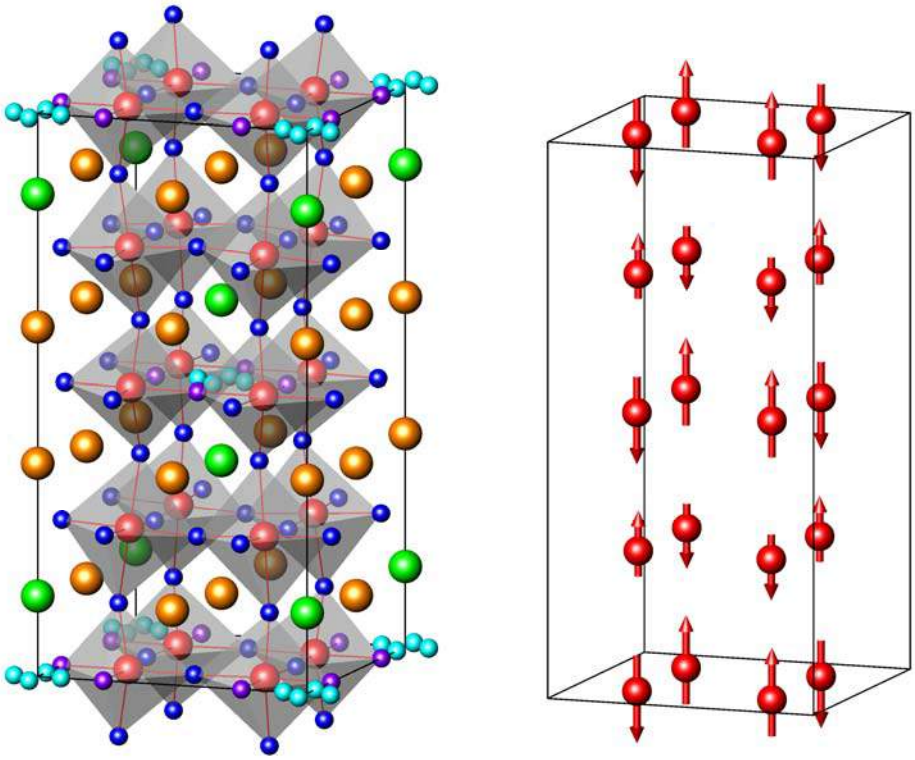

Рис. 2. Кристаллическая (слева) и магнитная (справа) структуры состава $Sr_3YCo_4O_{10.5}$. Большими шарами показаны атомы Y (зеленые), Sr (золотистые) и Co (в центре кислородных октаэдров). Атомы кислорода (малые шары) занимают заполненные (синие), частично заполненные (фиолетовые) и разупорядоченные (светло синие) позиции. Магнитный момент Co в слоях с заполненными кислородными позициями ($z \approx 0.25$ и $z \approx 0.75$) составляет около 1.5 μ_B, тогда как в слоях с $z = 0$ и $z = 1/2$ $\mu_{Co} \approx 2.8$ μ_B.

Продолжались исследования влияния высокого давления на кристаллическую и магнитную структуры сложных магнитных оксидов переходных металлов. В экспериментах с гексагональным фрустрированным манганитом $YMnO_3$, проявляющим свойства мультиферроика, обнаружено значительное усиление диффузного магнитного рассеяния и резкое подавление интенсивности магнитных рефлексов при повышении давления в области низких температур (**рис. 3**). Интерпретация этого явления основана на предположении о стабилизации под давлением состояния магнитной жидкости с сильными спиновыми флуктуациями [**3**].

В составе $La_{0.33}Ca_{0.67}MnO_3$, исследованном в диапазоне температур 10 – 300 K и давлений 0 – 5 ГПа, обнаружено, что под давлением исходное антиферромагнитное

состояние типа вигнеровского кристалла подавляется и происходит стабилизация антиферромагнитного состояния C-типа [**4**].

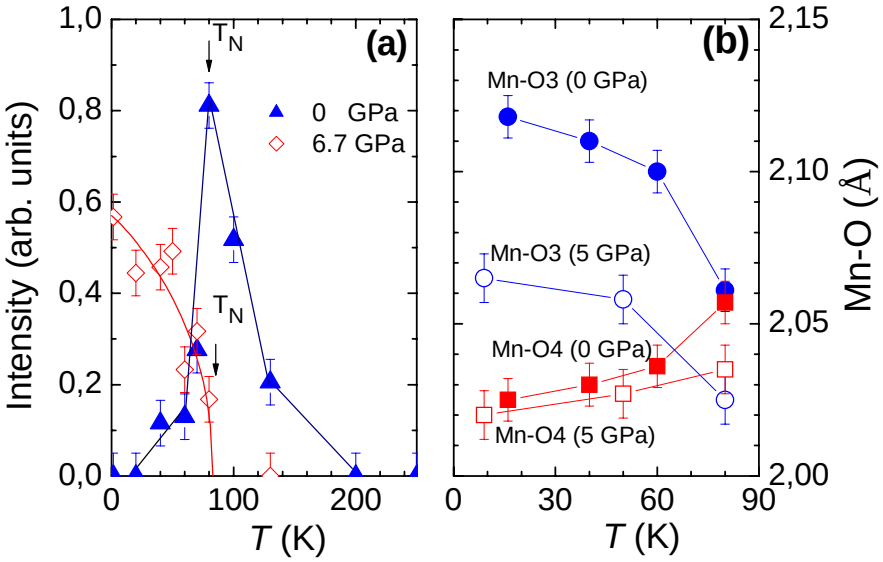

Рис. 3. Температурная зависимость магнитного диффузного рассеяния в $YMnO_3$ при различных давлениях (слева). Увеличение его интенсивности при высоком давлении и низких температурах связано с возникновением состояния спиновой жидкости с сильными флуктуациями, обусловленного симметризацией треугольной магнитной решетки, сформированной межатомными связями Mn-O3 и Mn-O4 (их зависимости от температуры и давления показаны справа).

1.1.2. Исследования модельных и биологических мембран

Впервые получена информация о структурной организации липидных мембран, построенных на основе фосфолипидов актинобактерий *S. Hygroscopicus*. Липидная фракция, выделенная из этих бактерий образует на кварцевых подложках многослойную мембранную структуру с периодом повторяемости d_0 = 85.8 ± 0.5 Å и d_0 = 83.5 ± 0.5 Å при внешних условия среды T = 20°C, RH = 97% и T = 40°C, RH = 96% соответственно. При этом часть липидов не входит в состав бислоя и образует жидкую мицеллярную фазу с размерами мицелл 54.2 ± 0.2 Å. Эти результаты доказывают жидкокристалическую структуру мембран, построенных из выделенных фосфолипидов актинобактерий. Жидкокристаллическая структура таких мембран позволяет применить методы дифракции рентгеновских лучей для исследования изменений ламеллярной и латеральной структуры при охлаждении многослойных мембран в избытке водных растворов криопротекторов. Будущие исследования процессов изменения структуры при охлаждении мембран до азотных температур с последующим нагревом позволят более эффективно подбирать криопротекторы для хранения бактерий.

Дифракция нейтронов применена для исследования структурной организации липидных мультислойных мембран на основе церамида 6 и смеси шести жирных кислот. Этот состав моделирует структуру верхнего слоя кожи млекопитающих stratum corneum (SC). Были использованы наиболее распространенные в липидной матрице SC пальмитиновая (C16:0), стеариновая (C18:0), арахиновая (C20:0), бегеновая (C22:0), лигноцериновая (C24:0) и церотиновая (C26:0) кислоты в мольном соотношении 1.3/3.3/6.7/41.7/36/6.7. Для этого состава определено влияние сульфата холестерина на процесс гидратации и структуру полностью гидратированной мембраны в экспериментах по исследованию кинетики набухания мембраны в избытке воды при 20°C. Пример измеренных

зависимостей для периода повторяемости мембран показан на **рис. 4**. Установлено, что мембраны на основе смеси жирных кислот имеют структуру, схожую со структурой модельной мембраны SC на основе пальмитиновой кислоты. Кроме того, оказалось, что использованная композиция жирных кислот ускоряет время гидратации мембраны в полтора раза.

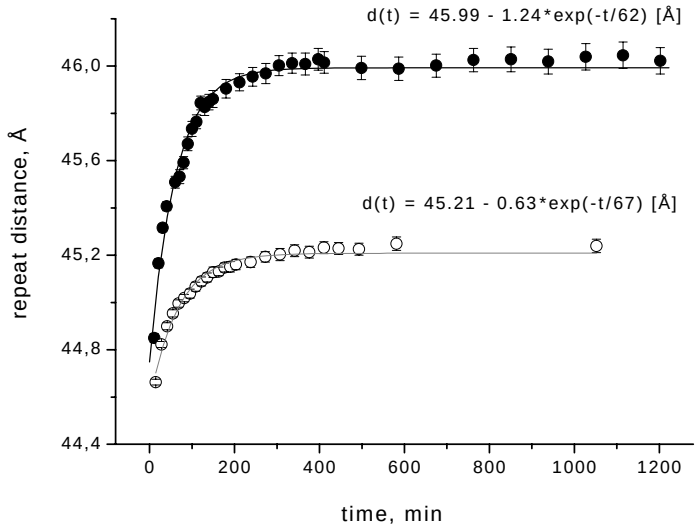

Рис. 4. Изменение во времени периода повторяемости мембран основе церамида 6 и смеси шести жирных кислот с двумя различными весовыми соотношениями компонент в процессе гидратации в тяжелой воде при 20^{o}C. Сплошные линии проведены в соответствии с экспоненциальной зависимостью периода от времени.

1.1.3. Наноструктурированные материалы

Исследована структура слабоконцентрированных (объемная доля магнитного диспергированного материала порядка 1%) магнитных жидкостей (наночастицы магнетита в декагидронафталене), стабилизированных с помощью насыщенных моно-карбоксильных кислот разной длины (лауриновая, миристиновая, пальмитиновая и стеариновая кислоты) [**5**]. Использован анализ намагниченности, электронная микроскопия и малоугловое рассеяние неполяризованных нейтронов (**Рис. 5**). Проведено сравнение с классической магнитной жидкостью, стабилизированной ненасыщенной олеиновой кислотой. Показано, что в отличие от олеиновой кислоты насыщенные кислоты стабилизируют магнетит меньшего размера и с меньшей полидисперсностью. Для изученных насыщенных кислот средние значения размера и индексы полидисперсности соответствуют приблизительно одной функции распределения по размерам (**Рис. 5*a***). На основе сравнения кривых малоуглового рассеяния неполяризованных нейтронов (**Рис. 5*b***) определена эффективная толщина стабилизирующей оболочки вокруг магнетита, которая коррелирует с длиной используемой кислоты. Таким образом, сделан вывод о том, что существенный вклад в стабилизационные свойства оболочки вносит ее упругость, которая приблизительно одинакова для насыщенных кислот, но сильно отличается от таковой для олеиновой кислоты. Работа выполнена совместно с Исследовательским центром фундаментальных и прикладных исследований Румынской Академии наук (Отделение Тимишоары, Румыния), Будапештским нейтронным центром (Венгрия) и Исследовательским центром Геестхахта ГКСС (Германия).

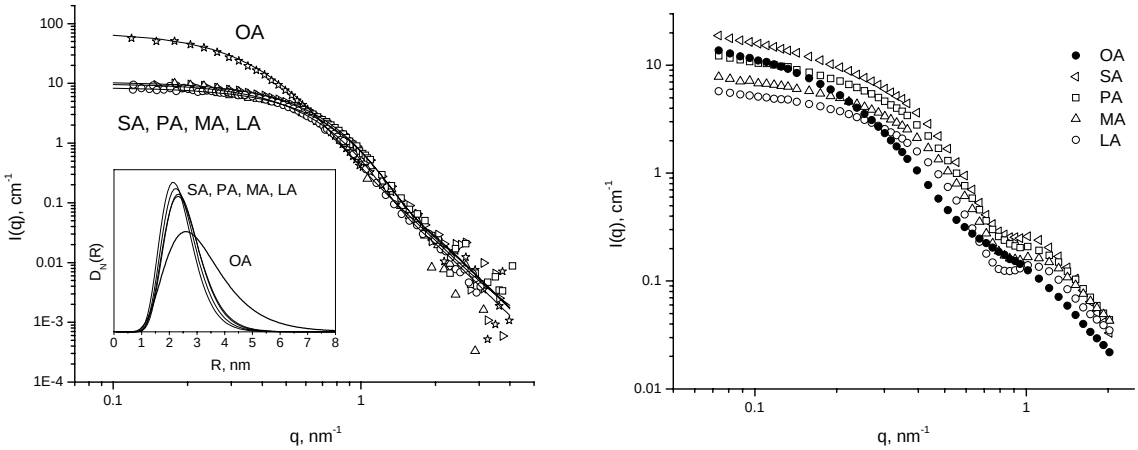

(*a*) (*b*)

Рис. 5. Исследование с использованием малоуглового рассеяния нейтронов структурных различий неполярных органических магнитных жидкостей (магнетит в декагидронафталене), стабилизированных одиночным слоем моно-карбоксильных кислот различной длины и насыщенности: олеиновая (OA), стеариновая (SA), пальмитиновая (PA), миристиновая (MA) и лауриновая (LA) кислоты. (*a*) Экспериментальные кривые рассеяния для обычного (недейтерированного) носителя. Из-за малого контраста между жидким носителем и стабилизирующей оболочкой, рассеяние преимущественно имеет место только на магнитных наночастицах. Вставка показывает восстановленные функции распределения по радиусу частиц. (*b*) Экспериментальные кривые рассеяния для носителя с 90% содержанием дейтерированного аналога. Для насыщенных кислот (SA, PA, MA, LA) заметна модуляция рассеяния от кислоты, свидетельствующая о корреляции между толщиной оболочки и длиной кислоты. При этом, как видно из (*a*), функции распределения по радиусу для магнитных наночастиц, стабилизированных насыщенными кислотами, очень близки и заметно отличаются от таковой для ненасыщенной кислоты OA.

В рамках проекта РФФИ – Сообщество Гельмгольца (Германия) продолжались эксперименты по изучению структуры слабо концентрированных (с 1% объемной долей магнитного материала) магнитных жидкостей, стабилизированных с помощью насыщенных моно-карбоксильных кислот разной длины. Проведен поиск подходящего источника магнитных наночастиц среди водных магнитных жидкостей со стерической стабилизацией на основе двойного покрытия магнетита различными поверхностно-активными веществами (ПАВ), включая лимонную (CA+CA), олеиновую (OA+OA), миристиновую (MA+MA) и лауриновую кислоты (LA+LA). Структурный анализ, включающий в себя эксперименты по намагниченности, просвечивающей электронной микроскопии и малоугловому рассеянию нейтронов, показал, что часть наночастиц магнетита (размер около 7 нм, полидисперсность 40%) в исследуемых системах образует стабильные агрегаты со средним размером до 40 нм в зависимости от типа оболочки ПАВ. Магнитные жидкости добавлялись в среду, в которой инкубировались клетки рака мозга различных серий. Проникновение наночастиц в клетки было определено через магнитную сепарацию клеток, атомную абсорбционную спектроскопию, флюоресценцию и оптическим анализом с использованием красителя. Обнаружено, что клеточная токсичность исследуемых наночастиц различна для разных стабилизирующих слоев ПАВ. Показано, что предпочтительным источником магнитных наночастиц является магнитная жидкость со стабилизацией LA+LA. С точки зрения структурных особенностей она обладала наименьшей агрегацией (**рис. 6**), что объясняет лучшее проникновение магнитных наночастиц в клетки и может являться причиной наименьшей токсичности для клеток.

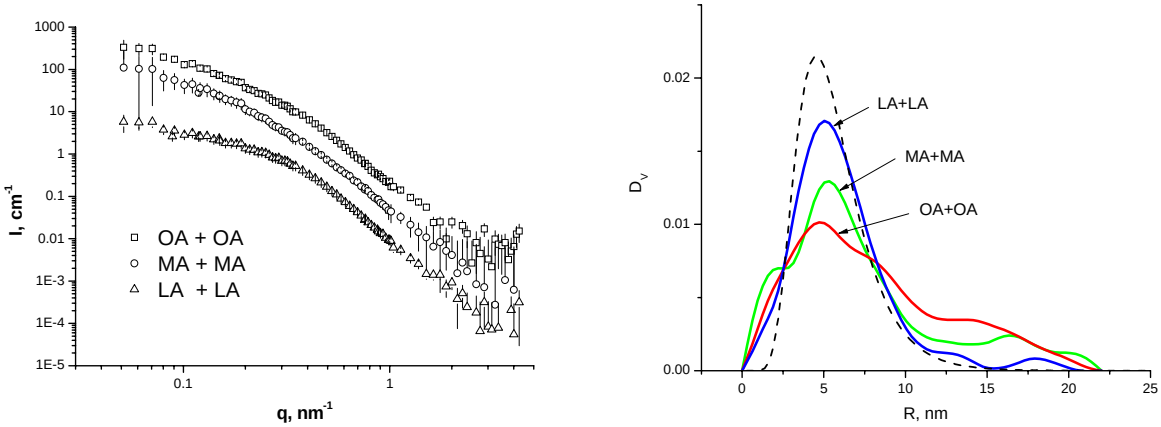

(*a*) (*b*)

Рис. 6. Малоугловое рассеяние нейтронов на магнитных наночастицах, диспергированных в воду и стабилизированных двойными слоями монокарбоксильных кислот разной длины и насыщенности: олеиновой (OA+OA), миристиновой (MA+MA) и лауриновой (LA+LA). (*a*) Экспериментальные кривые рассеяния. (*b*) Восстановленные функции распределения по объему для магнитных частиц. Штриховой линией показан расчет для отдельных частиц согласно данным электронной микроскопии.

В рамках теории нуклеации по аналогии со слабополярными растворителями рассмотрен [**6**] процесс кластерообразования фуллерена C_{60} в азот-содержащем растворителе NMP (растворитель средней полярности). Показано, что, как и в случае слабополярных растворителей, для объяснения стабилизации размера кластеров в NMP требуется привлечение модели ограниченного роста, отвечающей формированию эффективной стабилизирующей оболочки вокруг кластеров. Наиболее вероятным механизмом формирования такой оболочки видится образование донорно-акцепторных комплексов C_{60}/NMP, которое постепенно ограничивает рост кластеров. Рассмотрена также реорганизация кластеров фуллерена при добавлении воды в раствор C_{60}/NMP, которая, в частности, проявляется в резком увеличении интенсивности малоуглового рассеяния нейтронов для размеров порядка 10 нм. Показано, что критические изменения в растворе, наблюдаемые экспериментально при добавлении к нему воды, не могут быть описаны изменением концентрации и термодинамических характеристик системы. Работа выполнена совместно с Российским научным центром «Курчатовский институт» (Москва, Россия), Киевским национальный университетом им. Тараса Шевченко, Институтом химии поверхности им. А.А.Чуйко НАН Украины (Киев, Украина), Московским государственным университетом им. М.В.Ломоносова (Москва, Россия), Исследовательским институтом физики твердого тела и оптики Венгерской Академии (Будапешт, Венгрия).

Растворы феррожидкостей на основе Fe_3O_4 исследованы методом μSR-спектроскопии. Эксперименты проведены на пучке поляризованных положительных мюонов, на синхротроне с ориентацией внешнего магнитного поля в поперечном направлении к ориентации спина мюона. Эксперименты сделаны при температуре от 26 до 300 К. Обнаружено, что диамагнитная компонента существует в феррожидкости в том же количестве, как и в тяжелой воде, но релаксация спина мюона в феррожидкости протекает быстрее, чем в D_2O. Наблюдалось также существенное смещение частоты прецессии спина в феррожидкости. Показано что смещение частоты прецессии мюона как функция внешнего магнитного поля описывается функцией Ланжевена типичной для парамагнитных систем. Оценен средний радиус наночастиц (<D> = 12 nm) [**7**].

Совместно с Институтом синтетических полимерных материалов имени Н.С.Ениколопова проведены исследования нового класса полимеров, получаемых в результате регулируемого синтеза - дендримеров. По экспериментальным данным МУРН восстановлено пространственное распределение рассеивающей плотности исследуемого типа дендримеров (**рис. 7**). Методом вариации контраста доказано, что молекулы дендримеров в растворах не содержат закрытых внутренних полостей, не доступных растворителю. Определен парциальный объем дендримера в растворе. Показано гомогенное распределение рассеивающей плотности. Получено, что дендримеры 9-ой генерации монодисперсны в пределах экспериментальной ошибки. Получены экспериментальные доказательства того, что распределение плотности длины рассеяния внутри дендримера гомогенно. Показано, что простой моделью роста дендримерных ветвей невозможно объяснить анизометрию и пространственную неоднородность дендримера [**8**].

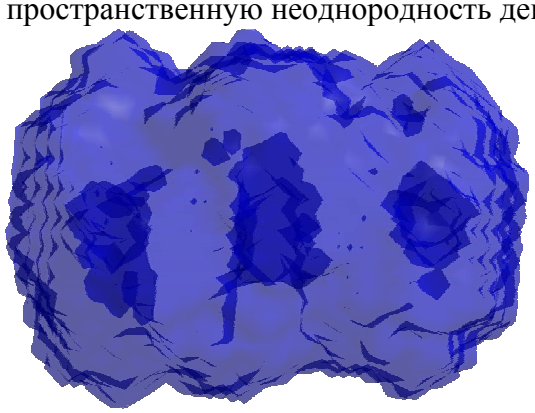

Рис. 7. Пространственное распределение рассеивающей плотности в дендримере, полученное из данных малоуглового рассеяния.

Методами малоуглового рассеяния нейтронов и рентгеновских лучей проведено исследование магнитных эластомеров – композитных материалов из полимерной матрицы и высокодисперсных магнитных частиц. Обнаружено, что полимерная матрица фрагментирована и имеет нанофазный характер, при этом геометрические размеры нанофазных областей зависит от концентрации внедренных магнитных частиц и величины магнитного поля, прилагаемого в процессе синтеза материала.

1.1.4. Физика тонких пленок

В рамках темы сосуществования ферромагнетизма (FM) и сверхпроводимости (S) в тонких мультислоях завершена обработка данных и интерпретация результатов, полученных на тройной системе (S)/(FM)/(S), а именно, (Nb)/(Fe)/(Si, Mo) на подложке из кремния. Теоретический анализ показал, что благодаря эффектам близости между (S) и (FM) слоями возможны различные сценарии их взаимодействия: формирование доменной структуры, «перетекание» намагниченности от (FM) к (S) слою, изменение прямого и косвенного обменного взаимодействия (FM) слоёв. Практическая важность изучения таких систем связана с перспективой создания устройств записи информации одновременно по электрическому и магнитному каналам. Измерения проведены в магнитном поле напряжённостью 500 Э и в диапазоне температуры 2 – 60 К. Впервые одновременно наблюдены перестройка доменной структуры и понижение намагниченности насыщения в доменах при переходе слоя Nb(500 Å) и структуры [Si(34 Å)/Mo(34 Å)] в сверхпроводящее состояние (**рис. 8**). Впервые прямо показано, что в тройной системе (S)/(FM)/(S) при переходе слоёв в сверхпроводящее состояние происходит уменьшение величины обменного взаимодействия в ферромагнитном слое [**9**].

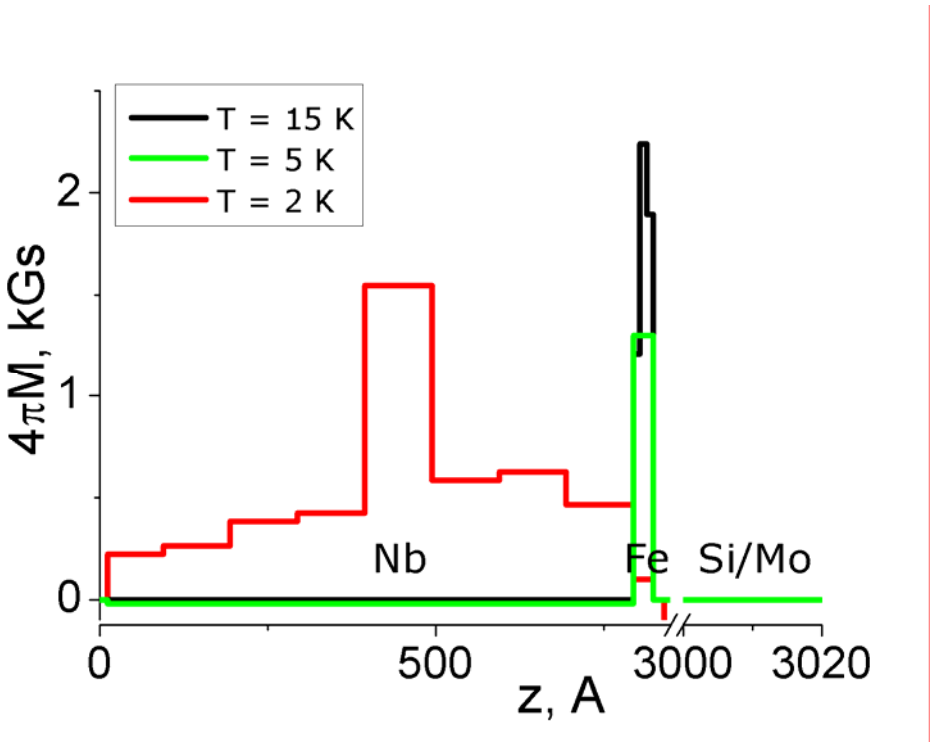

Рис. 8. Профиль намагниченности в мультислоях Nb/Fe/[Si/Mo] при 15, 5 и 2 К в магнитном поле 500 Э. При понижении температуры и переходе слоёв сверхпроводников (Nb) и (Si/Mo) в сверхпроводящее состояние происходит уменьшение величины средней намагниченности в ферромагнитном слое железа.

1.1.5. Атомная динамика

Изучены изомеры диметил-бутанола $C_6H_{13}OH$, (2,2DM-1B, 3,3DM-1B, 2,3DM-2B и 3,3DM-2B), состоящие из глобулярных молекул, которые в твердом состоянии образуют ориентационно неупорядоченные кристаллические фазы. Калориметрические исследования полиморфизма этих соединении выявили значительные различии температур плавления, а также кинетики и числа фазовых превращений, наблюдаемых при охлаждении и нагреве. Одновременные исследования дифракции и неупругого некогерентного рассеяния нейтронов (HHPH) позволили идентифицировать стеклообразные и кристаллические фазы, которые могут сосуществовать при низких температурах [**10**]. Предварительная интерпретация спектров HHPH основана на квантово-химических расчетах динамики изолированных молекул, с применением базиса B3LYP/6-311G** в теории функционала электронной плотности (DFT). Расчетные спектры плотности колебательных состояний для изолированных молекул, $G_{cal}(\nu)$, имеют качественное согласие с экспериментальными спектрами, $G_{exp}(\nu)$, но не удовлетворительно определяют частоты колебании характерные для водородных связей [**11**]. Компьютерное моделирование структуры и динамики молекулярных кластеров изомеров диметил-бутанола (DMB) позволило определить длины и характерные частоты колебаний водородных связей в зависимости от количества молекул и структуры кластеров. Сравнение расчетных и экспериментальных спектров плотности колебательных состоянии полученных для изомера 2,2DM-1B представлено на **рис. 9**. Образование водородных связей приводит к существенным сдвигам частот колебаний гидроксильных групп OH изолированных молекул. Частоты вне-плоскостных колебаний водорода, γ(C-O-H), увеличиваются примерно в два раза (100%). Частоты колебаний в плоскости связи, δ(C-O-H), увеличиваются примерно на 30%, тогда как частоты растяжения

связи, ν(O-H), уменьшаются примерно на 10%. Спектры $G_{cal}(\nu)$, полученные для циклических тетрамеров молекул DMB, достаточны для удовлетворительной интерпретации колебательных полос наблюдаемых в спектрах HHPH и инфракрасного поглощения (ИК). Средняя длина водородных связей для расчетных структур циклических тетрамеров DMB, хорошо совпадает с оценкой длин водородной связи по частотам моды ν(O-H), определенным из спектров ИК. Все компьютерные расчеты проведены в Суперкомпьютерном центре (PCSS) в Познани.

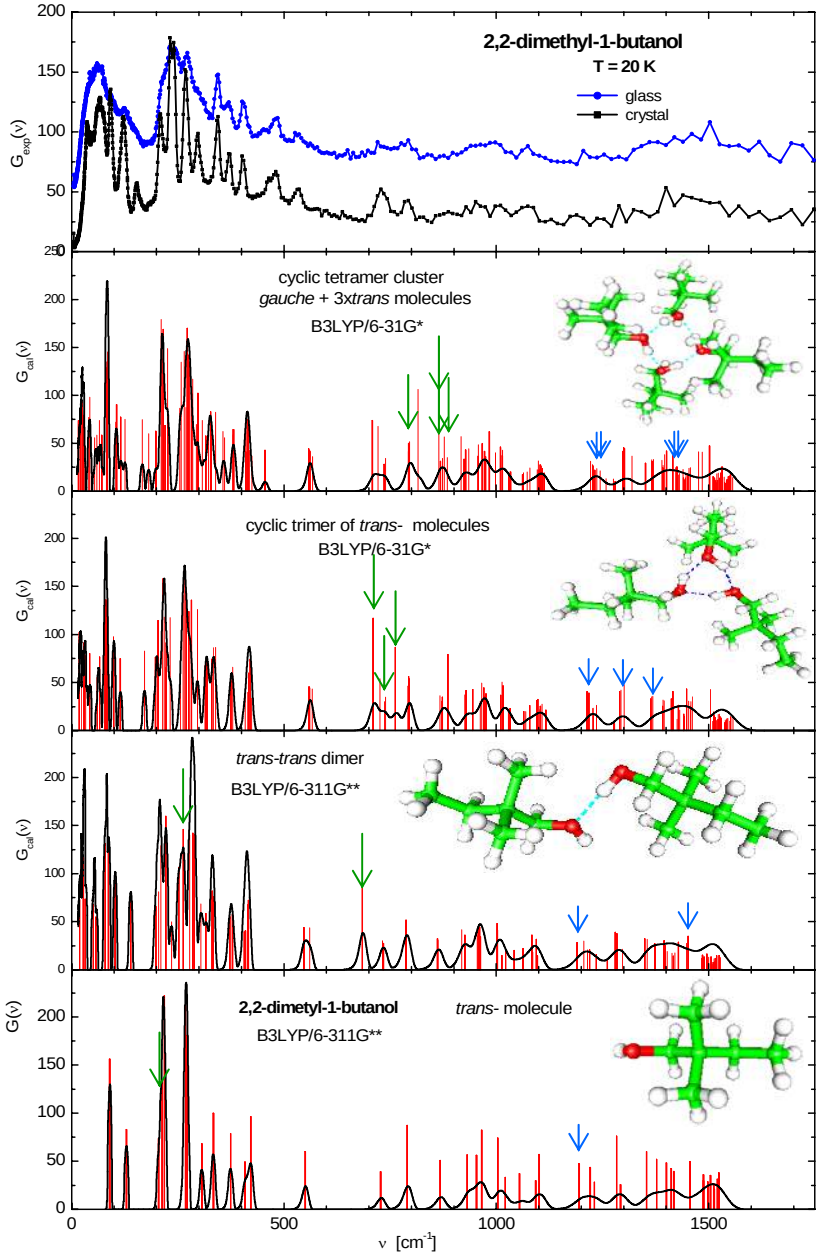

Рис. 9. Пример сравнения экспериментальных и расчетных спектров HHPH для 2,2-диметил-1-бутанола.

Проведен подробный анализ экспериментальных данных по квазиупругому рассеянию нейтронов водной дисперсией наноалмазов (концентрация частиц ~ 80 мг/мл, средний размер частиц ~ 8 нм, температура раствора ~12°C). Анализ данных велся с использованием модели, согласно которой вода, входящая в состав дисперсии,

предполагалась двухкомпонентной системой, включающей в себя обычную (объемную) воду и воду, непосредственно примыкающую к поверхности наночастицы и испытывающую ее влияние на свои структурно-динамические свойства (далее, гидратационная вода). Относительная доля этой воды была оценена как ~3%, что соответствует примерно двум – трем слоям молекул воды, примыкающим к поверхности наночастицы. Анализ диффузионных процессов в обеих водных компонентах велся на основе метода «stretched exponent», позволяющего оценить эффекты α-релаксации (диффузионные процессы, приводящие к разрушению ближайшего окружения молекулы) в обеих водных компонентах. Было установлено, что имеет место явное замедление диффузионной подвижности молекул гидратационной воды по сравнению с объемной (**рис. 10**). Интенсивность диффузионных процессов в гидратационной воде оказалась близка к параметрам диффузии переохлажденной воды с температурой -(15–20)°C.

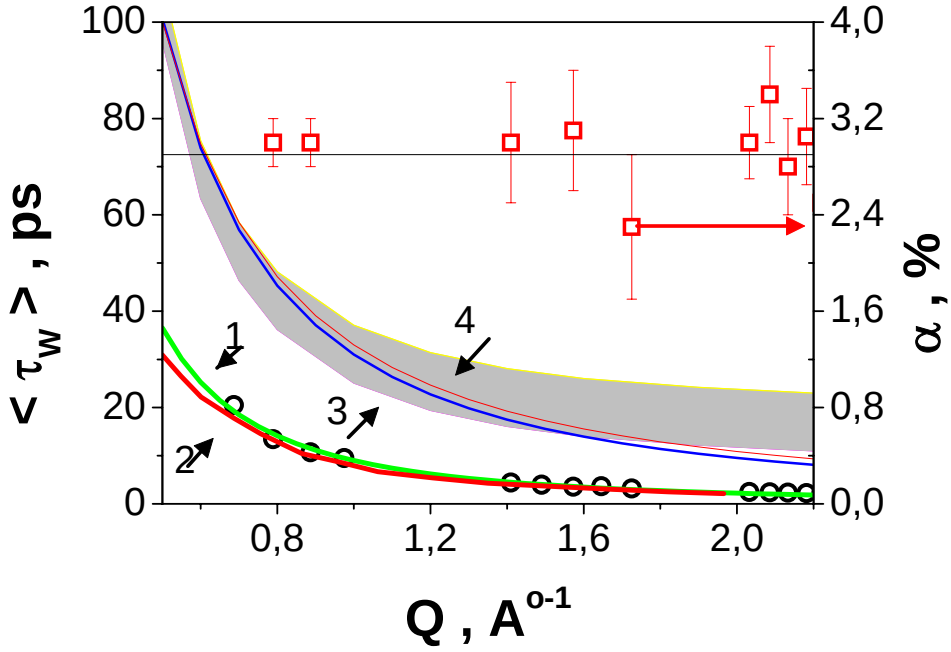

Рис. 10. Зависимость среднего времени α – релаксации $<\tau_W>$ в объемной и гидратационной воде от передачи волнового вектора нейтрона Q. Правая ось ординат: относительная доля гидратационной воды - $< \alpha > = (2.9 \pm 0.3)\%$. Обозначены кривые 1 – 4, где 1 - объемная вода ($<\tau_W>(Q) = 9.0*Q^{-2.02}$), 2 - МД данные для T = 11°C, 3 - гидратационная вода ($<\tau_W>(Q) = 31*Q^{-1.7}$ и $\gamma = 1.7 \pm 0.1$, получены в области 0.5 $A^{-1} < Q < 1.4$ A^{-1}), 4 - $<\tau_W>$ в переохлажденной воде, МД данные для T = - 20°C.

На спектрометре ДИН-2ПИ методом неупругого рассеяния медленных нейтронов исследованы коллективные моды в жидком литии [**12**]. Измерения проведены при температуре 500 К ($T_{пл}$(Li) = 453.7 К). Из экспериментальных спектров выделена и проанализирована составляющая когерентного рассеяния. Получен участок дисперсионной кривой коллективных атомных возбуждений для расплава лития, который в пределах ошибок эксперимента согласуется с результатами других авторов. На **рис. 11** в приведенных единицах показана обобщенная дисперсионная кривая для жидких щелочных металлов из экспериментальных работ. Видно, что результат для лития не противоречит общей картине. Вся совокупность точек образует единую дисперсионную кривую, что подтверждает вывод о микродинамическом подобии жидких щелочных металлов.

Измерены спектры неупругого рассеяния нейтронов для нитрида урана UN в интервале температур от комнатной до 1273 К. Нитрид урана рассматривается как базовый материал для создания комбинированного топлива реакторов на быстрых нейтронах, с

которыми связывается перспектива развития крупномасштабной ядерной энергетики. На **рис. 12** приведены функции плотности фононных состояний UN для нескольких температур, восстановленные из экспериментальных спектров. Нитрид урана обладает заметным магнитным рассеянием, вклад которого не учитывался при обработке экспериментальных спектров, поэтому эти данные носят предварительный характер.

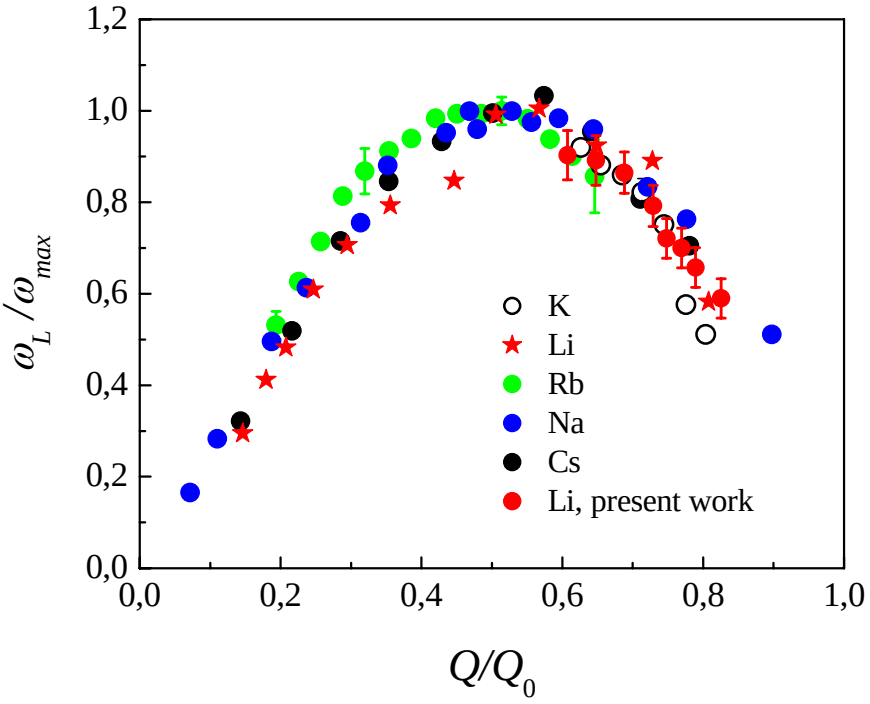

Рис. 11. Обобщенная дисперсионная зависимость для жидких щелочных металлов в приведенных координатах.

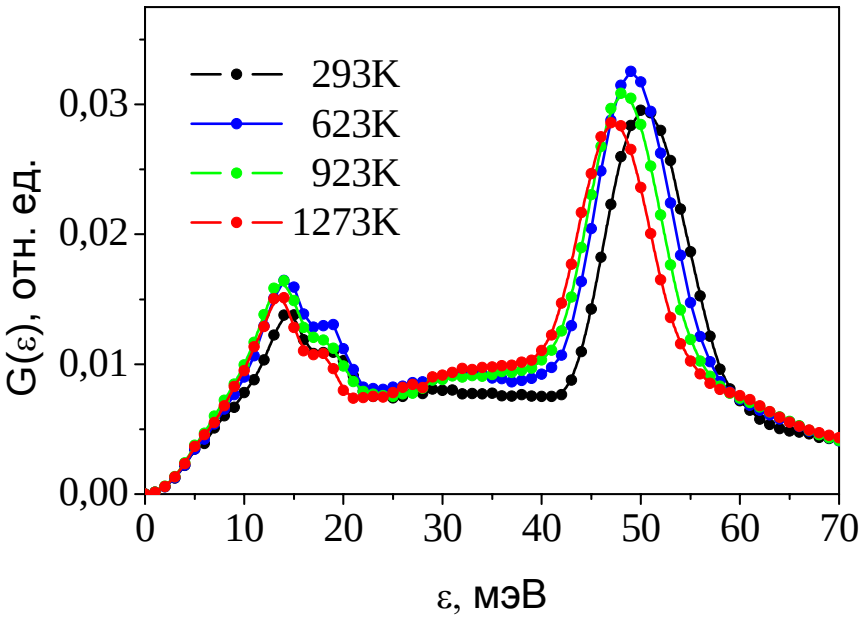

Рис. 12. Функции плотности фононных состояний UN при температурах 293 – 1273 К. Наблюдаются две области колебаний с максимумами при передачах энергии ε ~ 14 мэВ и ~50 мэВ. Первая (акустическая) отвечает колебаниям тяжелых атомов урана, вторая (оптическая) – легких атомов азота. С ростом температуры происходит смягчение спектра колебаний за счет сдвига оптической части в область меньших энергий и трансформации акустической части спектра.

1.1.6. Прикладные работы

К прикладным работам в отделе НИКС ЛНФ традиционно относятся экспериментальные исследования текстуры горных пород и минералов, внутренних напряжений в них и определение внутренних напряжений в объемных материалах и изделиях, включая инженерные материалы и детали машин и устройств. В основном, эти исследования ведутся с помощью дифракции нейтронов.

На основе результатов комплексных нейтронных и акустических экспериментов образцов монокристаллического и поликристаллического кварца в области полиморфного α-β перехода обоснована флюидометаморфогенная (ФМ) модель сейсмотектогенеза. В такой модели причиной разрушения при сейсмическом процессе является рост величины микронапряжений и уменьшение прочности твердых тел в ходе твердофазных превращений. Формулировка модели приведена в монографии [**13**].

С использованием метода количественного текстурного анализа установлены основные четыре типа кристаллографических текстур кварца в природных горных породах. Для оценки ожидаемой степени анизотропии различных физических свойств впервые использован метод описания преимущественной ориентировки с помощью построения гистограмм для функции распределения ориентаций (ФРО) и ФРО-спектров (**рис. 13**).

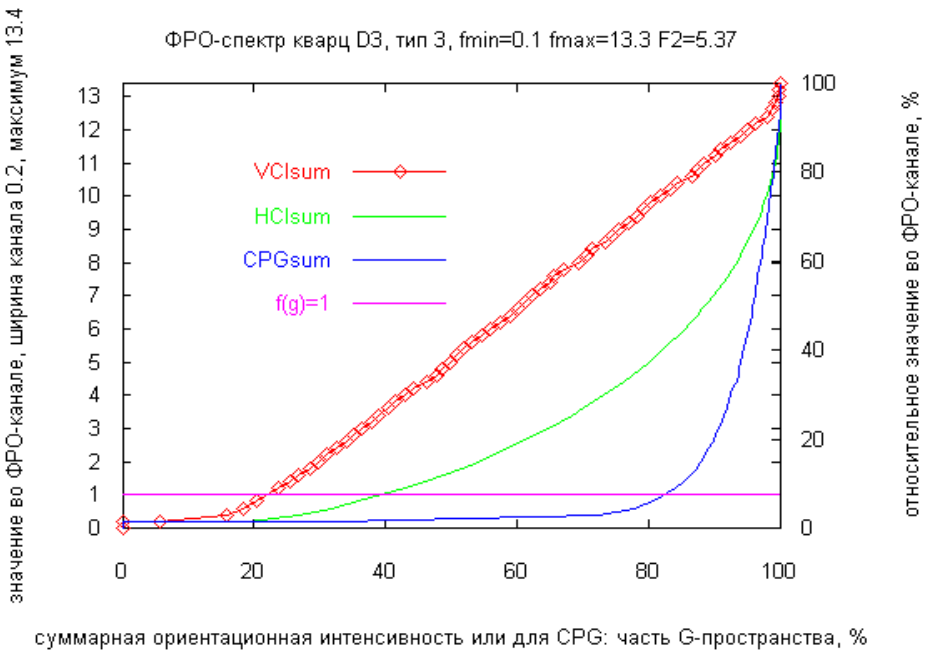

Рис. 13. Пример ФРО-спектра кристаллического кварца.

Проведены комплексные нейтронографические и акустические исследования образцов биотитовых гнейсов, которые выявили противоречия между значениями скоростей упругих волн, измеренных и реконструированных на основе данных количественного текстурного анализа. Теоретическое рассмотрение [**14**] взаимодействия анизотропной (текстурированной) среды с распространяющимися в ней упругими волнами позволило установить несколько фактов, объясняющих указанное противоречие. В частности, показано, что при наличии одного вектора анизотропии в текстурированной среде могут распространяться одна чисто поперечная волна и две волны со смешанной продольно-поперечной поляризацией. При наличии двух векторов анизотропии все волны имеют в общем случае смешанную продольно-поперечную поляризацию. При отражении от

поверхности раздела сред, различающихся направлениями векторов анизотропии и (или) величиной параметра анизотропии, происходит в общем случае тройное расщепление преломленных и отраженных волн. Закон Снеллиуса при отражении волн в анизотропных средах в общем случае не выполняется. Продольные колебания содержатся в разных модах, распространяющихся с совершенно разными скоростями.

Горные породы на основе ангидрид-доломитовых минералов ("Zuckerdolomit") изучены на предмет корреляции внутрикристаллических напряжений и текстуры. Образцы породы были извлечены из месторождения Piora Mulde (центральные Альпы, Швейцария). Эксперименты проведены на нейтронном дифрактометре с использованием метода времени пролета. Основные составляющие породы (доломит и ангидрид) характеризуются высокой симметрией структуры (тригональная и ромбическая, соответственно). Внутренние напряжения в доломите и ангидриде имеют, как правило, противоположные знаки, характеризуя сжатие или растяжение. Принимая во внимание то, что упругие константы обоих минералов могут сильно различаться в зависимости от направления в кристалле, следует ожидать проявления специфического гео-механического поведения породы, определяемого комбинацией текстуры, упругости и внутренних напряжений. Анализ показал, что взаимодействие этих факторов приводит к хрупкому разрушению породы, если упругие волны распространяются по направлениям, близким к плоскостям спайности [**15**].

Завершен цикл работ по исследованию мартенситной трансформации и усталостных свойств аустенитных нержавеющих сталей, широко используемых в технике из-за своих выдающихся механических, сварочных и антикоррозионных характеристик. Экспериментальная симуляция усталостной деградации проводилась с помощью циклических нагрузок растяжение – сжатие в пластической области с частотами от 0.1 до 100 Гц. Выявлены области характерных частот, сильно различающихся по воздействию на сталь. Определены закономерности образования мартенситной фазы в исходно однофазном (аустенитном) материале. Показано, что в некоторых случаях имеется значительное рассогласование (**рис. 14**) в упругих константах фаз, образующих материал, что оказывает значительное влияние на его прочностные свойства.

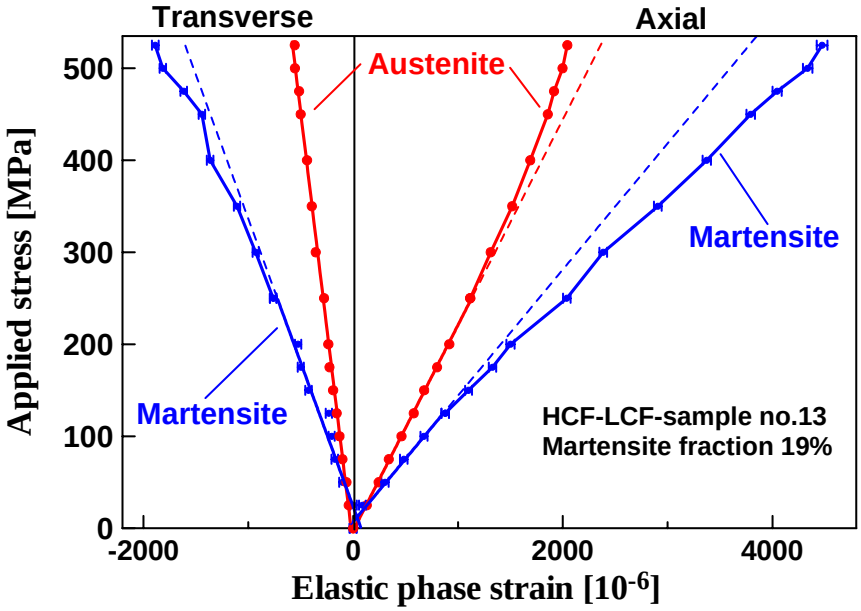

Рис. 14. Соотношения деформация – напряжение в аустенитной (исходно) нержавеющей стали после высоко- и низкочастотной усталостной нагрузки для аксиальной (справа) и тангенциальной (слева) компонент. Возникающая в ходе циклирования мартенситная фаза имеет другие, чем аустенит, упругие константы.

II. Методические результаты

Начато изготовление головной части зеркального вакуумного нейтроновода в рамках реализации проекта создания дифрактометра для исследования микрообразцов ДН-6 (канал 6Б ИБР-2М).

Проведены первые эксперименты на рефлектометре Будапештского нейтронного центра в рамках исследования возможности создания нейтрон-оптических зеркал нового поколения, основанных на специальном принципе усиления брэгговского рассеяния для заданного значения волнового вектора. Этот подход (развитый в работе [**16**]) к созданию зеркал с высоким критическим углом полного отражения является альтернативным по отношению к широко используемой методике создания подобных зеркал с апериодической структурой методом магнетронного напыления. Проведено изучение отражательной способности новых зеркал. Модельное описание кривых отражения для изучаемых систем показало хорошее совпадение с экспериментальными данными. Работа выполнена в сотрудничестве с Исследовательским институтом физики твердого тела и оптики Венгерской Академии (Будапешт, Венгрия) и компанией МИРРОТРОН (Будапешт, Венгрия).

В 2008 продолжалась работа по проекту создания многофункционального рефлектометра ГРЭЙНС на реакторе ИБР-2М. На нем планируется изучение разнообразных границ раздела с жидкими фазами методом рефлектометрии нейтронов (включая поляризованные нейтроны для исследования границ раздела с магнитными наночастицами). ГРЭЙНС откроет принципиально новые возможности в исследованиях наносистем на реакторе ИБР-2М. Дополнительные режимы на рефлектометре включают в себя: (1) возможности изучения незеркального отражения и рассеяния GISANS; (2) угловое кодирование в горизонтальной плоскости на основе Ларморовской прецессии спина нейтронов; (3) 3D поляриметрия на основе Ларморовской прецессии спина нейтронов. Уже начато изготовление головной части рефлектометра, которая состоит из системы расщепления пучка на два. Сдана в производство коллимационная система, включающая в себя массивную подставку для размещения отдельных узлов установки (коллимационные щели, отклоняющие зеркала). Специальные направляющие позволяют передвигать узлы вдоль оси пучка. Вся конструкция размещается в специальном вакуумном кожухе, где организованы специальные входы для локального доступа к элементам без полной разборки конструкции. Как элементы коллимационной системы начато изготовление отклоняющих зеркал (длина 1 м, суперзеркало, m=2) для неполяризованного и поляризованного пучков. Назначение этих элементов – направление нейтронов первичного пучка под заданным углом к поверхности образца, расположенного горизонтально. Такое отклонение позволяет регулировать угол падения на образец, и отделять тепловые и холодные нейтроны от быстрых нейтронов, проходящих через зеркала, не отражаясь, что исключает прямую видимость зоны реактора и улучшает фоновые условия на установке. В течение года проводилась разборка канала 10 и освобождение его под новое оборудование рефлектометра. Работа выполнялась в рамках целевого взноса BMBF (Германия) совместно с ИЛЛ (Гренобль, Франция), Университетом Халле, Техническим университетом Мюнхена и Петербургским институтом ядерной физики им. Б.П.Константинова.

Завершен технический проект зеркального вакуумного нейтроновода для спектрометра ДИН-2ПИ и проведены работы по подготовке рабочей площадки для установки нейтроновода. Работа ведется в кооперации с организациями-пользователями: ЛНФ ОИЯИ и ПИЯФ РАН (Гатчина). Создаваемый зеркальный нейтроновод позволит повысить интенсивность холодных нейтронов ($E < 5$ мэВ) на образце в 4 – 6 раз и при этом уменьшить размеры исследуемых образцов в 2 – 3 раза, что будет означать существенное улучшение качества спектрометра ДИН-2ПИ и приближение его характеристик к лучшим зарубежным аналогам.

Подготовлен к утверждению технический проект зеркального вакуумного нейтроновода для канала 7А на реакторе ИБР-2М, который будет строиться в соответствии с соглашением ОИЯИ – BMBF (Германия). Реализация этого проекта позволит решить две главные задачи: увеличение потока тепловых нейтронов на спектрометрах SKAT и EPSILON, улучшение соотношения эффект – фон для этих спектрометров. Кроме того, в рамках проекта предусматривается установка дополнительного прерывателя, с помощью которого можно будет варьировать рабочий диапазон по длине волны, а именно, станет возможным его расширение до 14 Å. Новая схема размещения спектрометров показана на **рис. 15.**

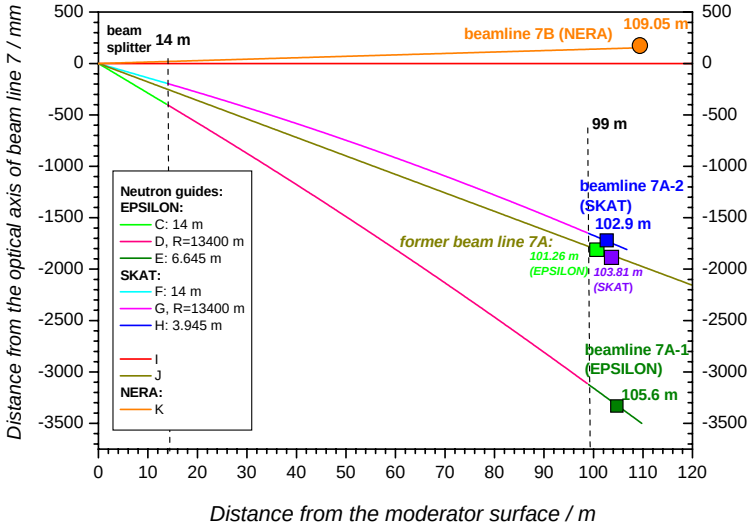

Рис. 15. Разводка нейтронных пучков на каналах 7А и 7В (спектрометры NERA, SCAT, EPSILON) с помощью новой нейтроноводной системы. По оси абсцисс указано расстояние от замедлителя в метрах. По оси ординат – смещение пучка относительно центральной линии в мм. В головной части предполагается установка единого узла (splitter) для разделения пучков. После отметки 14 м пучки формируются отдельными нейтроноводами. Для пучка 7А показан нейтроновод, действовавший на реакторе ИБР-2, на котором располагались спектрометры SCAT и EPSILON.

Изготовлена установка для измерения низкотемпературного магнитосопротивления в области низких температур. Установка потребовалась для оперативного анализа свойств манганитов типа $La_{1-x}Sr_xMnO_3$, которые являются ферромагнетиками со свойствами “плохого металла”. Синтез манганитов выполнялся по золь-гель технологии. Их магнетосопротивление было успешно измерено в поле H_{max} = 1.2 Т в диапазоне температур 7 - 300 К.

References

1. I.V.Nikolaev, H.D’Hondt, A.M.Abakumov, J.Hadermann, A.M.Balagurov, I.A.Bobrikov, D.V.Sheptyakov, V.Yu.Pomjakushin, K.V.Pokholok, D.S.Filimonov, G. Van Tendeloo, E.V.Antipov. “Crystal structure, phase transition and magnetic ordering in the perovskitelike $Pb_{2-x}Ba_xFe_2O_5$ solid solutions”. **Phys. Rev. B**, 2008, v.78, pp.024426 (1-12).
2. D.V.Sheptyakov, O.A.Drozhzhin, V.Yu.Pomjakushin, S.Ya.Istomin, I.A.Bobrikov, E.V.Antipov, A.M.Balagurov. “Correlation of spin and charge ordering in $Sr_3YCo_4O_{10.5+\delta}$, δ=0.02 and 0.26”. **Phys. Rev. B**, 2008, accepted.
3. D.P.Kozlenko, I.Mirebeau, J.-G.Park, I.N.Goncharenko, S.Lee, J.Park, B.N.Savenko. “High pressure induced spin liquid phase of multiferroic $YMnO_3$”. **Phys. Rev. B**, 2008, v.78, pp.054401 (1-5).

4. D.P.Kozlenko, L.S.Dubrovinsky, B.N.Savenko, V.I.Voronin, E.A.Kiselev, N.V.Proskurnina. “Pressure-induced suppression of Wigner-crystal antiferromagnetic state in $La_{0.33}Ca_{0.67}MnO_3$”. **Phys. Rev. B**, 2008, v.77, pp. 104444 (1-6).
5. M.V.Avdeev, D.Bica, L.Vekas, V.L.Aksenov, A.V.Feoktystov, L.Rosta, V.M.Garamus, R.Willumeit. “Structural aspects of stabilization of magnetic fluids by mono-carboxylic acids”. **Advanced Materials Research**, 2008, accepted.
6. V.L.Aksenov, T.V.Tropin, E.A.Kizima, M.V.Avdeev, M.V.Korobov, L.Rosta. “On fullerene cluster formation in nitrogen-containing solvents”. **Physics of the Solid State**, 2008, accepted.
7. M.Balasoiu, S.G.Barsov, D.Bica, et al. “MSR Study of the Properties of Fe_3O_4-Based Nanostructured Magnetic Systems”. **JETP Letters**, 2008, v.88, pp.210-213.
8. A.V.Rogachev, A.Yu.Cherny, A.N.Ozerin, A.M.Muzafarov, E.A.Tatarinova, A.Kh.Islamov, V.I.Gordeliy, A.I.Kuklin. “Revealing inner structure of the polycarbosilane dendrimers from small-angle neutron scattering data”. **Journal of Physics: Conference Series.** v.129, 2008, 012041.
9. V.L.Aksenov, Yu.V.Nikitenko, Yu.N.Khaidukov, S.N.Vdovichev, M.M.Borisov, A.N.Morkovin, E.H.Mukhamedzhanov. “Coexistence of superconductivity and ferromagnetism in the nanostructure Nb(500 Å)/Fe(39 Å)/[Si(34 Å)/Mo(34Å) $]_{40}$/Si”. **Journal of Surface Investigations,** 2008, accepted.
10. E.Juszyńska, M.Massalska-Arodź, I.Natkaniec, J.Krawczyk “Neutron scattering studies of solid-state polymorphism in dimethyl butanol glass formers”. **Physica B**, 2008, v.403, p.109.
11. E.Juszyńska, K.Hołderna-Natkaniec, M.Massalska-Arodź, I.Natkaniec, E.Ściesińska, J.Ściesiński. “IINS, MIR and DFT investigations of vibrational spectra of 3,3-dimethyl-1-butanol and 3,3-dimethyl-2-butanol”. **Acta Physica Polonica A**, 2008, v.113, pp.1131-1143.
12. N.M.Blagoveshchenskii, V.A.Morozov, A.G.Novikov, M.A.Pashnev, A.L.Shimkevich, O.V.Sobolev. “Quasielastic neutron scattering and diffusion in liquid lithium and lithium–hydrogen melt”. **Journal of Physics: Condensed Matter**, 2008, v.20, pp.104201-104204.
13. M.V.Rodkin, A.N.Nikitin, R.N.Vasin. “Seismotectonic effects of solid-state transformations in geomaterials”. **Moscow: Geos**, 2008, p.220.
14. A.N.Nikitin, T.I.Ivankina, V.K.Ignatovich. “Peculiarities of p- and s-wave propagation through textured rocks.” JINR Communications, 2008, P18-2008-50, p.19.
15. K.Walther, Ch.Scheffzük, A.Frischbutter, R.Naumann, I.A.Brovkin. “A “Zuckerdolomit”-sample from the Piora Mulde (Switzerland), studied by an *in situ* applied load experiment using neutron time-of-flight diffraction”. **Z. geol. Wiss.**, 2008, v.36, pp.123-138.
16. I.Carron, V.Ignatovich “Algorithm for preparation of multilayer systems with high critical angle of total reflection” **Phys. Rev. A**, 2003, v.67, p.043610.

1.2. NEUTRON NUCLEAR PHYSICS

Introduction

In 2008, at the Frank Laboratory of Neutron Physics the main investigations in the field of neutron nuclear physics were carried out on neutron beams of nuclear research centers in Russia, Germany, Republic of Korea, China, France and at the EG-5 accelerator in FLNP. The studies were conducted in the following traditional directions: investigation of time and spatial parity violation processes in neutron-nuclear interactions; studies of quantum-mechanical characteristics, energy and dynamics of fission; experimental and theoretical investigations of electromagnetic properties of the neutron and of its beta-decay; gamma-spectroscopy of neutron-nuclear interactions, atomic nucleus structure, obtaining of new data for reactor applications and for nuclear astrophysics; experiments with ultracold neutrons; applied research. Concurrently, the preparation of experiments at the first stage of the IREN facility and at the IBR-2M reactor in FLNP was conducted.

I. Experimental investigations

1.2.1 Work to prepare and carry out an experiment on the direct measurement of the neutron-neutron scattering cross section at the YAGUAR reactor (RFNC-VNIITF, Snezhinsk)

Calibration measurements with inert gases.

Calibration measurements with inert gases are needed to perfect the technique and to test the reliability of the obtained results. The idea of the measurements is to measure a well-known cross section of thermal neutron scattering by an inert gas at the facility for measuring nn-scattering cross-section. If the obtained result coincides with the table one, it means that the measurements are carried out methodically correctly and this technique can be used for measuring the nn-scattering cross section. It should be noted that our information about the detector efficiency is not quite accurate. Thus, we should proceed from the assumption that we do not know the efficiency of the detector. Therefore measurements should be carried out with different gases. For example, using ^{4}He, the detector efficiency is determined and using Ar, the scattering cross-section can be measured.

Figure 1 shows the results of calibration measurements using ^{4}He and Ar.

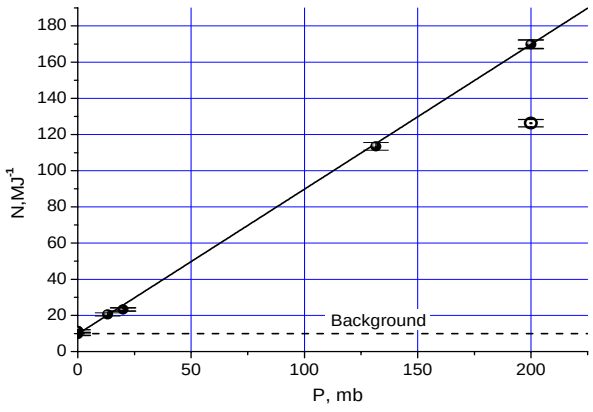

Fig. 1. The results of calibration measurements. The ordinate axis is the detector count per 1 MJ reactor energy, the abscissa axis is the gas pressure at 20^{o}C. Black circles are the measurements with ^{4}He and an open circle – with Ar, solid line is the linear approximation of the experimental data.

The presented data shows clear linear dependence of the detector count on the gas pressure, which points to the methodical correctness of the conducted measurements.

The table scattering cross sections are $\sigma_T(^4\text{He}) = (0.79\pm0.02)$ b, $\sigma_T(\text{Ar}) = (0.656 \pm 0.003)$ b. The experimentally obtained cross section on Ar is $\sigma_Э(\text{Ar}) = (0{,}642 \pm 0{,}024)$ b, which is in good agreement with the table value.

First attempt to measure n-n scattering cross section

The equation for calculation of the number of nn-scattering events in the nn-scattering pool of the reactor JAGUAR can be written as:

$$N_{nn} \sim \iint \frac{\Phi^2(t,\vec{r})}{v_0} \sigma_{nn} dt dV ,$$

where t is the time, V is the volume of the nn-scattering pool, $\Phi(t,\vec{r})$ is the thermal neutron flux density, v_0 = 2200 m/s, σ_{nn} is the nn-scattering cross section.

As is seen from the equation the number of the nn-scattered neutrons is proportional to the product of squared flux density and pulse duration. The neutron flux density is proportional to the reactor power. As a result, the dependence of the number of neutrons detected during a pulse on the energy of the pulse allows one to understand what the source of the detected neutrons is. For example, the number of neutrons scattered on the walls of the channel or on the edges of the collimator is a linear function of the pulse energy but does not depend on the pulse duration. Since the pulse duration in the JAGUAR reactor is about inversely proportional to its energy, the dependence of the number of nn-scattered neutrons on the pulse energy will be nearly cubic.

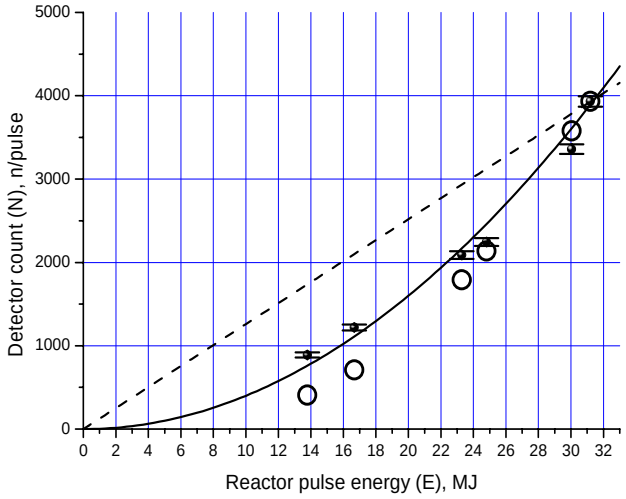

Fig. 2. The dependence of the number of neutrons counted per pulse on the JAGUAR reactor pulse energy. Black points – experimental data; dashed line – linear dependence: N ~ E; solid line – quadratic dependence: N ~ E^2; open circles – calculated dependence of the number of scattered neutrons taking into account true pulse shape.

Figure 2 shows the dependence of the number of neutrons counted during a pulse on the JAGUAR pulse energy. In the Figure all the calculated functions are reduced to the experimental value at 31 MJ. It is seen that the experimental data are close to quadratic dependence and are noticeably different from both linear dependence and the one for nn-scattering. The difference from linear dependence reflects the fact that in the nn-scattering pool the number of objects, on which neutrons are scattered, changes. In the case of quadratic dependence the number of such objects is proportional to the energy pulse or fluence, but not to the neutron flux density, which means the objects are accumulated in the nn-scattering pool during the pulse. Most probable candidates as such objects are the gas molecules flying off the walls under the action of reactor radiation. In other words, we observe radiation desorption here.

The radiation desorption can be suppressed by degassing the nn-scattering pool surface just before the reactor pulse and by using low-absorption materials as a wall material. Work to investigate radiation desorption in the instrument for nn-scattering cross-section measurements is planned to be carried out next year.

1.2.2. Experiment to study cold neutron quasi-specular reflection off the nanopowder surface

Sequential scattering of particles/quanta at small angles in the medium – small-angle scattering, results in the fact that if a beam of particles/quanta falls on the medium at a grazing angle, the angular

distribution of the reflected particles/quanta has a pronounced maximum at an angle close to the incident one. A similar situation must also take place for neutrons if they fall on a medium with effective small angle scattering at a small angle. Nanoparticles with a size of a few nanometers can effectively scatter cold neutrons at small angles. At the same time, smallness of the neutron wavelength in comparison with the particle, which provides for smallness of the angle at scattering, allows one to consider the interaction of neutrons with nanoparticles in the powder as that with individual particles.

We tried to determine experimentally the parameters of the discussed phenomenon in the reflection of neutrons off a nanodiamond powder. To this end, we measured the dependence of the angular distribution of neutrons reflected off the surface of a diamond nanopowder for different wavelengths of incident neutrons at an angle of neutron beam incidence on the surface of 2°, 3° or 4°. The experimental lay-out is shown in **Fig. 3.** The sample in the form of a prism 15 cm long, 5 cm high and 4 cm deep is placed inside a special cryostat. The surface of the powder is covered with a 100 μm thick aluminum foil. Scattering on the walls of the cryostat is negligibly small in comparison with that on the sample. The neutron beam has an outlet diaphragm 15 mm high by 0.3 mm wide. The scattered neutrons are registered within the angle ±12° of the incident beam in the vertical plane.

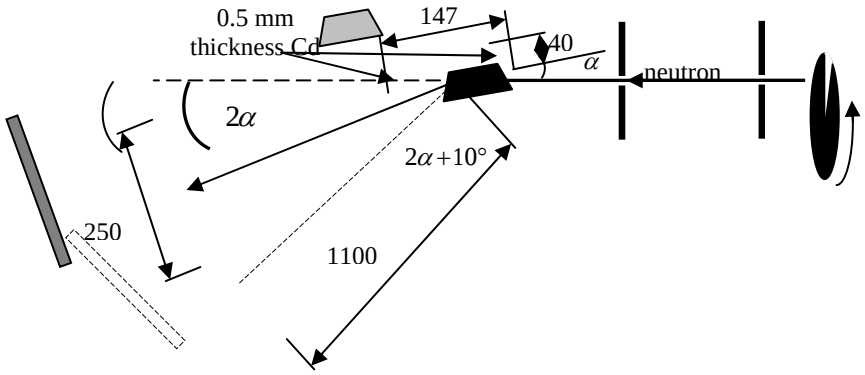

Fig. 3. The experimental lay-out.

The results of measurements are shown in **Figs. 2**, **3**, and **4**. As expected, multiple scattering on nanoparticles results in neutron reflection off the surface with a relatively narrow angular distribution whose maximum is at an angle close to the specular reflection one. The smaller the incident neutron wavelength, the wider the angular distribution of the scattered neutrons is. If the angle of neutron beam incidence increases, the angular distribution becomes wider as well. Thus, for cold neutrons with the wavelength λ from 4 Å to 8 Å at small angles of incidence (smaller than 6 - 7) quasispecular albedo in the scattering plane is observed with a probability of ~25%. For wavelengths smaller than 4 Å the quasi-specular albedo is suppressed by Bragg scattering, and for λ larger than 8 Å the angular distribution becomes too wide to speak about the quasi-specular effect. For neutron incidence at angles larger than 6 -7 the probability of quasi-specular reflection is commensurable with that of scattering at angles much larger than the specular reflection angle.

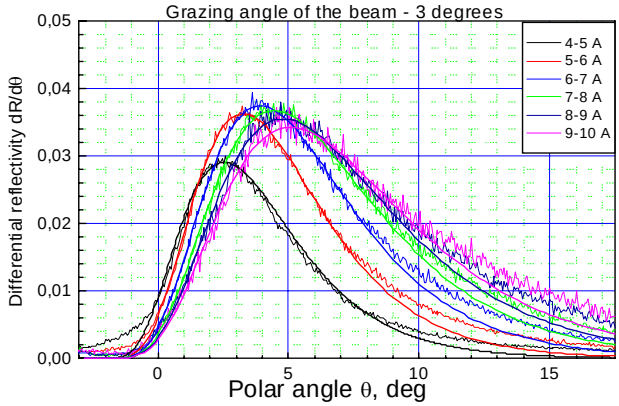

Fig. 4. The dependence of the reflected neutron flux on the polar angle for neutrons with energies lying in different energy intervals (indicated in the Figure) at a grazing angle of neutron incidence on the surface of 3º. The experimental dependence is approximated to the logarithmically normal distribution whose dispersion is chosen as a width parameter of the flux angular distribution.

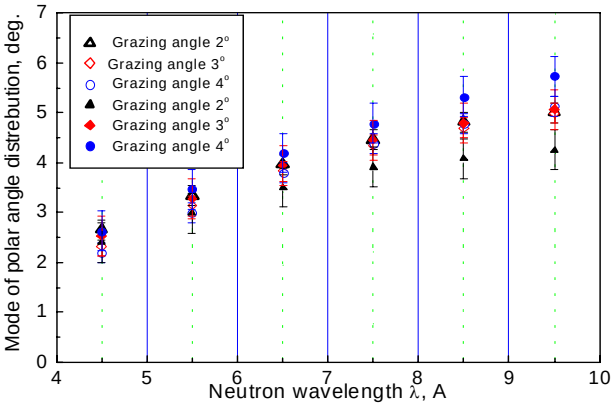

Fig. 5. The position of the maximum in the polar angle distribution of the reflected neutrons as a function of neutron wavelength for different angles of incidence and temperatures.
Open points — liquid nitrogen temperature measurements, filled points — room temperature measurement results.

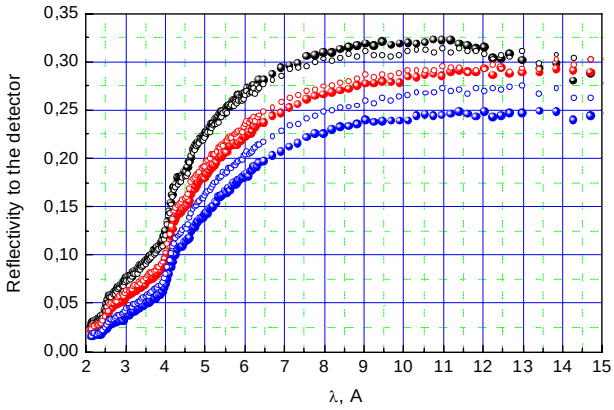

Fig. 6. The dependence of the reflectivity to the detector on the neutron wavelength at different angles of incidence and temperatures.
Black points — angle of incidence 2º.
Red points — angle of incidence 2º.
Blue points — angle of incidence 2º.
Open points — liquid nitrogen temperature measurements, filled points — room temperature measurement results.

For large angles and large λ (when the transverse component of neutron velocity exceeds ~50 m/s) such quasispecular albedo exceeds the probability of reflection off the existing supermirrors (reflection off which is also quasispecular at such velocities)

The measurements were done twice: at room temperature with a preliminarily prepared sample (long pumping-out and outgasing at 150°C), and at -150°C. At sample cooling the channel of inelastic, practically isotropic, scattering on carbon and hydrogen impurity atoms must be suppressed. Contrary to expected, cooling of the sample resulted in an increase of reflection probability due to the quasispecular component in the main.

1.2.3. Experiments with ultracold neutrons

On the UCN beam built at the reactor TRIGA in the University of Meinz, time-of-flight measurements to investigate the properties of cBN – boron nitride with a cubic structure, as a material with a high boundary energy for UCN chambers, were conducted.

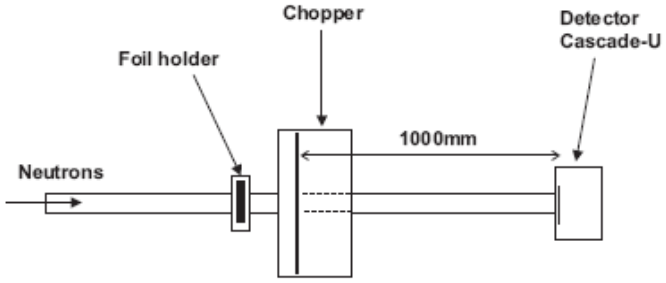

Fig. 7. The experimental lay-out.

The material is very strong, nonmagnetic, has a high electric resistance, including that to surface currents, and may therefore be a very promising material for building chambers to search for EDM of the neutron.

For a known boron nitride density of 3.5 g/cm^3 it is expected that the boundary energy is 324 neV for a material with a natural content of boron isotopes, and E=351 neV for a material enriched with the isotope B-11.

The investigated materials were deposited on the surface of 380μ monocrystalline plates by the method of magnetron sputtering. The layer thickness was 300 nm.

By analyzing time-of-flight spectra obtained with and without a sample the boundary energies of boron nitride, E=305±15 neV, and of nickel used for calibration, E=240±15 neV, were determined.

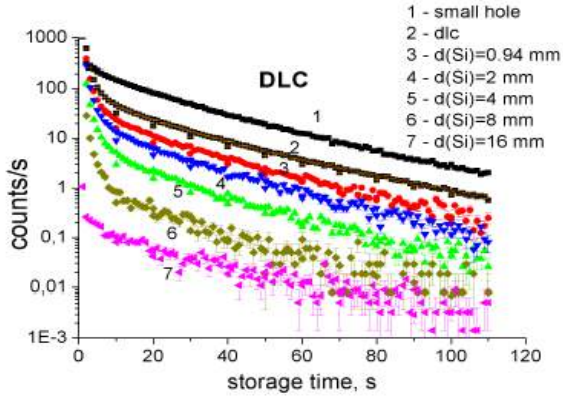

Fig. 8.

Figure 4: The typical measured time dependent count rate (DLC sample foil): 1 – the UCN flux density measured through 2.5 mm diameter hole in the sample foil, 2 – the count rate through the DLC foil at the 100 μm Al substrate, no additional absorber, 3-7 – the count rate through the DLC foil with different Si absorbers between the scatterer and the neutron detector. The time shown from the moment of opening of the UCN valve after the filling time 20 seconds.

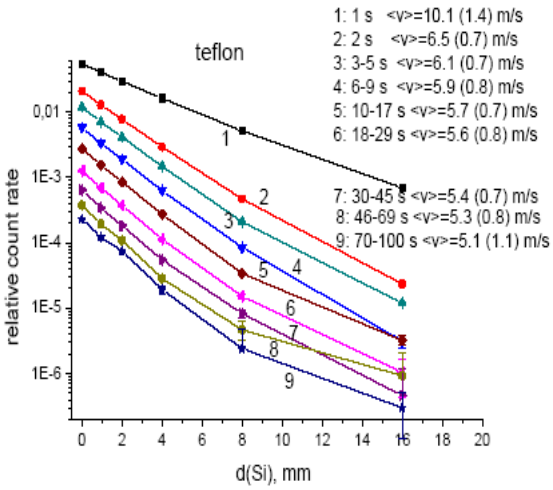

Fig. 9.

Figure 8: The neutron count rate (relative to the incident UCN flux) for the teflon sample as a function of Si thickness after subtracting the contribution of up-scattering to the thermal energy range. The inferred neutron mean velocities and half-widths of the Gaussian distributions (in brackets) for corresponding storage time intervals are shown in the insert. The straight lines connect the experimental points.

On the beam of the ILL reactor, measurements of the UCN “low heating” effect were conducted with copper, teflon, and diamond-like carbon samples. Spectra of heated neutrons at energies from UCN to thermal and also, evolution with time of UCN spectra in the trap were measured. The method of “calibration absorbers” for the measurement of neutron spectra was developed. Monocrystalline silicon plates and rhodium foils were used as absorbers. Neutron spectra were determined from absorption curves in the monoenergy and in a more detailed approximation.

Figure 9 exemplifies the detector count rate as a function of time for different absorbers and absorption curves from which the energy of stored or heated neutrons is determined.

It is found that different materials give different spectra of heated neutrons and also, that the spectrum of heated neutrons extends to the μeV energy region.

1.2.4. Neutron-nucleus interaction mechanism studies

Studies of the interaction mechanism of neutrons with nuclei are of importance from the viewpoint of understanding the laws of nature. Neutron reactions with emission of charged particles have not been adequately investigated so far. Investigations of reactions with neutrons, (n,p), (n,t), (n,alpha), carried out in many laboratories supply valuable information about the mechanism of nuclear reactions and the structure of the atomic nucleus, including that about the role of single-particle and many-particle components in the process of compound nucleus excitation and in discovery of effects of selective intensification or decay of collective-cluster states of nuclei with respect to pure statistical distribution. Neutron beams with an energy of a few MeV do not only allow one to do averaging over a

large number of initial states of excited nuclei but also to raise the Coulomb barrier penetrability of the nucleus for the reactions (n,p), (n,t), (n,alpha) in comparison with resonance neutron induced reactions by several orders of magnitude as well as to observe changes in decay characteristics with increasing excitation energy of the nucleus as the region of giant dipole resonances is being approached. It is planned to conduct experimental investigations of the reactions (n,p), (n,t) or (n,alpha) on limit light (6Li, 9Be, 10B), light (14N, 20,21Ne, 24Mg, 28Si, 35Cl), medium A~40-70 (39K, 54,57Fe, 58Ni, 63Cu, 64, 67Zn, 95Mo), and on heavy A~150 (143Nd, 147,149Sm) nuclei over a wide range of neutron energies from a few keV to 6.5 MeV. Comparison of the presently available data shows that in the energy interval 3 to 10 MeV experimental data are not numerous and there is considerable discrepancy between values cited by different authors. In the majority of cases such reactions were investigated with the help of the activation method, which appears to be insufficient for reliable separation of direct, pre-equilibrium and compound processes. We use the method of direct detection and spectrometry of emitted particles in neutron beams. The method allows direct measurement of spectra of emitted charged particles, determination of the total cross section of the reaction, and of the angular distribution of reaction products.

The experiments are carried out at Van de Graaf accelerator EG-5 in the Laboratory of Neutron Physics of the Joint Institute for Nuclear Research and EG-4.5 of the Institute of Heavy Ions in Beijing University in collaboration with Lodz (Poland) and Mongolian national universities.

In 2008:

- A system of targets to obtain fast neutrons on the EG-5 channel was developed (and in presently in the process of manufacturing in the FLNP experimental workshop (EW));
- Design drawings of the ionization chamber to be operated at EG-5 and IREN were made;
- Design drawings of the «proton telescope» for EG-5 were made;
- An article on the measurement of the reaction 64Zn(n,a) at neutron energies 2.54; 4.00, and 5.50 MeV was written and published in the journal Nucl.Sci.Eng.
- The reaction 147Sm(n,a)143Nd measurement data at neutron energies 5.0, 6.0 MeV were processed and the corresponding article was written and accepted for publication in the journal Applied Radiation and Isotopes
(attached to this annual report);
- The reaction 143Nd(n,a)140Ce measurements at En=4, 5, and 6 MeV were conducted; data processing started;
- The reaction 95Mo(n,a)92Zr measurements at при En=4, 5, and 6 MeV were conducted; background measurements are under preparation.

1.2.5 Preparation of first-stage experiments at IREN

In the course of the year experiments for the first stage of operation of the neutron source IREN were prepared.

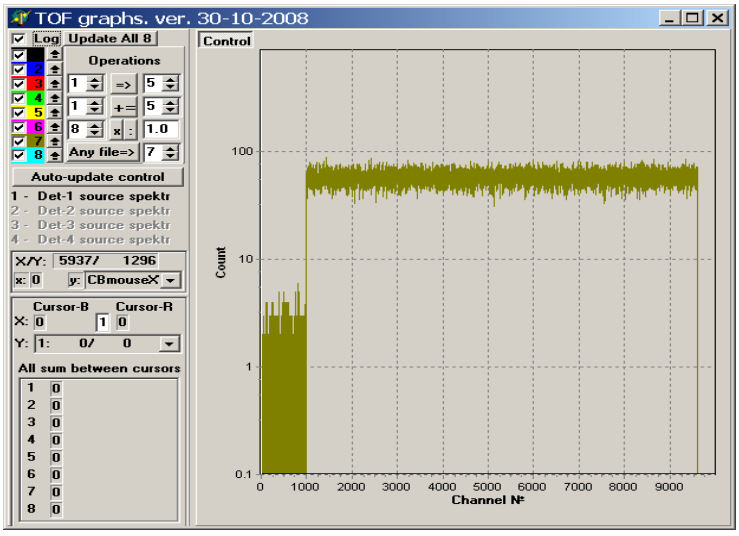

Fig. 10. The demonstrative window for visualization of the measured spectra under the program «Tof_usb».

a) The measuring module of the gamma-spectrometer «KOKOS» was modernized, which increased essentially its operation speed: a new USB-1 interface was designed and built and a new program for experimental data storage, «Lada», was written.

b) Fast time analysis blocks with a channel width of 10 – 20 ns for time-of-flight neutron spectrometry were designed, built, and tested. Fast time analysis system software for registration of 4 TOF spectra, «TOF_usb», was developed. The system is designed for investigation of IREN neutron beam parameters. Also, additional algorithms were developed and included in the given program with the aim of conducting precision experiments.

1.2.6 Gamma-spectrometry of neutron-nuclear interactions

Analysis and interpretation of experimental data on the intensity of two-quanta cascades following thermal neutron capture by different nuclei continued.
Semi-phenomenological function approximation of the sums of radiation strength functions of primary dipole gamma-transitions over the primary gamma-transition energy interval $0.5 < E_1 < B_n$-0.5 MeV is done with a high accuracy for a large number of nuclei. As a basic hypothesis there is used a hypothesis that experimental data can be presented as a superposition of two strongly different functions. A smooth function describes changes in the probability of gamma-quanta emission due to excitation of fermion-type nuclei, pronounced peaks are due to excitation of boson-type nuclei.

The approximation resulted in a self-coordinated consistent picture of processes occurring in the nucleus for practically all nuclei in the periodic system and confirmed the earlier result of level density analysis showing that the parameters of the cascade decay of the neutron resonance are determined by coexistence and interaction of a superfluid and an ordinary phase in a heated nucleus.

It is obtained that the form of radiation strength functions in the investigated nuclei is a dynamic quantity (changing in a cyclic manner as the mass of the nucleus changes), and the value of *k(E1)+k(M1)* for particular energies of gamma-transitions and particular nuclei is determined by the structure of decaying or excited levels at least at energies down to the neutron binding energy B_n. The result defines the smallest area of excitation of nuclei where it is necessary to account for and from where one can get information about the dynamics of changes in the transition of the nucleus from Bose- to Fermi system on heating.

The same experimental data continue to be used to obtain new spectroscopic data on deformed nuclei over a much larger excitation energy interval than that accessible to conventional nuclear spectroscopy and also, to verify different models of the nucleus. In particular, it is found that total experimental gamma-spectra of two even tin isotopes are reproduced most accurately in the calculation if just step-like density of levels and strength functions accounting for intensification of the strength functions of primary and secondary gamma-transitions to the excitation region corresponding to such structure of the excited level spectrum of the nucleus, are used. Although due to some peculiarities of the experimental method for measurement of the two-quanta cascade intensity, both level density and strength functions are determined more accurately than using any other competing technique, there exists a necessity to reveal main sources of systematic errors and reduce them essentially. In particular, it is necessary to develop new independent methods for determination of such parameters of the nucleus.

Independent confirmation of existence of a considerable step-like structure of the level density was obtained by reanalysis of published to date experimental data on primary gamma-transition intensities averaged over neutron resonances at 2 and 24 keV. The distribution of intensity dispersion from the average was first approximated over different energy intervals of primary gamma-transitions within the framework of the representation that their intensities depend on the excited level structure and their random deviation dispersion is not described by a χ^2 distribution with one degree of freedom (as assumed before).

The level densities and radiation strength function sums determined in this way confirm characteristic features of similar data obtained from intensities of two-quanta cascades of thermal neutron capture for nuclei with $40 \leq A \leq 200$. Also, they allow estimation of the sign and value of their resulting systematic error which is mainly due to very strong dependence of radiation strength functions of cascade gamma-transitions on the structure of the excited nucleus. The conclusion is correct at least for excitation energies smaller than half neutron binding energy. Comparison with model representations of level density shows, for example, that the nucleus ^{174}Yb is in the superfluid state for most excited nuclei below 3.5-4 MeV at least. Furthermore, preliminary information about the ratio of the number of levels with prevailing components of the quasiparticle- to those of phonon-type was first obtained down to the same excitation energy of the even-even deformed nucleus (the dependence of vibrational amplification of the density of quasiparticle levels on the excitation energy was determined).

Combined analysis of experimental data on two-quanta cascade intensities promises an increase in the accuracy of determination of the properties of the nucleus at energies below the neutron binding energy at least.

1.2.7. Measurements of the nuclear charge of fission fragments on miniFOBOS

Searching for and investigation of rare, including many-body, decay modes of weakly excited nuclei is still an urgent problem in experimental nuclear. It is just the region of excitation energies where earlier unknown manifestations of nuclear system clusterization can be expected. Reliable identification of unusual decay channels implies simultaneous measurement of an as large as possible number of different parameters of the process, including mass and energy of decay products, their angular distribution, neutron multiplicity, etc. It is natural that measurement of the nuclear charge of the formed fragments is quite desirable.

In a series of experiments to search for triple collinear cluster decay (TCCD) of heavy nuclei the two-shoulder gas-filled-detector-based time-of-flight spectrometer of charged particles of nuclear reactions mini-FOBOS was used. The spectrometer allows measurement of the velocity vector and energy of fragments. Knowing velocity one can determine so-called primary masses of fragments from binary fission (Mtt), and known velocity and energy allows determination of the mass of the fragment after neutrons are emitted (Mte). The energy of fragments is measured using big ionization chambers (BIK) earlier operated on the spectrometer 4π-spectrometer FOBOS.

Measurement of the nuclear charge of fission fragments by measuring the time of their track drift in the chamber is technically a more difficult problem than measurement of energy. Charge resolution directly depends on electric field homogeneity and uniformity of gas mass in the working volume of the chamber. To secure the second condition it does not suffice to stabilize the pressure and composition of the gas mixture. Additionally, thermostabilization of the chamber is required. The enumerated conditions were created in the experiment for investigation of the reaction $^{235}U(n_{th},f)$ on the wide-aperture spectrometer miniFOBOS on the IBR-2 reactor beam. For calculation of the nuclear charge of fragments on the basis the data obtained in the experiment two variants of charge calibration were developed. Model tests showed that the charge parametrization used in calibration allows satisfactory reproduction of the nuclear charge of fission fragments in a wide energy range. The charges of light ions from He to C predicted within the framework of the given approach appear to shift two charge units to a larger side.

1.2.8. Parameter investigations of the TIMEPIX detector in radiation registration from ^{244}Cm and ^{252}Cf

In FLNP JINR, investigations of pixel detectors MEDIPIX and of their application in nuclear physics, particularly in fission studies, are carried out in collaboration with the Polytechnic Institute (Prague). The MEDIPIX detector is two silicon plates one of which is a sensor of bombarding particles and the other consists of a large number of pixels each of which is a spectrometric tract that includes an

amplifier, a discriminator and a counter. The two plates are connected to each other in every pixel by means of the “bump-bonding” method.

In JINR, investigations were conducted of whether it is possible to measure fission fragments and charged light particles (from the spontaneous radiation sources 244Cm and 252Cf) with detectors of two types, MEDIPIX2 and TIMEPIX. As soon as a particle falls into the sensitive layer of the detector a so-called charge sharing effect takes place in which the charge is shared between several pixels and a cluster is formed as a result. The size of the cluster depends on the specified thresholds as well as on the energy and charge of the bombarding particle. In the detector MEDIPIX2 one can see a two-dimensional picture showing distinct difference between the size of the cluster for alpha particles and that for fission fragments. In addtion, after appropriate calibration we succeeded in measuring the two-hump curve of the energy distribution of fission fragments on the basis of cluster sizes alone.

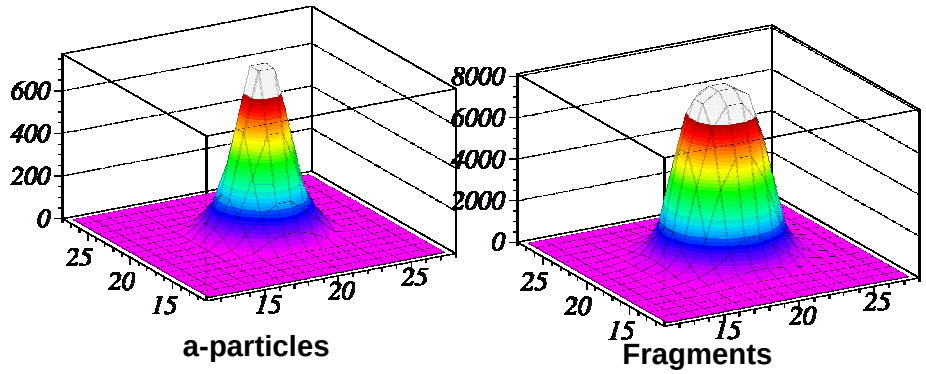

Fig. 11. The energy distribution in the cluster for alpha-particles and fission fragments.

The new type of MEDIPIX detectors, TIMEPIX, allows registration of the discriminator operating time in each pixel. With proper tuning this time can be converted into amplitude and the charge in the pixel can be measured. As a result, a three-dimensional picture is obtained (see on the right). This makes it possible to determine the energy of the bombarding particle more precisely. The possibility of particle identification by charge and mass, and also by the angle at which the particle falls into the detector with the help of such three-dimensional “snaps” of each event is investigated

In future it is planned to use the detectors of the type to study rare nuclear fission modes.

II. Theoretical investigations

1.2.9. Neutron scattering on proton studies

The amplitude spin structure of *s*–wave elastic scattering of slow neutrons on free protons is investigated in theory. A formula for the effective scattering cross section of a polarized slow neutron on a polarized proton is obtained and it is shown that in the effective cross section, triplet (total spin $S = 1$) and singlet (total spin $S = 0$) scattering contributions add together incoherently. At the same time, the maximum value of the integral cross section $\sigma_{max} \approx 37.1$ *barn* corresponds to anti-parallel spin orientation ($\mathbf{P}_n \mathbf{P}_p = -1$, where $\mathbf{P}_n$ and $\mathbf{P}_p$ are polarization vectors) and the minimum value of $\sigma_{min} \approx 3.64$ *barn* – to parallel spin orientation ($\mathbf{P}_n \mathbf{P}_p = +1$) of totally polarized neutrons and protons.
If at least one of the nucleons is not polarized and also, in the case of mutually perpendicular polarization of the vectors ($\mathbf{P}_n \mathbf{P}_p = 0$), the integral cross section of *s* –wave elastic neutron-proton scattering is ≈ 20.4 *barn* at zero energy.

For comparison, low-energy *s* –wave scattering of polarized neutrons, which is only possible in the singlet state if identity is taken into account, is analyzed.

A significant difference, $| b^{(np)} / b^{(nn)} | \approx 1.4$, between the singlet length of *s*- wave *np*-scattering $b^{(np)} = - a^{(np)}(0) = - 23.7$ Fm and the length of *s*- wave *nn*- scattering $b^{(nn)} = - a^{(nn)}(0) = - 17.0$ Fm (which, at first glance, must coincide because of isotopic invariance) is explained by the fact that the scattering length becomes very sensitive to nucleon interaction potential parameters if the nucleon scattering amplitude module is much larger than the radius of force action. In this case, the notion of isotopic invariance is actually applicable not to scattering amplitudes but to potentials of neutron-proton and neutron-neutron interaction that must differ by not more than (2 ÷ 3) %, which, nevertheless, results in a difference between the corresponding amplitudes of several tens of percent. This is confirmed by the calculation in the framework of spherical rectangular well model: a change in the depth or width of the well by only (1.5 ÷ 3) % results in a considerable change in the scattering length.

III. Applied research

1.2.10. Analytical investigations at the reactor IBR-2

Preparation for NAA Sector accreditation

Harmonization of QA/QC Systems According to ISO and International Standards in Nuclear Analytical Laboratories of the Russian Federation

In the framework of the project for technical cooperation with IAEA «Harmonization of Quality Control Systems according to ISO and international standards in nuclear analytical laboratories of the Russian Federation» (RUS7003) the NAA Sector held three IAEA workshops at which IAEA experts gave instructions on how to organize accreditation, including preparation of documentation, equipment, laboratory rooms, and personnel training. In 2008, an extensive documentation package was prepared, a program for rebuilding the chemical laboratory was developed and part of the necessary equipment was purchased with IAEA financial support. The project allowed three members of the sector to work as a trainee in accredited nuclear physics laboratories in Germany, Belgium, Austria, and the Netherlands in late 2008 and early 2009.

NAA Sector experimental base development

IBR-2M. In 2008 work to improve spectrometric and service equipment of the facility REGATA at the reactor IBR-2 continued. Semi-conducting germanium detectors and a set of electronic blocks of *Canberra* make were purchased. The detector is calibrated with respect to efficiency and the obtained data are included in the program for element concentration calculation. Background measurements in different rooms of the laboratory building, including bomb-proof shelter, were conducted with the aim of finding a place for natural radioactivity measurements of the sample. To reduce the background, germanium detector shielding was taken for temporary use and was assembled. The program package for experimental data processing is being updated. On the basis of design documentation earlier developed by FLNP DB new irradiation channels for REGATA at the reactor IBR-2M were built by JINR Experimental Workshops in 2008. A delivery pipe to fill detectors with liquid nitrogen was manufactured and assembled. Under Technical Cooperation Project, IAEA supplied a lyophilizer (low temperature drying device) for sample preparation; in near future sample homogenizing equipment (ball mill), *etc.* will be purchased.

IREN. In the reported period possibility of NAA experiments at the new neutron source IREN was estimated theoretically. Flux density distributions of thermal, resonance, and fast neutrons around the target were calculated and an optimal site for irradiation channel positioning was found. Together with «Development and Application Base in Physics (DAB-Physics)», Sofia, Bulgaria, and JINR DB a design of pneumatic system for NAA studies at IREN was developed.

Biomonitoring

In 2008 a cycle of studies and publications in the framework of the international program «Heavy metal atmospheric deposition in Europe – estimations based on moss analysis», completed. The work covered some regions in Central Russia, South Urals, Belarus, Bulgaria, Slovakia, Poland, Romania, Serbia, Macedonia, Croatia, and Greece as well as in Mongolia and Vietnam. The results for the European part are reflected in a regular issue for 2008 of the Atlas "Spatial and Temporal Trends in Heavy Metal Accumulation in Mosses in Europe (1990-2005)" published by the UN Commission for Transboundary Transfer of Air Pollution in Europe.

In collaboration with Opole University (Poland) there was carried out an integrated study to assess the environmental condition over an "anomalous territory" in the west of Poland characterized by an increased radioactive background due to Chernobyl accident and impact of industry. The first results were published in the Polish journal «*Ecological Chemistry and Engineering*» in 2008.

In 2008, in collaboration with the Institute of Physics in Belgrade, Serbia, and the Norwegian University of Science and Technology in Trondheim an extended methodological investigation in calibration measurement of element content in atmospheric precipitation and moss-transplants used for assessment of deposition of heavy metals and other elements was conducted. The related article is accepted for publication in the international journal *Environmental Pollution* (IF 3.2).

Work to study atmospheric pollution over the territory of the Udmurt Republic using the moss-biomonitor analysis method is completed. The related article is accepted for publication in the Russian general science journal «*Regional Ecology Problems*». In the work the moss-biomonitor method was first applied to assess the situation in the region of a chemical weapon destruction polygon.

Ecosystem condition assessment

Under the auspices of the RFFI-Romanian Academy project «Geochronology and retrospective study of pollution of unconsolidated sediments from oxygenated and anoxic territories of the Western Black Sea», retrospective assessment of pollution in the region was carried out in 2008. Six publications were prepared together with Romanian colleagues. RFFI approved prolongation of the project for 2009.

In 2008, many-year collaboration with Mongolian scientists in the field of ecology resulted in a landmark project «Development of a system of complex monitoring heavy metals and radionuclides in Mongolia based on nuclear and related analytical techniques» with financial support of RFFI and Mongolia.

In collaboration with Macedonia (University in Scopje) an atlas containing maps of distribution of a number of heavy metals around the lead-zinc industrial plant in the town of Veles is published in 2008.

The results of multielement NA-analysis of a collection of aerosol filters for different years obtained from Bratislava are reflected in the article accepted for publication in one of the most prestigious international journals in ecology "*Atmospheric Environment*" (IF 2.6) in 2008.

Food products and human health

In 2008 at the reactor of Moscow Physics Engineering Institute (Moscow) food product analysis in connection with the NAA Sector-NICSA (South Africa) project "Comparative Nuclear Physics Analytical Studies of Consumption Effect of Food Products Grown in Some Industrial Regions of Russia and South Africa on Children's Health" continued. The results are presented as a review of investigations conducted in JINR and NECSA, South Africa.

In 2008, in the framework of the IAEA coordination program «Impact of Toxic and Potentially Toxic Elements on Women of Reproductive Age in Developing Countries», work on multielement

analysis of blood samples of specially selected patients from one of the industrial regions in Moscow carried out in collaboration with the RF State Medical University (Moscow), Analytical Center of the Geological Institute, RAS and I.P.Sechenov Medical Academy, completed. The study confirmed the hypothesis that there exists correlation between such toxic elements as lead, zinc and antimony and Body Mass Index in the examined patients. The results are reported to the International Congress of Epidemiologists in Brazil in September, 2008 and are published in the journal "*Public Health and Disease Prevention*", Moscow in 2008.

Biotechnologies

Work in the field of biotechnological methods of removing toxic elements (mercury, chromium, *etc*) from the environment is carried out by the NAA Sector in collaboration with E.Andronikashvili Institute of Physics (Tbilisi, Georgia). New results on the use of natural bacterial strains extracted from basalt rock to reduce toxic chromium (VI) to nontoxic chromium (III) published in 2008. It is found that as toxic chromium (VI) load in the bacterium *Arthrobacter oxidans* increases the concentration of other elements changes essentially in the direction of either increase or decrease. The results are of importance for biochemists working in the field of biotechnologies.

Material sciences

Fine-crystalline diamond synthesis

The investigation of the behavior of defects in fine-crystalline diamonds under the action of neutron radiation in the presence of a catalyst conducted together with specialists from the Institute of Solid State and Semiconductor Physics of NASB, Minsk, Belarus, completed and the results are presented as a separate chapter in the book «Diamond and Related Materials» (USA) in print.

Radioecology

The method of moss-biomonitors was applied in Belarus for the first time to estimate atmospheric deposition of radioactive nuclides 20 years after the Chernobyl accident. Measurements of long-lived radioactive nuclides – nuclear fuel fission products – were performed together with Slovakian specialists from the Low Background Laboratory of Bratislava University in 2008. Part of the collected samples was analyzed by NECSA (South Africa) specialists. It is shown that ^{137}Cs activity levels in mosses collected in the territory of the Gomel region are 4 times the background. An increased content of ^{210}Pb was also noted. The results were presented at "The 22nd Task Force Meeting of the UNECE ICP Vegetation" in Germany in February 2009.

Training

On the basis of the REGATA facility, training courses were organized for senior-year students of the University of Dubna and for students of International Summer Schools held by the JINR University Center (from Bulgaria, Czech Republic, Slovakia in July and from the South African Republic in September-October). In the period of report two term papers, one bachelor' degree paper and three master's degree papers on investigations performed in the NAA sector.

Organization of Scientific Meetings

- Second Workshop in the framework of the Project for Technical Cooperation between IAEA and NAA Sector FLNP «Harmonization of Quality Control Systems according to ISO and international standards in nuclear analytical laboratories of the Russian Federation» (May 26-30, 2008, Dubna;
- A third IAEA workshop of the same name (October 27-31, 2008, Dubna).

1.2. НЕЙТРОННАЯ ЯДЕРНАЯ ФИЗИКА

Введение

В течение 2008 основные работы в области нейтронной ядерной физики в ЛНФ им. И. М. Франка проводились на нейтронных пучках ядерных центров России, Германии, Республики Корея, Китая, Франции, а также на ускорителе ЭГ-5 в ЛНФ. Исследования проводились в традиционных направлениях: изучение процессов нарушения пространственной и временной четности при взаимодействии нейтронов с ядрами; изучение квантово-механических характеристик, энергетики и динамики процесса деления; экспериментальное и теоретическое исследование электромагнитных свойств нейтрона и его бета-распада; гамма-спектроскопия нейтронно-ядерных взаимодействий; структура атомного ядра; получение новых данных для реакторных приложений и для ядерной астрофизики; эксперименты с ультрахолодными нейтронами; прикладные исследования. Параллельно велась подготовка экспериментов на первой очереди установки ИРЕН, а также на реакторе ИБР-2М в ЛНФ.

I. Экспериментальные исследования

1.2.1 Работы в рамках подготовки и проведения эксперимента по прямому измерению сечения рассеяния нейтрона на нейтроне на реакторе ЯГУАР (РФЯЦ-ВНИИТФ, г.Снежинск)

Калибровочные измерения на инертных газах.

Калибровочные измерения на газах нужны для отработки методики и проверки достоверности получаемых результатов. Смысл измерений состоит в том, чтобы на установке для измерения сечения nn-рассеяния измерить хорошо известное сечение рассеяния тепловых нейтронов на инертном газе. Если полученное значение совпадет с табличным, то значит, измерения проведены методически верно, и по этой же методике можно измерять сечение nn-рассеяния. Нужно отметить, что наше знание об эффективности детектора не совсем точное. Поэтому нужно исходить из того, что эффективность детектора нам не известна. Соответственно измерения нужно проводить на различных газах. На одном газе, например на ^{4}He, определяется эффективность детектора, а на Ar измеряется сечение рассеяния.

На рис. 1 представлены результаты калибровочных измерений на ^{4}He и на Ar.

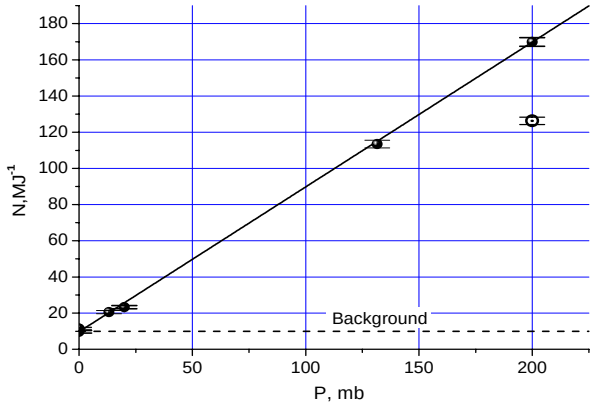

Рис. 1 ***Результаты калибровочных измерений. По оси ординат отложен счет детектора на 1 МДж энерговыделения реактора, по оси абсцисс – давление газа при 20^{o}C. Черные точки – измерения на ^{4}He, светлая точка – на Ar,сплошная линия – линейная аппроксимация экспериментальных данных.***

Из представленных данных видна четкая линейная зависимость счета детектора от давления газа, что указывает на методическую правильность проведения измерений.

Табличные значения сечений рассеяния: $\sigma_T(^4\text{He}) = (0.79\pm0.02)$ б, $\sigma_T(\text{Ar}) = (0.656 \pm 0.003)$ б.

Полученное экспериментальное сечение рассеяния на Ar: $\sigma_Э(\text{Ar}) = (0{,}642 \pm 0{,}024)$ б, что хорошо согласуется с табличным значением.

Первая попытка измерения сечения n-n рассеяния.

Формулу для расчета числа nn-рассеяний в полости nn-рассеяния реактора ЯГУАР можно записать в виде:

$$N_{nn} \sim \iint \frac{\Phi^2(t,\vec{r})}{v_0} \sigma_{nn} dt dV$$

Где t – время, V – объем полости nn-рассеяния, $\Phi(t,\vec{r})$ – плотность потока тепловых нейтронов, v_0 = 2200 м/с, σ_{nn} – сечение nn-рассеяния.

Из этой формулы видно, что число nn-рассеянных нейтронов пропорционально произведению квадрата плотности потока на длительность импульса. Плотность потока нейтронов пропорциональна мощности реактора, поэтому по зависимости числа зарегистрированных за импульс нейтронов от энергии импульса можно понять, что является источником регистрируемых нейтронов. Так, например, число нейтронов рассеянных на стенках канала или на краях коллиматоров имеет линейную зависимость от энергии импульса и не зависит от его длительности. Т.к. длительность импульса реактора ЯГУАР приблизительно обратно пропорциональна его энергии, то зависимость числа nn-рассеянных нейтронов от энергии импульса будет близка к кубической зависимости.

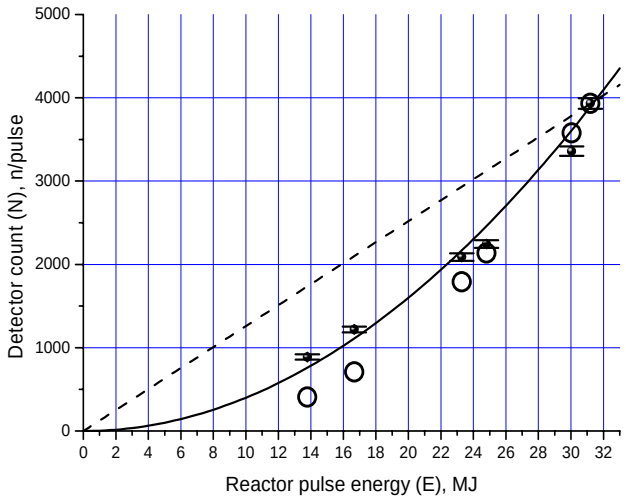

Рис. 2 ***Зависимость числа сосчитанных за импульс нейтронов от энергии импульса реактора ЯГУАР. Черные точки – экспериментальные данные; штриховая линия – линейная зависимость: N ~ E; сплошная линия – квадратичная зависимость: N ~ E^2; светлые точки – расчетная зависимость числа nn-рассеянных нейтронов с учетом реальной формы импульсов.***

На Рис. 2 представлена зависимость числа сосчитанных за импульс нейтронов от энергии импульса реактора ЯГУАР. На этом рисунке все расчетные зависимости приведены к экспериментальному значению при 31 МДж. Как видно, экспериментальные данные близки к квадратичной зависимости и значительно отличаются как от линейной зависимости, так и от зависимости для nn-рассеяния. Отличие от линейной зависимости указывает на то, что в полости для nn-рассеяния меняется число объектов, на которых рассеиваются нейтроны. При квадратичной зависимости число таких объектов будет пропорционально энергии импульса, или флюенсу, а не плотности потока нейтронов. Т.е. эти объекты в течение импульса накапливаются в полости для nn-рассеяния. Наиболее вероятная кандидатура для них – молекулы газа, слетающие со стенок под воздействием излучения реактора. Иначе говоря, мы наблюдаем радиационную десорбцию.

Подавление радиационной десорбции возможно обезгаживанием поверхности полости nn-рассеяния непосредственно перед импульсом реактора и заменой материала стенок на низкоабсорбционные материалы. Работы по исследованию радиационной десорбции на установке для измерения сечения nn-рассеяния планируется провести в следующем году.

1.2.2. Эксперимент по изучению квазизеркального отражения холодных нейтронов от поверхности нанопорошка

Последовательное рассеяние частиц/квантов на малые углы в среде – малоугловое рассеяние приводит к тому, что при падении пучка частиц/квантов на среду под скользящим углом, угловое распределение отражённых частиц/квантов имеет выраженный максимум при угле, близким к углу падения. Аналогичная ситуация должна быть и для нейтронов при падении нейтронов под малым углом на среду с эффективным малоугловым рассеянием. Наночастицы с

размером в несколько нанометров могут эффективно рассеивать на малые углы холодные нейтроны. В тоже время малость длины волны нейтрона по сравнению с частицой, обеспечивающая малость угла при рассеянии, позволяет рассматривать взаимодействие нейтронов с наночастицчами в порошке как с независимыми частицами.

Мы попытались экспериментально определить параметры данного явления при отражении нейтронов от порошк ананоалмазов. Для этого измерили зависимость углового распределения нейтронов, отражённых от поверхности алмазного нанопоршка, для различных длин волн падающих нейтронов при углах падения нейтронного пучка на поверхность в 2°, 3° и 4°. Схема измерения показана на **рис. 3**. Образец был изготовлен в виде призмы, габариты которой 15 см в длину, 5 см в высоту и 4 см в глубину и помещён в специальный криостат. Поверхность порошка закрыта алюминиевой фольгой толщиной 100 мкм. Рассеяние на стенках криостата пренебрежимо мало с рассеянием на образце. Пучок нейтронов имел выходную диафрагму 15 мм в высоту и 0.3 мм в ширину. Рассеянные нейтроны регистрировались в угле ±12° от падающего пучка в вертикальной плоскости.

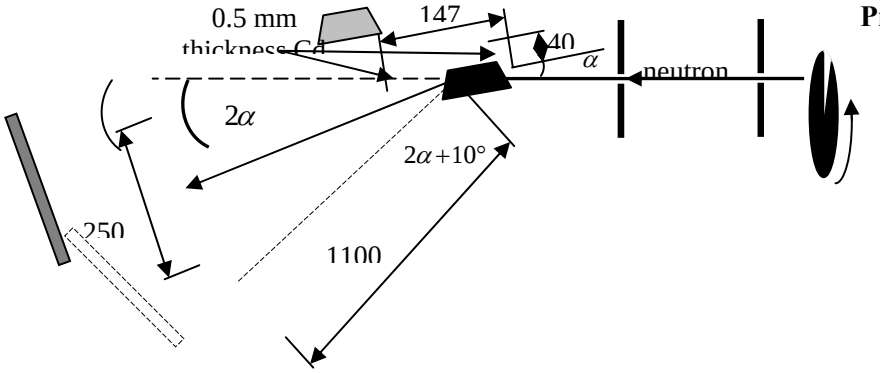

Рис. 3 Схема измерения.

Результаты измерений представлены на **рис. 2, рис. 3 и рис.4.** Как и ожидалось, в результате многократного рассеяния на наночастицах нейтроны отражаются от поверхности с относительно узким угловым распределением, максимум которого находится под углом близким угол зеркального отражения. Чем меньше длина волны падающих нейтронов, тем шире угловое распределение рассеянных нейтронов. При увеличении угла падения нейтронного пучка угловое распределение так же уширяется. Таким образом для холодных нейтронов с длинной волны λ от 4 Å до 8 Å наблюдается квазизеркальное в плоскости рассеяния альбедо на малых углах падения (меньше 6 -7) с вероятностью ~25%. При длинах волн меньше 4 Å квазизеркальное альбедо подавлено бреговским рассеянием, а при λ больше 8 Å угловое распределение становится слишком широким, что бы говорить о квазизеркальности. При падении нейтронов под углами большеми чем 6 -7 вероятность квазиупругого отражения становится соизмеримой с вероятностью рассеяния на углы много больше угла зеркального отражения.

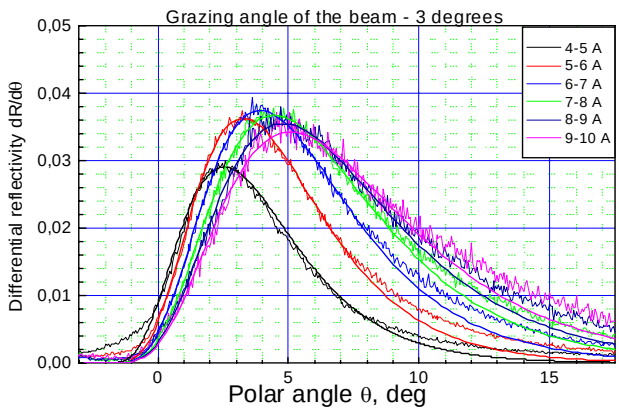

Рис. 4 Зависимость потока отражённых нейтронов от полярного угла для нейтронов с энергиями в различных диапазонах (указано на картинке) при скользящем угле падения нейтронов на поверхность 3º. Экспериментальные зависимости аппроксимированы логнормальным распределением, дисперсия которого выбрана в качестве характеристики ширины углового распределения потока.

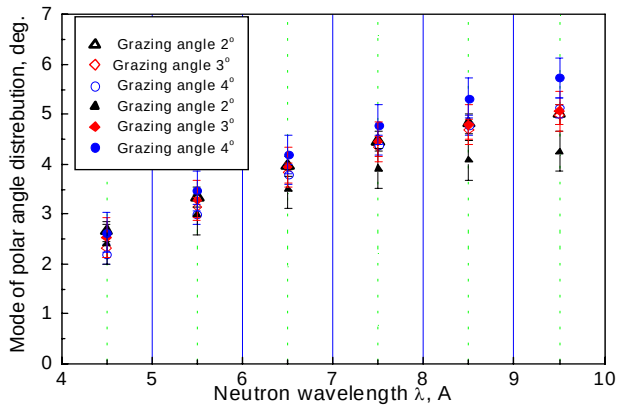

Рис. 5 Положение максимума в распределении потока отраженных нейтронов от полярного угла в зависимости от длины волны нейтронов, при различных углах падения и температуре.
Открытые точки — результаты измерений при температуре жидкого азота, закрашенные точки — результаты измерений при комнатной температуре.

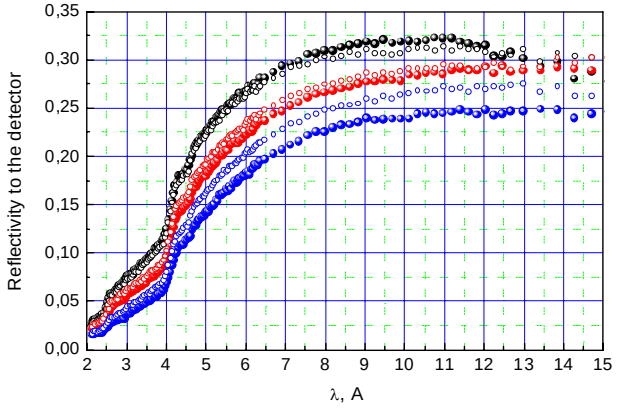

Рис. 6 Зависимость вероятности отражения в детектор от длины волны нейтронов при различных углах падения и температуре.
Чёрные точки — угол падения 2º.
Красные точки — угол падения 2º.
Синие точки — угол падения 2º.
Открытые точки — результаты измерений при температуре жидкого азота, закрашенные точки — результаты измерений при комнатной температуре.

Для больших углов и больших λ (когда поперечная составляющая скорости нейтрона превышает ~50 m/s такое квазизеркальное альбедо превышает вероятность отражения от существующих суперзеркал (отражение от которых при таких скоростях также имеет квазизеркальный характер)

Измерения проводились дважды: при комнатной температуре на образце после его предварительной подготовки (длительной откачки и обезгаживании при 150°C), а затем при температуре -150°C. При охлаждении образца канал неупругого практически изотропного рассеяния на углероде и примесных атомах водорода должен быть подавлен. В противоположность нашим ожиданиям, охлаждение образца привело к увеличению вероятности отражения, в основном, за счёт квазизеркальной компоненты.

1.2.3. Эксперименты с ультрахолодными нейтронами

На созданном пучке УХН на реакторе TRIGA в Университете г.Майнц проведены времяпролётные измерения по исследованию свойств cBN – нитрида бора с кубической структурой как материала для построения камер УХН с высокой граничной энергией.

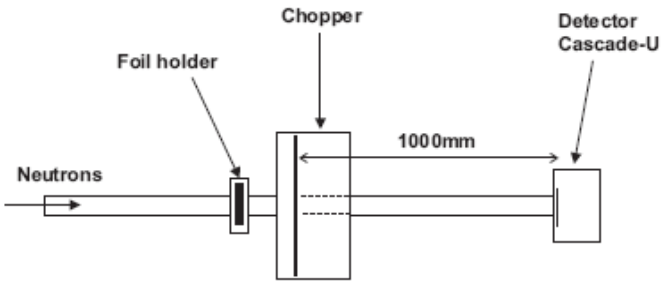

Рис. 7 Схема эксперимента

Этот материал очень прочен, не магнитен, имеет высокое электрическое сопротивление, в том числе и по отношению к поверхностным токам и поэтому может быть перспективным материалом для построения камер для поиска ЭДМ нейтрона.

При известной плотности нитрида бора 3.5 г/см^3 мы ожидаем величину граничной энергии 324 нэВ для вещества с естественным содержанием изотопов бора, а для обогащённого по изотопу B-11 значения E=351 нэВ.

Исследуемые материалы наносились на поверхность монокристаллических пластин толщиной 380 мк методом магнетронного осаждения. Толщина слоёв была 300 нм.

На основе анализа времяпролётных спектров с образцом и без образца были определены граничные энергии нитрида бора: E=305 $\pm$ 15 нэВ и используемого для калибровки никеля: E=240 $\pm$ 15 нэВ.

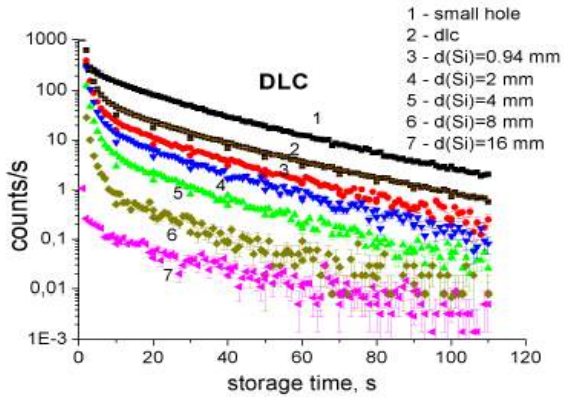

Рис. 9

Figure 4: The typical measured time dependent count rate (DLC sample foil): 1 – the UCN flux density measured through 2.5 mm diameter hole in the sample foil, 2 – the count rate through the DLC foil at the 100 μm Al substrate, no additional absorber, 3-7 – the count rate through the DLC foil with different Si absorbers between the scatterer and the neutron detector. The time shown from the moment of opening of the UCN valve after the filling time 20 seconds.

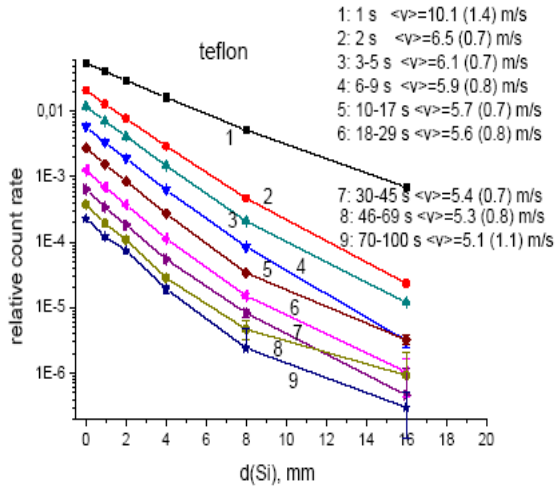

Рис. 8

Figure 8: The neutron count rate (relative to the incident UCN flux) for the teflon sample as a function of Si thickness after subtracting the contribution of up-scattering to the thermal energy range. The inferred neutron mean velocities and half-widths of the Gaussian distributions (in brackets) for corresponding storage time intervals are shown in the insert. The straight lines connect the experimental points.

На пучке реактора ИЛЛ проведены измерения «малого нагрева» УХН на образцах меди, тефлона и алмазоподобного углерода. Измерены спектры нагретых нейтронов при энергиях от УХН до тепловых а также эволюция во времени спектров УХН в ловушке. Разработан метод «калиброванных поглотителей» для измерения спектров нейтронов. В качестве поглотителей применялись монокристаллические пластины кремния и родиевые фольги. Спектры нейтронов определялись из кривых поглощения в моноэнергетическом и более детальном приближениях.

На рис. 8 показаны: пример скорости счета детектора в функции времени для разных поглотителей и кривые поглощения, из которых определяется энергия хранящихся и нагретых нейтронов.

Обнаружено, что разные материалы дают разные спектры нагретых нейтронов, а также, что спектр нагретых нейтронов простирается в область мкэВ-энергий.

1.2.4. Изучение механизма взаимодействия нейтронов с ядрами

Изучение механизма взаимодействия нейтронов с ядрами представляет большой интерес для понимания законов природы. К настоящему времени нейтронные реакции с вылетом заряженных частиц были исследованы недостаточно. Исследование реакций (n,p), (n,t), (n,альфа) на нейтронах, производящихся в различных лабораториях, дают ценную информацию о механизме протекания ядерных реакций и структуре атомного ядра, в частности, сведения о роли одночастичной и многочастичных компонент в возбуждении компаунд-ядер и выявлении эффектов селективного усиления и распада коллективно-кластерных состояний ядер

относительно чисто статистического распределения. Использование пучков нейтронов с энергией в несколько МэВ позволяет не только получить усреднение по большому числу начальных состояний возбужденного ядра, но и повысить на несколько порядков проницаемость кулоновского барьера ядра для реакций (n,p), (n,t), (n,альфа) по сравнению с реакциями, вызванными резонансными нейтронами, а так же проследить изменение характеристик распада с увеличением энергии возбуждения ядра по мере приближения к области гигантских дипольных резонансов. Планируется проведение экспериментальных исследований реакций (n,p), (n,t) или (n,альфа) на предельно легких ядрах (6Li, 9Be, 10B,), легких (14N, 20,21Ne, 24Mg, 28Si, 35Cl), а так же на ядрах средней массы A~40-70 (39K, 54,57Fe, 58Ni, 63Cu, 64, 67Zn, 95Mo) и тяжелых A~150 (143Nd, 147,149Sm)в широком диапазоне энергии нейтронов от нескольких кэВ и пока до 6.5 МэВ. Сравнение существующих данных показывает, что в диапазоне энергий от 3 до 10 МэВ экспериментальные данные немногочисленны, и существуют значительные расхождения между значениями, приводимыми разными авторами. В большинстве случаев исследования этих реакций велись с использованием активационного метода, который оказался недостаточным для надежного разделения прямых, предравновесных и компаунд-процессов. Нами используется метод прямой регистрации и спектрометрии вылетающих частиц на пучках нейтронов, позволяющий непосредственно получать спектры вылетающих заряженных частиц, определять полное сечение реакций, угловое распределение продуктов реакций.

Эксперименты проводятся на ускорителях Ван-де-Граафа ЭГ-5 в Лаборатории нейтронной физики ОИЯИ и ЭГ-4,5 Института физики тяжелых ионов Пекинского университета совместно с Пекинским университетом и при сотрудничестве с Лодзинским (Польша) и Монгольским национальным университетами.

В 2008 г.:

- Разработана система мишеней для получения быстрых нейтронов на канале ЭГ-5 (в стадии изготовления в ОП ЛНФ);
- Подготовлены чертежи Ионизационной камеры для работы на ЭГ-5 и ИРЕН;
-Подготовлены чертежи «протонного телескопа» для работы на ЭГ-5;
- По измерениям реакции 64Zn(n,a) при энергии нейтронов 2,54; 4,00 и 5,50 МэВ подготовлена и опубликована статья в журнале Nucl.Sci.Eng.
- Закончена обработка измерений реакции 147Sm(n,a)143Nd при энергии нейтронов 5,0 и 6,0 МэВ, подготовлена и принята к печати статья в журнале Applied Radiation and Isotopes (см. прилагаемую к отчету статью);
-Проведены измерения реакции 143Nd(n,a)140Ce при En=4, 5 и 6 МэВ; начата обработка данных;
-Проведены измерения реакции 95Mo(n,a)92Zr при En=4, 5 и 6 МэВ; готовится измерение фона;

1.2.5. Подготовка экспериментов на первой очереди ИРЕН

В течение года проводились работы по подготовке к экспериментам на первой очереди нейтронного источника ИРЕН.

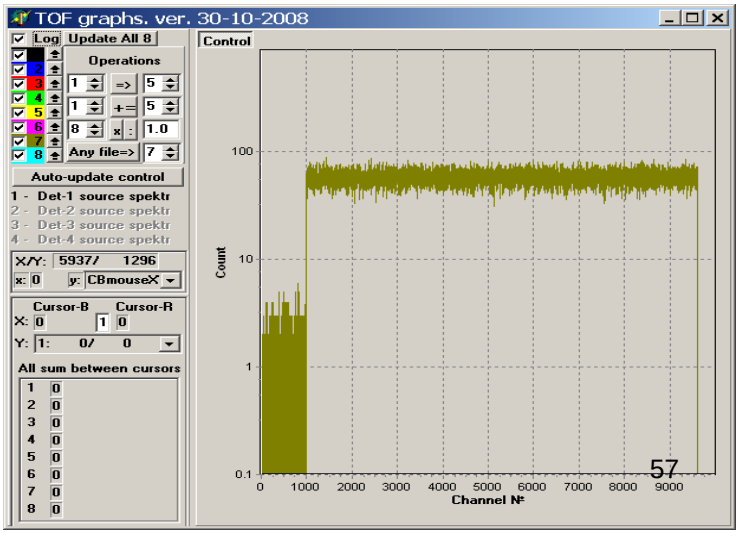

Рис. 10 Иллюстративное окно визуализации измеряемого спектра программы «Tof_usb».

а) Осуществлена модернизация измерительного модуля гамма-спектрометра «КОКОС», позволившая существенно увеличить его быстродействие: разработан и изготовлен интерфейс под USB-1 и создана новая программа накопления экспериментальной информации «Lada».
б) Разработаны, изготовлены и испытаны блоки быстрого временного анализа с шириной канала 10 – 20 нс для проведения спектрометрии нейтронов по времени пролёта. Разработано программное обеспечение системы с быстрым временным анализом для регистрации 4-х TOF спектров «TOF_usb». Система предназначена для исследования параметров пучка нейтронного источника ИРЕН. Помимо этого, разработаны дополнительные алгоритмы и включены в данную программу для выполнения прецизионных экспериментов.

1.2.6. Гамма-спектроскопия нейтронно-ядерных взаимодействий

Продолжался анализ и интерпретация экспериментальных данных по интенсивностям двухквантовых каскадов при захвате тепловых нейтронов различными ядрами.
Суммы радиационных силовых функций дипольных первичных гамма-переходов аппроксимированы с высокой точностью полуфеноменологической зависимостью в области энергий первичных гамма-переходов $0.5 < E_1 < B_n$-0.5 МэВ для большого количества ядер. В качестве основной гипотезы использована гипотеза: экспериментальные данные можно представить в виде суперпозиции двух сильно различающихся функций. Плавно изменяющаяся функция – описывает изменение вероятности эмиссии гамма-кванта, обусловленное возбуждениями ядра фермионного типа, ярко выраженные пики - обусловлены возбуждениями ядра бозонного типа.

Результаты аппроксимации дали внутренне согласованную и непротиворечивую картину происходящих в ядре процессов практически для всей периодической системы и подтвердили полученный ранее при анализе плотности уровней результат: параметры процесса каскадного гамма-распада нейтронного резонанса определяются сосуществованием и взаимодействием в нагретом ядре сверхтекучей и обычной его фазы.

Получено, что форма радиационных силовых функций в исследованных ядрах являются динамической величиной (циклически изменяющейся при изменении массы ядер), а значения *k(E1)+k(M1)* для конкретных энергий гамма-переходов и конкретных ядер определяются структурой распадающегося и возбуждаемого уровней, по крайней мере, до энергии связи нейтрона B_n. Результат определяет наименьшие размеры области возбуждений ядра, в которой необходимо учитывать и из которой можно получать информацию о динамике изменения процесса перехода ядра из бозе- в ферми-систему при его нагревании.

Эти же экспериментальные данные продолжают использоваться как для получения новой спектроскопической информации о деформированных ядрах в значительно большем интервале энергий возбуждения, чем доступно традиционной ядерной спектроскопии, так и для тестирования различных моделей ядра. В частности, получено, что экспериментальные полные гамма-спектры двух четных изотопов олова воспроизводятся в расчете с наибольшей точностью при использовании именно ступенчатой плотности уровней и радиационных силовых функций, учитывающих усиление силовых функций первичных и вторичных каскадных гамма-переходов в область возбуждений, соответствующей этой структуре спектра возбужденных уровней ядра.

Хотя в силу методических особенностей эксперимента по измерению интенсивности двухквантовых каскадов и плотность уровней, и силовые функции определяются с наибольшей точностью по сравнению с конкурирующими методиками, существует необходимость в выявлении основных источников систематических погрешностей и в существенном уменьшении их величины. В частности – разработке новых и независимых методик определения этих параметров ядра.

Независимое подтверждение наличия значительной ступенчатой структуры в плотности уровней получено при реанализе опубликованных к настоящему времени данных об экспериментальных интенсивностях первичных гамма-переходов, усредненных по нейтронным резонансам в районе их энергий 2 и 24 кэВ. Распределение разброса этих интенсивностей

относительно среднего значения впервые аппроксимировано в различных интервалах энергий первичных гамма-переходов в представлении о том, что их интенсивности зависят от структуры возбуждаемого уровня, а дисперсия их случайных отклонений не описывается χ^2 распределением с одной степенью свободы (как то предполагается до сих пор).

Определенные таким образом плотности уровней и суммы радиационных силовых функций подтверждают характерные особенности аналогичных данных, извлеченных из интенсивностей двухквантовых каскадов радиационного захвата тепловых нейтронов для ядер с $40 \leq A \leq 200$, и позволяют так же оценить знак и величину их результирующей систематической погрешности, обусловленной прежде всего очень сильной зависимостью радиационных силовых функций каскадных гамма-переходов от структуры возбуждаемого уровня. Заключение справедливо, во всяком случае, для энергий возбуждения, меньших половины энергии связи нейтрона. Сопоставление с модельными представлениями о плотности уровней показывает, например, что ядро ^{174}Yb находится в сверхтекучем состоянии для основной части возбужденных уровней по крайней мере ниже 3.5-4 МэВ. Более того, впервые удалось получить предварительную информацию о соотношении числа уровней с доминирующими компонентами квазичастичного и фононного типа до этой же энергии возбуждения четно-четного деформированного ядра (определена зависимость коэффициента вибрационного усиления плотности квазичастичных уровней от энергии возбуждения).

Использование совместного анализа экспериментальных данных по интенсивностям двухквантовых каскадов обещает повысить точность определения свойств ядра, по крайней мере, ниже энергии связи нейтрона.

1.2.7. Измерение ядерного заряда осколков деления на установке миниФОБОС

Поиск и исследование редких, в том числе многотельных, мод распада слабо возбужденных ядер остается актуальной задачей экспериментальной ядерной физики. Именно в этой области энергий возбуждения можно ожидать ранее неизвестных проявлений кластеризации ядерных систем. Надежная идентификация необычных каналов распада предполагает одновременное измерение возможно большего числа различных параметров процесса – масс и энергий продуктов распада, их угловых распределений, множественности нейтронов и т.д. Естественно, весьма желательно измерение ядерного заряда образующихся фрагментов.

В серии экспериментов по поиску тройного коллинеарного кластерного распада (ТККР) тяжелых ядер использовался двух плечевой времяпролетный спектрометр заряженных продуктов ядерных реакций миниФОБОС на базе газонаполненных детекторов. Спектрометр позволяет измерять вектора скорости фрагментов и их энергии. Через скорости можно определить так называемые первичные массы осколков (Mtt) бинарного деления, а через скорости и энергии - массы осколков после сброса нейтронов (Mte). Для измерения энергии фрагментов служат большие ионизационные камеры (БИК), использовавшиеся в 4π-спектрометре ФОБОС.

Измерение ядерного заряда осколков деления по времени дрейфа образованного ими трека в ионизационной камере представляет собой технически более сложную задачу, чем измерение энергии. Разрешение по заряду непосредственно зависит от однородности электрического поля и постоянства массы газа в рабочем объеме камеры. Для обеспечения второго из условий недостаточно стабилизировать только давление и состав газовой смеси – дополнительно необходима термостабилизация камеры. Перечисленные условия были обеспечены в эксперименте на широкоаппертурном спектрометре миниФОБОС по исследованию реакции ^{235}U(n_{th},f) на пучке реактора ИБР-2. Для вычисления ядерного заряда фрагментов по полученным в эксперименте данным было разработано два варианта калибровки по заряду. Тестирование на модельных данных показало, что использованная параметризация заряда в рамках процедуры калибровки позволяет удовлетворительно восстанавливать ядерный заряд осколков деления в широком энергетическом диапазоне. Предсказываемые в рамках этого

подхода заряды легких ионов от He до C оказываются смещенными в большую сторону приблизительно на две зарядовых единицы.

1.2.8. Исследование свойств детектора TIMEPIX при регистрации излучения из источников ^{244}Cm и ^{252}Cf

В ЛНФ ОИЯИ совместно с Политехническим институтом (г. Прага) ведутся исследования пиксельных детекторов MEDIPIX и возможности их применения в области ядерной физики, в частности, для изучения процесса деления. Детектор MEDIPIX представляет собой две кремниевые пластины, одна из которых является сенсорной частью, в которой регистрируются налетающие частицы, а другая состоит из множества пикселей, каждый из которых является спектрометрическим трактом, включающим в себя усилитель, дискриминатор и счетчик. Обе пластины соединены между собой в каждом пикселе методом “bump-bonding”.

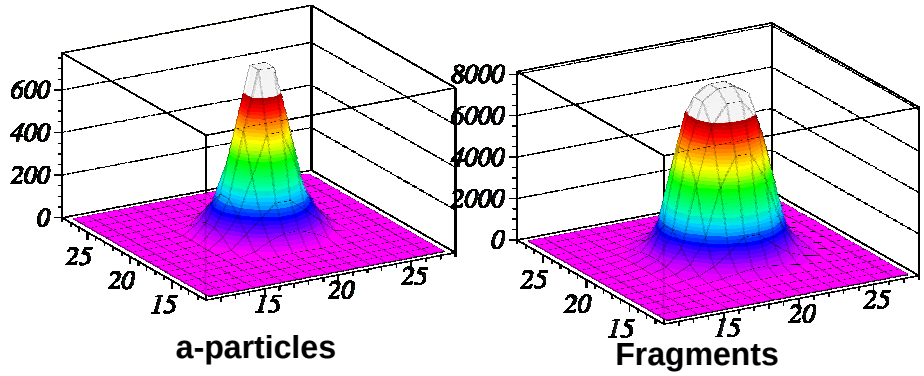

Рис. 11 Распределение энергии в кластере для альфа-частиц и осколков деления.

В ОИЯИ исследовалась возможность измерения осколков деления и легких заряженных частиц (из спонтанных источников 244Cm и 252Cf) с помощью двух типов детекторов: MEDIPIX2 и TIMEPIX. При попадании частицы в чувствительный слой детектора, возникает так называемый эффект распределения заряда (charge sharing effect), при котором заряд распределяется на несколько пикселей, формируя таким образом кластер. Размер кластера зависит от установленных порогов, а также от заряда и энергии налетающей частицы. В детекторе MEDIPIX2 можно наблюдать двумерную картинку, на которой четко видна разница в размере кластера для альфа-частиц и для осколков деления. Более того, проведя соответствующую калибровку, удалось измерить двугорбую кривую энергетических распределений осколков деления, используя только размеры кластеров.

Новый тип MEDIPIX детекторов - TIMEPIX позволяет регистрировать время срабатывания дискриминатора в каждом пикселе. При соответствующих настройках это время можно конвертировать в амплитуду, таким образом измеряя величину заряда в пикселе. Получается трехмерная картинка (см. рис справа). Это позволяет более точно определять энергию налетающей частицы. Ведутся исследования по возможности идентификации частиц по заряду и массе, а также по определению угла вхождения частицы в детектор, используя такого рода трехмерные «снимки» каждого события.

В перспективе планируется использование такого рода детекторов в экспериментах по изучению редких мод деления ядер.

II. Теоретические исследования

1.2.9. Исследование рассеяния нейтрона на протоне

Теоретически исследована спиновая структура амплитуды s -волнового упругого рассеяния медленного нейтрона на свободном протоне. Получена формула для эффективного

сечения рассеяния медленного поляризованного нейтрона на поляризованном протоне и показано, что в эффективном сечении вклады триплетного (полный спин $S = 1$) и синглетного (полный спин $S = 0$) рассеяния складываются некогерентно. При этом максимальное значение интегрального сечения $\sigma_{max} \approx 37{,}1$ *барн* соответствует антипараллельной ориен-тации спинов ($\mathbf{P}_n \mathbf{P}_p = -1$, где $\mathbf{P}_n$ and $\mathbf{P}_p$ – векторы поляризации) , а минимальное значение $\sigma_{min} \approx 3{,}64$ *барн* – параллельной ориентации спинов ($\mathbf{P}_n \mathbf{P}_p = +1$)
полностью поляризованных нейтрона и протона . В случае, когда хотя бы один из нуклонов не поляризован, а также в случае, когда векторы поляризации взаимно перпендикулярны ($\mathbf{P}_n \mathbf{P}_p = 0$) , интегральное сечение s -волнового упругого рассеяния нейтрона на протоне при нулевой энергии составляет $\approx 20{,}4$ *барн* .

Для сравнения, выполнен также анализ низкоэнергетического s -волнового рассеяния поляризованных нейтронов, которое с учетом тождественности возможно только в синглетном состоянии.

Существенное различие $-\,|\, b^{(np)} / b^{(nn)} \,| \approx 1{,}4$ – между синглетной длиной s- волнового np- рассеяния $b^{(np)} = -a^{(np)}(0) = -23{,}7$ Фм и длиной s- волнового nn- рассеяния $b^{(nn)} = -a^{(nn)}(0) = -17{,}0$ Фм (которые, на первый взгляд, должны были бы совпадать ввиду изотопической инвариантности) объясняется тем, что длина рассеяния становится очень чувствительной к параметрам потенциала взаимодействия нуклонов при условии, что модуль амплитуды рассеяния нуклонов сильно превосходит радиус действия сил. В этом случае понятие изотопической инвариантности фактически применимо не к амплитудам рассеяния, а именно к потенциалам нейтрон-протонного и нейтрон-нейтронного взаимодействия, которые должны отличаться не более чем на (2 ÷ 3) % – приводя, тем не менее, к отличию соответствующих амплитуд на несколько десятков процентов. Это подтверждается проведенными расчетами в модели сферической прямоугольной ямы : изменение глубины или ширины ямы всего на (1,5 ÷ 3) % приводит к весьма значительному изменению длины рассеяния

III. Прикладные исследования

1.2.10. Аналитические исследования на реакторе ИБР-2

Подготовка к аккредитации сектора НАА

В рамках проекта Технической кооперации с МАГАТЭ «Гармонизация системы контроля качества в соответствии с ISO-17025 и международными стандартами в лабораториях Российской Федерации, использующих ядерно-физические аналитические методы» (RUS7003), сектор НАА провел три Рабочих совещания МАГАТЭ, на которых были заслушаны лекции экспертов МАГАТЭ по организационным вопросам аккредитации, включающим подготовку документации, оборудования, помещений и тренинга персонала. В 2008 году подготовлен большой пакет документов, план реконструкции химической лаборатории и приобретена при финансовой поддержке МАГАТЭ часть необходимого оборудования. Этот проект обеспечил стажировку трем сотрудникам сектора в аккредитованных ядерно-физических лабораториях Германии, Бельгии, Австрии и Нидерландов в конце 2008 и начале 2009 гг.

Развитие экспериментальной базы сектора НАА

ИБР-2М В 2008 году продолжались работы по усовершенствованию спектрометрического и сервисного оборудования установки РЕГАТА на реакторе ИБР-2. Приобретены полупроводниковый германиевый детектор и ряд электронных блоков фирмы *Canberra*. Проведена калибровка детектора по эффективности с занесением полученных данных в программу расчета концентраций элементов. Проведены измерения фонов в различных помещениях лабораторного корпуса, в том числе и в бомбоубежище с целью выбора места для проведения измерений естественной радиоактивности образцов. Для уменьшения фона во временное пользование получена и собрана защита германиевого детектора. Совершенствуется пакет программ для обработки экспериментальных данных. По разработанной ранее в КБ ЛНФ

конструкторской документации в Опытном производстве ОИЯИ в 2008 году были изготовлены новые каналы облучения для установки РЕГАТА на реакторе ИБР-2М. Изготовлена и смонтирована магистраль для заполнения детекторов жидким азотом. МАГАТЭ в рамках проекта Технической кооперации поставило лиофилизатор (сушка при низкой температуре) для пробоподготовки; в ближайшее время будет приобретено оборудование для гомогенизации образцов (шаровая мельница) и др.

ИРЕН За отчетный период была проведена теоретическая оценка возможности проведения НАА на новом источнике нейтронов ИРЕН. Были рассчитаны распределения плотностей потоков тепловых, резонансных и быстрых нейтронов вокруг мишени и выбрано оптимальное место расположения каналов облучения. Совместно с «Базой развития и внедрения по физике (БРВ-физика)», София, Болгария, и КБ ЛНФ проведена разработка технического проекта на изготовление пневмотранспорта для проведения НАА на установке ИРЕН.

Биомониторинг

В 2008 году завершен цикл работ и публикаций, выполненных в рамках международной программы «Атмосферные выпадения тяжелых металлов в Европе – оценки на основе анализа мхов-биомониторов». Эти работы охватывают некоторые регионы Центральной России, Южного Урала, Белоруссии, Болгарии, Словакии, Польши, Румынии, Сербии, Македонии, Хорватии и Греции, а также Монголии и Вьетнама. Европейская часть результатов отражена в очередном выпуске 2008 года Атласа “Spatial and Temporal Trends in Heavy Metal Accumulation in Mosses in Europe (1990-2005)”, издаваемого Комиссией ООН по трансграничному переносу воздушных загрязнений в Европе.

Совместно с Университетом в Ополе (Польша) выполнено комплексное исследование по оценке состояния окружающей среды на «аномальной территории» на западе Польши, характеризующейся повышенным радиоактивным фоном вследствие Чернобыльской аварии и техногенного воздействия промышленности. Первые результаты опубликованы в 2008 году польским журналом «*Ecological Chemistry and Engineering*».

В 2008 году совместно с Институтом физики в Белграде, Сербия, и Норвежским Университетом науки и технологии в Трондхейме выполнена большая методическая работа по калибровочным измерениям содержания элементов в атмосферных осадках и мхах-трансплантах, используемых для оценки атмосферных выпадений тяжелых металлов и других элементов. Работа принята в печать международным журналом *Environmental Pollution* (IF 3.2).

Завершенная в 2008 году работа по изучению атмосферных загрязнений на территории Удмуртской Республики – оценки на основе анализа мхов-биомониторов – принята в печать российским общественно-научным журналом «*Проблемы региональной экологии*». В этой работе впервые метод мхов-биомониторов был применен для оценки экологической ситуации в районе полигона по уничтожению химического оружия.

Оценка состояния экосистем

В рамках проекта РФФИ – Румынская Академия «Геохронология и изучение ретроспективных загрязнений незатвердевших донных отложений из кислородосодержащих и бескислородных акваторий западной части Черного моря» в 2008 проведена оценка ретроспективного загрязнения этого региона. Совместно с румынской стороной подготовлены шесть публикаций. РФФИ поддержал продление проекта на 2009 год.

Многолетнее сотрудничество с монгольскими учеными в области экологии привело в 2008 году к этапному проекту «Разработка системы комплексного мониторинга тяжелых металлов и радионуклидов в Монголии с использованием ядерно-физических аналитических методов», финансируемому РФФИ-Монголия.

В сотрудничестве с Македонией (Университет в Скопье) в 2008 году подготовлен и сдан в печать Атлас карт распределения ряда тяжелых металлов в районе свинцово-цинкового комбината в г. Велес.

Результаты многоэлементного НАА коллекции аэрозольных фильтров разных лет, полученных из Братиславы, отражены в статье, принятой в 2008 году к опубликованию в одном из наиболее престижных международных экологических журналов "*Atmospheric Environment*" (IF 2.6).

Продукты питания и здоровье человека

В 2008 году на реакторе МИФИ (Москва) продолжены работы по анализу продуктов питания в связи с проектом сектора НАА с NECSA, ЮАР: «Сравнительное изучение воздействия на здоровье детей потребления продуктов питания, выращенных в некоторых промышленных районах России и Южной Африки, с использованием ядерно-физических аналитических методов». Результаты анализа продуктов питания подготовлены в виде обзора работ, выполенных в ОИЯИ и NECSA, ЮАР.

В рамках координационной программы МАГАТЭ «Воздействие токсичных и потенциально токсичных элементов на женщин репродуктивного возраста в развивающихся странах» совместно с Российским государственным медицинским университетом (Москва), Аналитическим центром Геологического института РАН и Медицинской Академией им. И.П. Сеченова в 2008 году завершена работа по определению многоэлементного анализа образцов крови специально подобранных пациентов из одного из промышленных районов Москвы. Эти исследования подтвердили гипотезу о корреляции таких токсичных элементов, как свинец, цинк и сурьма, с индексом массы тела (Body Mass Index) обследуемых пациентов. Результаты доложены на Всемирном конгрессе эпидемиологов в Бразилии в сентябре 2008 года и опубликованы в 2008 году в журнале "*Общественное здоровье и профилактика заболеваний*", Москва.

Биотехнологии

Работы по биотехнологии очистки окружающей среды от токсичных элементов (ртуть, хром и др.) ведутся в секторе НАА совместно со специалистами Института физики им. Э. Андроникашвили (Тбилиси, Грузия). Подготовлены к печати новые результаты по использованию природных штаммов бактерий, выделяемых из базальтов, для восстановления токсичного хрома (VI) в нетоксичную форму хром (III). Было установлено, что при увеличивающихся нагрузках бактерий *Arthrobacter oxidans* токсичным хромом (VI) существенно изменяется содержание других элементов, причем как в сторону увеличения, так и уменьшения. Эти эксперименты имеют большое значение для биохимиков, работающих в области биотехнологий.

Материаловедение

Синтез мелкокристаллических алмазов

Выполненное совместно со специалистами Института твердого тела и полупроводников Беларуси исследование о поведении дефектов в мелкокристаллических алмазах под воздействием нейтронного облучения в присутствии катализаторов нашло завершение в виде отдельной главы в книге «Diamond and Related Materials» (США), находящейся в печати.

Радиоэкология

Впервые на территории Беларуси был применен метод мхов-биомониторов для оценки атмосферных выпадений радионуклидов спустя 20 лет после Чернобыльской аварии. Измерения долгоживущих радионуклидов – продуктов деления ядерного топлива – были проведены в 2008 году совместно со словацкими специалистами в низкофоновой лаборатории Братиславского Университета. Часть проб была проанализирована специалистами NECSA в ЮАР. Показано, что уровни активности ^{137}Cs в образцах мха, собранных на территории Гомельской области, в 4 раза превышают фоновые. Отмечено также повышенное содержание ^{210}Pb. Эти результаты будут доложены на "The 22nd Task Force Meeting of the UNECE ICP Vegetation" в Германии, в феврале 2009 года.

Учебный процесс

На базе установки РЕГАТА в 2008 году проводился Практикум для студентов старших курсов Университета «Дубна» и студентов Международных Летних Школ, организуемых УНЦ ОИЯИ (июль – Болгария, Чехия, Словакия; сентябрь-октябрь – ЮАР). За отчетный период на базе сектора НАА были выполнены две курсовых, одна бакалаврская и три магистерских работы.

Организация совещаний

- Второе рабочее совещание в рамках проекта Технической кооперации сектора НАА ЛНФ с МАГАТЭ «Гармонизация системы контроля качества в лабораториях РФ, использующих ядерно-физические аналитические методы (26-30 мая 2008, Дубна).
- Третье одноименное совещание МАГАТЭ (27-31 октября 2008, Дубна).

2. NEUTRON SOURCES

2.1. The IBR-2 pulsed reactor

In 2008 the following works on the IBR-2 modernization were performed:

1. Dismantling of all replaced equipment of the IBR-2 was completed:

1.1. In accordance with the project of NIKIMT (Research and Development Institute of Construction Technology) two rolling shieldings (RS), which house stationary reflectors (SR) with control and emergency protection blocks, water moderators and pneumatic rabbit systems (overall weight of each RS is about 10 t) were moved one after another to a ring corridor. The dismantling of RS was complicated by a high level of induced activity (~ 1000 R/h) and space-limited working conditions. Special protection devices manufactured in JINR EW and FLNP were used to reduce the level of radiation. In January-February, 2008, both RS were successfully moved to a storage by the personnel of the FLNP Mechanical and Technological Department (MTD).

1.2. In the first quarter of 2008 the equipment in the reactor control room (control panel and cabinets for electronic safety control system equipment) was dismantled.

2. Installation of new equipment of the IBR-2M reactor:

2.1. After the RS of IBR-2 were removed (see 1.1.), new RS-1M and RS-2M of the IBR-2M reactor with new stationary reflectors SR-1 and SR-2 were installed. This work, which lasted from January till June, 2008, demanded significant operational development of the equipment to meet the specifications of the design documentation (DD) and under hazardous radiation conditions called for efficient organization of work. Upon installation, the operation of RS-1M and RS-2M was tested and the mating of SR-1 and SR-2 with each other as well as of shutters 1 and 9 with RS-1M and RS-2M, respectively, was checked. The work was conducted by the MTD personnel.

2.2. The preparatory work on the installation of the reactor vessel was performed: necessary installation devices as well as components for the Na-collector jacket were manufactured; a contract with the specialized organization "Energospetsmontazh" on welding the vessel with the sodium collector was concluded.

2.3. The preparation of a reserve control room was completed and the installation of equipment started.

3. Manufacturing of new equipment for IBR-2M:

3.1. In the middle of November, 2008 the manufacturing of the reactor vessel in NIKIET (N.A.Dollezhal Research and Design Institute of Power Engineering) was completed and on 17.11.2008 it was delivered to JINR. The delay in delivery of the vessel for 6 months made it impossible to complete welding operations for the vessel and sodium collectors by the end of 2008.

3.2. Manufacturing of 3 grooved water moderators was completed. The inclined moderator (beams 4-6) underwent geometrical try-on tests in its regular place in the central part of the reactor biological shielding. The mating of the moderator with the stationary reflector was tested showing positive results.

3.3. Manufacturing of all executive mechanisms of the safety and control system (SCS) was completed.

3.4. For the most part the manufacturing of equipment of automatic safety and control system (ASCS) and a new control panel was completed.

3.5. In INEUM (I.S.Bruk Institute for Electronic Control Machines) the equipment of the technological parameters control system (TPCS) was manufactured and passed factory acceptance tests. The equipment was delivered to FLNP and its installation started.

4. Complex of cryogenic moderators (CM) of IBR-2M.

4.1. In 2008 the design documentation for CM 202 for beams 7-11 was worked out. A contract with the NPO “Atom” (Research and Production Association "Atom") on manufacturing CM 202 was concluded.

4.2. In NIKIET the development of design documentation for CM 203 for beams 2-3 started.

4.3. The GSPI (State Specialized Design Institute) completed the technological project (1^{st} stage) for the CM complex.

4.4. The design documentation on mesitylene supply pipelines for CM 202 and CM 203 was completed in the FLNP Design Bureau and forwarded to the NPO “Atom” for production.

4.5. In the NPO “Atom” the manufacturing of rolling shieldings for the installation of CM 202 and CM 203 was completed.

4.6. The NPO “Geliymash” (Research and Production Association of Helium Engineering) delivered the equipment for cryogenic helium refrigerator KGU-700/15. The metal constructions for the installation of KGU-700/15 are being assembled. A contract with "Energospetsmontazh" on assembling of cryogenic pipelines for CM 202 and CM 203 was concluded. In NPO “Geliymash” the manufacturing of cryogenic pipelines and two cryostats is nearing completion.

5. Building and construction activities:

5.1. Preparation of the reactor reserve control room was completed.

5.2. The main construction work in rooms of reliable power supply system was carried out.

5.3. The most part of the planned activities in the reactor control room was performed.

2.2 The IREN Project

The main tasks of the Frank Laboratory of Neutron Physics and the Laboratory of Particle Physics in 2008 were the completion of installation, testing and commissioning of the equipment of the first stage of the LUE-200 accelerator. By June, 2008 work on the installation of the equipment in the accelerator halls was completed. Starting at the end of June, 2008 work to transport the beam and to train various systems of the accelerator was in progress. On June 17, 2008 an electron beam with the specified parameters was obtained at the exit of the electron source (**Fig. 1**) whereupon work to adjust the klystron and the modulator of the first accelerating section began.

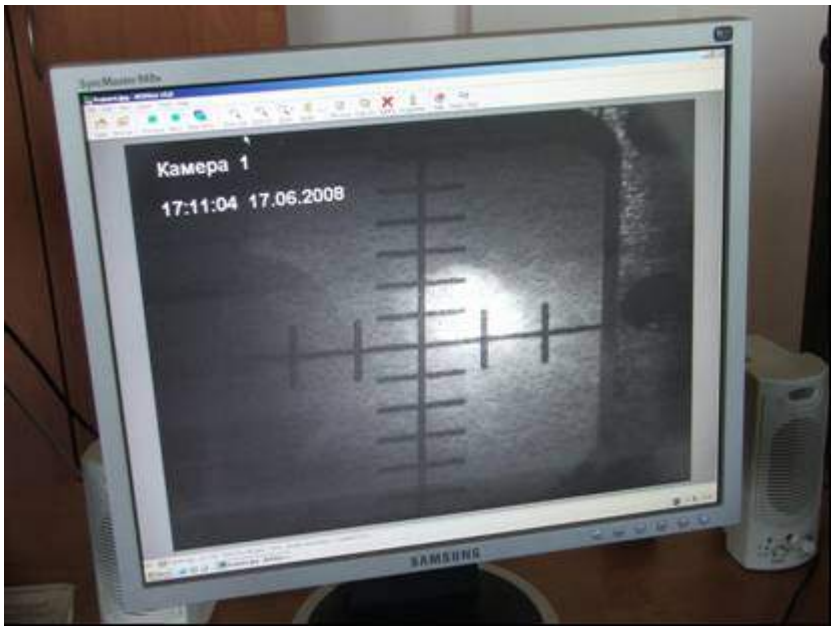

Fig. 1. An electron beam image captured by a fluorescent screen of the diagnostic box after the electron source (June 17, 2008).

By the end of November, 2008 the adjustment of HF systems of the accelerator was completed and an accelerated electron beam was transported through the first section. For independent verification of the results, a prototype tungsten target was manufactured and placed in the diagnostic box chamber at the exit of the first accelerating section. On December 5, 2008 the accelerated electron beam was transported to the prototype target and at the same time, in the time windows synchronized with the start of the accelerator the measuring module developed by the specialists from the FLNP Nuclear Physics Department detected high-energy gamma-quanta and neutrons. The presence of hard gamma-quanta and neutrons was independently confirmed by the data from the radiation monitoring equipment.

As a control experiment the measurements of gamma-quanta and neutrons were carried out by placing a diagnostic fluorescent screen in the electron beam at the exit of the source. During the experiment there were no gamma-quantum and neutron counts in the corresponding detection channels as compared to the case when electrons from the source were injected to the accelerating section.

By December 15, 2008 the stage of transportation of the accelerated electron beam to the prototype tungsten target located in the ceiling between the lower accelerating hall and the target hall of the facility was completed. Using the focal length of quadrupole lenses and the measured value of the displacement of the beam center of gravity depending on the current in the correcting magnets, the average energy of the accelerated electron beam was estimated to be 20 MeV. On

December 15, 2008 the accelerated electron beam with a pulse current of 300-400 mA at a frequency of up to 5 Hz was transported to the prototype target. Neutrons produced as a result of interaction of bremsstrahlung gamma-quanta with the substance of the target, were detected by a gas proportional neutron counter placed at a distance of 11 m from the target on the floor of the target hall. The duration of fast neutron burst was estimated and time-of-flight spectra with time channel widths from 20 ns to 8 μs were accumulated. For half an hour of the measurements at a frequency of 5 Hz the statistics of detector counts in the time channels amounted to two hundred counts in the resonance neutron energy region.

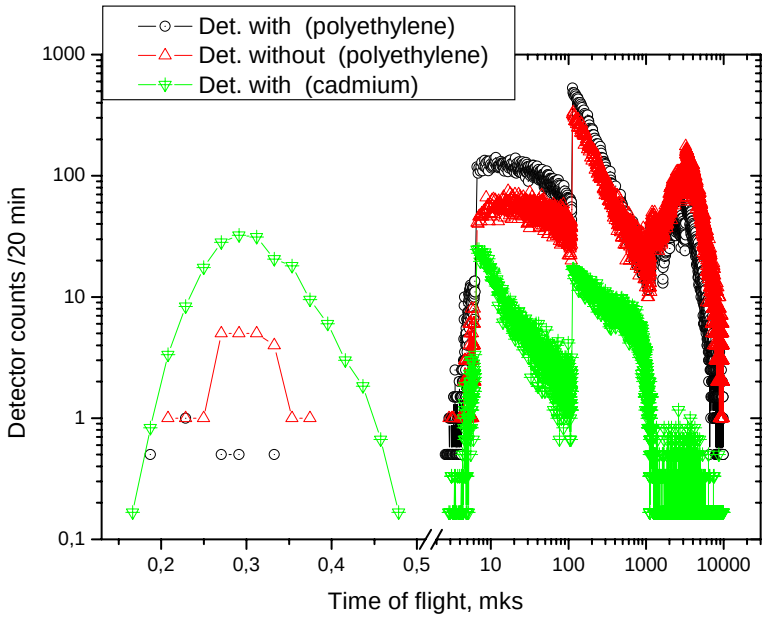

Fig. 2. Time-of-flight spectra from the prototype target detected by helium proportional counter in polyethylene (black circles), without polyethylene (red triangles) and in cadmium (green triangles); sharp changes in counts correspond to changes in time channel width.

At present, the installation of electron guide and focusing elements in the target hall has been completed and work to transport the beam to a regular non-multiplying target has started.

2. ИСТОЧНИКИ НЕЙТРОНОВ

2.1. Импульсный реактор ИБР-2

В 2008 г. по модернизации ИБР-2 выполнены следующие работы:

1. Завершен демонтаж всего заменяемого оборудования ИБР-2:

1.1. В соответствии с проектом НИКИМТ две откатные защиты (ОЗ), на которых размещались стационарные отражатели с блоками регулирования и аварийной защиты, водяные замедлители и пневмопочты (общий вес каждой ОЗ около 10 т) были последовательно выдвинуты в кольцевой коридор. Работа по их демонтажу осложнилась высокой наведенной активностью (~ 1000 р/час) и стесненными условиями для выполнения работ. Для снижения уровня излучения были применены специальные защитные приспособления, изготовленные в ОП ОИЯИ и ЛНФ. В январе-феврале 2008 г. обе ОЗ были успешно перенесены в хранилище персоналом МТО.

1.2. В I кв. 2008 г. было демонтировано оборудование в пультовой реактора: пульт управления и шкафы электронной аппаратуры системы управления и защиты.

2. Монтаж нового оборудования реактора ИБР-2М:

2.1. После удаления ОЗ ИБР-2 (см. п. 1.1.) был выполнен последовательно монтаж новых ОЗ-1М и ОЗ-2М реактора ИБР-2М с новыми стационарными отражателями СО-1 и СО-2. Эта работа, продолжавшаяся с января по июнь 2008 г., потребовала существенной доводки оборудования для обеспечения технических требований конструкторской документации (КД) и четкой организации работ в условиях сложной радиационной обстановки. После монтажа ОЗ-1М и ОЗ-2М были опробованы в работе, проверена сопрягаемость (mating) СО-1 и СО-2 друг с другом, проверена сопрягаемость 1-го и 9-го шиберов с ОЗ-1М и ОЗ-2М соответственно. Работа выполнялась персоналом МТО.

2.2. Выполнены подготовительные работы к монтажу корпуса реактора: изготовлены необходимые монтажные приспособления, детали для кожуха коллектора, заключен договор со специализированной организацией «Энергоспецмонтаж» о сварке корпуса с натриевым коллектором.

2.3. Завершена подготовка помещения резервного пульта, начат монтаж оборудования.

3. Изготовление нового оборудования ИБР-2М:

3.1. В середине ноября 2008 г. завершилось изготовление корпуса реактора в НИКИЭТ, а 17.11.2008 г. корпус был доставлен в ОИЯИ. Задержка с поставкой корпуса в 2008 г. на 6 месяцев не позволяет в полном объеме выполнить до конца 2008 г. сварку корпуса с натриевыми коллекторами.

3.2. Завершено изготовление 3-х водяных гребенчатых замедлителей. Наклонный замедлитель (пучки 4-6) прошел геометрическую примерку на штатном месте в защитном массиве реактора. Проверена сопрягаемость замедлителя со стационарным отражателем, полученные результаты положительные.

3.3. Завершено изготовление всех исполнительных механизмов СУЗ.

3.4. В основном завершено изготовление оборудования АСУЗ и нового пульта.

3.5. Изготовлено в ИНЭУМ оборудование системы контроля технологических параметров (СКТП), проведена заводская приемка СКТП, оборудование доставлено в ЛНФ, начат его монтаж.

4. Комплекс криогенных замедлителей (КЗ) ИБР-2М.

4.1. В 2008 г. завершен выпуск КД КЗ 202 для пучков 7-11. Заключен договор с НПО «Атом» на изготовление КЗ 202.

4.2. В НИКИЭТ начата разработка КД по КЗ 203 для пучков 2-3.

4.3. ГСПИ выпустил технологический проект (1 этап) комплекса КЗ.

4.4. Завершена КД по трубопроводам подачи мезитилена в КЗ 202 и КЗ 203 в КБ ЛНФ. КД передана в НПО «Атом» для изготовления.

4.5. В НПО «Атом» завершено изготовление откатных блоков для размещения в них КЗ 202 и КЗ 203.

4.6. От НПО «Гелиймаш» получено оборудование холодильной установки КГУ-700/15. Ведется монтаж металлоконструкций для установки КГУ-700/15. Заключен договор с «Энергоспецмонтаж» на монтаж криогенных трубопроводов для КЗ 202 и КЗ 203. В стадии завершения изготовление в НПО «Гелиймаш» криогенных трубопроводов и 2-х криостатов.

5. Строительные работы:

5.1. Завершена подготовка помещения резервного пульта.

5.2. Выполнены основные строительные работы по помещениям для системы надежного питания.

5.3. Выполнена большая часть запланированных работ по пультовой реактора.

2.2. Проект ИРЭН

Главными задачами Лаборатории нейтронной физики и Лаборатории физики частиц в 2008 году являлось завершение монтажа, тестирование и запуск оборудования первой очереди ускорителя ЛУЭ-200. К июню 2008 года были завершены работы по монтажу оборудования в ускорительных залах. С конца июня 2008 года велась работа по проводке пучка и тренировке различных систем ускорителя. 17 июня 2008 года был получен пучок электронов с заданными параметрами на выходе источника электронов (Рис. 1) после чего началась работа по настройке клистрона и модулятора первой ускоряющей секции.

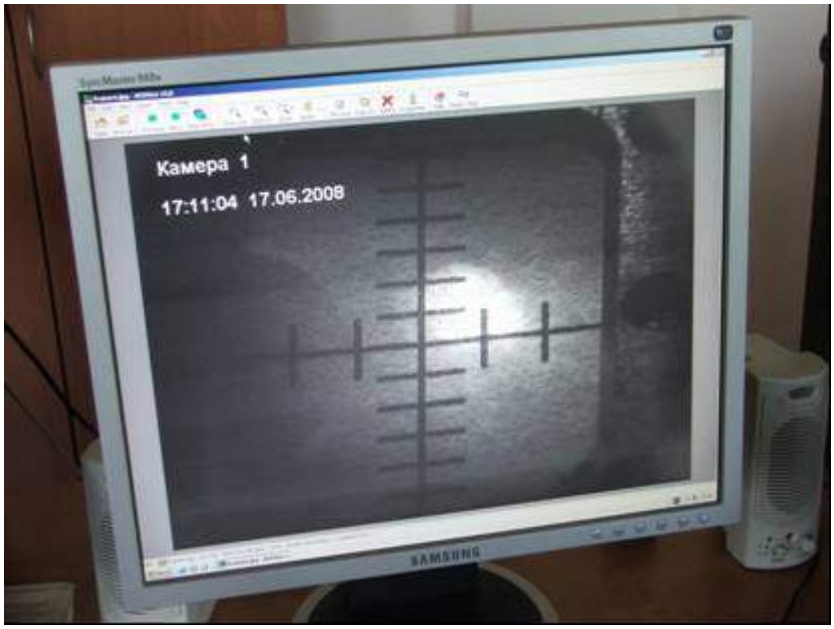

Рис. 1: изображение пучка электронов на люминофоре диагностического бокса после источника электронов (17 июня 2008г.)

К концу ноября 2008 года была завершена настройка ВЧ систем ускорителя, и пучок электронов в режиме ускорения был проведен через первую секцию. Для независимого подтверждения этих результатов была изготовлена временная мишень из вольфрама, которая была размещена в камере диагностического бокса на выходе из первой ускорительной секции. Пятого декабря 2008 года ускоренный пучок электронов был подан на временную мишень, при этом, измерительным модулем, подготовленным специалистами НЭОФЯ ЛНФ, во временных окнах, синхронизованных со стартом ускорителя, регистрировались жесткие гамма-кванты и нейтроны. Наличие жестких гамма-квантов и нейтронов было независимо подтверждено данными, полученными от аппаратуры дозиметрического контроля.

В качестве контрольного эксперимента были выполнены измерения гамма-квантов и нейтронов при перекрытии пучка электронов на выходе из источника диагностическим люминофором. При этом счет гамма-квантов и нейтронов в соответствующих регистрирующих каналах отсутствовал по сравнению со случаем, когда электроны от источника подавались в ускоряющую секцию.

К 15 декабря 2008 года был завершен этап проводки пучка ускоренных электронов до промежуточной вольфрамовой мишени, размещенной в перекрытии между нижним ускорительным и мишенным залами установки. По фокусному расстоянию квадрупольных линз и измеренной величине смещения центра тяжести пучка в зависимости от тока в корректирующих магнитах была оценена средняя энергия пучка ускоренных электронов,

которая составила 20 МэВ. Пятнадцатого декабря 2008 года пучок ускоренных электронов с импульсным током 300-400 мА при частоте до 5 Гц выводился на промежуточную мишень. Нейтроны, образованные в результате взаимодействия тормозных гамма-квантов с веществом мишени, регистрировались газовым пропорциональным нейтронным счетчиком, располагавшимся на расстоянии 11 метров от мишени на полу мишенного зала. Была оценена длительность вспышки по быстрым нейтронам и накоплен времяпролетный спектр с шириной временных каналов от 20 нс до 8 мксек. За полчаса измерений при частоте 5 Гц статистика отсчетов во временных каналах составила до двухсот отсчетов в области резонансных нейтронов.

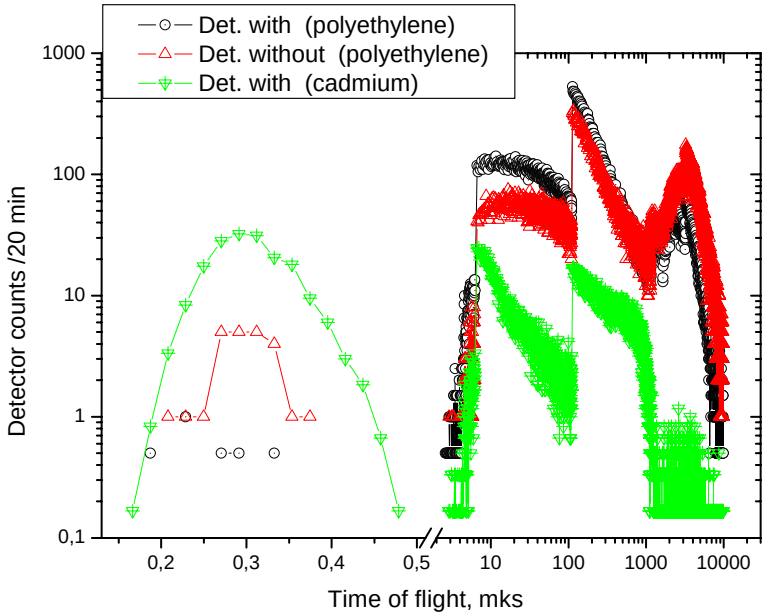

Рис. 2: Времяпролетные спектры от промежуточной мишени, зарегистрированные гелиевым пропорциональным счетчиком в полиэтиленовом чехле (черные кружки), без полиэтиленового чехла (красные треугольники) и в кадмии (зеленые треугольники); резкие изменения величины отсчетов соответствуют изменению ширины временного канала.

В настоящее время завершен монтаж электроновода и фокусирующих элементов в мишенном зале и начата работа по проводке пучка на штатную неразмножающую мишень.

3. DEVELOPMENT AND CONSTRUCTION OF ELEMENTS OF NEUTRON SPECTROMETERS FOR CONDENSED MATTER INVESTIGATIONS

In 2008 within the framework of the theme the following main results were obtained:

Neutron beam-forming systems

In cooperation with the German Institutes and PNPI (Gatchina) within the framework of the project aimed at constructing curved mirror neutron guides for the EPSILON and SKAT spectrometers on beam 7a of the IBR-2 reactor the work to design and manufacture mechanical and optical units of neutron guides continued. In particular, additional vacuum housings, supporting platform and installation-loading mechanism for a single-volume demountable vacuum housing of the head part of the neutron guide system (splitter, see **Fig. 1**) for beam 7 of IBR-2M were developed and manufactured. In PNPI optical elements for the head and curved parts of the neutron guide were produced as well.

Fig. 1. Splitter housing at a vacuum test site.

In the JINR Experimental Workshops (JINR EW) 44 beam-positioning support pillars for curved neutron guides were manufactured (**Fig. 2**). Also, the drawings of posts and beam-positioning support pillars of the head part were forwarded to JINR EW and put into production. The head part of the neutron guide on beam 7b (NERA-PR spectrometer) was dismantled and the shielding of the chopper in the reactor ring corridor was partially disassembled. The technical project of reconstruction of the supporting column in bldg. 117 was prepared.

Fig. 2. Beam-positioning support pillars for curved neutron guides

It has been suggested that a test beam for testing neutron detectors and other elements of spectrometers be positioned on IBR-2M channel 13. The parameters and infrastructure of the test beam were determined and the preparation of the technical project started. The design parameters of beam 13 are: neutron guide cross-section – 314 cm²; neutron flux on the moderator surface – ~ 2×10^{12} n/ cm² /s, at a distance of 10 m – up to 10^8 n/ cm² /s.

Cryogenic investigations

Under the contract with the RRC «Kurchatov Institute» a bore cryostat for cooling high-pressure sapphire anvil cells for working in the temperature range of 6.5-300 K was designed and manufactured (**Fig. 3**). The diameter of the cryostat orifice opening for loading high-pressure cells is 120 mm, which corresponds to the cell sizes and makes it possible to place them in either a vertical or horizontal position. The temperature is measured and controlled by Scientific Instruments Model 9700 temperature controller and silicon diodes DT470. The cryostat also uses SUMITOMO SRP-062B cryocooler.

Fig. 3. General view of the cryostat and auxiliary equipment.

Work on the FLNP cryogenic test stand (**Fig. 4**) continued. In 2008 the basic element of the test stand – CRYOMECH PT403 cryocooler – was purchased and installed. The main components of the cryostat, which makes it possible to carry out tests in the temperature range of 2.5 – 300 K, were designed and manufactured as well.

Tests of vacuum explosion welded joints of titanium - nickel-chromium stainless steel were carried out. The joints were subjected to thermocycling treatment in the temperature range of 6-300K under simulated real-life conditions. This work is of crucial importance for accelerator engineering, which uses superconducting magnets and resonators operating in liquid helium, and also opens up new prospects for ultra-low temperature engineering.

Control systems of actuating mechanisms

The software was upgraded and the SMC-32-CAN controller developed in FLNP for the control systems of actuating mechanisms on the IBR-2M spectrometers was tested:

- The control module with controlled parameters (current pulse duration and pause duration) for direct-current motors was embedded into the Sonix + software package;

- To improve the accuracy of actuating mechanisms, the encoder installed on the step motor shaft was incorporated in their design, which significantly enhances the resolution.

Fig. 4. Cryogenic test stand.

The investigations demonstrating the possibility of using TOSHIBA VFAS1-4370PL drives for phasing the rotation of motors with power up to 500W were carried out. Corresponding recommendations to replace obsolete and worn-out drives EKT2 used in beam choppers on the IBR-2 spectrometers were made. A stand to test characteristics of choppers was assembled. Work to introduce control systems of actuating mechanisms on the spectrometers of the IR-8 reactor in the RRC «Kurchatov Institute» was performed.

Gas detectors

The prototype of a position-sensitive neutron detector based on a multi-wire proportional chamber with individual data readout from each wire was constructed. The detector uses 36(X)*18(Y) cathode wires spaced 1mm apart. Signals are read out via 8-channel current preamplifiers and discriminators; there are also analog outputs. Amplitude spectra of signals from the wires were obtained. Pulse width is about 200 ns. The prototype of the detector was prepared for stand tests.

In cooperation with INRNE BAS (Sofia) a curved PSD intended for x-ray and neutron diffraction studies was designed and constructed. It is a curved 1D gas-filled position-sensitive detector based on a multiwire proportional chamber with delay line data readout.

The detector is housed in a steel case. A panel with a system of electrodes is fixed to its front wall. Signals are output via BNC connectors; high voltage is supplied via SHV connectors. There are two Swagelok connectors on the detector case, which makes it possible to use it in a continuous-flow mode of operation. The front wall is detachable, and when the device is used as an x-ray detector the entrance window is an aluminum plate 0.1 mm thick, when detecting neutrons the thickness of the entrance window is 7 mm. For greater rigidity the entrance window is buried in the detector case. The cathode and anode wires are spaced 1 mm apart. The prototype model of the detector is shown in **Fig. 5**.

As well as the 1D and 2D PSD developed earlier in FLNP, the given detector uses unified electronic blocks:

- NIM crate with Phillips Scientific PS715 constant-fraction discriminator, Iseg NHQ206L 2-channel HV power supply and fast charge-sensitive preamplifiers;
- Personal computer with a built-in PCI DAQ board.

At present, the prototype of the detector is being tested at the stand.

Fig. 5. Prototype model of the curved PSD.

In 2008 two MWPC position-sensitive detectors were manufactured: for the GRAINS spectrometer (financed by the grant of the Hungarian Academy of Sciences) and for the monitoring system of the IBR-2M reactor cold moderators (financed by the grant of the Federal Agency for Science and Innovations of the RF Ministry of Science and Education). The basic characteristics of the detectors and a photo of the detector case are presented in **Fig. 6**. Tests of the 2D PSD for controlling the level of mesitylene in the cold moderator chamber were successfully carried out at the reactor of the Obninsk Branch of the Karpov Institute of Physical Chemistry.

Type	2D MWPC
Active area	200×200 mm^2
Resolution	2.0×2.0 mm^2
Wavelength range	0.4 - 12 Å
Efficiency (λ=2Å)	65 %
Position determination	Delay lines

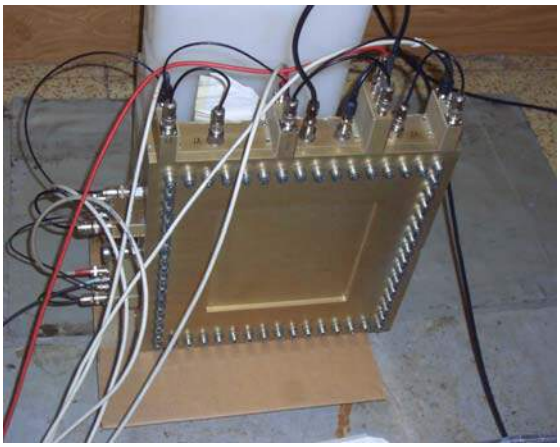

Fig. 6. 2D PSD for the GRAINS spectrometer and the monitoring system.

Scintillation detectors

The design documentation on the detector system for the DN-6 diffractometer was prepared. A number of works were performed to equip the STOIK diffractometer at the IR-8 reactor in the RRC «Kurchatov Institute», in particular, control system electronics and software on the basis of step motors and CAN network were developed. A 10-channel high-contrast detector with a resolution of 2 mm was put into operation.

Development of LAN, DAQ electronics and software

Work to lay and install fiber-optic communication lines between bldg. 119 and experimental halls 1,2 and the IBR-2M control room was completed. The installation of the corresponding communication equipment in 2009/10 will allow 1-10 Gbit/s data transfer rate in the given segment of the network. An optical cable was laid in the IREN network segment as well and a 100 Mbit/s switch was put into service; access to the Internet was provided to the first top-priority users. Lower level network switches in buildings 42 and 42a were upgraded.

Firmware programs were developed and two sets of electronic blocks for the IBR-2M spectrometers were manufactured and debugged with a programmable event generator. Drivers and program interfaces for the Sonix + software package were developed.

The development of the Sonix+ software package proceeded both by including new hardware control modules and by improving the user interface and visualization means. Service possibilities of the WebSonix remote control system were extended.

In cooperation with HZB, Berlin, the work on the integration of the DeLiDAQ software package (acquisition and accumulation of data from PSD) to the CARESS and SPEC packages continued.

In cooperation with the Jülich Research Center the development and preliminary testing of the PHASE SPACE TRANSFORMER module for the VITESS software package were performed and work on computer simulation of a backscattering spectrometer started. The parameters of a number of other VITESS modules (SPACE, SPACEWINDOW_MULTIPLE, etc.) were improved and new options (consideration of neutron attenuation by air at various temperatures and humidities, simulation of geometrically non-ideal neutron guides, etc.) were added. Using the above-mentioned modules the simulation and optimization of the beam-forming system for channel 7a of the IBR-2 reactor were performed. Work on simulation and development of neutron spin-echo spectroscopy with rotating/pulsating magnetic fields continued. Computer simulation for a new neutron reflectometer for the planned European Spallation Source (ESS) started.

3. РАЗРАБОТКА И СОЗДАНИЕ ЭЛЕМЕНТОВ СПЕКТРОМЕТРОВ ДЛЯ ИССЛЕДОВАНИЯ КОНДЕНСИРОВАННЫХ СРЕД

В 2008 году по теме получены следующие основные результаты:

Системы формирования нейтронных пучков

В рамках проекта создания изогнутых зеркальных нейтроноводов спектрометров ЭПСИЛОН и СКАТ на канале 7а реактора ИБР-2 совместно с институтами ФРГ и ПИЯФ г. Гатчина продолжались работы по проектированию и изготовлению механических и оптических узлов нейтроноводов. В частности, разработаны и изготовлены дополнительные вакуумные кожуха, несущая платформа и монтажно-загрузочный механизм однообъёмного разборного вакуумного кожуха головной части нейтроноводной системы (сплиттера, ***Рис.1***) 7 канала ИБР-2М. В ПИЯФ изготовлены также оптические элементы для головной и изогнутых частей нейтроновода.

Рис.1.Кожух сплиттера на участке вакуумных испытаний.

В ОП ОИЯИ изготовлены 44 юстировочные опоры изогнутых нейтроноводов (**Рис.2**), а также сданы в производство чертежи стоек и юстировочных опор головной части. Произведен демонтаж головной части нейтроновода на канале №7б (спектрометр НЕРА-ПР) и частичный демонтаж защиты прерывателя в кольцевом коридоре реактора. Подготовлен технический проект реконструкции несущей колонны в здании 117.

Рис.2. Юстировочные опоры изогнутых нейтроноводов

На 13 канале ИБР-2М предложено создать тестовый пучок для проведения испытаний нейтронных детекторов и других элементов спектрометров. Проектные параметры пучка: сечение нейтроновода – 314 см²; нейтронный поток с поверхности замедлителя – $\sim 2 \times 10^{12}$ нейтр./ см² /с, на расстоянии 10м – до 10^8 нейтр./ см² /с. Определена инфраструктура тестового пучка и начата подготовка технического проекта.

Криогенные исследования

По контракту с РНЦ «Курчатовский институт» выполнена конструкторская разработка и изготовлен шахтный криостат (**Рис.3**) для охлаждения камер высокого давления с сапфировыми наковальнями для работы в диапазоне температур 6,5-300К. Диаметр проходного отверстия криостата для загрузки камер высокого давления равен 120мм, он соответствует размерам самих камер и позволяет располагать камеры как в вертикальной, так и горизонтальной ориентации. Контроль и измерение температуры осуществляется при помощи контроллера Scientific Instruments модели 9700 и кремниевых диодов DT470. Для охлаждения в криостате применен криокулер SRP-062B фирмы SUMITOMO.

Рис.3. Общий вид криостата и вспомогательного оборудования

Продолжались работы по созданию криогенного стенда ЛНФ (**Рис.4**). В 2008 г. приобретен и установлен основной элемент стенда – криокулер РТ403 фирмы CRYOMECH, были также сконструированы и изготовлены основные детали криостата, позволяющего проводить тесты в диапазоне температур 2.5 – 300К.

Проведены испытания вакуумных швов титан - нержавеющая хромоникелевая сталь, выполненные при помощи взрыва. При этом производилось термоциклирование швов в диапазоне температур 6-300К в условиях, имитирующих реальные. Данная работа имеет решающее значение для ускорительной техники, использующей сверхпроводящие магниты и резонаторы, работающие в жидком гелии, а также открывает новые перспективы в технике сверхнизких температур.

Системы управления исполнительными механизмами

Модернизировано программное обеспечение и проведены испытания разработанного в ЛНФ контроллера SMC-32-CAN для систем управления исполнительными механизмами на спектрометрах ИБР-2М:

- в состав комплекса Sonix+ введен модуль управления двигателями постоянного тока с регулируемыми параметрами (длительность импульса тока и длительность паузы);
- для повышения точности исполнительных механизмов в их конструкцию введен энкодер, устанавливаемый на валу шагового двигателя, что существенно улучшает разрешение.

Рис.4. Криогенный стенд

Проведены исследования, показавшие возможность использования приводов VFAS1-4370PL фирмы TOSHIBA для фазировки вращения двигателей с мощностью до 500Вт. Сделаны соответствующие рекомендации по замене устаревших и выработавших ресурс приводов ЭКТ2, используемых в прерывателях пучков на спектрометрах ИБР-2. Собран стенд для проверки характеристик прерывателей. Выполнен ряд работ по внедрению систем управления исполнительными механизмами на спектрометрах реактора ИР-8 в РНЦ «Курчатовский институт».

Газовые детекторы

Создан прототип MWPC детектора с индивидуальным съемом информации с каждой нити. Детектор содержит 36(X)*18(Y) катодных нитей, намотанных с шагом 1мм. Съем сигналов осуществляется через 8-канальные токовые предусилители и дискриминаторы; имеются также аналоговые выходы. Получены амплитудные спектры сигналов с нитей. Ширина импульсов около 200 нс. Прототип детектора подготовлен к испытаниям на стенде.

В сотрудничестве с INRNE BAS, Sofia разработан и изготовлен изогнутый ПЧД, предназначенный для рентгеновской и нейтронной дифрактометрии. Он представляет собой изогнутый однокоординатный газонаполненный позиционно-чувствительный детектор, выполненный на основе многопроволочной пропорциональной камеры. Съем сигналов осуществляется с линии задержки.

Конструктивно детектор выполнен в стальном корпусе, к передней стенке которого крепится сборка с системой электродов. Вывод сигналов осуществляется через разъемы BNC, высокое напряжение подается через разъемы SHV. На корпусе детектора имеются 2 разъема Swagelock, что позволяет использовать его в проточном режиме. Передняя стенка съемная, при работе в качестве рентгеновского детектора входным окном является алюминиевая пластинка, толщиной 0,1мм, при регистрации нейтронов толщина входного окна будет составлять 7мм. Для большей жесткости входное окно утоплено в корпусе детектора. Шаг намотки анодных и катодных нитей равен 1мм. Опытный образец детектора показан на **Рис.5**.

Рис.5. Опытный образец изогнутого ПЧД

Так же как и в ранее разработанных в ЛНФ 1D и 2D ПЧД, в данном детекторе используются унифицированные электронные блоки и программное обеспечение:

- NIM крейт, дискриминатор с точной временной привязкой Phillips Scientific PS715, в/в источник питания Iseg NHQ206L, быстродействующие зарядо-чувствительные предусилители;
- персональный компьютер со встроенной платой PCI DAQ.

В настоящее время опытный образец детектора проходит тестовые испытания на стенде.

В 2008 г. изготовлены два MWPC ПЧД: для спектрометра GRAINS (финансирование из гранта Венгерской Академии Наук) и для системы мониторинга холодных замедлителей реактора ИБР-2М (финансирование по Госконтракту с Федеральным агентством по науке и инновациям Минобрнауки РФ). Основные характеристики детекторов и фотография корпуса детектора показаны на **Рис.6**. На реакторе филиала НИИФХИ им. Карпова, г. Обнинск успешно проведены испытания 2D ПЧД, предназначенного для контроля уровня мезитилена в камере холодного замедлителя.

Тип	2D MWPC
Рабочая область	200x200 мм^2
Разрешение	2,0x2,0 мм^2
Диапазон длин волн	0,4 - 12 A
Эффективность (λ=2Å)	65%
Определение позиции	Линии задержки

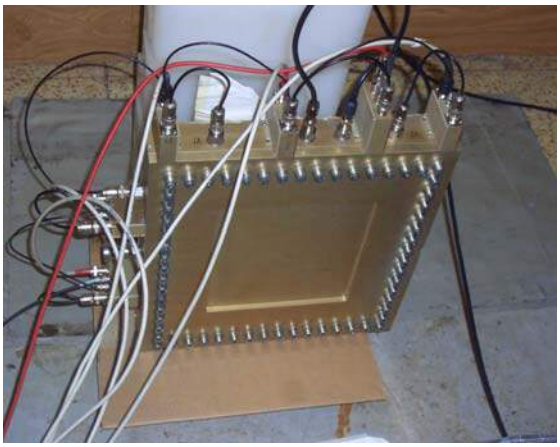

Рис. 6. Двухкоординатный ПЧД для спектрометра GRAINS и системы мониторинга

Сцинтилляционные детекторы

Оформлена рабочая документация на изготовление детекторной системы дифрактометра ДН-6. Выполнен ряд работ по оснащению оборудованием дифрактометра СТОИК на реакторе ИР-8 в РНЦ «Курчатовский институт», в частности, разработаны электроника и программное обеспечение системы управления дифрактометром на основе шаговых двигателей и сети CAN. Введен в эксплуатацию 10-канальный детектор высокой контрастности с разрешением 2мм.

Развитие локальной вычислительной сети, электроники систем сбора данных и программного обеспечения

Завершены работы по прокладке и монтажу волоконно-оптических линий связи между зданием 119 и экспериментальными залами 1,2 и пультом управления ИБР-2М. После установки соответствующего коммуникационного оборудования в 2009/10 г.г. это позволит работать в данном сегменте сети со скоростью 1-10 Гбит/с. В сетевом сегменте установки ИРЕН также проложен оптический кабель и введен в эксплуатацию коммутатор на 100 Мбит/с; осуществлено подключение первоочередных пользователей сети. Выполнена модернизация сетевых коммутаторов нижнего уровня в зданиях 42 и 42а.

Разработаны firmware программы, а также изготовлены два комплекта новых электронных блоков для спектрометров ИБР-2М и выполнена их отладка с генератором событий. Разработаны драйверы и программные интерфейсы к Sonix+.

Продолжались работы по развитию комплекса Sonix+, как за счет включения новых модулей для управления устройствами, так и за счет совершенствования пользовательского интерфейса и средств визуализации. Расширены сервисные возможности системы удаленного управления WebSonix.

Совместно с HZB, Berlin продолжались работы по интеграции программного комплекса DeLiDAQ (сбор и накопление данных с ПЧД) с пакетами CARESS и SPEC.

В сотрудничестве с исследовательским центром FZ-Juelich выполнены разработка и предварительное тестирование модуля PHASE SPACE TRANSFORMER для программного комплекса VITESS и начаты работы по моделированию спектрометра обратного рассеяния. Улучшены параметры ряда других модулей VITESS (SPACE, SPACEWINDOW_MULTIPLE и др.) и добавлены новые возможности (учет затухания на воздухе при разных температурах и влажности, моделирование геометрически неидеальных нейтроноводов и др.). С помощью вышеуказанных модулей проведены моделирование и оптимизация системы проводки пучка для канала 7а реактора ИБР-2. Продолжены работы по моделированию и развитию нейтронной спин-эхо спектроскопии с вращающимися/пульсирующими магнитными полями. Начаты работы по моделированию нового нейтронного рефлектометра для планируемого европейского источника нейтронов ESS.

4. EXPERIMENTAL REPORTS

4.1. CONDENSED MATTER PHYSICS

1. High Pressure-Induced Spin Liquid Phase of Multiferroic $YMnO_3$.
D. P. Kozlenko, I. Mirebeau, J.-G. Park, I. N. Goncharenko, S. Lee, Junghwan Park, and B. N. Savenko.

2. Неупругое рассеяние медленных нейтронов нитридом урана при температурах 293 – 1273К
В.А.Семенов, В.М.Морозов, А.В.Пучков, Ж.А.Козлов, Е.Л.Ядровский

3. Structural Phase Transitions of Pyridinium Perchlorate at High Pressures.
S.E.Kichanov, D.P.Kozlenko, B.N. Savenko, J.Wasicki, W.Nawrocik, P.Czarnecki, C. Lathe

4. Autocorrelative Microdynamics of Liquid Lithium And Lithium–Hydrogen Melt: The Inelastic Neutron Scattering Study
N.M. Blagoveshchenskii, A.G. Novikov, V.V. Savostin

5. Structural Aspects of Ferrogfluids Stabilization By Mono-Carboxylic Acids
Avdeev M.V., Feoktystov A.V., Aksenov V.L., Vekas L., Rosta L., Garamus V.M., Willumeit R.

6. Investigation of Periodic Multilayers
Bodnarchuck V.I., Ignatovich V.K., Yaradaikin S.P., Czer L, Veres T

7. SANS Contrast Variation on Water-Based Magnetic Fluids Stabilized by Different Monocarboxylic Acids
Feoktystov A.V., Avdeev M.V., Bulavin L.A., Vekas L., Garamus V.M., Willumeit R.

8. Contrast Variation in Small-Angle Neutron Scattering by Water-Based Ferrofluid With Surfactant/Polymer Stabilization
Feoktystov A.V., Avdeev M.V., Bulavin L.A., Garamus V.M., Kopcansky P., Timko M., Koneracka M., Zavisova V.

9. Solutions of Dodecylbenzene Sulfonic Acid in Polar Carrier Studied by Small-Angle Neutron Scattering.
V.I.Petrenko, M.V.Avdeev, V.L.Aksenov,V.M.Garamus,L.A.Bulavin, L.Rosta

10. Analysis of the Structure of Water-Based Ferrofluids by Small Angle Neutron Scattering
V.I.Petrenko, M.V.Avdeev, A.V.Feoktystov, V.L.Aksenov, L.A.Bulavin, L.Rosta, V.M.Garamus, L.Vekas

11. Study of Proximity Effects in Superconductor/Ferromagnet Interface Using Waveguide Enhancement of Neutron Standing Waves
V.L. Aksenov, K.N. Zhernenkov, Yu. N. Khaidukov, Yu.V. Nikitenko, L.Bottyán, F. Tanczikó, D. Merkel, B. Nagy, L.Deák, D.L. Nagy, E. Szilágyi, Zs.E. HorváthL. KissA. Csík, K. VadG. LangerA. Rühm

12. Phase State and Structure of the Ceramide 6 Based Model Membranes of the Stratum Corneum
M.A. Kiselev, A. Ruettinger, N.Yu. Raybova, S. Dante, Th. Hauss

13. Neutron Wave Resonances and Off-Specular Scattering from Waveguides
S.V. Kozhevnikov, F. Ott, A. Paul, L. Rosta

14. X-ray investigation of comb-like liquid crystal polymers, oriented by a strong magnetic field for SANS measurements
A.I.Kuklin, A.Yu.Cherny, V.G.Cherezov, S.Kostromin, A.V.Rogachev, V.P.Shibaev

15. Neutron Diffraction Study OF Texture Evolution OF ECAPed Magnesium Alloys
T.A. Lychagina, D.I. Nikolayev, H.-G. Brokmeier, W. Gan

16. Correlation of Spin and Charge Ordering in $Sr_3YCo_4O_{10.5+\delta}$, δ=0.02 and 0.26
D.V. Sheptyakov, O.A. Drozhzhin, V.Yu. Pomjakushin, S.Ya. Istomin, I.A. Bobrikov, E.V. Antipov, A.M. Balagurov

17. Successive Structural Phase Transitions in $Pr_{0.5}Sr_{0.5}CoO_3$ in the Range 10–1120 K
A. M. Balagurov, I. A. Bobrikov, D. V. Karpinsky, I. O. Troyanchuk, V. Yu. Pomjakushin, and D. V. Sheptyakov

18. Melting Behavior of Water Confined in Carbon Nanopores; Structure of the Confined Ice.
M.Jazdzewska, M.Sliwinska-Bartkowiak, A.I. Beskrovnyy, S.G. Vasilovskiy

19. Residual Strain and Texture of an Anhydrite-Dolomite-Specimen (central Alps)
Ch. Scheffzuek, K. Walther, A. Frischbutter, R. Naumann, and I.V. Brovkin

20. Автокорреляционная микродинамика жидкого лития и расплава литий–водород: исследование методом неупругого рассеяния нейтронов.
Н.М. Благовещенский, А.Г. Новиков, В.В. Савостин

4.2. NEUTRON NUCLEAR PHYSICS

1. Elemental Content of Indigenous Bacteria under Different Cromium Loadings
M.V. Frontasyeva, S.F. Gundorina, T.M. Ostrovnaya, I. Zinicovscaia, N.Ya. Tsibakhashvili[1,2], L. Mosulishvili, E. Kirkesali, T. Kalabegishvili, S. Kerkenjia, H-Y. Holman

2. Precise Approximation of Sums of Experimental Radiative Strength Functions of Dipole Gamma-Transitions IN THE Region $E_\gamma \approx B_n$ FOR THE Atomic Masses $40 \leq A \leq 200$
Sukhovoj A.M., Furman W.I., Khitrov V.A.

3. Epithermal NAA for Marine Geoecology
C. Cristache, O. Culicov, M. Toma, M.V. Frontasyeva, S.S. Pavlov, O.G. Duliu, G. Oaie

4. Heavy Metals AND Ree IN Bottom Sediments AND Dreissenids OF THE Rybinsk Reservoir
Goryaynova Z.I., Pavlov D.F., Frontasyeva M.V.

4.3. NEUTRON SPECTROMETERS FOR CONDENSED MATTER INVESTIGATIONS

1. Optimization of a Moderator-Neutron Guide System for Spectrometers of Beam 7a of the IBR-2M Reactor.
Manoshin S.A., Belushkin A.V., Kulikov S.A., Shabalin E.P., and Zhuravlev V.V.

НЕУПРУГОЕ РАССЕЯНИЕ МЕДЛЕННЫХ НЕЙТРОНОВ НИТРИДОМ УРАНА ПРИ ТЕМПЕРАТУРАХ 293 – 1273К

В.А.Семенов[a], В.М.Морозов[a], А.В.Пучков[a]
[a] *State Scientific Centre – Institute for Physics and Power Engineering, 249033, Obninsk, Kaluga Region ,Russia*

Ж.А.Козлов[b], Е.Л.Ядровский[b]
[b] *Joint Institute for Nuclear Research, Dubna, Russia*

Нитрид урана рассматривается в настоящее время как базовый материал для создания комбинированного топлива реакторов на быстрых нейтронах, с которыми связывается перспектива развития крупномасштабной ядерной энергетики [1]. Поэтому, нейтронографические исследования, дающие прямую информацию о микроскопических параметрах вещества, имеют не только научное, но и большое практическое значение. В рамках общей задачи по созданию базы нейтронографических данных для ядерных топливных материалов, были измерены спектры неупругого рассеяния нейтронов для нитрида урана UN в интервале температур от комнатной до 1273К.

UN имеет кубическую кристаллическую решетку типа NaCl с постоянной решетки a_0 =0,4890 нм (при 300К) и расстоянием между атомами урана d = 0,345 нм. Рентгеновская плотность равна 14,4 г/см^3. Теплопроводность нитрида урана на порядок выше, чем у оксидного топлива, что позволяет снизить рабочие температуры в тепловыделяющих элементах активной зоны реактора. UN обладает магнитными свойствами, которые зависят от температуры, давления, радиационного облучения. Это создает предпосылки для их прикладного использования, в частности, создания новых магнитных методов неразрушающего контроля нитридного ядерного топлива в условиях радиационного облучения [2].

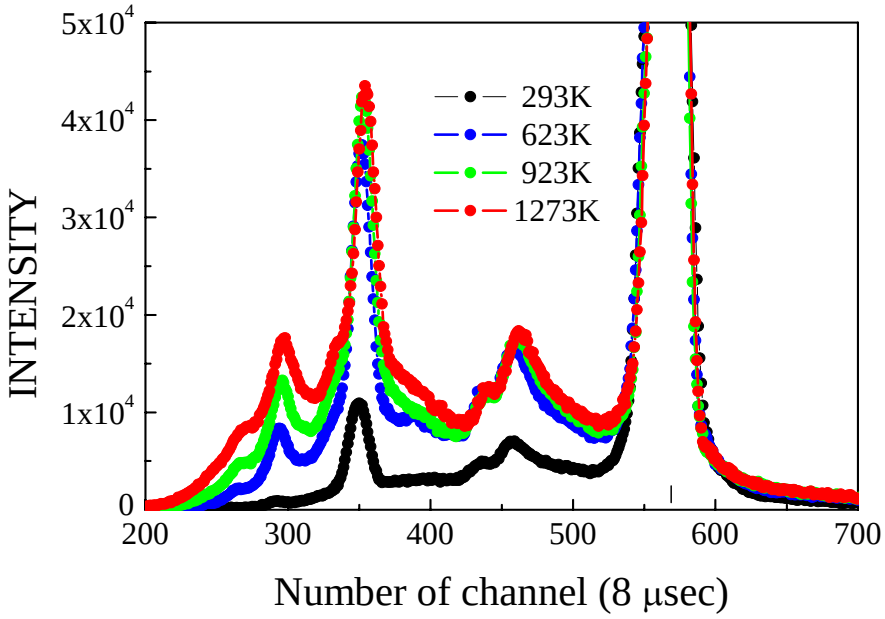

Рис.1. Экспериментальные спектры нейтронов, рассеянных UN. Учтены эффекты рассеяния нейтронов конструкционными материалами термостата и контейнером.

Измерения выполнены совместно с ЛНФ ОИЯИ на спектрометре ДИН-2ПИ с использованием термостата TS3000K [3]. Образцы мононитрида урана были изготовлены в ВНИИНМ им.А.А.Бочвара [4] в виде таблеток UN диаметром 7,9 мм, герметично запакованных в тонкостенные контейнеры из нержавеющей стали. Образец,

сформированный из пяти таких контейнеров, располагался на столике внутри цилиндрического танталового нагревателя, который, в свою очередь, был окружен четырьмя цилиндрическими тепловыми экранами из листового тантала толщиной 0,05 мм. Измерения с UN были выполнены при температурах 293, 623, 923 и 1273К. Предельная температура лимитировалась материалом оболочки (нержавеющая сталь ЭП-823). Предварительно обработанные спектры рассеянных нейтронов, просуммированные по всем углам рассеяния, приведены на рис.1. Из этих спектров с использованием программного комплекса SLOWN [5] впервые восстановлены функции плотность фононных состояний UN для высоких температур (рис.2). Основные детали спектра, полученного для комнатной температуры, находятся в согласии с данными работы [6]. Нитрид урана обладает заметным магнитным рассеянием, вклад которого не учитывался на данном этапе обработки экспериментальных спектров, поэтому эти данные носят предварительный характер.

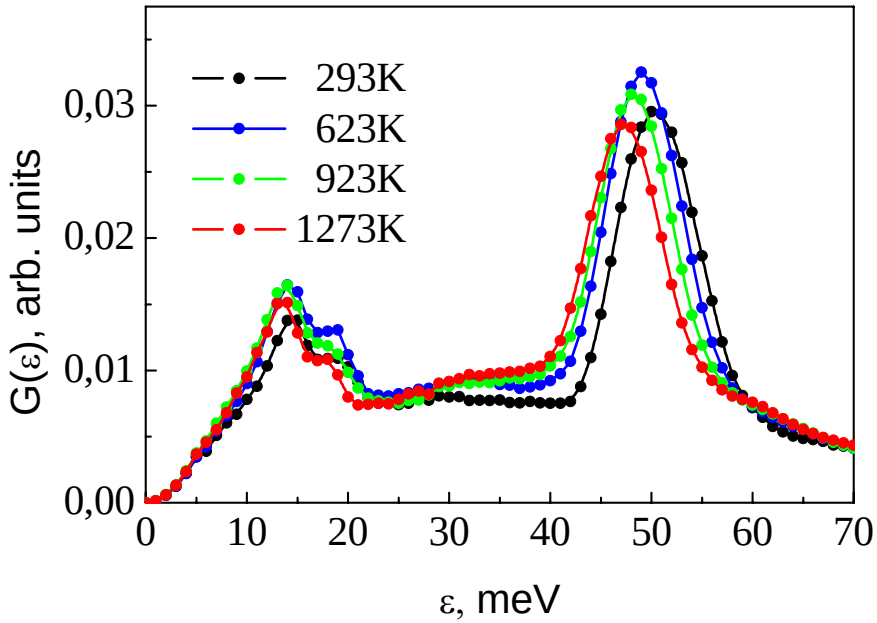

Рис.2. Функции плотности фононных состояний UN при высоких температурах. Наблюдаются две области колебаний с максимумами при передачах энергии ε =~14мэВ и ~50мэВ. Первая (акустическая) отвечает колебаниям тяжелых атомов урана, вторая (оптическая) – легких атомов азота. С ростом температуры происходит смягчение спектра колебаний за счет сдвига оптической части в область меньших энергий и трансформации акустической части спектра.

Литература

1. E.Adamov, V.Orlov et.al. The next generation of fast reactors, Nuclear Engineering and Design, 173 (1997), p. 143-150.
2. А.З.Солонцов, В.П.Силин. Препринт ФИАН-24, 2003, 40 с.
3. М.Ион, Ж.А.Козлов, Г.Матееску, И.Падуреану, В.А.Семенов, Л.Крачун, С.Н. Рыпеану, В.М. Морозов, А.И.Опреа, К.Опреа, А.В.Пучков. Сообщение ОИЯИ Р13-2008-66, Дубна, 2008, 11с.
4. Б.Д.Рогозкин., Н.М.Степеннова, А.А.Прошкин, Атомная энергия **95**(3), 208 (2003).
5. Ю.В.Лисичкин, А.Г.Довбенко, В.А.Ефименко, А.Г.Новиков, Л.Д.Смиренкина, С.И.Тихонова. Вопросы атомной науки и техники. Сер. «Ядерные константы», вып.2(33), 12 (1979).
6. F.A.Wedgwood, J.Phys.C: Solid State Phys. **7**, 3203 (1974).

HIGH PRESSURE-INDUCED SPIN LIQUID PHASE OF MULTIFERROIC $YMnO_3$

D. P. Kozlenko[1], I. Mirebeau[2], J.-G. Park[3,4], I. N. Goncharenko[2], S. Lee[3], Junghwan Park[3], and B. N. Savenko[1]

[1] *Frank Laboratory of Neutron Physics, Joint Institute for Nuclear Research, 141980 Dubna, Russia*
[2] *Laboratoire Léon Brillouin, CEA-CNRS, CE Saclay, 91191 Gif-sur-Yvette, France*
[3] *Department of Physics, SungKyunKwan University, Suwon 440-746, Korea*
[4] *Center for Strongly Correlated Materials Research, Seoul National University, Seoul 151-742, Korea*

The hexagonal manganites $RMnO_3$ (R = Ho, Er, Tm, Yb, Lu, Y, Sc and In) are unique class of materials, exhibiting multiferroic phenomenon in combination with frustrated low dimensional magnetism on triangular lattice. In these compounds, the ferroelectric transition temperature T_C ~ 600 - 900 K is much higher in comparison with the antiferromagnetic (AFM) ordering temperature, T_N ~ 70 – 130 K [1]. In the hexagonal $RMnO_3$ structure of $P6_3cm$ symmetry Mn ions are located at the centers of MnO_5 bipyramids and they form a natural 2D edge-sharing triangular network separated along the *c*-axis by a noncoplanar layer of R atoms. The distance between the nearest Mn atoms is ~ 3.5 Å in the *ab* plane and ~ 6 Å along the *c*-axis, respectively. This then leads naturally to geometrically frustrated magnetism with strong in-plane Mn-O-Mn antiferromagnetic superexchange interactions, while the Mn-O-O-Mn superexchange between adjacent triangular planes is about 2 orders of magnitude weaker.

Recent high pressure studies found that the ordered Mn magnetic moments of $YMnO_3$ and $LuMnO_3$ are strongly suppressed at low temperatures, implying significantly enhanced spin fluctuations in both compounds at high pressures [2]. However, latest muon spin relaxation (μSR) experiments observed T_N of $YMnO_3$ to increase with pressures up to 1.4 GPa, while no evidence of the spin liquid state was found below T_N [3]. These somewhat contrasting observations clearly show that the nature of the magnetic state of $YMnO_3$ at high pressures, especially the relationship between the pressure-enhanced T_N and the spin-fluctuations, still remains unanswered.

In neutron diffraction patterns of $YMnO_3$, measured at the G6.1 diffractometer (Orphee reactor, Laboratoire Leon Brillouin, France) at different pressures and temperatures, a broad diffuse scattering appears at $40 < 2\theta < 80°$ for temperatures well above T_N = 75 K. Upon cooling the diffuse scattering gets stronger and reaches a maximum at T_N (Fig. 1). Below T_N, however, the magnetic diffuse scattering is rapidly suppressed and, at the same time, new magnetic peaks (100) and (101) appear at d = 5.31 and 4.82 Å, respectively, indicating an onset of the triangular 120° AFM state of Γ_1 symmetry. At high pressure of P = 6.7 GPa we observed a substantial decrease and a visible relative change in the intensities of the magnetic peaks at low temperatures. Our subsequent analysis using Rietveld refinement duly found that at 6.7 GPa the ordered Mn magnetic moments get further reduced from 3.2 to 1.6 μ_B and, simultaneously, undergo a pressured-induced reorientation in the *ab* plane as reported in the previous studies for a smaller pressure range [2].The angle φ between the Mn magnetic moments and the hexagonal axes decreases continuously from 90 to 38° with increasing external pressure from 0 to 6.7 GPa. It implies that the symmetry of the triangular AFM state of $YMnO_3$ changes from a pure Γ_1 (φ = 90°) to a mixed $\Gamma_1+\Gamma_2$ irreducible representation.

Of particular notice is that at high pressures the temperature evolution of the diffuse scattering is drastically modified (Fig. 1). For example, it is almost negligible above T_N at P = 6.7 GPa whereas it becomes stronger and reaching a maximum near T_N at ambient pressure (Fig. 3a). However, under high pressure it increases gradually on cooling below T_N and reaches a maximum

intensity at the lowest measured temperature of our study, T = 1.5 K. This striking difference in the temperature dependence of the diffuse scattering between ambient pressure and 6.7 GPa (Fig. 1) is a very strong piece of evidence supporting the idea of the coexistence of the suppressed long-range order and the pressure-induced spin liquid ground state in $YMnO_3$ at high pressures.

How can we understand these experimental observations? In the hexagonal crystal structure of $YMnO_3$ there are two types of in-plane bonds, Mn-O3 and Mn-O4, whose values control the delicate balance of the dominant Mn-O3-Mn and Mn-O4-Mn superexchange AFM interactions within the Mn triangular network. In order to study the pressure dependence and, in particular, the temperature dependences of the in-plane Mn-O bonds, we measured neutron diffraction data for T < 80 K and P = 0 and 5 GPa with the DN-12 spectrometer. Interestingly enough, we observed in these new data that the Mn-O3 and Mn-O4 bonds become very close to one another at ambient pressure and T = 80 K, where the diffuse scattering reaches a maximum, with the difference being just about 0.005 Å above T_N (Fig. 1). As one can see in the figure, upon cooling below T_N the onset of the AFM triangular state is accompanied by a noticeable splitting of these two bonds. The difference between their lengths reaches a value of 0.09 Å at T = 10 K. This splitting in the Mn-O bonds then lifts up the geometrical frustration effects in the ordered phase at ambient pressure. In marked contrast to the ambient pressure data, the splitting of Mn-O3 and Mn-O4 bonds is less pronounced below T_N at high pressure of 5 GPa: the difference of 0.04 Å at T = 10 K is smaller than half of the corresponding value at ambient pressure. The reduced distortion of Mn-O3 and Mn-O4 bonds leads to a further symmetric and ideal triangular network of the Mn spins and so enhanced frustration. The enhanced geometrical frustration effects can then explain the observed appearance of the strong spin fluctuations at low temperatures and a sharp decrease in the ordered magnetic moment [4].

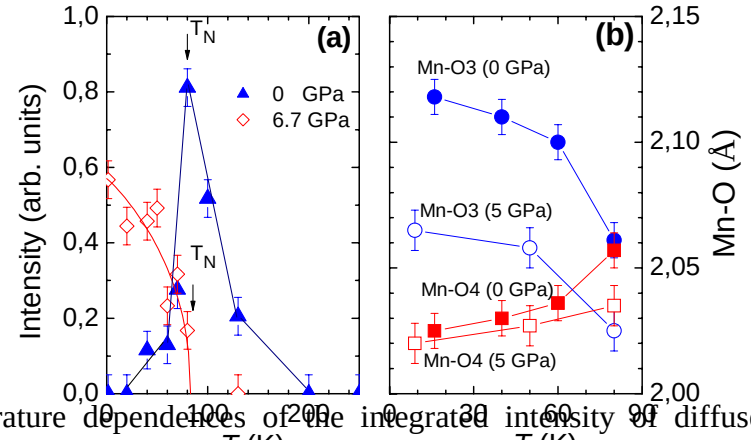

Fig. 1. (a). Temperature dependences of the integrated intensity of diffuse scattering peak in $YMnO_3$ at P = 0 and 6.7 GPa. (b) Temperature dependences of Mn-O3 and Mn-O4 bond distances below and in vicinity of T_N in $YMnO_3$ at P = 0 and 5 GPa.

References:

[1] J. Park, J-G. Park, G. S. Jeon et al., Phys. Rev. B **68**, 104426 (2003).
[2] D.P.Kozlenko, S.E.Kichanov, S.Lee et al., JETP Letters **82**, 193 (2005).
[3] T. Lancaster, S. J. Blundell, D. Andreica et al., Phys. Rev. Lett. **98**, 197203 (2007).
[4] D.P.Kozlenko, I.Mirebeau, J.-G.Park, et al., Phys. Rev. B, v. 78, pp. 054401-1-5 (2008).

STRUCTURAL PHASE TRANSITIONS OF PYRIDINIUM PERCHLORATE AT HIGH PRESSURES

S.E.Kichanov*, D.P.Kozlenko, B.N. Savenko
Frank Laboratory of Neutron Physics, JINR, Russia
* *E-mail: ekich@nf.jinr.ru*

J.Wasicki, W.Nawrocik, P.Czarnecki
Faculty of Physics, A.Mickiewicz University, Poland

C. Lathe
HASYLAB am DESY, Germany

Introduction

Pyridinium salts belong to the group of molecular-ionic crystals with hydrogen bonds, which exhibit a reach variety of interesting phenomena such as structural phase transitions, ferroelectricity and dynamical orientational disorder of the pyridine cations [1-4]. The existence of ferroelectricity was discovered in pyridinium tetrafluoroborate $PyHBF_4$ ($C_5H_5NHBF_4$) [1], pyridinium perchlorate $PyHClO_4$ [2], pyridinium perrhenate $PyHReO_4$ [3] and pyridinium periodide $PyHIO_4$ [4].

In the recent study of the *P-T* phase diagram of $PyHClO_4$ by dielectric and NMR measurements [5] at pressures up to 0.4 GPa and low temperatures tree phases were observed. At ambient pressures and T>245 K the pyridinium prechlorate $PyHClO_4$ exhibits paraelectric phase I with the rhombohedral structure (space group R3m). At T=232 K the phase transition in to paraelectric phase III was observed. Under pressure, a linear increase of the transition temperatures to phases II and III was found. However, the direct structure studies of phase II and III of the pyridinium perchlorate $PyHClO_4$ wasn't performed.

In order to study structural modifications of deuterated pyridinium perchlorate we have performed energy dispersive X-ray diffraction measurements at high pressure up to 3.5 GPa in temperature range 297 – 380 K.

Experimental

The $(d_5PyH)ClO_4$ salt was prepared by allowing the d_5-pyridinium base (95%) dissolved in 80% ethanol to react with perchloric acid. The substance obtained in this way was recrystallized three times.

The X-ray diffraction experiments at high pressures up to 3.5 GPa in temperature range 294 – 380 K were carried out using the multianvil X-ray system MAX80 at F2.1 beamline of storage ring DORIS-III. Diffraction patterns were recorded in an energy dispersive mode using white synchrotron X-rays from the storage ring DORIS-III. The Bragg angle 2θ was fixed at 9.093°, counting times for each diffraction pattern were about 7 min. The refinement of X-rays diffraction patterns were made by means of Fullprof [6] program.

Results and discussions

At ambient conditions the rhombohedral phase I with space group R3m was evidenced and its calculated lattice parameters were a=8.675(9) Å and c=8.497(4) Å. This result agrees well with experimental data from Ref. [5]. At high pressure P>0.5 GPa the some changes in diffraction patterns were observed. These changes were corresponding with the phase transition from phase I to phase II in deuterated pyridinium perchlorate at high pressure. With a further pressure increase, sharp changes of diffraction patterns were indicated for P > 0.9 GPa, evidencing appearance of the phase III. The program VMRIA [7] were used for structure of high pressure phase II and III solving and its lattice parameters obtaining. The diffraction peaks for the phase II and III can be properly indexed within the monoclinic structural model of Cm and Pm symmetry, respectively. The

expected unit cell parameters of phase II at P=0.5 GPa are a=8.286(8) Å, b=14.758(7) Å, c=8.605(8) Å and β=90.9(6)^o Å and the phase III parameters are a=7.948(7) Å, b=14.444(9) Å, c=8.526(9) Å and β=93.2(9)^o. The unit cell volume as function of pressure was fitted by the Birch-Murnaghan equation of state [8]. The calculated values of bulk modules are B_0 = 15*(3)* GPa and B' = 4*(1)* for the phase I; B_0 =6(2) and B' = 4*(1)* for the ferroelectric phase II and B_0 = 11*(3)* GPa, B' = 4*(1)* for high pressure phase III.

The addition temperature experiments shown shift of temperatures of phase transition from phase III to II and from II to I at high pressure. The changes of temperature of phase transition from phase I to phase II is described T_{I-II}=245K+79.6(4)×P (GPa) and from monoclinic phase II to phase III T_{II-III}=233K+64.4(4)×P (GPa). The temperature range where ferroelectric phase exist increase from 12 K at ambient pressure to 42 K at pressure P=2.0 GPa. The *P-T* phase diagram of deuterated pyridinium perchlorate constructed on the basis of the obtained experimental data and data from Ref. [5] are shown in Fig. 1.

References

[1] P. Czarnecki, W. Nawrocik, Z. Pajak and J. Wasicki, Phys. Rev. B, **49**, 1511(1994).
[2] P. Czarnecki, W. Nawrocik, Z. Pajak and J. Wasicki, J. Phys.: Condensed Matter, **6,** 4955 (1994).
[3] J. Wasicki, P. Czarnecki, Z. Pajak, W. Nawrocik and W. Szczepanski, J. Chem. Phys., **107**, 576 (1997).
[4] Z. Pajak, P. Czarnecki, J. Wasicki and W. Nawrocik, J. Chem. Phys., **109**, 6420(1996).
[5] P. Czarnecki, J. Wasicki, Z. Pajak, R. Goc, H. Małuszynska, S. Habriło, J. Mol. Str., **404**, 175-180 (1997).
[6] J. Rodriguez-Carvajal, Physica B, **192**, 55 (1993).
[7] Zlokazov V.B., in thesis book of «IV Workshop on investigations at the IBR-2 pulsed reactor», (2005) p.75.
[8] F. J. Birch, J. Geophys. Res., **91**, 4949 (1986).

Fig.1. Phase diagram of $(d_5PyH)ClO_4$ constructed on the basis of the present data (open stars) and data from ref. [5] (open triangles).

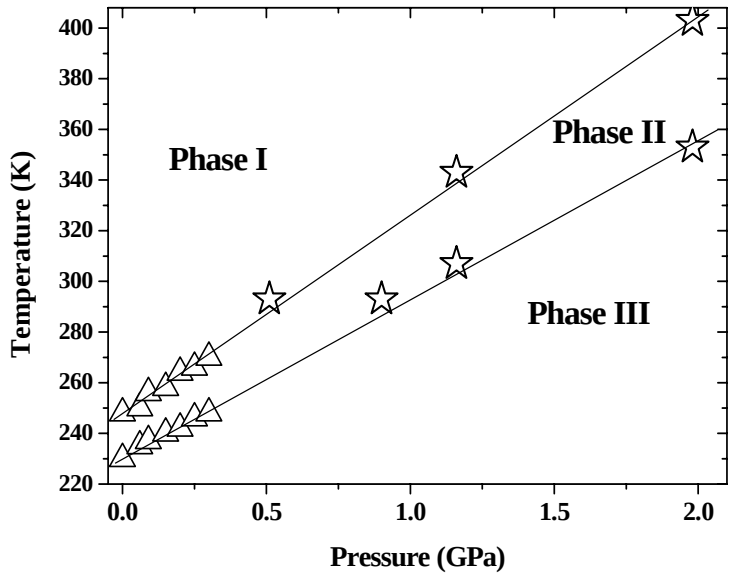

AUTOCORRELATIVE MICRODYNAMICS OF LIQUID LITHIUM AND LITHIUM–HYDROGEN MELT: THE INELASTIC NEUTRON SCATTERING STUDY

N.M. Blagoveshchenskii, A.G. Novikov, V.V. Savostin

State Scientific Center of Russian Federation – Institute for Physics and Power Engineering, Obninsk, Russia

Among numerous microdynamic characteristics of matter the valuable role plays the so called velocity autocorrelation function (VACF), which describes the correlations between velocities of particle at two different times, $t_1 = 0$ and $t_2 = t$. VACF is widely discussed function of the matter. The VACF can explain mainly by its theoretical manipulation access, and for the other hand, VACF is the direct output of molecular dynamics (MD) simulation. Time dependence of VACF follows from the frequency spectrum, $g(\omega)$, of the substance in such a way [1]:

$$\Psi_{VACF}(t) = \frac{<V(0)V(t)>}{<V^2(0)>} = \int_0^\infty g(\omega)\frac{h\omega}{kT}cth(\frac{h\omega}{2kT})\cos(\omega t)d\omega \ . \qquad (1)$$

Fig.1 represents the VACF of liquid lithium atoms at different temperatures. It is seen that at t > 0.12 ps atom «forgets» its primary velocity. The local minimum of VACF disposition marks the time of «nearest neighbors» regime, and allows the characteristic interatomic oscillation frequency to be determined, as well as average oscillation energy of atoms in the liquid onder investigation.

For the comparison Fig. 2 contains the VACFs of liquid lithium for different temperatures obtained by the present study, and VACFs from MD-simulation [2] at approximate temperatures.

Fig. 2 reveals three main divergencies of the experiment from modeling. Firstly, experiment shows more weak VACF *vs*. T dependence. Secondly, the minimum of VACF corresponds to the more high oscillation energies inferred from experimental data than from MD-simulation. Thirdly, the experimental curves possess more deep minima. These divergencies we understand as the result of some inadequacy of interatomic interaction potential explored in MD-simulation.

Fig. 3 and 4 represent the VACF describing by the simple one-or-two component formula [3]:

$$\Psi(t) \sim \sum_{i=1}^{2}\exp(-\frac{t}{t_0})\cos(\frac{\varepsilon_i}{\hbar}t) \qquad (2)$$

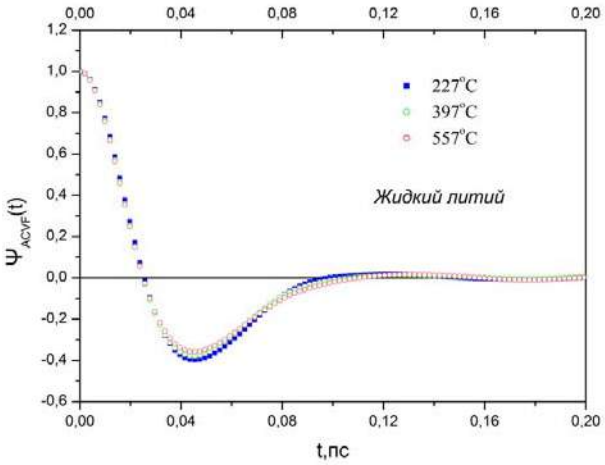

Fig. 1. VACF of liquid lithium atoms at different temperatures.

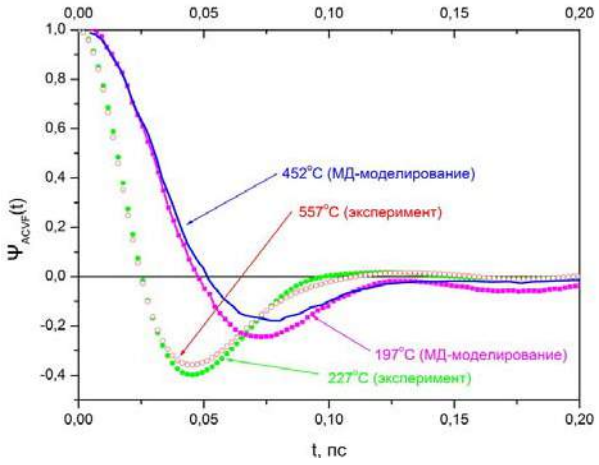

Fig. 2. VACF of liquid lithium atoms in comparison with VACF from MD-simulation at approximate temperatures [2].

As it seen from Fig. 3 and 4, the use of two components of formula (2) approximates the experimental curve VACF better than the use of one component. The t_0 value of expression (2) usually treats as particle life-time in the given surroundings, or by another words, can be called as a time of structural relaxation.

As a contemporary liquids theory regards, the fluctuation relaxation process mechanism is twofold: fast, linked with the binary atom-atom collisions, and slow, taking place through the atom-neighboring (clusters) interaction [2]. Hence, there exist also two different times of structural relaxation, related with the fast and slow mechanisms, correspondingly.

Our data treatment procedure includes the separation of neutron scattering spectra into the inelastic and quasi-elastic components with next their separate analysis. So, all the analysed VACFs do not contain any diffusion effects, being of pure oscillatory nature. As a matter of fact, one can suppose that the characteristic time t_0 extracted from the VACF's decomposition (2) is related to the fast (i.e. binary) process.

Difference of the frequency spectra of lithium and hydrogen in the Li–H alloy [4] absolutely reflects itself in the lineshape of VACF shown in Fig. 5. The difference of relaxation times for lithium and for hydrogen in the Li–H alloy [4] demonstrates that the nearest neighboring in pure lithium is more long living than it takes place in Li–H alloy.

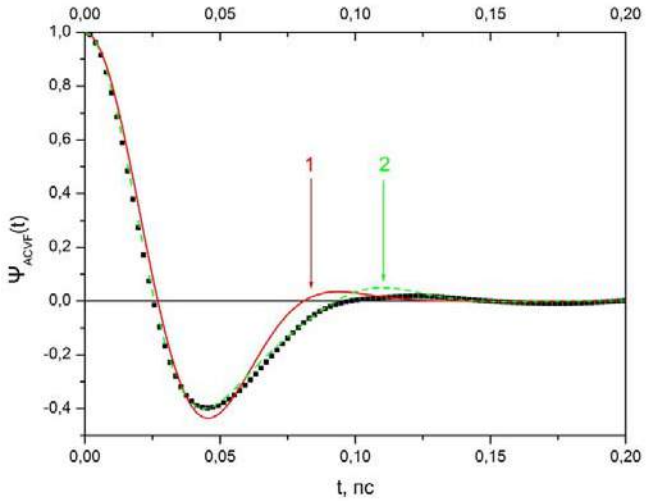

Fig. 3. The experimental VACF (T = 227°C) description by one-component model (2) – 1, and by two-component model (2) – 2: ε_1 = 35.1 meV, ε_2 = 66.3 meV, t_0 = 0.067 ps.

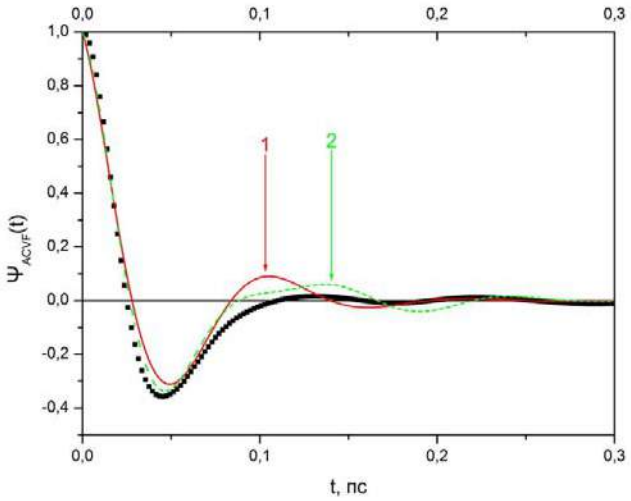

Fig. 4. The experimental VACF (T = 557°C) description by one-component model (2) – 1, and by two-component model (2) – 2: ε_1 = 32.7 meV, ε_2 = 52.5 meV, t_0 = 0.061 ps.

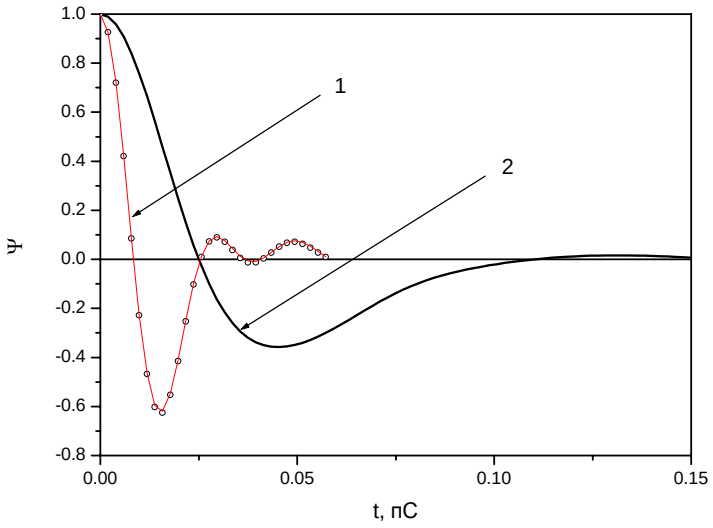

Fig. 5. Comparison of the VACF for lithium (1) and for hydrogen in the Li–H melt (2). T = 557°C.

References

1. Киттель Ч. Введение в физику твердого тела. М.: Наука, 1978.
2. Canales M., Gonzalez D., Gonzalez L., Alemany M., Gallego L. Density fluctuations and single-particle dynamics in liquid lithium. 2000, Phys. Rev. B, v. 62, p. 12095.
3. Sharma S.K., Tankeshwar K. Self-diffusion coefficients of expanded rubidium. J. Phys.: Condens. Matter, 1996, v. 8, p. 1089.
4. Blagoveshchenskii N.M., Morozov V.A., Novikov A.G., Pashnev M.A., Savostin V.V., Shimkevich A.L. Study of the microdynamics of liquid lithium and lithium–hydrogen melt by inelastic neutron scattering. Crystallography Reports, 2007, v. 52(3), p. 460.

STRUCTURAL ASPECTS OF FERROGFLUIDS STABILIZATION BY MONO-CARBOXYLIC ACIDS

Avdeev M.V. *, Feoktystov A.V. **, Aksenov V.L. ***
Frank Laboratory of Neutron Physics, Joint Institute for Nuclear Research, Dubna, Russia
*E-mail: *avd@nf.jinr.ru, **feoktystov@gmail.com, ***aksenov@nf.jinr.ru*

Vekas L.
Center for Fundamental and Advanced Technical Research RAS, Timisoara Division, Romania

Rosta L.
Research Institute for Solid State Physics and Optics HAS, Budapest, Hungary

Garamus V.M., Willumeit R.
GKSS Research Centre, Geesthacht, Germany

Colloidal stability of magnetic fluids (MFs), especially at a high volume fraction of magnetic nanoparticles, φ_m, is a complex issue connected to the synthesis procedure, including the nature of surfactant(s) and carrier liquids used. In this work we report our recent results on structural studies of stabilization factors in MFs based on non-polar organic carriers.

It is well known [1] that one of the best molecules for stabilizing magnetite nanoparticles in organic non-polar liquids is oleic acid (OA), a non-saturated mono-carboxylic (fatty) acid, which has a C_{18}–tail with a double bond kink in the middle. Despite wide use of this surfactant in stabilization procedures of magnetic fluids, still there is no full understanding what factors responsible for the resulting stabilization distinguish oleic acid from its straight-chain saturated analogue, stearic acid, which is always considered as a poor stabilizer. Here, we investigate the structure of magnetic fluids based on decahydronaphtalene (DHN) and stabilized by various chain length molecules from a series of saturated and straight carboxylic acids, namely lauric (LA), myristic (MA), palmitic (PA) and stearic (SA) acids with C_{12}, C_{14}, C_{16}, C_{18}- tails, respectively, and compared them with the classical fluid stabilized by OA. Magnetization analysis and small-angle neutron scattering are used to find out and compare the particle size distribution in the studied MFs and the effective thickness of the surfactant (acid) shell. This work is a continuation of [2].

All studied fluids were prepared by the same procedure [3,2] standard for OA stabilization. Magnetite nanoparticles, Fe_3O_4, were obtained by the co-precipitation in aqueous solution of Fe^{2+} and Fe^{3+} ions (salts $FeSO_4.7H_2O$; $FeCl_3.4H_2O$) in the presence of NH_4OH sol. 25% (temperature 80-82^{o}C). A surfactant from the above mentioned series with a significant excess (30 vol. %) was added to the system right after the co-precipitation starts following its chemisorption on the magnetite surface. Then, several steps including washing with magnetic decantation, flocculation, re-dispersion in light hydrocarbon and filtration were performed to remove residues of salts, free surfactant in solution and large aggregates of non-dispersed magnetite particles, respectively. Finally, magnetite particles coated with a single surfactant layer were extracted by flocculation with acetone and, then, re-dispersed into the required carrier, DHN (Merck, chemically pure). The particle concentration in the MF strongly depends on the acid used. Despite the fact that exact quantitative analysis of the dispersing efficiency is quite a difficult topic for colloidal solutions, qualitatively we conclude that as compared to OA such efficiency is just several times less for MA, and more than 10 times less for other saturated acids (LA, PA, SA). Again, qualitatively, SA is the worst stabilizant among the considered saturated acids. Repeating the above procedure in the case of saturated acids several times (depending on dispersing efficiency) we succeeded in concentrating the samples up to φ_m within 6 - 10 %. It is important that the final flocculation-redispersing cycle was additionally performed

until free surfactants were completely removed from the fluids. The ratio between volume fractions of magnetite and covering surfactants was determined from the density measurements and constituted ~1:1 for OA sample and between 1:2 and 1:3 for samples with saturated acids. All of the fluids were stable at least a year after preparation.

The main structural difference revealed for the fluids with saturated acids as compared to the OA case concerns the size distribution function of the stabilized magnetite nanoparticles. First, it was judged from the magnetization curves (Fig.1). They were treated in terms of the polydisperse Langevin approximation [5] with the log-normal distribution of the magnetite core radius R:

$$D_N(R)=(1/(2\pi)^{1/2}SR)\exp[-\ln^2(R/R_0)/(2S^2)], \quad (1)$$

where R_0, S are the varied parameters. Because of the low volume fraction of magnetite both the concentration effect and the magnetic interparticle interaction were not taken into account.

The SANS curves from solutions in DHN are given in Fig.2. In this case the scattering from the surfactant layer is almost matched, because the values of the mean scattering length density for the surfactants and carrier are close [4]. Also, the nuclear scattering dominates strongly over the magnetic part, which is a result of the large contrast between magnetite and carrier [4]. So, the curves in Fig.2 correspond to the nuclear scattering from magnetite and are treated in the frame of the model of homogeneous polydisperse spheres [4] with $D_N(R)$ as in Eq.1.

The difference in the data of magnetization analysis and SANS can be seen for $D_N(R)$. It is most significant for the case of the OA stabilization. In [2] this difference was related to the size dependence of the thickness of the non-magnetic layer. However, there is no clear reason for such effect. The discussed difference can also reflect the magnetic interaction effect, which concerns both the magnetization analysis and SANS. In the first case, it influences the used Langevin approximation. The larger the particles dispersed in the liquid (OA sample), the stronger the interaction; hence, a larger deviation in the parameters of the Langevin approximation can take place. In SANS the attraction between particles results in appearance of the structure-factor increasing the apparent atomic size of the particles and making it different from the magnetic size.

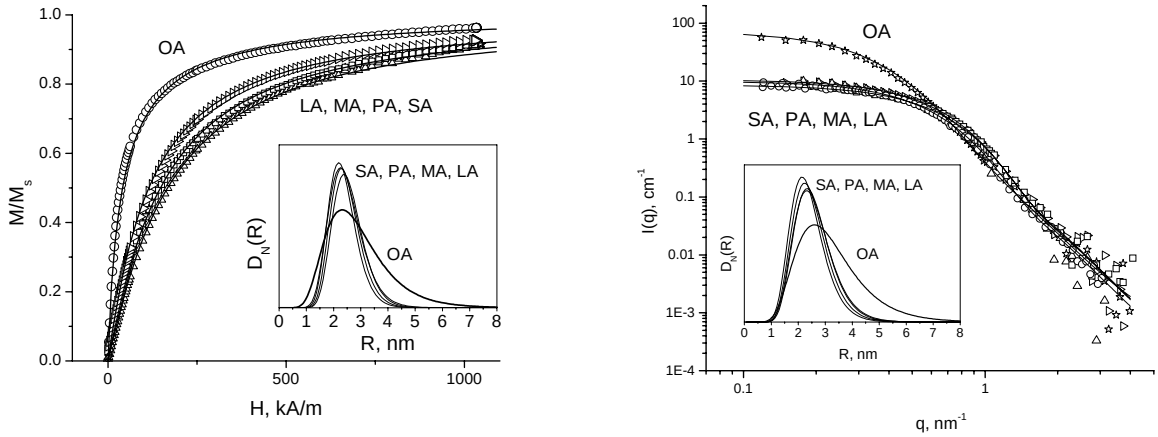

Fig.1. Magnetization curves (points) for magnetic fluids stabilized by various mono-carboxylic acids in DHN, φ_m = 1.5 %. Lines are results of polydisperse Langevin approximation. Inset shows corresponding particle size distributions of magnetite (magnetic size).

Fig.2. Experimental (points) SANS curves for MFs in DHN normalized to φ_m = 1.5 %. Lines are the results of approximation by the model of poly-disperse independent spheres. Inset shows the corresponding particle size distributions of magnetite (atomic size).

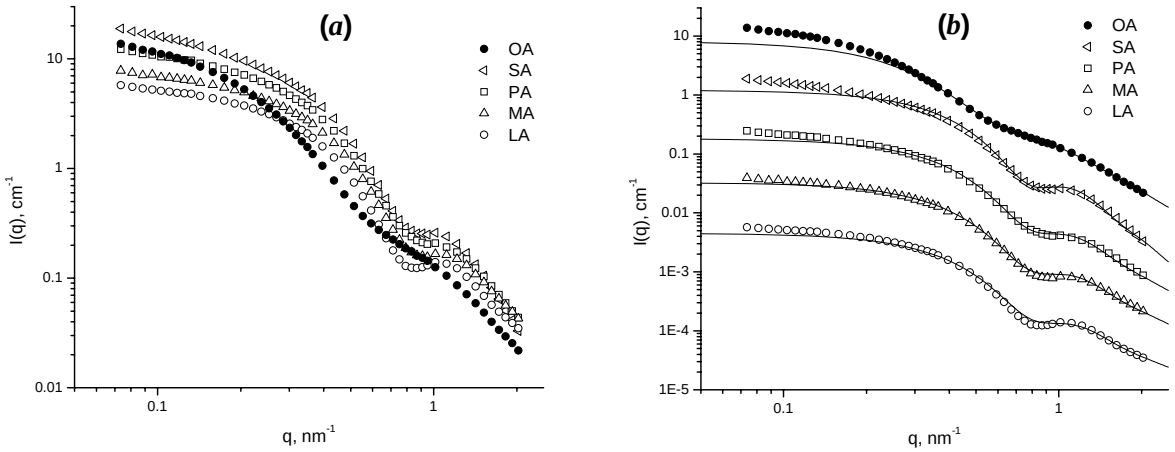

Fig.3. SANS curves for MFs in 90 % d-DHN. (*a*) curves are normalized to φ_m = 0.6 %. (*b*) approximation by the model of independent core-shell particles with polydisperse core; for convenient view the curves are additionally divided by factors of 10 (SA), 50 (PA), 200 (MA), 1000 (LA).

Table 1.

Sample	R_0 (nm)		S		h (nm) (scattering)	L (nm)
	magnetization	scattering	magnetization	scattering		
OA	2.70	3.40	0.39	0.38	1.40	2.3
SA	2.50	2.55	0.22	0.28	1.85	2.3
PA	2.40	2.48	0.22	0.28	1.55	2.1
MA	2.40	2.65	0.22	0.28	1.35	1.8
LA	2.30	2.51	0.22	0.28	1.25	1.6

The thickness of the surfactant layer around magnetite can be deduced from SANS data for 90% d-DHN solutions in Fig.3. In this case, due to a significant contrast the scattering from the layer contributes much in the curves making their behavior quite different from the previous case with usual DHN. The modulation of the scattering with the chain length of the saturated acids is clearly seen in Fig.3*a*. Since the particle size distribution does not change much with the surfactant, and the scattering length densities of the saturated acids are very close, the surfactant chain length is the only factor determining the difference in the curves for saturated acids. The given data differ from those in Fig.2, where no modulation on the surfactant length takes place. Again, the curve for the fluid with the OA stabilization in Fig.3*a* shows qualitatively different behavior as compared to saturated acids, which confirms the conclusion about the difference in the $D_N(R)$ function for the two cases. In Fig.3*b* all curves are fitted to the core-shell model for particles with poldisperse cores [4, 6]. Here, the magnetic scattering contribution is neglected. As it was shown previously, [7, 6, 8], it is difficult to model this contribution because of the complex magnetic correlations. Nevertheless, its effect is small for $q > 0.1$ nm^{-1}. At smaller q-values it results in systematic deviation of the experimental data from the model curves (see Fig.3*b*). Together with the thickness of the shell, h, the dimensionless parameter η=-(ρ_1 - ρ_s)/(ρ_1-ρ_0) comprising the scattering length densities of magnetite, $\rho_0 = 6.9\times10^{10}$ cm^{-2}, shell, $\rho_1 \approx 0$ cm^{-2}, and solvent, $\rho_s = 6.545\times10^{10}$ cm^{-2}, was varied around the calculated value of –0.95. Also, the parameters of the $D_N(R)$ function were free only over 5 % vicinities around values taken from

the data in Fig.2. The resulting *h*-values are presented in Table 1. They confirm the conclusion that the thickness of the surfactant layer correlates with the surfactant length, *L*, whose value calculated according to Tanford's formula [9] is given in Table 1 for comparison. Taking into account the fact that saturated fatty acids of various chain lengths stabilize magnetite nanoparticles with approximately the same $D_N(R)$, one can conclude that this $D_N(R)$ is not determined by the acid length, but rather the acid organization on magnetite surface. Our data show that a stabilizing layer of a saturated acid possesses worse elastic properties than the layer of OA. The other reason, which can affect the stabilized particle size distribution, as well as the dispersing efficiency of the acids, is connected with chemical factors during the preparation. Thus, the possible micelle formation in intermediate water solutions can decrease the number of free surfactant molecules required for full coating of magnetite surface. The critical micelle concentration is inversely proportional to the molecule length, which correlates with the worst dispersing efficiency of the longest SA. Also, the addition of the surfactants during the synthesis of the studied MFs is performed using concentrated solutions of the acids in light hydrocarbon. The nematic interaction between the elongated acid molecules can affect the number density of free surfactant in solution. The careful consideration of these two points is the subject of our further research.

Acknowledgments. The work is done in the frame of the project RFBR-Helmholtz (HRJRG-016). This research project has also been supported by the European Commission under FP6 through the Key Action: Strengthening the European Research Area, Research Infrastructures. Contract nr: RII3-CT-2003-505925, GKSS, Germany; and by the CEEX research program of the Romanian Ministry of Education and Research, contract NanoMagneFluidSeal nr.83/2006.

References:

[1] R.E.Rosensweig: *Ferrohydrodynamics* (Cambridge University Press, UK 1985)
[2] M.V.Avdeev, D.Bica, L.Vékás, et al., J. Mag. Mag. Mater. 311 (2007) 6
[3] D.Bica, Rom. Rep. Phys. 47 (1995) 265
[4] M.V.Avdeev, V.L.Aksenov, M.Balasoiu, et al., J. Coll. Interface Sci. 295 (2006) 100
[5] M.Rasa, Eur. Phys. J. 2 (2000) 265
[6] M.V.Avdeev, M.Balasoiu, V.L.Aksenov, et al., J. Mag. Mag. Mater. 270 (2004) 371
[7] M.V.Avdeev, M.Balasoiu, Gy.Torok, et al., J. Mag. Mag. Mater. 252 (2002) 86
[8] M.V.Avdeev, Physics Uspekhi 50 (2007) 1083
[9] C.Tanford, J. Phys. Chem. 76 (1972) 3020

INVESTIGATION OF PERIODIC MULTILAYERS

Bodnarchuck V.I.†, , Ignatovich V.K., Yaradaikin S.P.
FLNP JINR
E-mail: † bodnarch@nf.jinr.ru

Czer L, Veres T
Research Institute for Solid State Physics, Konkoly, Th.u. 29-33, P.O.B. 49, H-1525, Budapest XII, Hungary

Introduction

Neutron supermirrors are used in many physical experiments now. They are multilayer systems usually composed as a set of bilayers every one of which consists of two materials with high and low optical potentials. The supermirrors increase the angular or wave length range of total reflection comparing to mirrors consisting of a single material with high optical potential. If the single material gives total reflection for normal component k of the incident neutrons in the range $0 < k < k_c$, where k_c is the limiting wave number for the given material, the supermirror can increase the interval up to nk_c. A multilayer system that gives reflectivity ~ 1 in the interval $0 < k < nk_c$ is called Mn mirror. It became a usual practice to fabricate M2 and M3 mirrors. However there are many attempts to produce mirrors with higher n also. The last record belongs to Japanese [1] who prepared mirror M6.7.

Last time all the mirrors were prepared in aperiodical fashion, which meant that thicknesses of layers in bilayers varied with the bilayer number. The algorithm for thickness variation was proposed by Hayter and Mook [2]. According to this algorithm the change of thicknesses of neighboring bilayers is very small and does not match interatomic distance. It leads to creation of unavoidable roughnesses on layers interface.

There exists also another algorithm proposed in [3], according to which the supermirror is to be produced as a set of periodic chains with some number N of identical bilayers. The variation of thicknesses of neighboring chains in this case is larger, which may help to improve quality of interfaces and therefore of the whole supermirror.

Experiment

The goal of the given work is to investigate at the Budapest Neutron Center how well we can control the thickness and quality of periodic multilayer systems prepared by Mirrotron Ltd, Budapest. In other words we want to see how well the neutron reflectivity of produced systems match theoretical expectations, how large is diffuse scattering because of technological imperfectness and whether we can explain and control them.

For that purpose we measured at the neutron reflectometer of KFKI reflectivities of 4 samples containing 1, 2, 4 and 8 Ni/Ti bilayers on a boron float glass substrate. The scheme of the experiment is shown in Fig. 1. In this experiment the incident beam was monochromatized by crystal of pyrolytic graphite and had wave length 4.28 Å. The sample mirror could be rotated to change the grazing angle θ of the incident neutrons, and the detector was stationary and wide enough to percept all the reflected neutrons in a given range of θ variation.

From fitting of measured data to theoretical curves we could find the parameters of samples and resolution of installation. Variation of parameters of samples shows how far the technological conditions are varied from sample to sample. Comparison of angular distribution of the incident beam at the reflectometer and angular distribution of the reflected beam gives information on intensity of diffuse scattering and its dependence on number of bilayers.

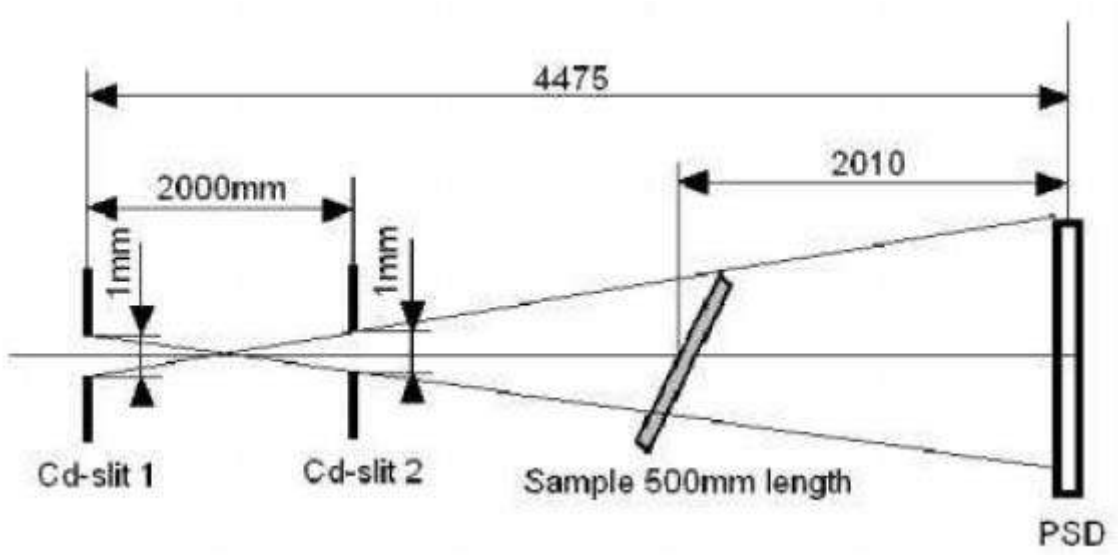

Fig. 1. The scheme of the neutron reflectometer at KFKI. The sample mirror can be rotated around an axis perpendicular to the plane of the picture. The position sensitive detector is stationary and sufficiently large to register all the reflected neutrons, when grazing angle is sufficiently small according to experimental requirements. Collimation angle was 0.5 mrad and the neutron beam was monochromatic with wave length 4.28 Å and presumable resolution.

In Figure 2 in linear scale are shown the results of fitting experimental data for 2, 4 and 8 periods with the formula [3]:

$$R(k) = \int_{k-\delta}^{k+\delta} \left| \vec{R}_{Ns}(p) \right|^2 \frac{dp}{2\delta} + n_b \,, \tag{1}$$

where

$$\vec{R}_{Ns}(p) = \vec{R}_N(p) + T_N^2(p) \frac{r_{s0}(p)}{1 - \overleftarrow{R}_N(p) r_{s0}(p)} \tag{2}$$

is the reflection amplitude from a periodic chain of N periods evaporated over a semiinfinite substrate, and the substrate reflection amplitude is

$$r_{s0} = \frac{k - k_s}{k + k_s}, k_s = \sqrt{k^2 - u_s} \,. \tag{3}$$

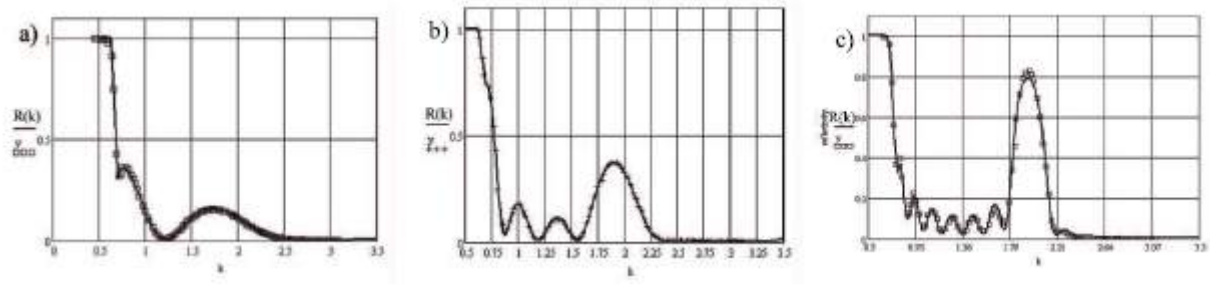

Fig. 2. Fitting of the reflectivity data for periodic chains of bilayers evaporated on a thick float glass substrate. The fitting function is given by Eq. (1). The data were obtained in Hungary at the reflectometer with wide stationary detector. The results are shown in linear scale for a) 2; b) 4; c) 8 bilayers. The solid curves are theoretical curves with parameters found from fitting.

Eq. (1) takes into account the final resolution of the installation, scheme of which is shown in Fig. 2, and possible existence of background, nb, in the system. The resolution δ and background n_b were two fitting parameters. Besides them we took as fitting parameters the real parts of all the potentials u_b, u_w, the potential of substrate u_s in terms of that of Ni, and thicknesses of Ni and

Ti layers in units of $\lambda_c/2\pi$ of Ni. Imaginary parts of the potentials were put to table ones. The results for fitted parameters are presented in the first three lines of the Table 1. The last column of the table shows χ^2 of the fitting. The pictures in Fig. 2 show a good fit of all the samples, however the thicknesses of the Ni layers are more than 20% higher and thicknesses of the Ti layers are more than 20% lower than in the project. The Ni potential was found to be slightly lower than is expected, which can be explained by presence of some oxygen or nitrogen impurities. The resolution $\delta \approx 3.5$ % and background $n_b = 0.003$ are also quite acceptable. The worst was the value of the χ^2. It is especially high in the case of the 8 periods sample.

Table 1. Fitted values of real parts of potentials u′ for Ni (b-barrier), Ti (w-well) and substrate (s), their thickness *l*, resolution δ, background n_b and χ^2 for periodic chains with N=2,4,8 bilayers. Imaginary parts u″ of the potentials were fixed. The results are given in dimensionless units. The unit of energy is equal to real part of Ni optical potential $u'_{Ni} = 0.245$ μeV, and unit of length is the reduced critical wavelength $\lambda_c/2\pi = 92$Å for Ni.

N	u_b'	u_w'	u_s'	u_b''	u_w''	u_s''	l_b	l_w	δ	n_b	χ^2
2	**0.964**	**-0.258**	**0.452**	**0.00014**	**0.00012**	**0.0001**	**1.121**	**0.59**	**0.036**	**0.003**	**25**
4	**0.934**	**-0.388**	**0.446**	**0.00014**	**0.00012**	**0.0001**	**1.182**	**0.525**	**0.033**	**0.003**	**114**
8	**0.993**	**-0.242**	**0.398**	**0.00014**	**0.00012**	**0.0001**	**1.061**	**0.649**	**0.035**	**0.0089**	**349**

Perhaps, so high value of χ^2 could be explained by taking into account the off-specular scattering that we not regarded in our model. Unfortunately we can not measure the off-specular scattering on our samples in BNC and the checking of its influence on the fit is a deal of the future experiment.

Conclusions

The experiment confirms the rightness of algorithm given in [3] for the samples with few periods. At the same time the experiment clearly shown that achieving of the good agreement between the experimental results and theoretical model is possible with taking into account both the specular and diffuse off specular reflection on the sample imperfections.

References:

[1] Maruyama R, Yamazaki D, T. Ebisawa T, M. Hino M, Soyama K. Development of neutron supermirror with large critical angle. Thin solid films 2007;515:5704-6.

[2] Hayter JB, Mook HA. Discrete Thin-Film Multilayer Design for X-ray and Neutron Supermirrors. J.Appl.Cryst. 1989;22:35-41.

[3] Carron I., Ignatovich VK. Algorithm for preparation of multilayer systems with high critical angle of total reflection Phys.Rev. 2003;A67:043610.

[4] Ignatovich VK. “Neutron optics.” M: Fizmatlit, 2006 (in Russian).

[5] Steyerl A. Effect of surface roughness on the total reflection and transmission of slow neutrons. Z.Phys. 1972;254:169-88.

[6] Sinha SK, Sirota EB, Garoff G, Stanley HB. X-ray and neutron scattering from rough surfaces. Phys.Rev.B 1988;38(4):2297-311.

[7] Chiarello R, Panella V, Krim J, Thompson C. X-ray reflectivity and adsorption isotherm study of fractal scaling in vapor-deposited films. Phys.Rev.Lett. 1991; 67(24):3408-11.

[8] Pynn R. Neutron scattering by rough surfaces at grazing incidence. Phys.Rev.B. 1992;45(2):602-12.

SANS CONTRAST VARIATION ON WATER-BASED MAGNETIC FLUIDS STABILIZED BY DIFFERENT MONOCARBOXYLIC ACIDS

Feoktystov A.V. [*], Avdeev M.V. [**]
Frank Laboratory of Neutron Physics, Joint Institute for Nuclear Research, Dubna, Russia
E-mail: [*] *feoktystov@gmail.com*, [**] *avd@nf.jinr.ru*

Bulavin L.A.
Kyiv Taras Shevchenko National University, Kyiv, Ukraine

Vekas L.
Center for Fundamental and Advanced Technical Research RAS, Timisoara Division, Romania

Garamus V.M., Willumeit R.
GKSS Research Centre, Geesthacht, Germany

Magnetic fluids are colloidal dispersions of magnetic nanoparticles in liquids. To prevent aggregation of the particles because of the dipole-dipole interaction (especially in the magnetized state under external magnetic field) particles are usually covered with a stabilizing surfactant layer [1]. For polar magnetic fluids the double stabilization, conventionally the formation of the additional second layer, is required [2]. The first layer forms due to chemisorption of surfactant polar heads on the surface of the magnetic particles. The second layer is the result of the physical sorption: tails of the second layer's molecules are turned to the tails of the first layer's molecules, thus polar heads are turned outside, which makes it possible to dissolve the particles in polar carriers. Such kind of double-layer stabilization requires some excess of the surfactant molecules in the solution, so that exchange of molecules of the second stabilization layer with free molecules in the solvent is in equilibrium. This type of magnetic fluids is promising for synthesis of biocompatible magnetic systems to be used in various medical applications.

The initial concentrated magnetic fluids were synthesized in the Laboratory of Magnetic Fluids at the Center of Fundamental and Advanced Technical Research of the Romanian Academy of Sciences (Timisoara, Romania). The samples were water-based magnetic fluids with magnetite nanoparticles stabilized by myristic (MA) or oleic acids (OA). The volume fraction of dispersed magnetite, φ_m, constituted 11% in the LA sample and 13% in the MA sample. Fluids showed good stability (at least in one year after preparation) in the absence of external magnetic field.

To perform contrast variation measurements samples were diluted ten times with different mixtures of light water (H_2O) and heavy water (D_2O) in a way that the D_2O content in the final sample was varied from 0% up to 90%.

The measurements were done at the SANS-1 instrument at the steady-state reactor FRG-1 of the GKSS Research Centre (Geesthacht, Germany). As buffer solutions the corresponding mixtures of H_2O/D_2O with the same D_2O content were used.

The contrast variation method in SANS experiments is based on detecting changes in the scattering from the system when varying the contrast, a difference between mean scattering length densities (SLDs) of the particles and the carrier. In the classical generalized approach for monodisperse non-magnetic particles [3] the SANS intensity is analyzed in terms of the basic functions (q-dependent coefficients in the expansion of I over the contrast). For polydisperse and magnetic particles in magnetic fluids the scattering can be treated [4] in similar manner:

$$I(q) = \tilde{I}_s(q) + \Delta\tilde{\rho}\tilde{I}_{cs}(q) + (\Delta\tilde{\rho})^2 \tilde{I}_c(q), \quad (1)$$

where

$$\Delta\tilde{\rho} = \overline{\rho}_e - \rho_s \quad (2)$$

is the modified contrast, the difference between the effective mean SLD of the particles, $\overline{\rho}_e$, and SLD of the liquid carrier, ρ_s; and $\tilde{I}_c(q)$, $\tilde{I}_s(q)$, $\tilde{I}_{cs}(q)$ are the modified basic functions which contain information about the nuclear and magnetic SLD distributions within particles, as well as the polydispersity function. The term $(\Delta\tilde{\rho})^2\tilde{I}_c(q)$ prevails in the scattering intensity at sufficiently large contrast and corresponds to the average particle shape. The contrast independent term $\tilde{I}_s(q)$ comprises the residual nuclear scattering at the effective match point and magnetic scattering contribution, which is determined by the magnetic SLD of the particles. The $\tilde{I}_{cs}(q)$ is the cross-term. In the general case, the choice of $\overline{\rho}_e$ is arbitrary [4]. It does not affect the $\tilde{I}_c(q)$ function, which is the most transparent for interpretation.

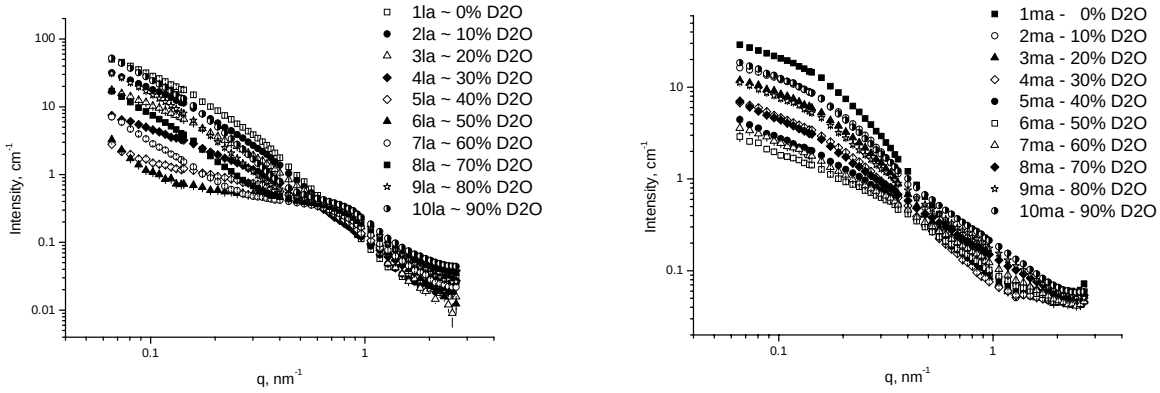

a) b)

Fig.1. SANS contrast variation on magnetic fluids with double-layer stabilization by lauric acid (LA) (a) and myristic acid (MA) (b). Percent volume fraction of D_2O in the solvent is indicated. Volume fraction of dispersed magnetite in the samples, φ_m, is ~1.1% (LA) and ~1.3% (MA).

All scattering curves measured at various D_2O content are presented in Fig.1a (LA) and Fig.1b (MA). We failed in fitting the experimental curves to the model of separate core-shell particles imitating spherical magnetite cores coated with surfactant shell. This indicates a significant aggregation effect on the scattering, which differs much the studied type of magnetic fluids from those based on non-polar carriers and stabilized by a single surfactant layer [5]. The scattering from the aggregates does not make it possible to treat the obtained curves with the Guinier approximation. As the choice of effective match-point is arbitrary, here we used another method which connects this choice with the inner structure of the considered systems. We have found minima positions in the dependencies of scattering intensities on D_2O content in the liquid carrier at different q-values. The found dependences of the minimum positions as a function of q are given in Fig.2. The important observation is that for the MA sample the minimum does not change at q-interval of 0.06 – 0.3 nm^{-1}. From the well-known relation between direct and reciprocal spaces, $D \sim 2\pi/q$, one can conclude that the aggregates in this sample can be considered as homogeneous at the scale of more than 20 nm. The corresponding effective match point, 51 % of D_2O, gives the mean aggregate SLD of 2.93×10^{10} cm^{-2}. For the LA sample the situation is different. No q-interval where the match point does not change is distinguishable, so in this case we deal with quite polydisperse aggregates whose mean SLD depends strongly on the aggregate size.

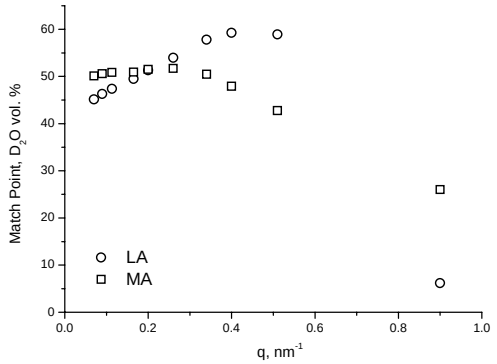

Fig.2. Dependence of the effective match point on q-value for both magnetic fluids.

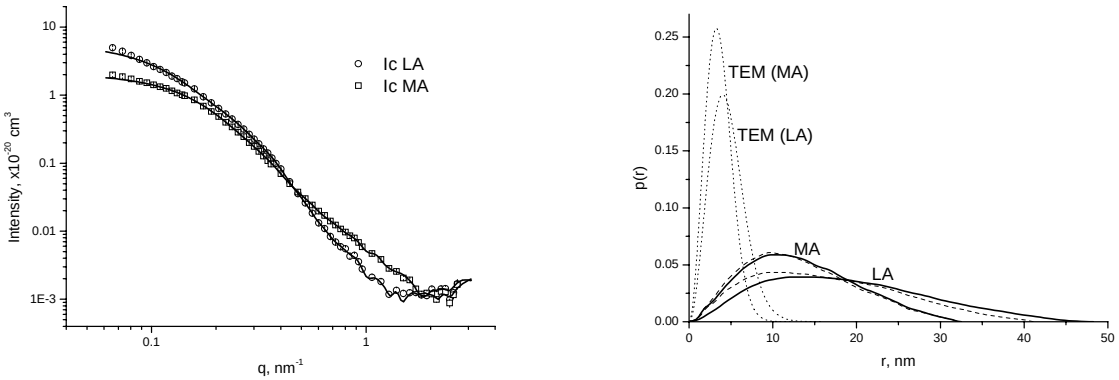

a) b)

Fig.3. Experimentally obtained shape scattering modified basic functions for each of magnetic fluids. The line shows fits of the curves according to obtained $p(r)$ function (a); Pair distance distribution functions of particles found from shape scattering modified basic functions for both magnetic fluids (solid lines) compared with the pair distance distribution functions found from the curves with 0% D_2O content (dashed lines) and from the TEM measurements of the separated particles (doted lines) – MA: D_0= 6.08 nm, S=0.20; LA: D_0=7.42 nm, S=0.23 (b).

To find the modified basic functions we solved system of equations of type (1) using value of contrast at q = 0.09 nm^{-1}. The most informative of the modified basic functions is the $\tilde{I}_c(q)$ function (Fig.3a). From the comparison of $\tilde{I}_c(q)$ for the LA and MA samples one can see that particles of the LA magnetic fluid have larger sizes than those of the MA fluid. It is clearly supported by the Indirect Fourier Transform (IFT) [6] of the $\tilde{I}_c(q)$ functions, which produces the pare distance distribution (PDD) function $p(r)$ shown in Fig.3b. For polydisperse systems this function reflects mainly the particle size distribution. The maximal value, where $p(r)$ is non-zero, corresponds to the maximal aggregate size, which is 49 and 33 nm for the LA and MA samples, respectively, in full agreement with above conclusion. DLS measurements on the same samples [7] conducted to average hydrodynamic sizes of 77 nm for LA and 48 nm for MA double layer stabilized magnetic fluids, which include the stabilizing layer contribution and show the same difference between the two kind of magnetic fluids; average size ratios are 1.5 (SANS) and 1.6 (DLS), respectively. The radius of gyration, R_g, calculated from the $p(r)$ function, 15.2 ± 0.2 nm (LA) and 10.2 ± 0.1 nm (MA), is connected with the radius of gyration of the particle shape, R_c, and volume, V_c, in a way $R_g^2 =< R_c^2\ V_c^2 >/< V_c^2>$, where brackets denote the averaging over the particle radius distribution $D_N(R)$ [4]. Assuming the quasi-spherical shape of the aggregates, which allows one to use the relation $R_c^2 = (3/5)R^2$, one obtains the characteristic radii of the particles $(< R^2\ V_c^2 >/< V_c^2>)^{1/2}$ to be equal to 19.5 ± 0.3 nm and 13.8 ± 0.1 nm for the LA and MA magnetic fluids, respectively. In Fig.3b the PDD functions from $\tilde{I}_c(q)$ are also compared with those obtained for the scattering curves at zero content of D_2O. The later case is determined

only by the scattering from magnetite. Additionally, the calculated PDD functions for single magnetite nanoparticles in the magnetic fluids are shown. The calculations were based on the data [8] of the transmission electron microscopy (TEM).

From Fig.3b one can see a significant difference in the organization of aggregates in the two fluids. If for the LA sample there is an observable difference in PDD functions from $\tilde{I}_c(q)$ and from the H2O curve, for the MA sample the PDD functions of the two kinds almost coincide. For the LA sample the difference in the maximal size of the two PDD functions, about 3.5 nm, can be related to the effective thickness of the surfactant layer around magnetite nanoparticles. As to the MA sample, we suppose that here one deals with the homogeneous agglomeration with quite small effective thickness of the surfactant around single magnetite nanoparticles. The estimate of the volume fractions of magnetite gives ε_m = 0.44, which means that the surfactant content in the aggregates does not exceed 56 %. Using the $D_N(R)$ function from TEM for single magnetite particles we obtain that the maximal effective thickness of the surfactant around magnetite, which satisfies the obtained surfactant content, is restricted by 1.3 nm. This value is very small, which mean that particles in aggregates are nanomagnetite covered with one incomplete layer of myristic acid. In opposite, the LA magnetic fluid can be considered as more close to the non-polar organic magnetic fluids [5] with the core-shell particle structure, where the surfactant covers completely the magnetite surface and forms the stabilizing shell.

Conclusions

Structure analysis based on contrast variation in small-angle neutron scattering on water-based magnetic fluids sterically stabilized with short-chain length lauric (C12) and myristic (C14) acids revealed that the fluids differ principally with respect to the aggregate formation. In the LA sample quite polydisperse associations of magnetite nanoparticles coated with double surfactant layer (effective thickness about 3.5 nm) mainly appear. The MA sample is characterized by the formation of homogeneous and less polydisperse aggregates as a result of the non-full covering of magnetite with the surfactant. The reason for this can be connected with the possible formation of micelles of mono-carboxylic acids in water, which decrease the number of free surfactant molecules required for full coating of magnetite surface. The critical micelle concentration is inversely proportional to the molecule length [9], which correlates with the worse stabilization for the longer MA.

Acknowledgments. The work is done in the frame of the project RFBR-Helmholtz (HRJRG-016). This research project has also been supported by the European Commission under FP6 through the Key Action: Strengthening the European Research Area, Research Infrastructures. Contract nr: RII3-CT-2003-505925, GKSS, Germany; and by the CEEX research program of the Romanian Ministry of Education and Research, contract NanoMagneFluidSeal nr.83/2006.

References:

[1] R.E.Rosensweig, *Ferrohydrodynamics*, Cambridge Univ. Press (1985)
[2] D.Bica, L.Vekas, M.V.Avdeev, et al.,J. Mag. Mag. Mater. 311 (2007) 17
[3] H. B.Stuhrmann, In *Modern aspects of small-angle scattering*. Ed. Brumberger, H., Kluwer Acad. Publishers, Dordrecht, (1995) 221
[4] M.V.Avdeev, J. Appl. Cryst. 40 (2007) 56
[5] M.V.Avdeev, D.Bica, L.Vékás, et al., J. Mag. Mag. Mater. 311 (2007) 6
[6] J.Skov Pedersen, Adv. Coll. Inter. Sci. 70 (1997) 171
[7] E. Tombácz, D. Bica, A. Hajdú, et al., J.Phys.: Condens. Matter 20 (2008) 204103 p. 6
[8] M.V.Avdeev, D.Bica, L.Vekas, et al., Book of abstracts, 7th International Conference on the Scientific and Clinical Applications of Magnetic Carrier, Vancouver, Canada, May 21-24, 2008 (The University of British Columbia: Vancouver)
[9] B.Jounsson, B.Lindman, K.Holmberg, B.Kronberg, *Surfactants and polymers in aqueous solution* (John Wiley & Sons, Chichester, England, 1998)

CONTRAST VARIATION IN SMALL-ANGLE NEUTRON SCATTERING BY WATER-BASED FERROFLUID WITH SURFACTANT/POLYMER STABILIZATION

Feoktystov A.V. [*], Avdeev M.V. [**]
Frank Laboratory of Neutron Physics, Joint Institute for Nuclear Research, Dubna, Russia
E-mail: [*] *feoktystov@gmail.com*, [**] *avd@nf.jinr.ru*

Bulavin L.A.
Kyiv Taras Shevchenko National University, Kyiv, Ukraine

Garamus V.M.
GKSS Research Centre, Geesthacht, Germany

Kopcansky P., Timko M., Koneracka M., Zavisova V.
Institute of Experimental Physics, Slovak Academy of Sciences, Kosice, Slovak Republic

The key parameters of the behavior of magnetic particles in ferrofluids (fine liquid dispersions of magnetic materials stabilized usually with surfactants) are related to the nature of their surface. Magnetic fluids are very promising in the use of future medical applications. In such biocompatible systems the chemical composition of the surface is especially important to avoid the action of the reticuloendothelial system (RES), which is a part of the immune system, in order to increase the half-life of magnetic fluid in the blood stream. Coating the magnetic particles with a neutral and hydrophilic compound – poly(ethylene glycol) (PEG), the circulatory half-life increases from minutes to hours or days [1]. The object of investigations in the present study is the water based magnetic fluid stabilized with double layer surfactant/polymer [2].

The investigated magnetic fluids were synthesized in Instute of experimental physics of Slovak academy of sciences (Kosice, Slovak Republikc). The samples were magnetite nanoparticles coated with double layer of soidium salts of oleic acid ($C_{17}H_{33}COONa$). An additional layer of PEG was formed on so stabilized nanoparticles.

The magnetic fluid was investigated by small-angle scattering of non-polarized neutrons (SANS). The contrast variation with H/D substitution was used to reveal features of the internal structure of the ferrofluid at the scale 1-100 nm. The initial sample (volume fraction of magnetite about 2%) was dissolved with the ratio 1:4 by different mixtures of light/heavy water to achieve the D_2O contents of 0, 10, 20, 30, 40, 50, 60 and 70% in the final fluid. The H_2O content in the initial solution was estimated to be 95% from the mass density measurements (1.02 g/ml). Pure H_2O/D_2O mixtures with the same D_2O contents as in the experimental samples were used as buffer solutions. The studied fluid shows good stability in the absence of the external magnetic field. No significant changes in its properties were observed within period of one year after preparation.

Experiments were carried out on the SANS-1 small-angle instrument at the FRG-1 steady-state reactor of the GKSS Research Center (Geesthacht, Germany) [3]. No external magnetic field was applied to the samples.

The studied ferrofluid shows a complex multi-level and multicomponent structure. The experimental data were treated in terms of approach [4], which takes into account these aspects in addition to the classical contrast variation technique [5]. The advanced basic function approach takes the following view:

$$I(q) = \tilde{I}_s(q) + \Delta\tilde{\rho}\tilde{I}_{cs}(q) + (\Delta\tilde{\rho})^2 \tilde{I}_c(q), \quad (1)$$

where

$$\Delta\tilde{\rho} = \bar{\rho}_e - \rho_s \quad (2)$$

is the modified contrast, the difference between the effective mean scattering length density (SLD) of the particles, $\overline{\rho}_e$, and SLD of the liquid carrier, ρ_s. The modified basic functions $\tilde{I}_c(q)$, $\tilde{I}_s(q)$, $\tilde{I}_{cs}(q)$ comprise information about the nuclear and magnetic SLD distributions within particles, as well as the polydispersity function [4]. Among three basic functions the most transparent for interpretation is $\tilde{I}_c(q) = < I_c(q) >$, the average of the scattering shape function $I_c(q)$ of the Stuhrmann's type [5]. The corresponding term $(\Delta\tilde{\rho})^2 \tilde{I}_c(q)$ prevails in the scattering intensity (1) at sufficiently large contrast. The other basic function $\tilde{I}_s(q)$ describes scattering at the effective match point ($\Delta\tilde{\rho} = 0$). It comprises both the residual nuclear scattering and magnetic scattering. Finally, the $\tilde{I}_{cs}(q)$ contribution is a cross-function. In the general case, in contrast to the other two basic functions it can take negative values.

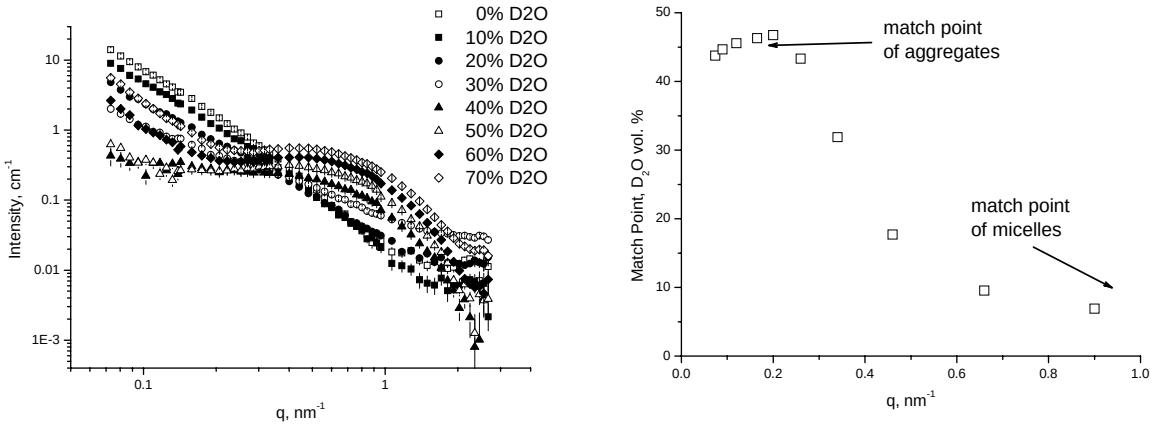

Fig.1. Changes in the SANS curves with the contrast variation on the studied ferrofluid. Percent volume fraction of D_2O in the solvent is indicated. Volume fraction of dispersed magnetite in the samples, φ_m, is less than 0.5%.

Fig.2. Dependence of the effective match point on *q*-value for the studied magnetic fluid. Two specific regions are distinguished.

The experimental SANS curves at different D_2O content in the carrier are presented in Fig.1. The change in the character of the curves repeats that seen in similar experiments [6] on a water-based ferrofluid with nanomagnetite sterically stabilized by a double layer of dodecylbenzenesulphonic acid (DBS). Samples with the small content of D_2O in the solvent (below 30%) show signal mainly from magnetite, because of the slight contrast between water and sodium oleate/PEG layer. The behavior of these curves differs from the scattering by single separated nanoparticles and corresponds rather to large (characteristic size more than 120 nm) aggregates. A specific feature clearly appears at *q*-values above 0.5 nm^{-1} at high D_2O content (above 50%), which corresponds to significantly smaller particles consisting mainly from H-components of the ferrofluid.

Because of the large size of the mentioned aggregates no specific Guinier regime can be resolved in the initial parts of the curves. In this case the effective match point of the system (effective content of D_2O when the scattering is minimal) cannot be related to forward scattering intensity. Nevertheless, as it was noted [4] that the choice of this parameter for polydisperse systems is entirely arbitrary. Here, we have built dependences of scattering intensities on D_2O content in the solvent at different values of *q* and found out their minima (i.e. effective match points). The full *q*-dependence of the effective match point is shown in Fig.2. Two regions where it does not change much can be seen. They can be related to match points of about 45 and 5%

corresponding to two kinds of particles in the fluid, which are aggregates containing magnetite particles and, most probable, micelles of free surfactant in the solution. Using the value of the match point, η, and the scattering length densities (SLDs) of light water ($\rho_{H2O} = -0.56 \times 10^{10}$ cm^{-2}), heavy water ($\rho_{D2O} = 6.34 \times 10^{10}$ cm^{-2}) and of magnetite ($\rho = 6.9 \times 10^{10}$ cm^{-2}) we estimated the volume fraction of magnetite in the aggregates as 37%. This value is close to that concluded for water based fluid with double DBS stabilization [6]. Since the SLDs of sodium oleate and PEG are almost the same, it is impossible to say from the mean SLD what fractions take these components. Also, the empty space in the aggregates, which also has zero SLD, should affect the mean SLD.

The shape of both the aggregates and micelles can be analyzed by the basic functions approach (1). To define the modified contrast (2) we used the D_2O content dependences of the scattering intensities at $q = 0.09$ nm^{-1}. The found minimum gave the effective match point of 44.6% of D_2O content (corresponding SLD 2.517×10^{10} cm^{-2}).

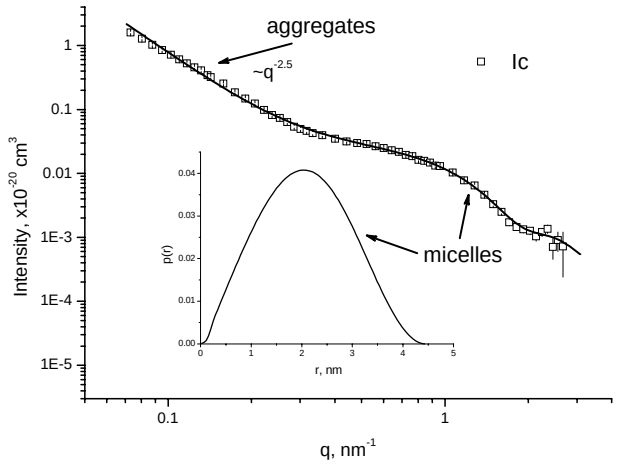

Fig.3. Experimentally obtained shape scattering modified basic function. Different scattering levels corresponding to two different kinds of particles are indicated. The line shows fit of the curve, which takes into account the power-law type scattering from aggregates (low q-values) and scattering from micelles (large q-values). Inset shows PDD for the "micelle part" of the scattering curve. Parameters of the IFT fit are $R_g = 1.59 \pm 0.05$ nm, $I(0) = (0.021 \pm 0.001) \times 10^{-20}$ cm^3.

As it was mentioned above, our main goal is the $\tilde{I}_c(q)$ basic function (Fig.3). It clearly shows two different scattering levels. The first level (small q-values) reflects the power-law type scattering $\sim q^{-2.5}$, which is a linear dependence in the double logarithmic plot in Fig.3. The obtained exponent (−2.5) indicates the presence of fractal aggregates with the dimension of 2.5 (mass fractals). Their size, as it was mentioned above, exceeds 120 nm that is why their Guinier region is out of the instrument resolution. The second level (large q-values) shows well-defined Guinier regime for significantly smaller particles. After subtracting the extrapolated power-law scattering at large q-values the second level can be treated well by the Indirect Fourier Transform (IFT) procedure [7] to obtain the pair distance distribution (PDD) of small particles. The resulting PDD is given in the inset to Fig.3. Parameters of the IFT fit are indicated in the caption to Fig.3. We relate the obtained PDD with spherical micelles formed as a result of the excess of the stabilizing agents (surfactant and PEG) in the solution. The micelle radius, ~2.1 nm, correlates well with the length of the sodium oleate, thus indicating that this molecule is responsible for the micelle formation.

Conclusions

Despite the good stability of the studied sample its inner structure is far from the general concept of the ferrofluid structure. Significant aggregates are seen in the SANS curves which are large (size more than 120 nm) fractal clusters. The origin of these clusters is to be clarified. It is well known [8-10] that in water-based ferrofluids with the double sterical stabilization two types

of aggregates are observed. The first type is the temperature stable comparatively small and compact (several magnetite particles) aggregate, formed presumably during the dispersing procedure. The second type is large (predominantly fractal) agglomerates, which form with time in the ferrofluids after preparation. Specific features of such aggregates are that they are destroyed at various rates by the temperature increase [8] and can change their structure under the effect of the external magnetic field [11]. In the given case, we can see that in the SANS curves only one type of the discussed aggregation (large clusters) dominates. Its sensitivity to temperature and external magnetic field should be measured in further experiments.

The formation of spherical micelles of sodium oleate in the studied system is evidenced by the SANS contrast variation, which is a result of the excess of the stabilizing agent. The comparison of their properties with those in pure aqueous solutions of the surfactant is the aim of our further research.

Acknowledgments. Projects VEGA 0077, APVV -0509-07, APVV-99-02605, as well as project RFBR-Helmholtz (HRJRG-016) are acknowledged.

References:

[1] N.Tomašovičová, M.Koneracká, P.Kopčanský, M.Timko, V. Závišová, Meas. Sci. Rev. 6 (2006) 32
[2] M.Timko, M.Koneracka, P.Kopcansky, et al., Indian J. Eng. Mater. Sci. 11 (2004) 276
[3] Zhao J, Meerwinck W, Niinkoski T., Rijillart A., Schmitt M, Willumaeit R., Stuhrmann H.B. Nucl Instr Meth A 356 (1995) 133
[4] M.V.Avdeev, J. Appl. Cryst. 40 (2007) 56
[5] Stuhrmann, H. B. In *Modern aspects of small-angle scattering*. Ed. Brumberger, H., Kluwer Acad. Publishers, Dordrecht, (1995) 221-254
[6] M.Balasoiu, M.V.Avdeev, V.L.Aksenov, D.Hasegan, V.M.Garamus, A.Schreyer, D.Bica, L.Vékás, J. Mag. Mag. Mater. 300 (2006) e225
[7] J.Skov Pedersen Adv. Coll. Inter. Sci. 70 (1997) 171
[8] M.V. Avdeev, V.L. Aksenov, M. Balasoiu, V.M. Garamus, A. Schreyer, Gy. Török, L. Rosta, D. Bica, L. Vékás, J Coll Interface Sci 295 (2006) 100
[9] L.Vekas, D.Bica, M.V.Avdeev, China Particuology 5 (2007) 43
[10] A. Wiedenmann, A. Hoell, M. Kammel, J. Magn. Magn. Mater. 252 (2002) 83
[11] V.L.Aksenov, M.V.Avdeev, M.Balasoiu, D.Bica, L.Rosta, Gy.Török, L.Vekas J. Mag. Mag. Mater., 258-259 (2003) 452

SOLUTIONS OF DODECYLBENZENE SULFONIC ACID IN POLAR CARRIER STUDIED BY SMALL-ANGLE NEUTRON SCATTERING

V.I.Petrenko, M.V.Avdeev, V.L.Aksenov
Joint Institute for Nuclear Research, Frank Laboratory of Neutron Physics, Russia

V.M.Garamus
GKSS Research Centre, Geesthacht, Germany

L.A.Bulavin
Kyiv Taras Shevchenko National University, Physics Department, Kyiv, Ukraine

L.Rosta
Research Institute for Solid State Physics and Optics, Budapest, Hungary

The given experiment is the continuation of the study of factors determining the stability of ferrofluids - fine liquid dispersions of magnetic nanoparticles coated with surfactant molecules [1]. The surfactant content in ferrofluids determines the stability of these systems. In practice, there exists an optimal content, deviations from which result in the deterioration of the ferrofluids quality. One can note that this problem is general for colloidal solutions. For organic non-polar ferrofluids with a single surfactant layer around magnetic nanoparticles the presence of the free surfactant molecules in the carrier worsens the ferrofluids stability. In polar ferrofluids with double stabilization the surfactant excess is necessary, still the knowledge of its optimal value is required. Thus investigation of the behavior of surfactant molecules in the solutions is very helpful for further research of ferrofluids stability. The goal of present work is the study of the behavior of dodecylbenzene sulfonic acid, $C_{18}H_{30}SO_3$, (DBS) in polar solvents (d-water). DBS surfactant is a component of various technical ferrofluids with double stabilization. The second surfactant layer in these fluids is formed by the physical adsorption under the surfactant excess. Small-angle neutron scattering (SANS) was used to find out the character of interaction in the system, structural parameters and possible micelle formation in solutions of free surfactants. The work was also initiated by recent detection from SANS contrast variation experiments on water based magnetic fluids with DBS as second surfactant shell that some aggregates with gyration radius 1.9 nm together with magnetic particles and their aggregates appear [2]. Since there is an excess of DBS in bulk of ferrofluids (water) it was supposed that aggregates with gyration radius of 1.9 nm are micelles of DBS, which initiated the current work on the study of micelle formation of DBS in water. We found a lack in the literature data on this question.

Small-angle neutron scattering (SANS) was used to conclude about structural features of DBS micelles at different acid concentration in solution. Scattering curves obtained at SANS instrument of the Budapest Neutron Center are shown in Fig.1. The expression for scattering intensity in standard form was used:

$$I(q) = n(\Delta\rho)^2 V^2 P(q) S(q), \qquad (1)$$

where $P(q)$ is particles form factor (sphere, ellipsoid), and $S(q)$ is structure factor responsible for interaction between micelles.

For calculation of the particles structure factor $S(q)$ the Hayter-Penfold model (charge spheres) was used:

$$S(q) \longrightarrow \begin{cases} U(r) = \pi\varepsilon D_{eff}^2 \Psi_{0,eff}^2 \dfrac{e^{-(r-D_{eff})/k_d}}{r}, & \text{for } r > D_{eff} \\ U(r) = \infty, & \text{for } r < D_{eff} \end{cases} . \qquad (2)$$

Results of fits are given together with the experimental data in Fig.1. Solid lines correspond to modeling by equation which was shown earlier with simultaneous approximation form- and structure factors (program FISH). The peaks on the curves reflect the micelle interaction. The obtained parameters are presented in the Table 1. As it is seen the micelles have spherical shape at low concentration. Then, with an increase in the acid concentration the micelles become ellipsoidal.

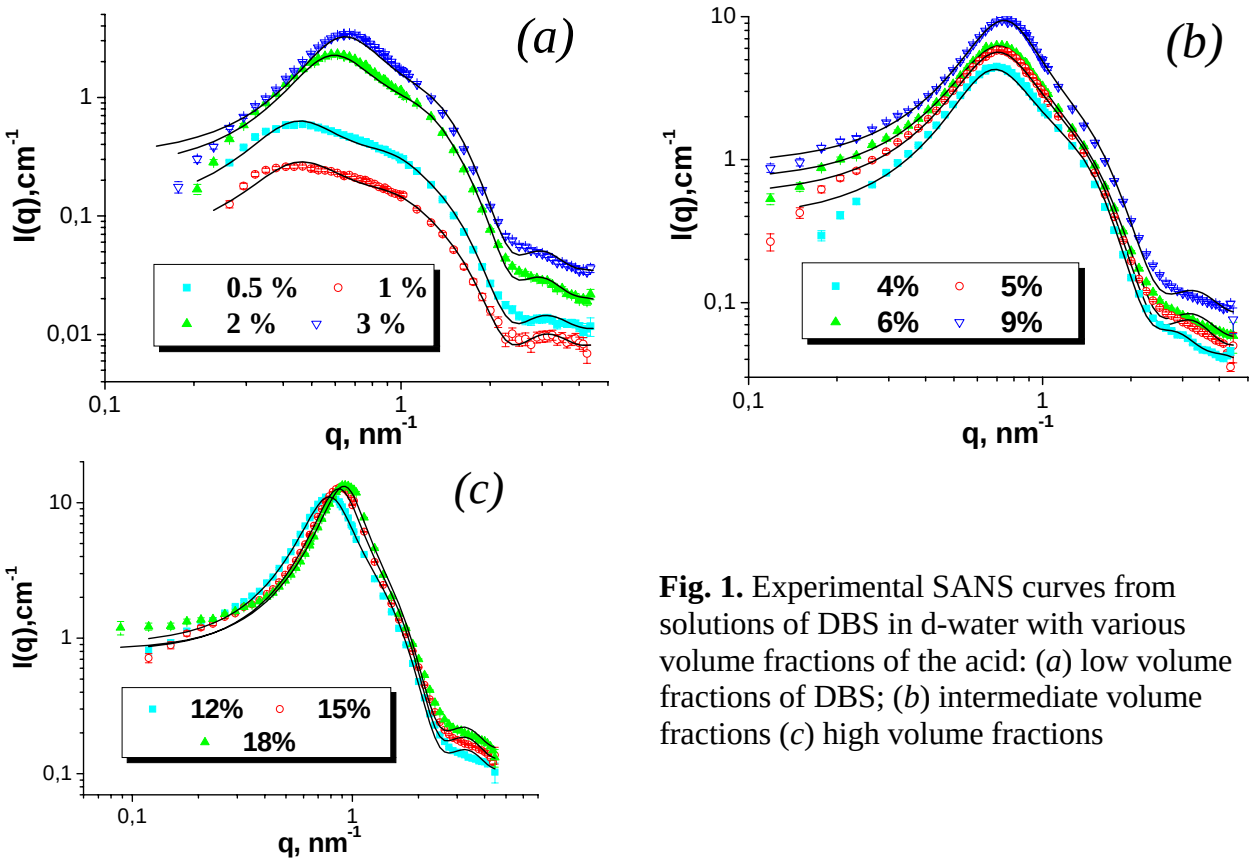

Fig. 1. Experimental SANS curves from solutions of DBS in d-water with various volume fractions of the acid: (*a*) low volume fractions of DBS; (*b*) intermediate volume fractions (*c*) high volume fractions

Table 1. Parameters derived from the SANS data

	"scale", cm^{-1}	R, A	X	H-P R, A	Charge	V_{mic}, A^3 x10^4	N_{agg}
DBS05	0.61	18	1	18	40	2.4	54
DBS1	0.28	18	1.08	23	35	2.6	59
DBS2	2.4	18	1.15	21	24	2.8	62
DBS3	3.5	17	1.3	22	20	2.7	59
DBS4	5	17	1.5	22	18	3.1	69
DBS5	7.4	17	1.7	23	16	3.5	78
DBS6	9	16	2	24	15	3.4	76
DBS9	15	16	2.4	26	15	4.1	92
DBS12	19	16	2.5	26	15	4.3	95
DBS15	25	16	2.4	25	15	4.1	92
DBS18	27	16	2.3	25	14	3.9	88

To summarize, we conclude that micelle formation of DBS was detected in SANS experiments on solutions of DBS in d-water. Micelle structure parameters including the aggregation number and charge of micelle were obtained. The increase in the micelle size is found at the increase in the acid concentration in DBS/water solutions.

The work is partially done in the frame of the project RFBR-Helmholtz (HRJRG-016).

References

1. R.E. Rosensweig, Ferrohydrodynamics, Cambridge Univ. Press, Cambridge, 1985.
2. M.Balasoiu, M.V.Avdeev, V.L.Aksenov, D.Hasegan, V.M.Garamus, A.Schreyer, D.Bica, L.Vékás, *J. Mag. Mag. Mater.* 300 (2006) e225

ANALYSIS OF THE STRUCTURE OF WATER-BASED FERROFLUIDS BY SMALL ANGLE NEUTRON SCATTERING

V.I.Petrenko, M.V.Avdeev, A.V.Feoktystov, V.L.Aksenov
Joint Institute for Nuclear Research, Frank Laboratory of Neutron Physics, Russia

L.A.Bulavin
Kyiv Taras Shevchenko National University, Physics Department, Kyiv, Ukraine

L.Rosta
Research Institute for Solid State Physics and Optics, Budapest, Hungary

V.M.Garamus
GKSS Research Centre, Geesthacht, Germany

L.Vekas
Centre for Fundamental and Advanced Technical Research, Timisoara, Romania

The investigation of ferrofluids (magnetic fluids) has fundamental, as well as applied interest for technical [1] and medical [2] applications. The prospects of ferrofluids in medical applications are determined by development in the synthesis of highly stable magnetic fluids in water. In contrast to classical ferrofluids based on non-polar organic carriers (single surfactant layer around magnetic particles is used for stabilization), the synthesis of stable water-based magnetic fluids is more complicated task. This case requires formation of the second stabilizing surfactant layer, which can be formed as result of the surfactant excess. In its turn, the surfactant excess can lead to the formation of micelles, which are unfavorable for stabilization procedure of magnetic particles.

In the given work the structure parameters of a number of water-based magnetic fluids are obtained by small-angle neutron scattering (SANS). Various combinations of surfactants were used in the stabilization procedure. Thus, the size distribution functions of colloidal particles are obtained when SANS is applied to the system based on light water. The degree of particles clusterization is derived from the comparison of the SANS results with the data of electron microscopy. The best, from the structural viewpoint, surfactant combinations are revealed.

Magnetic fluids were synthesized at the Center of Fundamental and Advanced Technical Research, Timisoara Branch of Romanian Academy of Sciences, in accordance with recently developed technique [3]. The different surfactants such as dodecylbenzenesulphonic acid (DBS), oleic (OA), myristic (MA) and lauric (LA) acids were used for the sample stabilization. Some information about the samples is presented in Table 1.

The experimental SANS curves for investigated ferrofluids 1-6 (Table 1) are shown in Fig. 1. Qualitatively, experimental curves have similar characters. Still, some difference allows us to conclude about various structural organizations of the fluids. From the given SANS data we obtain directly the information about structure of magnetic particles, since the contrast between surfactant and water carrier is minimal. Thus, the size distribution function of magnetic particles (called hereafter $D_V(R)$, the volume distribution function as a function of particles radius) can be obtained from the analysis of the SANS curves. The direct approximation to experimental data the model separate non-interaction spherical particles with lognormal size distribution does not give reliable results. This fact indicates that particle clusters form in the ferrofluids. The rate of clusterization in the fluids can be concluded from the $D_V(R)$ functions obtained by the indirect Fourier transform (program GNOM) and given in Figs.2 and 3.

Table 1. Description of the investigated water based ferrofluids

N	Magnetic material	Stabilization layers	Saturation magnetization, *M*, Gs	Volume fraction of magnetic material, φ	Density, ρ, g/cm^3
1	$CoFe_2O_4$	DBS + DBS	70	0.0165	1.066
2	Fe_3O_4	DBS + DBS	55	0.0160	1.066
3	Fe_3O_4	OA + OA	50	0.0125	1.051
4	Fe_3O_4	MA + MA	30	0.003	1.026
5	Fe_3O_4	LA +LA	100	0.024	1.101
6	Fe_3O_4	MA + DBS	128	0.030	1.125

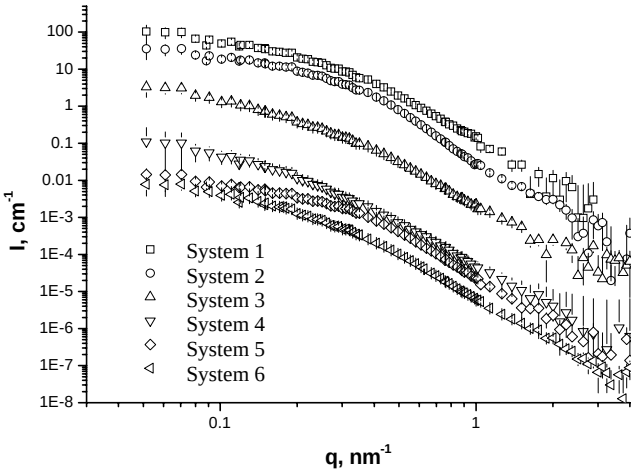

Fig. 1. The experimental SANS curves for systems 1-6 (Table 1) in the double logarithmic scale. For convenience view the curves are divided by 10 (system 2), 100 (system 3), 1000 (system 4), 10000 (system 5), 100000 (system 6).

The clusters in the systems 1 and 2 where two DBS layers were used for stabilization have a complex structure. Namely, two characteristic particle radii (approximately 6 and 16 nm) can be distinguished. The first value exceeds slightly the mean radius of magnetite (between 4-5 nm), which is formed in the condensation reaction (data of the electron microscopy). This fact allows us to conclude that in such systems the magnetite particles are dispersed into water as small compact aggregates (aggregation number ~10), which is typical for water-based magnetic fluids with double stabilization [4,5]. At the same time, the presence of relatively small quantity of large compact clusters with characteristic radius of 16 nm is revealed, which differs these fluids from the previous ones where large fractal formations were observed [4,5].

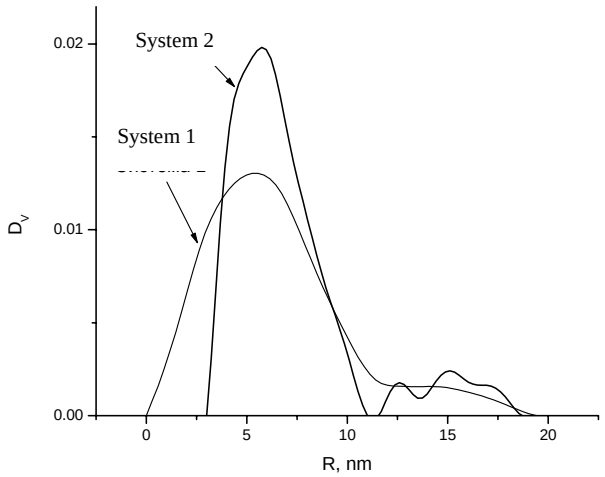

Fig. 2. Functions $D_V(R)$ for systems 1, 2 as result of IFT for SANS data (Table 1).

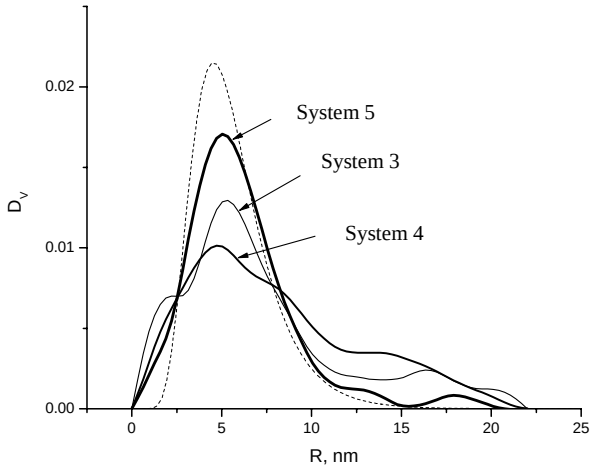

Fig. 3. Functions $D_V(R)$ for systems 3 - 5 as result of IFT for SANS data (Table 1). Dashed line is the model size distribution of nanomagnetite from the data of transmission electron microscopy [6].

The systems 3-5 (two layers of monocarboxylic acids are used for stabilization) are closer to the general concept of ferrofluids as systems of isolated magnetic particles covered by a surfactant shell. It is seen (Fig. 3) from the comparison of the obtained $D_V(R)$ functions with the model function for the separate magnetite nanoparticles revealed in the experiments on the transmission electron microscopy [6]. Large clusters (characteristic radius 10-20 nm) are present in the systems in addition to separate particles (radius of about 5 nm). As one can see, the system 5 with double stabilization by lauric acid is the closest to the distribution function $D_V(R)$ of separate particles.

The cluster organization for the system 6 is more complicated in comparison with cases discussed above. We failed in obtaining of reliable $D_V(R)$ function, which indicates that wider size distribution of primary and secondary clusters take place.

From the analysis of structure parameters of water-based ferrofluids with double stabilization synthesized by method [3] we can conclude that complex cluster formation in the magnetic fluids takes place in the case of stabilization by DBS. The primary clusters (radius about 6 nm) are associated into secondary aggregates (characteristic radius about 16 nm). The use of monocarboxylic acids for stabilization results in more stable ferrofluids from the viewpoint of structure. The observed characteristic radius of magnetic particles in such systems is about 5 nm and coincides with characteristic radius of magnetic nanoparticles, which are formed in the condensation reaction. Only some part of magnetic particles (depending on the used acid) is in large clusters with characteristic sizes of 19-20 nm. Thus, lauric acid (12 CH-groups) is the best surfactant for stabilization among three investigated mono-carboxylic acids. The given work shows the possibility for using mono-carboxylic acids in the synthesis of highly stable water-based ferrofluids. The important aspect of the given investigation is the biocompatibility of short chain length acids (lauric and myristic acids), which makes it possible to use the corresponding magnetic fluids in medical applications.

The work is partially done in the frame of the project RFBR-Helmholtz (HRJRG-016).

References

[1] Berkovski B. Ed. *Magnetic Fluids and Applications Handbook* – Beggel House, New York, 1996.

[2] Book of abstracts of the *6th International Conference on Clinical and Scientific Applications of Magnetic Carriers*, Krems, Austria, May 24-27, 2006.

[3] Bica D., Vekas L., Avdeev M.V. et al., *J. Mag. Mag. Mater.* 311 (2007) 17-21

[4] Avdeev M.V., Aksenov V.L., Balasoiu M. et al., *J. Col. Interface Sci.* 295 (2006) 100-107

[5] Balasoiu M., Avdeev M.V., Aksenov V.L. *Cryst. Rep.* 52 (2007) 551-558

[6] M.V.Avdeev, D.Bica, L.Vekas, V.I.Petrenko, V.M.Garamus, R.Turcu, B.Mucha, A.Schuster, K.Lamszus, R.Willumeit, Book of abstracts, *7th International Conference on the Scientific and Clinical Applications of Magnetic Carrier, Vancouver, Canada, May 21-24, 2008* (The University of British Columbia: Vancouver).

STUDY OF PROXIMITY EFFECTS IN SUPERCONDUCTOR/FERROMAGNET INTERFACE USING WAVEGUIDE ENHANCEMENT OF NEUTRON STANDING WAVES

V.L. Aksenov, K.N. Zhernenkov, Yu. N. Khaidukov†, Yu.V. Nikitenko
Frank Laboratory of Neutron Physics, JINR, Russia

E-mail: † khaiduk@nf.jinr.ru

L.Bottyán, F. Tanczikó, D. Merkel, B. Nagy, L.Deák, D.L. Nagy, E. Szilágyi
KFKI Research Institute for Particle and Nuclear Physics of the HAS, Budapest, Hungary

Zs.E. Horváth
Research Institute for Technical Physics and Materials Science of the HAS, Budapest, Hungary

L. Kiss
Research Institute for Solid State Physics and Optics of the HAS, Budapest, Hungary

A. Csík, K. Vad
Institute of Nuclear Research of the HAS, Debrecen, Hungary

G. Langer
Department of Solid State Physics, University of Debrecen, Debrecen, Hungary

A. Rühm
Max-Planck-Institut für Metallforschung, Stuttgart, Germany

Due to their incompatible nature, singlet superconductivity (S) and ferromagnetic (FM) order do not coexist. The exchange field, in a magnetically ordered state, tends to align spins of Cooper pairs in the same direction, thus preventing a pairing effect [1]. Conversely, ferromagnetic ordering is unlikely to appear in the superconducting phase. The energy for ferromagnetic ordering decreases and, instead of ferromagnetism, a non-uniform magnetic ordering ('cryptoferromagnetism') may appear in bulk materials [2]. However, due to the great progress of high-quality hybrid S/FM preparations, coexistence of S and FM can easily be realized in thin film heterostructures. On the one hand, Cooper pairs can penetrate the FM layer and in the interface region of a few nanometers may induce superconductivity even in the presence of a relatively large exchange field. On the other hand, magnetic order penetrates the SC layer and various novel FM and SC states may form with spatial oscillations and non-monotonic temperature variations with promising novel applications of structures like π-Josephson junctions, and S/FM spin-valves.

An S layer has been reported to affect the magnetic properties of the FM with scenarios – beside cryptoferromagnetism [2-4]– of magnetization leakage from FM into S layer [5,6], as well as a change of indirect exchange coupling of neighboring FM layers through S layer [7]. It is rather difficult to experimentally verify these theoretical predictions. This is why only a few experiments have been performed to study the influence of superconductivity on FM. In Refs. [3,4], for example, the observed reduction of magnetization below T_c in an S/FM bi-layer was interpreted as a cryptoferromagnetic effect, however, the experiment could also be interpreted as a consequence of magnetization leakage (an 'inverse proximity effect'), namely, by an induced negative magnetization in S layer and a suppression of the magnetization in the FM layer.

In order to judge upon the interpretations one has to perform experiments with methods of depth resolution matching the layer thicknesses, like Polarized Neutron Reflectometry (PNR). PNR is sensitive to the magnetic depth profile $\vec{M}(\vec{r})$. In order to be able to observe such proximity effects, samples of layer systems with ultra-thin FM layer and possibly with reduced exchange coupling strength (as manifested by a decreased Curie temperature T_{Curie}) are necessary. Simulations reveal that a straighforward usage of conventional PNR, it is impossible to detect such weak magnetic signals. In order to increase the magnetic signal the enhanced neutron standing wave ('waveguide') regime is to be used. In order to enhance standing waves, we place the S/FM interface between two layers with high scattering potentials. Such optimization study has been performed for several candidate materials [8]. Accordingly, using the Cu(32 nm)/V(40 nm)/^{57}Fe(0.5-1.5 nm)/MgO structure, one can increase the neutron flux by two orders of magnitude (Fig.1) near the S/FM interface (at $Q = Q_{WG}$ (0.009 Å^{-1} in the present case). Such a flux increase leads then to an enhancement of quasi-secondary radiations (spin-flip scattering and diffuse scattering) at the same value of Q.

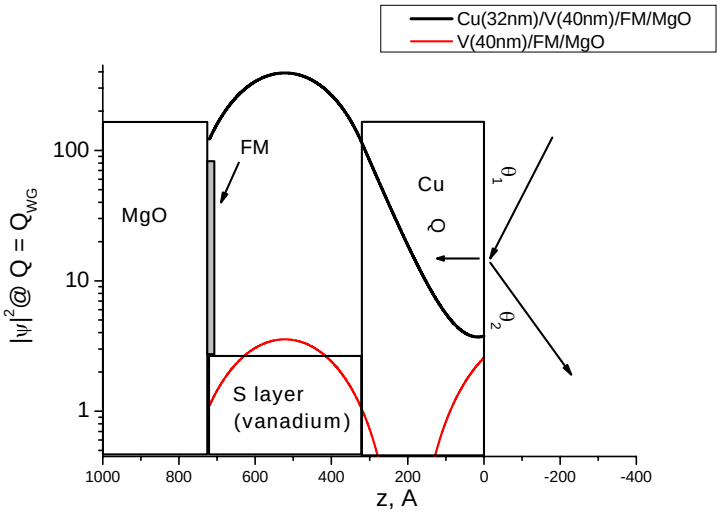

Fig. 1. Density of neutron flux inside a waveguide structure Cu(32 nm)/V(40 nm)/57Fe(0.5-1.5 nm)/MgO with and without Cu layer at Q = 0.009 Å-1 (solid black and dashed red lines, resp.). SLDs of materials are schematically shown by rectangular and incoming and reflected beams are shown by arrows.

Several Cu/V/^{57}Fe/MgO(001) samples (size ~20×10×2 mm^3) with FM layer thickness d_{FM} = [0.5 ÷4] nm, have been prepared in the KFKI Research Institute for Particle and Nuclear Physics, Budapest by molecular beam epitaxy (MBE) and, using magnetron-sputtering, further multilayers have been prepared in the Institute of Nuclear Research in Debrecen. To check structural, magnetic and superconducting properties of the samples, various experimental techniques were used, such as small- and wide-angle X-ray scattering, Rutherford backscattering (RBS) (of helium ions), Secondary Neutral Mass Spectrometry (SNMS) and SQUID magnetometry. Measurements have shown good quality of majority of the samples with layer structure close to nominal. The SQUID measurements allows to define magnetic properties of FM layer as well as superconducting properties of S layer. Saturation magnetization and coercivity of the FM layer at T ~ 10 K were found to be M_{sat} = [0.2-1.4] kOe and H_c = [0.04-0.18] kOe, respectively.he superconducting transition temperature T_C of the S layer for different samples were found to be between 3 and 3.5K.

In order to check the waveguide properties of the samples, room-temperature PNR measurements were performed on selected samples at the NREX+ reflectometer [9] of FRM-II, Munich, Germany. The presence of waveguide regime was searched for in the spin-flip channel. Spin-flip scattering originates from magnetization in FM layer non-collinear with the direction of the external magnetic field H. In order to induce such a magnetization in our samples, the samples were magnetized to saturation then rotated by 90^o for the reflectometric experiment in a magnetic field, H, with $0 < H < H_c$. In Fig. 2a, polarized neutron reflectivities in the different spin states for the sample with d_{FM} = 1nm are shown in black (R^{++}) and red (R^{+-}).

The presence of the waveguide mode is proved by the dip in the R^{++} and the peak in the R^{+-} reflectivity curves at Q = 0.008 Å^{-1}, at a value closed to the expected one.The change in the relative intensity at the dip and the peak are 74% and 10%, respectively.By fitting the reflectivity curve using the FitSuite code [10], the absolute value of the magnetization and the angle between the external field and the magnetization of the FM layer were found to be M = 0.9 ± 0.2 kOe and 35^o ±

5°, respectively. The intensity of the peak and the dip are very sensitive to the change of the magnetization vector.

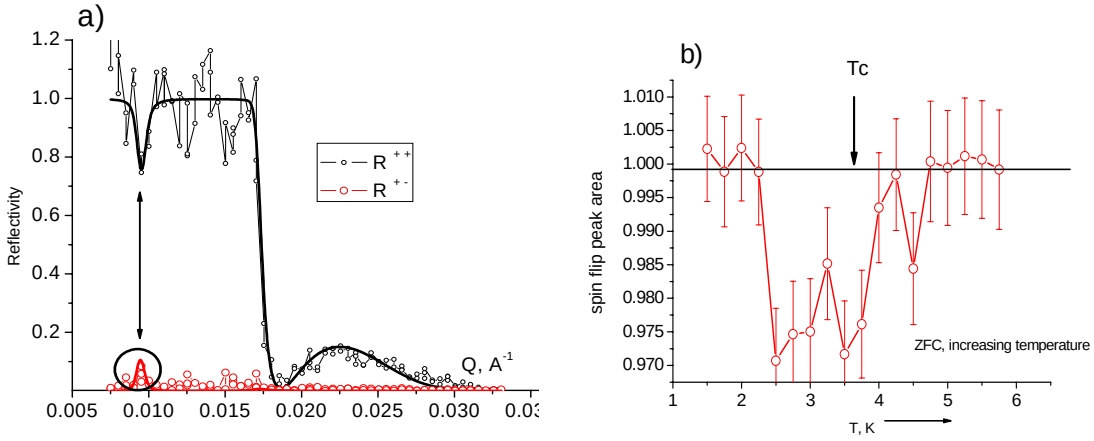

Fig. 2. a) Neutron reflectivities for different scattering channels from the sample Cu(32 nm)/V(40 nm)/Fe(1 nm)/MgO measured at RT in a magnetic field of 12 Oe. Arrow shows position of waveguide mode b) Intensity of spin-flip resonant peak area (shown at fig. 2a in circle) as a function of temperature

To prove this we performed low-temperature measurements on ADAM reflectometer [10] of ILL reactor. The scheme of the experiment is the same as it's described above. On fig. 2b area of spin flip (- +) resonant peak as a function of temperature in the vicinity of Tc is shown. A 3% drop of intensity (statistical error makes 1%) in the range of temperatures T = [0.6 ÷1] Tc is observed. This means that non-collinear part of FM magnetization decreased on 1.5%. Reason of this decrease will be discussed elsewhere.

In conclusion, strong waveguide enhancement of neutron standing waves have been foreseen by simulation and observed in various Cu/V/Fe/MO layer structures. Two series of samples were prepared by molecular beam epitaxy and by magnetron sputtering. The samples were well characterized by different techniques. Low temperature PNR measurements on Cu(32 nm)/V(40 nm)/Fe(1 nm)/MgO sample in the vicinity of resonant peak allow to say that there's a small drop of FM magnetization (of about 1%) in the temperature range T = [0.6 ÷ 1]Tc.

This work was supported by the Hungarian Academy of Sciences, the Hungarian National Fund (OTKA) and the National Office for Research and Technology of Hungary under Contract Nos. MTA-DUB/01, K62272 and NAPVENEUS'05, respectively. One of the authors (Yu. Kh.) gratefully acknowledges the financial support by The Foundation for Assistance to Small Innovative Enterprises of Russian Federation (grant № 8455 UMNIK-08-3)

References:

1. For a recent review, see e.g. I.A. Buzdin, Rev. Mod. Phys. 77, 935 (2005).
2. P.W. Anderson, H. Suhl, Phys. Rev., 116, 898 (1959).
3. Th. Muhge et al., Physica C 296, 325 (1998).
4. I.A. Garifullin et al., Appl. Magn. Reson. 22, 439 (2002).
5. V.N. Krivoruchko and E.A. Koshina, Phys. Rev. B 66, 014521 (2002).
6. F.S. Bergeret, A.F. Volkov and K.B. Efetov, Phys. Rev. B 69, 174504 (2004).
7. C.A.R. Sá de Melo, Phys. Rev. B 62, 12303 (2000).
8. Yu.N. Khaidukov, Yu.V. Nikitenko, V.L. Aksenov, http://arxiv.org/abs/0801.3967v1
9. http://www.mf.mpg.de/en/abteilungen/dosch/frmII/index.shtml
10. http://www.ill.eu/html/adam/
11. Program FitSuite is available at http://www.fs.kfki.hu/

PHASE STATE AND STRUCTURE OF THE CERAMIDE 6 BASED MODEL MEMBRANES OF THE STRATUM CORNEUM

M.A. Kiselev[1], A. Ruettinger[2], N.Yu. Raybova[1], S. Dante[3], Th. Hauss[3]

[1] *Frank Laboratory of Neutron Physics, Joint Institute for Nuclear Research, Dubna, Russia*
[2] *Institute of Pharmacy, Martin-Luther-University, Halle (Saale), Germany*
[3] *Berlin Neutron Scattering Center, Hahn-Meitner-Institute, Berlin, Germany*

The stratum corneum (SC), which is the outermost layer of the mammalian skin, has been in the focus of research for more than 30 years. The composition of the SC lipid matrix is completely different in comparison to cell membranes. The major lipids found in the SC are ceramides, cholesterol and its derivatives as well as free fatty acids [1], whereas cell membranes are mainly composed of phospholipids. The SC forms a continuous sheath of protein-enriched corneocytes which are embedded in an intercellular multilamellar lipid matrix. The SC represents the main barrier for substances leaving the skin, for example water, in addition to also acting as a barrier for substances which penetrate the skin such as drugs. Therefore, for any investigation of drug penetration through the SC and for the development of new delivery systems, it is essential to know its internal nanostructure and hydration behaviour on a molecular level. A series of experimental studies had to be carried out before it was accepted that the lipid part of the SC plays extremely important role in the barrier function of the skin.

Model membranes of SC are appropriate subject for the investigations by neutron diffraction. Firstly performed neutron diffraction experiment on a SC lipid model system composed of synthetic lipids as ceramide 6 (Cer6), cholesterol, palmitic acid and cholesterol sulphate characterized the internal membrane nanostructure by restoring a Fourier synthesis [2]. As a main result a low hydration of approximately 1 Å of the intermembrane space was detected which allows the fully extended conformation of ceramide 6. It was stated that the fully extended conformation creates an extremely strong intermembrane attraction which tighten adjacent bilayers to a steric contact. These insights lead to the suggestion of the armature reinforcement model as an independent theoretical model about the SC lipid matrix organization on a molecular level [3].

Investigations of the phase transitions in the SC model membranes could give important experimental information for the testing of the armature reinforcement model. Structural thermotropic phase transitions in the model SC membrane based on the ceramide 6 were characterized by neutron diffraction at V1 diffractometer of BENSC HMI. Two membranes were used. First one - mixed membrane with composition Cer6/Ch/6_FA/ChS, where 6_FA consists of fatty acids with chain length: C16:0, C18:0, C20:0, C22:0, C24:0, C26:0. Second one – two-phase membranes with composition Cer6/Ch/TA/ChS, where TA is Tetracosanoic Acid (C24:0). Fig. 1 presents the Fourier profiles of the main phase of Cer6/Ch/TA/ChS membranes at different temperature. Membrane structure is nearly the same at 30^{o}C and 50^{o}C. Structural phase transition

between 50°C and 80°C changes membrane structure mainly in the region of the polar head groups. Phase transition is not reversible, which is demonstrated by Fourier profile at 20°C (back cooling). Similar results were obtained for Cer6/Ch/6_FA/ChS membrane. Structural phase transition was detected at 57°C. Fourier analysis was done for T=20°C, 32°C, 57°C, 80°C, and again at 20°C. Fig. 2 demonstrates the membrane structure at T=20°C, 80°C, and back at 20°C. Transition is not reversible for the time of 12 hours. About 2-3 days is necessary for the full transformation of the membrane structure to the initially state at 57% relative humidity. Increasing of humidity decreases the time for membrane equilibrium. Our data shows that structural phase transitions in SC model membrane exist. Important property of the transition is slow molecule diffusion or slow conformation changes in the lipid structure [3].

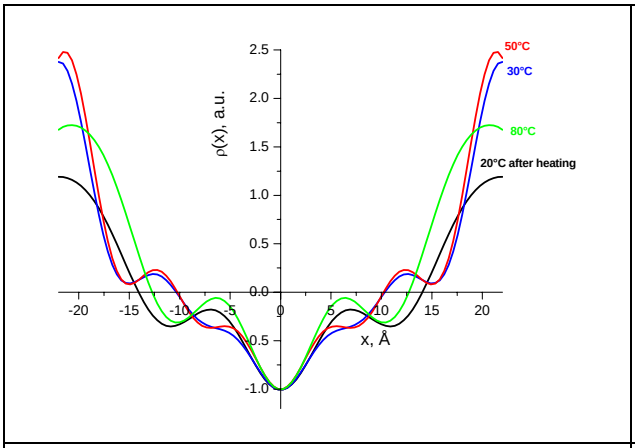

Fig. 1. Fourier profiles of Cer6/Ch/TA/ChS=55/25/15/5 at RH=57%, 8% D_2O at 30°C, 50°C, 80°C, and back 20°C after heating (black line)

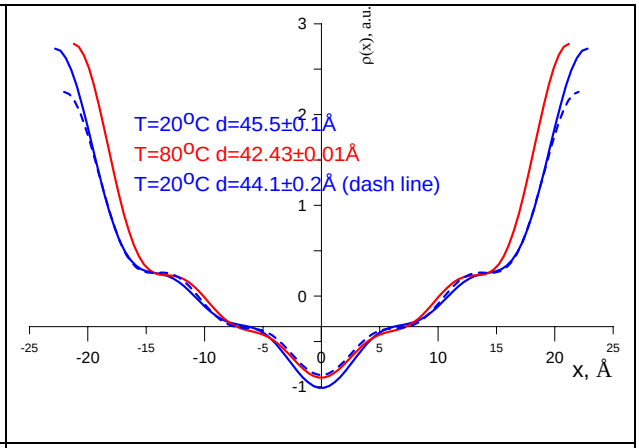

Fig. 2. Fourier profiles of Cer6/Ch/6_FA/ChS=55/20/15/10 at RH=57%, 8% D_2O at 20°C, 80°C, and back at 20°C after heating (dash line).

References:

1. D. Kessner, A.Ruettinger, M.A. Kiselev, S.Wartewig, R.H.H.Neubert. Properties of ceramides and their impact on the stratum corneum structure. A review, Part II: Stratum corneum lipid mixtures. *Skin Pharmacology and Physiology* 21 (2008) 58-74.
2. M. A. Kiselev, N. Yu. Ryabova, A. M. Balagurov, S. Dante, T. Hauss, J. Zbytovska, S. Wartewig, R. H. H. Neubert. New insights into structure and hydration of stratum corneum lipid model membrane by neutron diffraction. *European Biophys. J.* 34 (2005) 1030–1040.
3. M.A. Kiselev. Conformation of ceramide 6 molecules and chain-flip transitions in the lipid matrix of the outermost layer of mammalian skin, the stratum corneum. *Crystallography Reports* 52 (2007) 528-525.

NEUTRON WAVE RESONANCES AND OFF-SPECULAR SCATTERING FROM WAVEGUIDES

S.V. Kozhevnikov[a], F. Ott[b], A. Paul[c], L. Rosta[d]

[a]*Frank Laboratory of Neutron Physics, JINR, 141980 Dubna, Moscow Region, Russian Federation*
[b]*Laboratoire Léon Brillouin, CEA/CNRS, UMR12, CEA Saclay, 91191 Gif sur Yvette Cedex, France*
[c]*Institut für Festkörperforschung, Forschungszentrum Jülich, D-52425 Jülich, Germany*
[d]*Research Institute for Solid State Physics and Optics, POB 49, H-1525, Budapest, Hungary*

In carefully designed thin films hetero-structures, it is possible to create x-ray or neutron standing waves (NSW) which are resonantly enhanced. The theory of the neutron resonances in multilayer structures is described in [1]. During the last decade, resonant structures have been studied for various purposes. NSW in neutron wave-guides have been used to create sub-micron beams [2]. The use of NSW has also been experimentally developed for the investigation of thin films [3]. The thin layer to be investigated is placed inside the resonator at a position corresponding with the maximum amplitude of the NSW. The interaction between the neutrons and the investigating layer is thus strongly increased. This has been used to measure neutron spin-flip and beam-splitting for magnetically non-collinear layers [4,5] or generate secondary characteristic radiation (γ-rays with Gd layer [6,7] or α-particles with for Li [8]). It is also possible to use NSW to enhance the neutron interaction with interfacial roughness [9]. This was demonstrated in the system Fe/Cr/Fe where off-specular neutron scattering due to the interface roughness was measured [10]. This system was designed so as to have resonances near the Fe/Cr and the Cr/Fe interfaces. In this work we have investigated the interaction between neutron standing wave and the interfacial roughness in wave-guide structures of the type Py(permalloy)/Ti/Py. In such structures, off-specular neutron scattering is also strongly enhanced. We have more specifically investigated the regime of multiple resonances in the resonator layer. We have performed both fixed wavelength and Time-of-flight reflectometry characterisations of these systems. In the following we compare the experimental data obtained using both methods.

We have more specifically investigated tri-layer structures of the type Py(permalloy)/Ti/Py (Fig. 1a) where the resonator layer (Ti) with a low optical potential U is sandwiched between two permalloy layers with a high optical potential (Fig. 1b). Such a structure can be considered as a neutron wave-guide. It is possible to trap neutrons in the Ti layer which can then travel over macroscopic distances inside the layer (several mm). The different propagation modes of the neutrons inside the guide layer correspond to the resonant states. In such a structure, some neutrons can eventually channel down to the sample edge and create a submicron cross section neutron beam. Though the beam is very divergent it is also coherent and could be used for the investigation of nanostructures in biochemistry and semiconductor nanotechnology [2,11]. In our case, we will focus on the enhanced off-specular neutron scattering on the interface roughness of the guiding layer. This is actually a secondary effect of NWG. Nevertheless it is interesting since it demonstrates that it is possible to study *single* rough interfaces using neutron reflection which is often not possible in normal systems due to a very low scattered intensity.

The notations in Fig. 1 are the following: λ – the neutron wavelength, θ – glancing angle, k – neutron wave vector, p – projection of the neutron wave vector on the z-axis, Q – momentum transfer, d – thickness of guiding layer. Q_x and Q_y are the projection of the momentum transfer vector on the axis x and z. The subscript i corresponds to the incident beam (*i*nitial) and f corresponds to the reflected or refracted beams (*f*inal). There are three key scattering directions: specular reflection at $\theta_i = \theta_f$, the horizon at $\theta_i = 0$ and the direct beam at $\theta_i = -\theta_f$. For the refracted beam between the

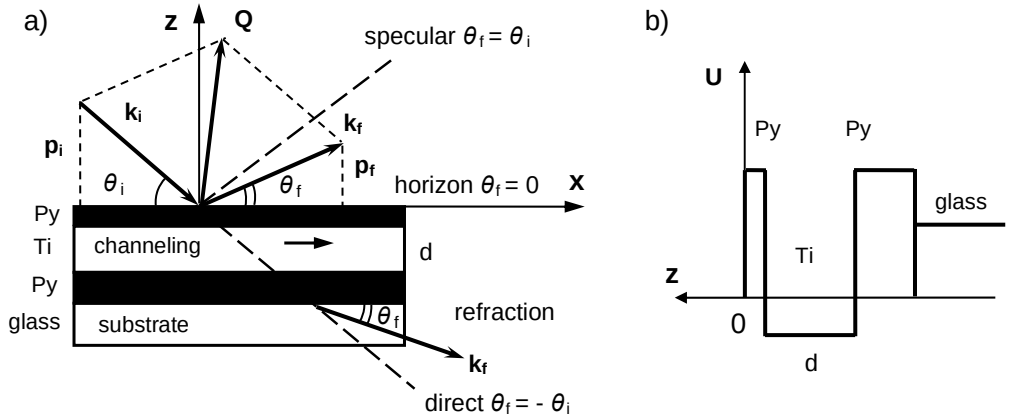

Fig. 1. a) Neutron waveguide structure; b) optical potential in the neutron waveguide.

horizon and the direct beam we have $\theta_f < 0$ and $p_f < 0$. The scattering wave-vector Q is related to the incidence and reflection angles by the relations:

$$Q = k_f - k_i = \begin{cases} Q_x = k_{fx} - k_{ix} = \dfrac{2\pi}{\lambda}\left(\cos\theta_f - \cos\theta_i\right) \approx \dfrac{\pi}{\lambda}\left(\theta_i - \theta_f\right)\left(\theta_i + \theta_f\right) \\ Q_z = k_{fz} - k_{iz} = \dfrac{2\pi}{\lambda}\left(\sin\theta_f + \sin\theta_f\right) \approx \dfrac{2\pi}{\lambda}\left(\theta_i + \theta_f\right) \end{cases} \quad (1)$$

The projections $p_{i,f}$ of the scattering wave-vectors are given by:

$$p_i = k_{iz} = \frac{2\pi}{\lambda}\sin\theta_i \approx \frac{2\pi}{\lambda}\theta_i \qquad p_f = k_{fz} = \frac{2\pi}{\lambda}\sin\theta_f \approx \frac{2\pi}{\lambda}\theta_f \quad (2)$$

The resonances take place (see Ref. [2]) when the phase Φ of the neutron wave function in the layered structure is equal to $2\pi n$, where n = 0, 1, 2, 3… is the resonance order. The main contribution into the phase comes from the guiding layer:

$$\Phi = 2\, p_n d = 2\pi n \quad (3)$$

Then from eqs. (2)-(3) we obtain the resonance conditions:

$$\frac{\theta_i}{\lambda} = \frac{n}{2d} \qquad \frac{\theta_f}{\lambda} = \frac{n}{2d} \quad (4)$$

The program SimulReflec [12] was used for the calculation of the neutron wave function density of "+" spin state in the magnetic structure Py(10 nm)/Ti(70)/Py(50)//glass. In Fig. 2, the distribution of neutron wave density is shown as a function of the layer thickness z and the incidence angle θ_i for a neutron wavelength λ = 4.52 Å. Three resonances n = 1, 2, 3 are seen in the guiding Ti layer at the incident glancing angles $\theta_{i1} = 0.25^\circ$, $\theta_{i2} = 0.4^\circ$ and $\theta_{i3} = 0.55^\circ$. The maximum of WF density reaches values up to 10 to 30. The maximum of the neutron wave function density for the different resonance orders can be changed by tuning the parameters of the system (the optical potentials and the thickness of layers).

In order to perform the characterization of the wave-guides, we have used two different reflectometry techniques: fixed wavelength and time-of-flight. We have used the fixed wavelength (λ = 4.52 Å) HADAS polarized reflectometer at the Forschung Zentrum Julich [13] which is equipped with a 2D detector and a multislit supermirror polarisation analyzer and the time-of-flight EROS neutron reflectometer in non-polarized mode [14] at the Laboratoire Léon Brillouin, CEA Saclay. The specular reflectivity of polarized neutrons "++" measured on HADAS is presented on Fig. 3. There are three dips corresponding to three resonances n = 1, 2, 3. The fitted structure is PyO_x(15 Å)/Py(78)/Ti(710)/Py(510)//*glass* with an interface roughness σ = 10 Å. The magnetization M is 0.8 μ_B/at. for the upper Py layer and 0.9 μ_B/at. for the bottom one. The regular dynamical reflectivity calculation cannot account for the resonance dips amplitude (10-15% of the total reflection). The diffuse off-specular scattering at one resonance position only represents about 2 % of the specular signal and thus can also not account for the dips amplitude.

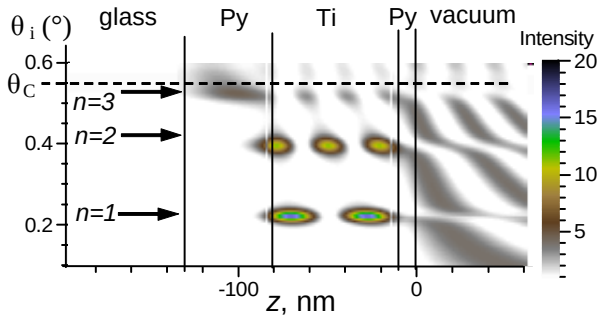

Fig. 2. Neutron wave function density "++" in the waveguide Py(10nm)/Ti(70)/Py(50)//*glass* calculated for λ = 4.52 Å in dependence on the incident angle θ_i and the sample depth *z*.

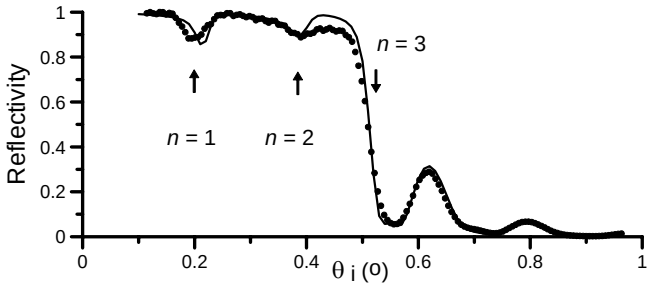

Fig. 3. Specular reflectivity "++" for tri-layer structure Py/Ti/Py//glass. The points are experimental data. The solid line is a numerical fit. The arrows indicate the resonances.

In order to fit the data, we introduced an artificially high absorption in the Ti guiding layer (60 times the tabulated value of 6.09 barn). This should be considered only as a trick to lose neutrons. However, we think that the neutrons are actually lost because they channel along the sample (over a distance up to 3 mm), exit at the edge of the sample and are lost for the specular reflectivity. This is difficult to account for in present reflectivity modelling programs.

The off-specular diffuse scattering signal measured on HADAS is presented on Fig. 4 in the coordinates (θ_i, θ_f). The diagonal line $\theta_i = \theta_f$ corresponds to the specular reflection. One can note that the diffuse scattering is enhanced along three vertical lines at $\theta_{in} = const$ and three horizontal lines at $\theta_{fn} = const$ corresponding to the resonances conditions n = 1, 2, 3 (Eq. 4). The scattered intensity is further increased at the intersection of different resonance orders (circles on Fig. 4). The diagonal lines of increased intensity correspond to Bragg-sheets (black rectangles). The intersection between resonant off-specular scattering and Bragg-sheets gives the enhancement in the resonant off-specular scattering (intersection between white lines and rectangles). The off-specular reflection due to neutron resonances has non-magnetic origin. We have observed the same off-specular scattering effect in non-magnetic neutron waveguide Cu(10nm)/Ti(65)/Cu(50)//glass.

On Fig. 5, the resonances and the off-specular scattering in reflection and refraction was measured in time-of-flight mode on the EROS reflectometer in non-polarized mode. The sample was saturated in the applied magnetic field 100 Oe and measured in the remanent state. On Fig. 5, off-specular scattering is presented: a) in the instrumental coordinates (λ, θ_f); b) in the (p_i, p_f) coordinates and c) in the intermediate coordinates $(p_i - p_f, p_i + p_f)$. The incident glancing angle is θ_i = 0.7°. One can see that Fig. 5b is very similar to Fig. 4 for the neutrons scattered above the horizon. There are off-specular reflection lines for the resonances at $p_i = const$ (vertical white lines) and $p_f = const$ (horizontal white lines). In Fig. 5c it is seen that there are Bragg-sheet lines (black rectangles). In the instrumental coordinates (Fig. 5a) the off-specular scattering signal is more difficult to interpret. The resonant reflection at $\lambda_n = const$ corresponds to p_i = const: λ_1 = 16 Å, λ_2 = 8 Å and λ_3 = 5.5 Å. This is close to the resonance conditions (4) with the resonator width d = 700 Å. The inclined white lines correspond to p_f = const where the reflection glancing angle θ_f depends on the wavelength. The wavelength dependence leads to the widening of the resonance lines and Bragg-sheet shown in Fig. 5a. The intersections between different resonances are marked by the circles in Figs. 5b and 5c and by the ellipses in Fig. 5a. Below the horizon, the arrow indicates the optical refraction of the neutron beam in the glass substrate. This critical wavelength 11 Å corresponds to the glass substrate nuclear potential of 95 neV. The transmitted diffuse scattering differs from the usual optical refraction. In Fig. 5c, the black rectangle indicates Bragg-sheet scattering at $p_i + p_f = const$. The resonances $p_i = const$ (vertical white lines in Fig. 5b) interfere with Bragg-sheet scattering and refracted beam (white rectangle). This leads to enhanced neutron scattering. Other type of transmitted beam is marked in Fig. 3a by the dotted line $\theta_f(°) = -0.61\theta_i - 0.064\lambda$ (Å). The origin of this beam may be neutrons transmitted above Bragg diffraction condition for the neutron wavelength.

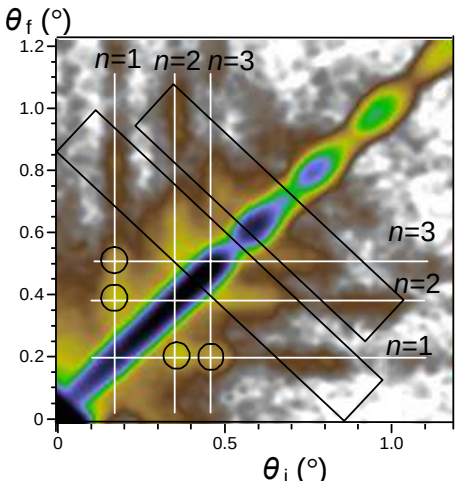

Fig. 4. Experimental off-specular scattering intensity "++" from a waveguide Py(10nm)/Ti(70)/Py(50)//*glass* measured on HADAS in the (θ_i , θ_f) representation.

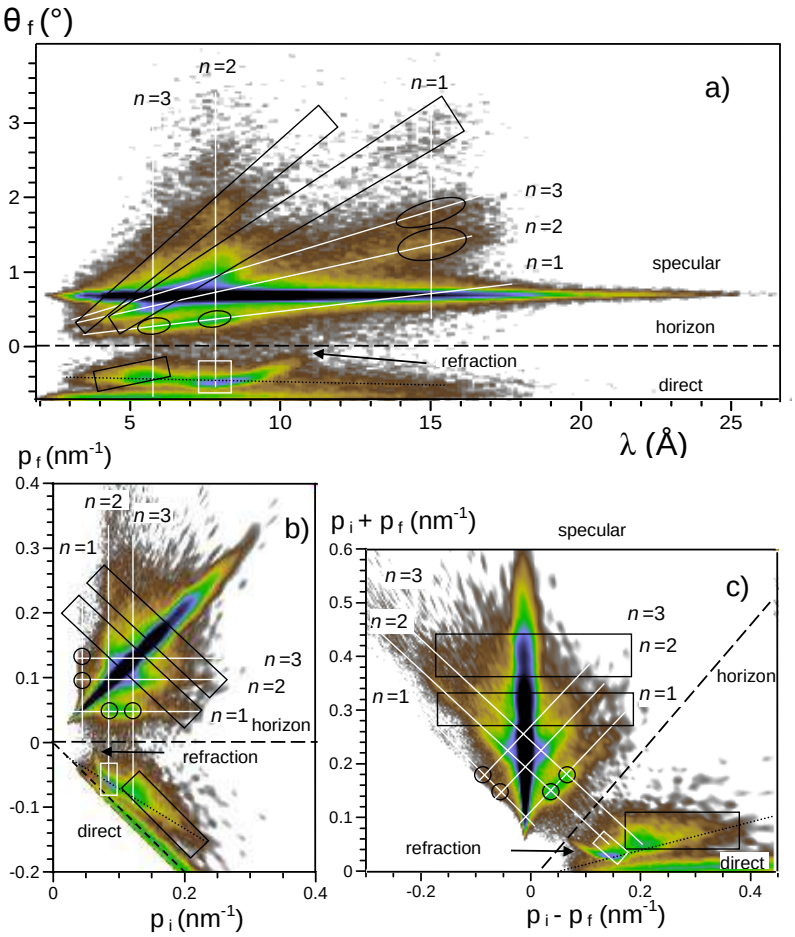

Fig. 5. Off-specular scattering (experiment) from Py/Ti/Py in TOF mode at $\theta_i = 0.7°$ in different representations: a) (λ, θ_f); b) (p_i, p_f); c) $(p_i + p_f, p_i - p_f)$.

The presented results will be published in [15].

This work has been supported by the European Commission under the 6th Framework Program through the Key Action: Strengthening the European Research Area, Research Infrastructures. Contract n°: RII3-CT-2003-505925 and ECONET project 16273ZA. The authors are thankful to Dr. Florin Radu for useful remarks.

[1] F. Radu, V.K. Ignatovich, Physica **B 292** (2002) 160.
[2] F. Pfeiffer, V. Leiner, P. Hoghoj, I. Anderson, Phys. Rev. Lett. **88** (2002) 055507.
[3] V.L. Aksenov, Yu.V. Nikitenko, Physica **B 297** (2001) 101.
[4] V.L. Aksenov, Yu. V. Nikitenko, S.V. Kozhevnikov, F. Radu, R. Kruijs, Th. Rekveldt, Surface investigation **116** (2001) 1225. Poverkhnost' **8** (2000) 10, in Russian.
[5] V.L. Aksenov, Yu.V. Nikitenko, S.V. Kozhevnikov, Physica **B 297** (2001) 94.
[6] H. Zhang, P.D. Gallagher, S.K. Satija, R.M. Lindstrom, R.L. Paul, T.P. Russell, P. Lambooy, J. Kramer, Phys. Rev. Lett. **72** (1994) 3044.
[7] V.L. Aksenov, L. Cser, N.A. Gundorin, Yu.V. Nikitenko, Yu.P. Popov, Physica **B 276-278** (2000) 809.
[8] V.L. Aksenov, Yu. V. Nikitenko, F. Radu, Yu.M. Gledenov, P.V. Sedyshev, Physica **B 276-278** (2000) 946.
[9] S.V. Kozhevnikov, F. Ott, E. Kentzinger, A. Paul, Physica B **397** (2007) 68-70.
[10] E. Kentzinger, U. Rucker, B. Toperverg, and T. Bruckel, Physica **B 335** (2003) 89.
[11] V.K. Ignatovich, F. Radu, Phys. Rev. **B 64** (2001) 205408.
[12] SimulReflec : http://www-llb.cea.fr/prism/programs/simulreflec/simulreflec.html
[13] U. Rücker, B. Alefeld, W. Bergs, E. Kentzinger, Th. Brückel, Physica **B 276-278** (2000) 95.
[14] A. Menelle, Physica **B 350** (2004) e767.
[15] S.V. Kozhevnikov, F. Ott, A. Paul, L. Rosta, Resonances and off-specular scattering from neutron waveguides, European Journal of Physics Special Topics (2009), in press.

X-ray investigation of comb-like liquid crystal polymers, oriented by a strong magnetic field for SANS measurements

A.I.Kuklin[1*], A.Yu.Cherny[2], V.G.Cherezov[3], S.Kostromin[4], A.V.Rogachev[1,5], V.P.Shibaev[4]

[1)] *Frank Laboratory of Neutron Physics, JINR, Dubna, Moscow reg., Russia*
[2)] *Bogoliubov Laboratory of Theoretical Physics, JINR, Dubna, Moscow reg., Russia*
[3)] *Department of Molecular Biology, The Scripps Research Institute, La Jolla, CA 92037, USA*
[4)] *A.N. Belozersky Institute of Physico-Chemical Biology, Moscow State University, Moscow, Russia*
[5)] *Skobeltsyn Institute of Nuclear Physics of Moscow State University, Moscow, Russia*

*E-mail: * kuklin@nf.jinr.ru*

At present, there is a growing interest in study of liquid crystalline polymers. Comb-like polymers with mesogenic molecules represent a large class of polymers that display liquid-crystalline properties. A lot of information is available on the properties of such polymers, both in dilute solutions and the bulk phase [1,2]. Investigations of the liquid-crystalline (LC) polymers are performed by various methods, such as X-ray diffraction, NMR spectroscopy, and optical diffraction. These measurements are mainly concerned with the structural changes due to new orientations, caused by strong magnetic field. However, so far the conformation of the main macromolecular chain has not been studied yet.

The labeling method allows us to extract direct information on the conformation of a single macromolecule from the neutron scattering data. Small Angle Neutron Scattering (SANS) method, used for this purpose, gives us the anisotropy parameter, that is, the ratio $R_\perp / R_\parallel$. Here $R_\parallel$ and $R_\perp$ are parallel and perpendicular mean square projections, respectively, of the radius of gyration of the main chain [3]. They are nothing else but "principal moments of inertia" of the main chain around the symmetry axis $R_\parallel$ and around a perpendicular axis $R_\perp$.

The first investigation, carried out by Kirste [3] and Keller [4], showed that the polymer coil of the liquid-crystalline (LC) polymer is not isotropic but has an axial symmetry. As discussed above, the anisotropy implies the difference in $R_\parallel$ and $R_\perp$. In turn, this leads to a strong anisotropy of the scattering data in Guinier-region.

In order to obtain $R_\parallel$ and $R_\perp$, we should measure the sample turned at various angles with respect to the neutron beam [5]. Technically, it is more convenient to polarize the sample in the form of a pill at 45° with respect to the normal of the "pill" and to make the experimental run for each turn of the "pill" about the normal [6]. One can consider the polymer coil as an ellipsoid, then the parameters $R_\perp$ and $R_\parallel$ are related to the radii of the ellipsoid: $a = b = \sqrt{5} R_\perp$ and $c = \sqrt{5} R_\parallel$. For the studied LC-polymer, we obtain [6] $a = b = 61{,}7 \pm 0.4$ Å and c=13.4±2 Å.

In Ref. [7], $R_\perp$ and $R_\parallel$ were determined. However, the measurements were made with a detector having no azimuthal sensitivity, which leads to significant experimental errors. So far, a full description of coil parameters has not been performed yet.

The main purpose of this paper is to determine the smectic phase parameters for the LC-polymer. In particulary, we experimentally obtain the data for the oriented comb-like LC polymers in strong magnetic field using X-ray diffraction method. From these data we extract the values of the lattice structure parameters.

We use the polymers consisting of 50% deuterated chains and 50% protonated chains, chemical formula is $(C_3D_5C_{20}O_3H_{23})_n$.

The samples were oriented in strong magnetic field (12 Tesla-up to 20 Tesla, see Fig. 1) in the Institute of Atomic Energy (Kurchatov Institute). At the beginning and the end of melting-frozen

process, we shake the samples by strong magnetic field up to 20 Tesla. The temperature and magnetic field evolution are represented in Fig. 1.

The results of X-ray diffraction experiment (DRON, FLNP, JINR) are depicted in Fig.2. Availability of the third Bragg pick, shown in the diagram, indicates that the process of orientation in strong magnetic field is well achieved. Using the Bragg equition with λ=1.54 Å one can calculate the periodicity 34,5±0,2 Å for the comb-like LC-polymers.

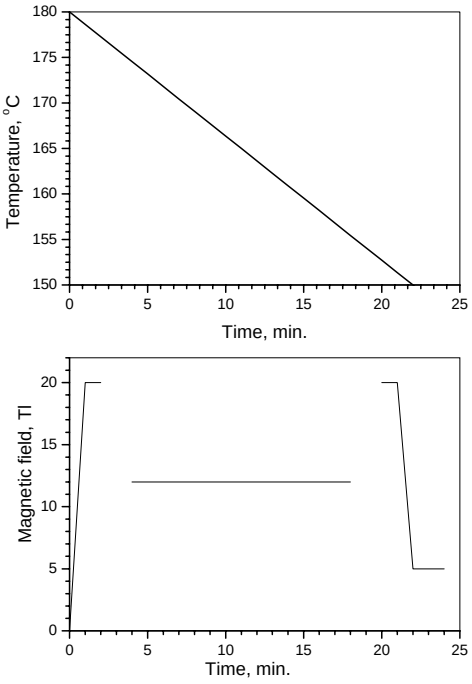

Fig. 1. Temperature and magnetic field evolution during the sample preparation

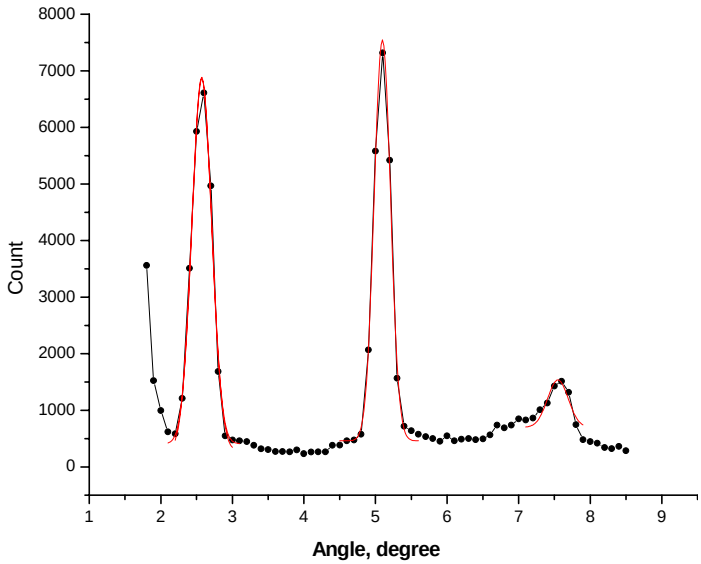

Fig. 2. X-ray scattering curves for the LC-polymer

Concluding, by means of X-ray diffraction we experimentally determine the period of the smectic layers. The method of obtaining $R_{\perp}$ and $R_{\parallel}$ with the SANS experiment will be discussed elsewhere.

References:

[1] *Liquid Crystalline Order in polymer*, ed. by A. Blumstein (Academic Press,1978).
[2] Shibaev, V.P., Plate, N.A, Adv. Polym. Sci., **60/61**, 173 (1984).
[3] Kirste, R.G., and Ohm, H.G., Makromolec. Chem. Rap. Commun., **6**, 179 (1985).
[4] Keller, P., Carvalho, B., Cotton, J.P., Lambert, M., Moussa, F., Pepy, G., J. Physique Lett., **46**, L-1065 (1985).
[5] Svetogorsky, D.A., J. Appl. Cryst., **23**, 79 (1990).
[6] A detailed description of the experiment will be published elsewhere.
[7] Kalus, J., Kostromin, S.G., Shibaev, V.P., Kunchenko, A.B., Ostanevich, Yu.M., Svetogorsky, D.A., Mol. Cryst. Liq. Cryst., **155**, 347 (1988).

NEUTRON DIFFRACTION STUDY OF TEXTURE EVOLUTION OF ECAPed MAGNESIUM ALLOYS

T.A. Lychagina[1], D.I. Nikolayev[1], H.-G. Brokmeier[2], W. Gan[2]

[1]*Frank Laboratory of Neutron Physics, Joint Institute for Nuclear Research, Dubna, Russia*

[2]*GKSS-Forchungszentrum, D-21502 Geesthacht, Germany*

Deformed magnesium alloys find wide application in various branches of mechanical engineering and, first of all, in aerospace, automobile and electronic industries. Though they have high specific strength, plasticity of semifinished products from these alloys (especially at temperatures of deformation below 250˚C) is not rather high [1]. It is connected in many respects to features of the structure and texture formation at plastic deformation of the given alloys. The situation can considerably be improved if to find ways of deformation of magnesium products allowing to generate in these materials the equiaxed fine-grained structure during deformation and diffuse or tilted basal texture. One of the promising ways of this problem decision is application of the severe plastic deformations with help of equal channel angular pressing (ECAP)[2-5]. The ECAP process consist of extruding a lubricated sample through two channels of equal and indentical area of cross-section. The process can be repeated multiple times. There is no change in area of cross-section due to the process.

The texture formed after ECAP for Mg-4.5%Al-1%Zn (MA2-1) alloy has been investigated. The bar extruded with backpressure at 345ºC was input for ECAP. The ECAP was carried out up to four passes following the routes A (a sample orientation is not changed after each pass), C (after each pass a sample is rotated about its longitudinal direction by 180º) and up to six passes following the route B_c (after the first two passes under the route C a sample is rotated about its longitudinal axis by 90º clockwise, then remaining two passes are achived again under the route C). The ECAP procedure was carried out using a specially designed die with an angle 90º between two channels of square cross section (20×20mm) without any rounding of the corners. In each route the sample had to be turned by 90º around its transverse axis in order to set the deformed sample back into the die. The first pass was carried out at 260ºC. Then temperature having been decreased up to 240ºC for the fourth pass. E_D is the extrusion direction (the direction of ECAP). The texture of the 8 samples was investigated by measuring the (002), (100), (101), (110) pole figures using the TEX-2 neutron diffractometer at the FRG-1 neutron source (GKSS Research Center). The samples size was 10×10×10mm. The all samples were measured so that the extrusion direction (the direction of ECAP) is in the center of the pole figures. The exposure time was about 40 hours for the 4 pole figures.

It was measured four complete pole figures (PFs) (002), (100), (101), (110) for each sample. The measurements for samples made in accordance with routes A, C and B_c were carried out. The experimental PFs measured for route A are given in Fig. 1. The fist row presents the PFs for the input extruded sample. In the second row it can be seen the PFs for sample after one ECAP pass. The initial texture (for input sample) is characterized by two strong axial components (basal and prismatic). The intensity of basal component is about 10mrd, and the intensity of prismatic component is about 18mrd. It should be underlined that the one prismatic texture component for common magnesium (AZ31, AZ61, MA2-1) alloys samples after extrusion is typical. The reason for the second component is backpressure combining with extrusion. After the first pass we observe the moving of the basal component (the intensity maximum) on the angle about 45° respectively to extrusion direction. After the second pass in route A this component moved on the angle about 90° respectively to extrusion direction. After the fourth pass in the route A the intensity of this component increased from the 6.06mrd (after the second pass) up to 8.97mrd. The moving of the texture components during the route C is rather close to one in the route A. The difference is velocity of intensity redistribution. So during the route C the maximum of basal texture component on the angle about 45° respectively to extrusion direction is more stable then in the route A. It

presents on the PFs for the samples after second and fourth passes as well in the route C. The maximum of this texture component increased from 6.35mrd after the second pass up to 8.42mrd after the fourth pass.

As for the route B_c we also observe the same component moving after the fourth pass. The maximum of this component increased from 8.61mrd after the fourth pass up to 11.9 mrd after the sixth pass.

The obtained results give information for the further improvement of ECAP technology aimed to required texture for MA2-1 alloy.

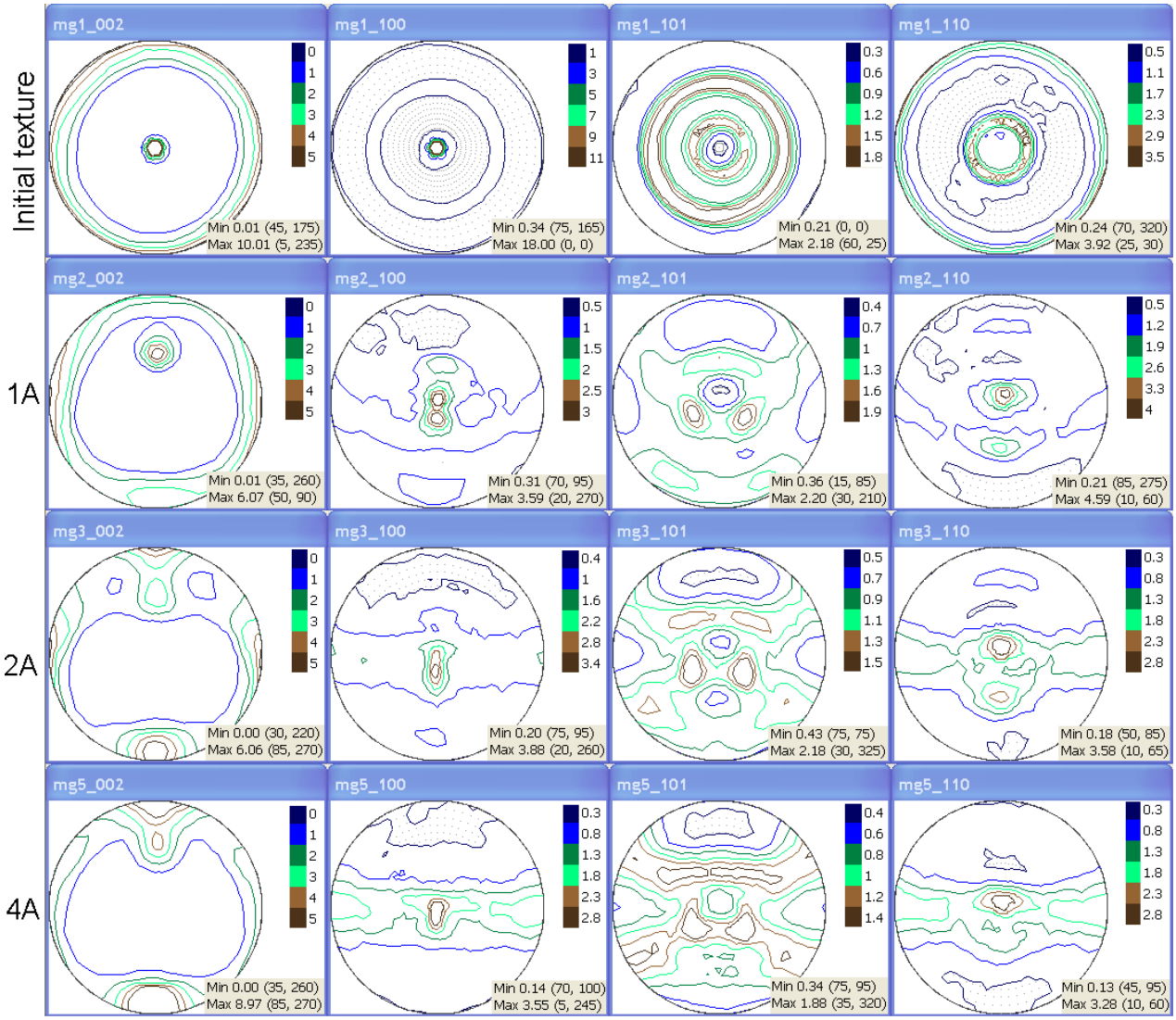

Figure 1: The experimental pole figures for the input sample and the samples in the route A of ECAP. The all samples are from alloy MA2-1. The extrusion direction (ED) is in the center for the all PFs. The position of the sample coordinate system (extrusion direction, transverse direction, normal direction) is the same for the all samples.

References

1. K.Xia, J.T. Wang, X.Wu, G.Chen, M.Gurvan, *Mater.Sci.Eng*. A 410-411, 324-327 (2005)
2. Z.Horita, T.Fujinami and T.G. Langdon, *Mater.Sci.Eng*., A318, 34 (2001)
3. R.Z.Valiev, R.K. Islamgaliev and I.V. Alexandrov *Prog.Mater.Sci.*, 45, 103 (2000)
4. A. Yamashita, Z.Horita and T.G. Langdon *Mater.Sci.Eng*., A300, 142 (2001)
5. T.Liu, W.Zhang, S.D.Wu, C.B.Jiang, S.X.Li, Y.B.Yu, *Mater.Sci.Eng.*, A 360, 345 (2003)

Correlation of spin and charge ordering in $Sr_3YCo_4O_{10.5+\delta}$, δ=0.02 and 0.26

D.V. Sheptyakov[1], O.A. Drozhzhin[2], V.Yu. Pomjakushin[1], S.Ya. Istomin[2], I.A. Bobrikov[3], E.V. Antipov[2], A.M. Balagurov[3]

[1] Laboratory for Neutron Scattering, ETH Zurich and Paul Scherrer Institut, CH-5232 Villigen PSI, Switzerland
[2] Department of Chemistry, Moscow State University, 119991 Moscow, Russia
[3] Frank Laboratory of Neutron Physics, Joint Institute for Nuclear Research, 141980 Dubna, Russia

Quite recently, the new perovskite-related cobaltites $Sr_{1-x}R_xCoO_{3-y}$, $0.1 \le x \le 0.5$, $0.2 \le y \le 0.4$, R=Y, Sm-Ho were discovered [**1**]. In the crystal structure of these compounds (possessing tetragonal unit cells with parameters *a* and *c* related to the parameter of cubic perovskite a_{per} as $a \approx 2 \times a_{per}$; $c \approx 4 \times a_{per}$, sp. gr. *I 4/m m m*), there are three different sites for the *A* cations occupying two 4*e* positions and one position 8*g*. It was found that Y or rare-earth cations preferentially occupy one of the 4*e* sites. Thus an idealized description of the chemical composition would then be $Sr_3R_1Co_4O_{12-y}$ and this type of structure is now frequently referred to as the 314-phase [**2**].

From the room temperature neutron powder diffraction data it was established [**2**] that $Sr_{0.7}Dy_{0.3}CoO_{2.62}$ is a G-type antiferromagnet with magnetic moments of Co atoms parallel to the *c*-axis of the tetragonal structure and the refined magnetic moment value of 1.2 μ_B at room temperature for Co-atoms. Independently the G-type long-range antiferromagnetic ordering has been found for $Sr_{0.67}Y_{0.33}CoO_{2.79}$ in Ref. [**3**]. The average for all Co-atoms low-temperature value of magnetic moment was found to be equal to 2.0 (3) μ_B, which corresponds to the intermediate spin state of Co^{3+}.

In this report some results of a new neutron diffraction study of atomic and magnetic structures of the Y-314 phases $Sr_3YCo_4O_{10.5+\delta}$ (or $Sr_{0.75}R_{0.25}CoO_{2.625+\delta/4}$) with two different oxygen contents: close to ideal ("as prepared" sample, $\delta = 0.02$) and a higher one ("oxidized" sample, $\delta = 0.26$) are presented. For both compounds the G-type AFM state was confirmed with different long-range magnetic moments for different Co-sites and without any indications for the long-range ferromagnetic order with substantial moment magnitudes.

The $Sr_3YCo_4O_{10.5+\delta}$ sample ("as-prepared" sample, about 6 g) was synthesized from the intimately mixed stoichiometric amounts of $SrCO_3$, Co_3O_4 and Y_2O_3 pressed into pellets and heated at 1150 °C for 24 h, then regrinded and reheated at 1170 °C for 48 h. In order to prepare the 314-phase with higher oxygen content, the "as prepared" sample (about 3 g) was placed in alumina crucible and heated at 600°C for 12 h under oxygen pressure of 150 atm. The oxygen content of the samples determined by iodometric titration corresponds to the formula $Sr_3YCo_4O_{10.5+\delta}$, with $\delta \approx 0.02$ and 0.26 for the "as prepared" and "oxidized" samples, correspondingly. Neutron diffraction patterns were collected with the powder diffractometers HRPT and DMC (both located at SINQ spallation neutron source, PSI Villigen). The refinements of the crystal and magnetic structure parameters were carried out with FullProf program suite, with the use of its internal tables for scattering lengths and magnetic form factors.

The crystal structures of $Sr_3YCo_4O_{10.5+\delta}$ ("as prepared" and "oxidized" samples) were refined at 298 K using neutron diffraction data from HRPT diffractometer and the structural model from Ref. [**4**]. In our refinements, we considered the differences in neutron scattering lengths of Sr (b_{Sr} = 7.02 fm) and Y (b_Y = 7.75 fm) to be too tiny in order to refine their possible mutual substitutions. Hence, we have positioned the smaller Y^{3+} cations exclusively in the A-positions *4e* (0,0,~0.14) with the lowest effective coordination number. The two other A-

positions are occupied in our refinement model exclusively by the Sr^{2+} cations: *4e* (0,0,~0.62) and *8g* (0,0.5,~0.13).

Upon cooling, the magnetic peaks appear in the neutron diffraction patterns of both samples in a similar manner. This is illustrated for the "oxidized" compound in the **Fig. 1**. The positions of all magnetic Bragg peaks marked by numbers coincide with those of the nuclear ones: 1 – with (110), 2 – with (112), 3 – with (312)/(116), 4 – with (332)/(316). The peak marked with * corresponds to the (1/2,1/2,1/2) magnetic diffraction peak of the CoO impurity and is not within the metrics of the Y314 compound.

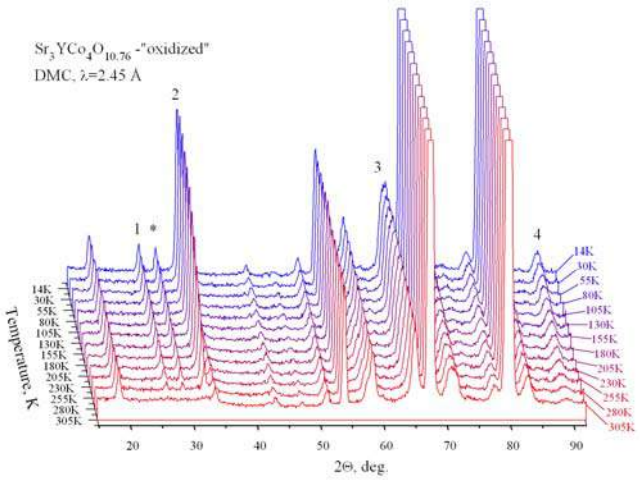

Fig. 1. The evolution of the neutron diffraction patterns (taken with DMC powder neutron diffractometer, λ=2.45 Å) of the "oxidized" $Sr_3YCo_4O_{10.76}$ compound with temperature. The magnetic peaks are marked with numbers 1–4.

Since the positions of magnetic peaks coincide with those for the allowed nuclear reflections, we conclude that the propagation vector of the magnetic structure of 314-phase is $\boldsymbol{\kappa} = (0,0,0)$. Using the determined propagation vector, we have performed the symmetry analysis of the possible magnetic ordering schemes which has been carried out with the program SARAh-2K. An important assumption done was that for both magnetic Co sites, the ordering occurs with one and the same irreducible representation (IR). This leaves out exactly three IR's, for which the decomposition for both Co sites has nonzero coefficients. An important finding is that the magnetic moments on the two sites are really different. The refined *c*-components of magnetic moments of the two sorts of atoms (Co1 and Co2) are in roughly the 2:1 proportion. The presence of a peak (110) at $2\Theta \sim 26.3°$ (marked as "1" in the ***Fig. 1***) unambiguously proves that the Co ions in different sites (Co1 and Co2) are in fact carrying different magnetic moments (its calculated intensity would drop to the exact zero if the moments on two Co sites were assumed equal). We note here that in the earlier papers, this very feature has been overlooked. In fact, in the Figure **5** of Ref. [**3**], the (110) peak is obviously absent at 350 K and definitely present at 10 K, but it is not modeled by the proposed in magnetic structure model with equal for *all* Co ions magnetic moments, and is certainly visible in the difference curve for the 10 K refinement.

We have to admit that from the diffraction data it is not possible to deduce which exactly of the two atoms – Co1 or Co2 possesses the larger magnetic moment magnitude since both possibilities provide roughly the same refinement quality. However since the Co1 atoms in oxygen deficient layers have a lower coordination number (on average 4.5), one can assume higher magnetic moments for them in comparison to the Co2 atoms in the octahedral coordination. The magnetic ordering in both samples occurs in the same manner, so all the considerations given above, are also valid for the "as prepared" sample as well. The temperature dependences of magnetic moments for both sublattices in all the samples are shown in the **Fig. 2**.

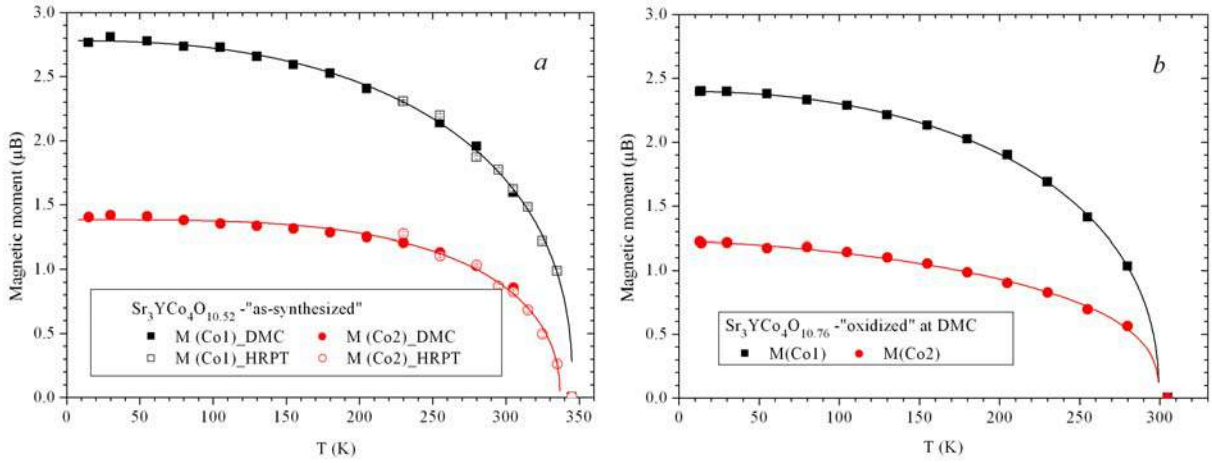

Fig. 2. Refined magnetic moments on the Co1 (squares) and Co2 (circles) sites for the investigated compounds: $Sr_3YCo_4O_{10.52}$ ("as prepared", panel a) and $Sr_3YCo_4O_{10.76}$ ("oxidized", panel b). The lines are guides to the eye. Filled circles correspond to the results obtained with DMC diffractometer ($\lambda = 2.45$ Å), opened ones – to the results from HRPT diffractometer ($\lambda = 2.955$ Å).

In summary, we have prepared $Sr_3YCo_4O_{10.5+\delta}$ compounds with the so called "314-phase" structure ($I4/mmm$, $a \approx 2\times a_{per}$; $c \approx 4 \times a_{per}$) possessing different oxygen content corresponding to δ=0.02, 0.26 and studied the temperature evolution of their crystal and magnetic structures by neutron powder diffraction. In contrast to the previous studies, refinement of the crystal structure of the "as-prepared" ($\delta = 0.02$) 314-phase revealed different distribution of oxygen atoms in oxygen-deficient layer over both the O2 and O2' positions. The main reason for this could be a considerable disorder of Sr^{2+} and Y^{3+} in the crystal structure and the degree of disorder could be associated with the amount of oxygen in O2' position.

Oxidation of the 314-phase leads to the decrease of the T_N from ~342 (±7) K for the "as prepared" $Sr_3YCo_4O_{10.52}$ compound to ~299 (±5) K for the "oxidized" $Sr_3YCo_4O_{10.76}$ one. Our detailed study of the magnetic structure confirmed the G-type AFM ordering, with the magnetic Co moments being aligned along the *c*-axis of the tetragonal cells. An important correction to the previous results is that we have experimentally observed ordering of different spin states of Co over octahedral and oxygen-deficient layers with the magnetic moments of the Co ions in the oxygen-deficient layers being significantly higher than those of the Co ions in the "completely filled" octahedral coordination. Thus, for the first time we demonstrate a direct correlation of the spin and charge ordering in these novel cobaltites.

References

1. S. Ya. Istomin, J. Grins, G. Svensson, O. A. Drozhzhin, V. L. Kozhevnikov, E V. Antipov, J. P. Attfield, Chem. Mater. **15**, 4012 – 4020 (2003).
2. S.Ya. Istomin, O.A. Drozhzhin, G. Svensson, and E.V. Antipov, Solid State Sciences **6**, 539-546 (2004).
3. D.J. Goossens, K.F. Wilson, M. James, A.J. Studer, and X.L. Wang, Phys. Rev. **B 69**, 134411 (2004).
4. R.L. Withers, M. James, and D.J. Goossens, J. Solid State Chem. **174**, 198-208 (2003).

Successive Structural Phase Transitions in $Pr_{0.5}Sr_{0.5}CoO_3$ in the Range 10–1120 K

A. M. Balagurov[a, *], I. A. Bobrikov[a], D. V. Karpinsky[b], I. O. Troyanchuk[b], V. Yu. Pomjakushin[c], and D. V. Sheptyakov[c]

[a] *Frank Laboratory of Neutron Physics, Joint Institute for Nuclear Research, Dubna, Moscow region, 141980 Russia*
[b] *Joint Institute of Solid State and Semiconductor Physics, National Academy of Sciences of Belarus, Minsk, 220072 Belarus*
[c] *Laboratory for Neutron Scattering, Paul Scherrer Institut, 5232 Villigen, Switzerland*

A fast growing interest to complex cobalt oxides (cobaltites) is caused by their peculiar magnetic and transport properties which are determined by the strong correlation between atomic structure of a particular compound and various ordering types: long range magnetic, charge or orbital order. In certain complex oxides $Ln_{1-x}M_xCoO_{3-\delta}$, where Ln is a lanthanide and M is an alkali earth element at certain relations between the ion radii of Ln and M, the ordered location of these elements and oxygen vacancies in the unit cell also appears. The feature of the magnetic structures in cobaltites is their relation with a particular spin state of the Co ion, which depends on its charge state, configuration of the CoO_6 octahedra, and can vary with the temperature [1].

An interesting and may be even special case of $Ln_{0.5}Sr_{0.5}CoO_3$ is $Pr_{0.5}Sr_{0.5}CoO_3$ (below, PSCO). The magnetic investigations [2] show that two phase transitions are observed in the Pr-containing compound at $T_C \approx 226$ K and $T_A \approx 120$ K, whereas compounds with other rare earth cations exhibit only one high-temperature transition at which the ferromagnetic ordering appears. Both transitions are manifested in the temperature dependence of the specific heat (in zero magnetic field), but only the transition at T_C is manifested as a change in the slope of the temperature dependence of the electric resistance. Below this temperature, the resistance decreases smoothly; for this reason, PSCO was classified as a metallic ferromagnet in the entire temperature range below T_C.

Noticeable anomalies were observed in the elastic properties of $Pr_{0.5}Sr_{0.5}CoO_3$ at T_A [3], which indicate the rearrangement of the structure. Nevertheless, the crystal structure of the low-temperature phase of PSCO and, correspondingly, the nature of the second magnetic phase transition at T_A remained unclear. We attempted to solve this problem by using high resolution neutron and synchrotron radiation diffraction. In addition, the experiments in a wide temperature range (10–1123 K) make it possible to reconstruct the complete sequence of structural transitions in $Pr_{0.5}Sr_{0.5}CoO_3$.

The $Pr_{0.5}Sr_{0.5}CoO_3$ powder was synthesized using the normal ceramic technology. To analyze the crystal symmetry, we used the diffraction data obtained on a neutron Fourier diffractometer (HRFD) at the IBR-2 pulsed reactor, Joint Institute for Nuclear Research (Dubna, Russia). The neutron spectra were measured in a wide temperature range (10-773 K) normally in the heating regime. In addition, PSCO was studied on high-resolution powder diffractometer on the synchrotron radiation source DORIS (DESY, HASYLAB, B2 line). The measurements on the DORIS were performed at room temperature and at higher temperatures up to 1123 K. The data were analyzed by means of the MRIA and FullProf programs.

The high-temperature structure of PSCO corresponds to ideal perovskite (space group *Pm3m)* with the unit cell parameter $a \sim 3.85$-3.88 Å. The structural transition to the rhombohedral phase (space group *R-3c)* occurs near 800 K. The structure is rhombohedral down to $T \sim 330$ K, whereas clear attributes of the orthorhombic structure appear below this temperature; i.e., the two-phase state is formed. The orthorhombic structure of PSCO is well described in the space group

Imma. A rapid decrease in the volume fraction of the *R*-3*c* phase and the corresponding increase in the volume of the *Imma* phase occur in the temperature range from 300 to 290 K, which corresponds to the minimum detected in [3] in the temperature dependence of the Young modulus. Down to $T\sim$ 120 K including T_C, no significant rearrangements of the structure are observed except for the disappearance of the traces of the rhombohedral phase at $T \sim 200$ K. The fraction of the *Imma* phase begins to rapidly decrease at 120 K and a new phase appears. We have to interpret the symmetry of this phase as a triclinic. Attempts to refine neutron or synchrotron spectra (even in the Profile Matching regime in the FullProf program) at any other symmetry (monoclinic or monoclinic + orthorhombic) did not provide satisfactory result. The description of the diffraction spectrum profile in the low temperature range (10 – 120 K) can be radically improved only with the reduction of the unit cell symmetry to triclinic. In this case, the χ^2 value decreases by a factor of 3 or 4. According to the neutron data, the volume of this low-symmetry phase in the sample heated from 10 K decreases sharply (by 20%) in the range from 90 to 110 K, but its noticeable amount is clearly observed up to 150 K. The temperature dependences of lattice parameters for all observed phases are shown in Fig. 1.

According to the above data, the crystal symmetry at $T_A \sim 120$ K is reduced from orthorhombic to triclinic and, correspondingly, the interatomic distances and valence angles change. These changes can be estimated by comparing the cell anisotropy parameter $\nu = b/(a^2 + c^2)^{1/2}$ before and after the transition. The CoO_6 octahedra in the orthorhombic phase have an almost regular shape (all Co-O distances are approximately equal to each other) and $\nu = 0.994$; in this case, $c > a \approx b'$, where $b' = b/\sqrt{2}$. The relation between the parameters in the low-symmetric phase is different, $b' > a \approx c$, and the noticeable anisotropy of the unit cell with $\nu = 1.016$ appears (Fig. 2); this anisotropy indicates at least a certain ordering degree of the e_g orbitals of cobalt along the *b* axis. The attendant changes in the interatomic distances and valence angles give rise to the rearrangement of the magnetic interactions and to the appearance of an anomaly in the temperature dependence of the magnetic susceptibility at $T_A \sim 120$ K.

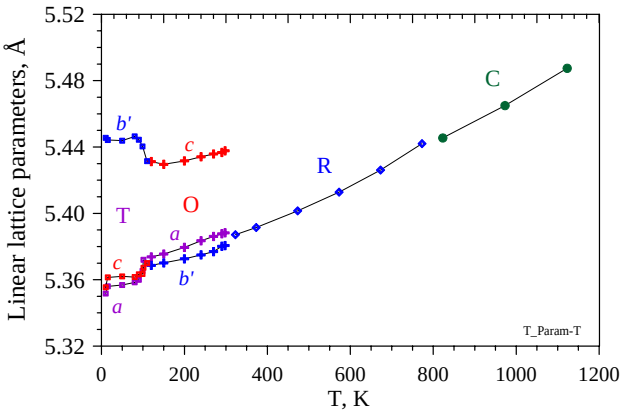

Fig. 1. Temperature dependence of the reduced linear parameters (for $Z = 4$, $b' = b/2$) of the unit cell of $Pr_{0.5}Sr_{0.5}CoO_3$ for all phases under consideration: cubic (*C*, *Pm3m)*, rhombohedral *(R, R-3c)*, orthorhombic (O, *Imma)*, and triclinic *(T, P1)*. The data for the cubic phase were obtained on the synchrotron radiation source and the other data, on the HRFD diffractometer.

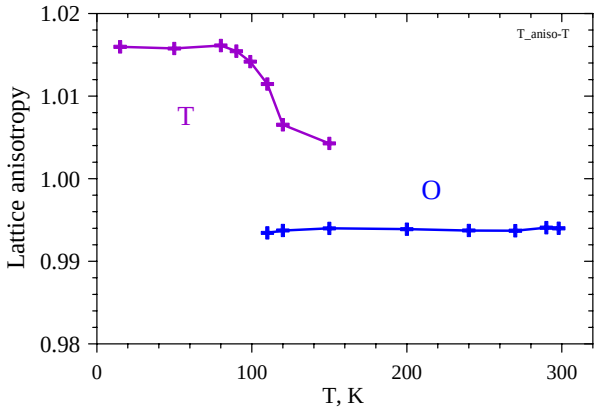

Fig. 2. Anisotropy $\nu = b/(a^2 + c^2)^{1/2}$ of the $Pr_{0.5}Sr_{0.5}CoO_3$ unit cell for the (*O*) orthorhombic and (*T*) triclinic phases. The CoO_6 octahedra in the *O* phase have an almost regular shape. The values $\nu > 1$ refer to the prevailing ordering of the e_g orbitals of cobalt along the *b* axis of the unit cell.

REFERENCES

1. P. G. Radaelli and S.-W. Cheong, Phys. Rev. B **66**, 094408 (2002).
2. R. Mahendiran and P. Schiffer, Phys. Rev. B **68**, 024427 (2003).
3. I. O. Troyanchuk, D. V. Karpinsky, A. N. Chobot et al., Pis'ma Zh. Éksp. Teor. Fiz. **84**, 180 (2006) [JETP Lett. **84**, 151 (2006)].

Melting behavior of water confined in carbon nanopores; structure of the confined ice.

M.Jazdzewska, M.Sliwinska-Bartkowiak
Faculty of Physics, A.Mickiewicz University, Poznan, Poland
A.I. Beskrovnyy, S.G. Vasilovskiy
Frank Laboratory of Neutron Physics. Joint Institute for Nuclear Research, Dubna, Russia

Water confined in a nanoscale environment exhibit unique properties and has been the subject of much attention. Of particular interest have been the effects of phase transitions on water in confined systems, structure of water and ice in nanopores [1,2,3] and dynamical properties of water in one-dimensional pores considered as a model of water channels [4,5]

Structure of water in nanopores has not been as fully explored as that of bulk water. There are at least 13 ice polymorphs of bulk water. The phase diagram of ice exhibits many different crystal forms depending on local molecular correlations that influence the ordered arrangement of hydrogen-bonded configuration. In addition to these stable structures there also a number of metastable states, which depend on less ordered hydrogen-bond arrangements. The inter-relation of these various structures has been a source of difficulties in establishing the complex behavior of the solid state of confinement water.

We experimental studies of melting transition for D_2O water confined in opened double wall carbon nanotubes (DWNT) of average inner diameter of 2,4 nm. (average external diameter: of 7 nm) produced by NANOCYL Belgium, using differential scanning calorimetry (DSC) and dielectric relaxation spectroscopy (DRS) The structure of the confined ice was determined by the neutron diffraction experiment (ND). Because D_2O water is typically used in neutron scattering to avoid the complications of incoherent scattering and inelasticity corrections that arise when H_2O is used, D_2O water for used in each experiments .

In our experiments we used the DWNT sample, which were heated to about 400K and kept under vacuum (10^{-3} torr) for a few days to remove the air prior to and during the introduction of D_2O (100% deuterium) purchased from Sigma.

DSC measurements. The melting temperatures were determined from the position of the peaks of the heat flow signals on heating and were reproducible to within 0,5K. DSC scan corresponding to the melting of D_2O water in DWNT is presented at Fig.1a. The large endothermic peak at 276.9K corresponds to the melting of the bulk D_2O water in which DWNT are suspended, so the pores are fully filed. In addition, a second peak at 271,4 K is observed, which can correspond to the melting of D_2O water in the DWNTs; the melting temperature of D_20 adsorbed in DWNT is shifted towards lower temperatures by about 5.5 K relative to that of the bulk water.

Neutron Diffraction experiments have been performed at DN-2 A sample in vanadium container (with diameter 5mm , height 15mm) was cooled to about 100 K and then warmed to 300 K. Structure refinement was carried out using FullProf program based on the multi-phase Rietveld analysis method. At Fig.2 the neutron diffraction spectra at temperatures 280K, 276K and 220K during a warming cycle for D_2O water encapsulated in DWNT and the results of Rietveld refinements are presented. At temperature 276K, slightly lower than the bulk D_2O water melting point but higher than the pore melting temperature, the neutron diffraction spectrum is typical for hexagonal ice (Ih) with the space group P63/mmc. The characteristic triplet of hexagonal ice is clearly visible at 3.44, 3.66, 3.89 Å, with additional single peaks at the positions: 1.47, 1,72, 2.25, 2.67. At lower temperature, below the pore melting point there is a broader peak structure characteristic of the cubic ice (Ic) with the space group Fd3m, where the additional peaks at the positions: 1.04, 1,46, 1.83, 1,91, 3,67 Å are observed. At temperature 280K D_2O bulk and inside the pores are the liquid and at the neutron diffraction spectrum only the peaks from dry DWCN are visible.

Suppression of the crystal growth of ice in the cylindrical mesopores can be a vital factor for the formation and the stability of cubic ice, which is a more packed form of ice (coordinate number l =12) than the hexagonal ice (l =8). In carbon nanotubes with diameter 2.4 nm the existence of cubic form of ice can be also affected by similar reason.

The similar experiments performed for D_2O placed in mesoporous carbon CMK-3, which is the carbon replica of SBA-15 silica template with pore size of 3.8nm, have shown the existence of cubic and ice-IX crystal form of D_2O in pores, below the pore melting point.

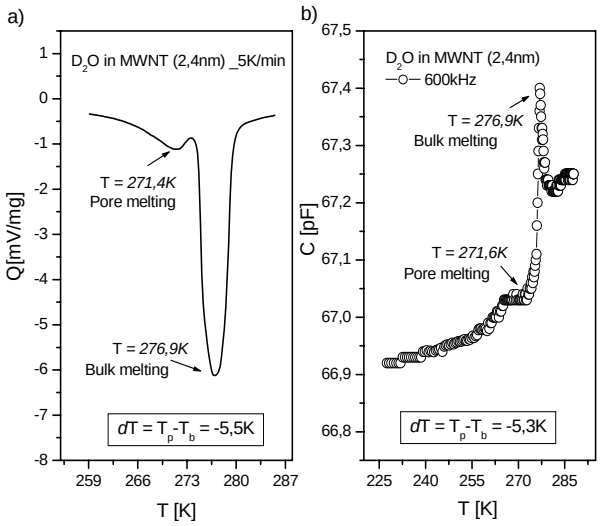

Fig.1, a) DSC scan for D_2O confined in DWNT, b) electric capacity C vs temperature for D_2O confined in DWNT. The melting temperature of D_2O water confined in DWNT is by 5.4K lower than of bulk water.

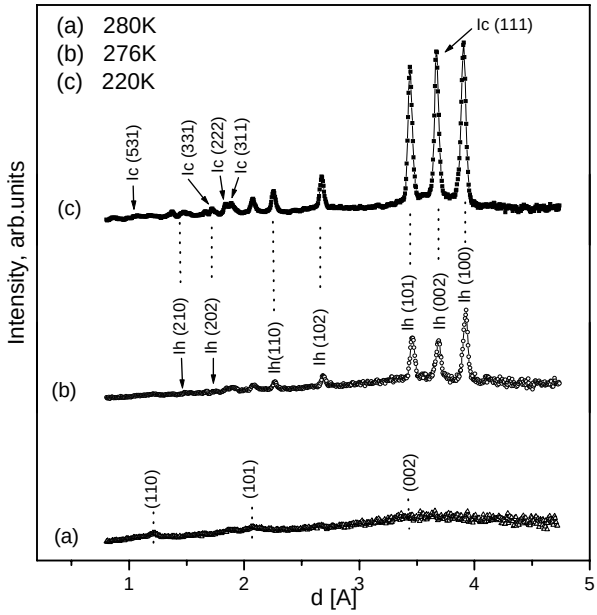

Fig.2 The diffraction pattern for D_2O in DWNT of 2,4nm diameter at temperatures: a).280K, b).276K and c).220K

1] A.Strilo, A.A. Chialvo, K.E. Gubbins and P.T.Cummings, *J.Chem.Phys.*, **122**, 234712
[2] A.I.Kolesnikov, J.M. Zanotti, C.K. Lonng, P.Thiyagarajan, A.P.Moravsky, R.O.Loufty and C.J. Burnham, Phys.Rev.Lett., 1999, 93, 035503
[3] H.Tanaka and K.Koga *J.Chem.Phys.*, 2005, **123**, 094706
[4] J.C.Dore, B. Webber and J.H.Strange, *Coll.Surf.Sci.A*, 2004, **241**, 191
[5] K.Matsuda, T.Hibi, H.Kadouaki, H.Kataura and Y.Maniwa, *Phys.Rev.B*, 2006, **74**, 073415

RESIDUAL STRAIN AND TEXTURE OF AN ANHYDRITE-DOLOMITE-SPECIMEN (CENTRAL ALPS)

Ch. Scheffzuek[a, c], K. Walther[a] , A. Frischbutter[b], R. Naumann[b], and I.V. Brovkin[c]
[a] *Freie Universitaet Berlin, FB Geowissenschaften, 12249 Berlin, Germany*
[b] *Helmholtz Centre Potsdam, GFZ German Research Centre for Geoscience, 14473 Potsdam, Germany*
[c] *Frank Laboratory of Neutron Physics, Joint Institute for Nuclear Research, 141 980 Dubna, Russia*

A rock composite, consisting of the minerals anhydrite and dolomite ("Zuckerdolomit") is known for special petrophysical behaviour. Frequently, it was observed, that Zuckerdolomit respond mountain releasing (mining, tunnelling) with a complete loss of cohesion within the grain structure. This behaviour may be of eminent importance, because operators as well as materials may be at risk of being buried. Zuckerdolomit is known inter alia from the central Alps between the Gotthard Massif and Leventina gneisses.

Intracrystalline strain measurements were carried out at the diffractometer EPSILON-MDS, texture was determined using the diffractometer SKAT (beamline 7A of the research reactor IBR-2, FLNP at JINR Dubna).

Measurements were carried out on a cylinder specimen (30 mm Ø, 60 mm in length). The rock was composed of ~55 % dolomite, ~36 % anhydrite, and <3% calcite.

A discriminating microstructural feature is the grain shape difference between its main components: Dolomite grains are bounded straight linear, often 120°-angular. The only rarely twinned dolomite has a grain size several orders lower than that of anhydrite. Furthermore, small marginal zones of deviating crystallographic orientation may be interpreted as strain-induced. In contrast, the anhydrite grains are arch-like (amoeboidic) bordered and interlocked among them, triggering a more explicit schistosed structure than typical for the dolomite layers. Relating to the sample's scale, foliation is parallel orientated to the plane of alternating stratification.

The crystallographic texture of anhydrite and dolomite was found to be fundamentally different. The dolomite (0001) pole figure is characterized by a split peak maximum near [y], girdle-like stretched over [z] and superimposed by a weak small circle structure. In contrast, the (010)-pole figure of anhydrite is characterized by a dominant maximum in [x], - girdle-like stretched parallel to the sample's (ss/s_x). The distribution intensity is much sharper than those for dolomite. The residual strain has been measured following a scan perpendicular to the foliation plane at seven points (a-g), see Fig. 1. In tendency anhydrite- and dolomite values seems to be contrarily aligned regarding dilatation and compression. Changes in composition between the different points of measurement are still disregarded.

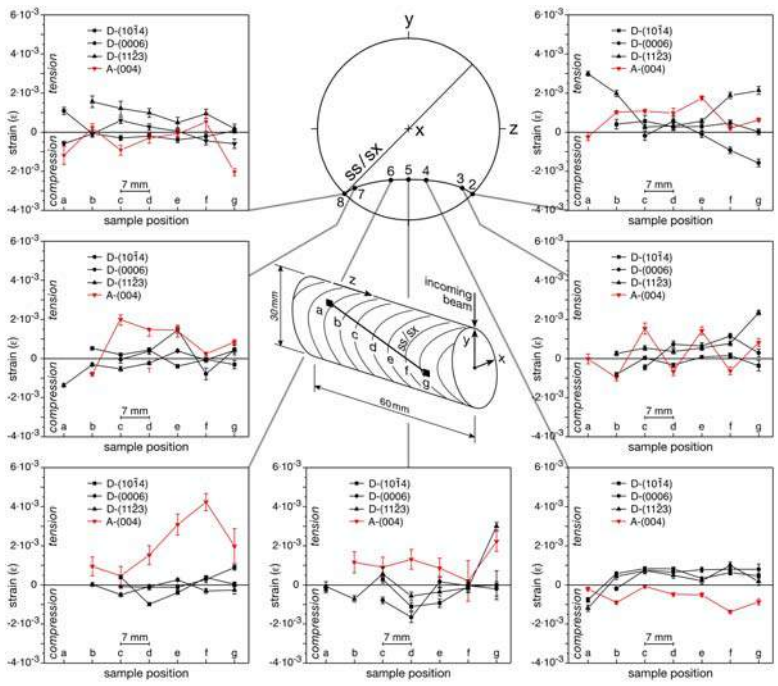

Fig. 1: Intracrystalline strain for three lattice planes of dolomite and one of anhydrite, measured for seven directions in relation to the sample's coordinate system and at seven points of measurements perpendicular to the sample's foliation trace.

In situ deformation experiments has been carried out at the same sample. All the observed lattice spacing of dolomite are characterised by a more or less continuous shift towards decreased spacing (increased compression of about $-0.4 \cdot 10^{-3}$ due for step by step load, Fig. 2). This tendency is not really interrupted up to the 17 days standstill period of the experiment. In contrast, the strain data for the

anhydrite lattice spacing are more varying. In particular, regarding the first steps of deformation we observed considerable variations of intracrystalline strain between dilatation and compression before we got strain values, comparable to those for the dolomite lattice spacing as we reached the period of experimental stop.

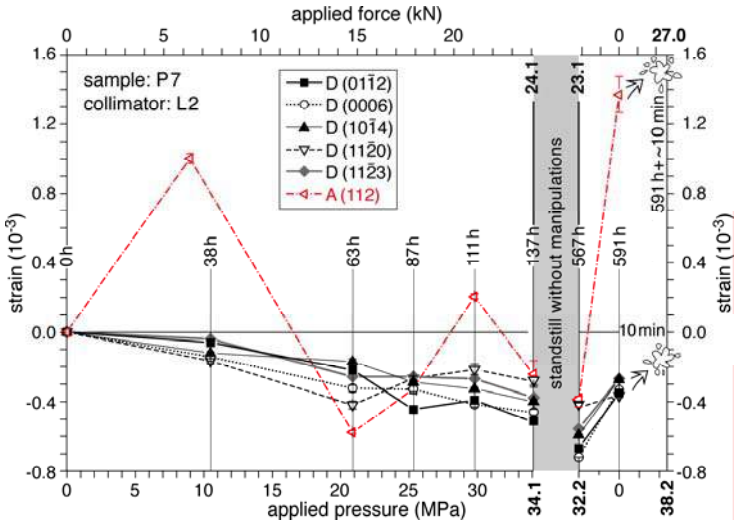

Figure 2: Strain-stress diagram for a 591h + 10min, uniaxial applied load (38 MPa) experiment on "Zuckerdolomit".

An oppositeness between strain evolution of dolomite and anhydrite, like to suggest from the results of the residual strain relations, may be possible but is not doubtless to indicate. Most interesting are the data, reflecting the evolution due to the state of interruption of the experiment: A clear increased compressive strain (of about $0.2 \cdot 10^{-3}$) for the value representing the first state after the 17 days interrupt (567 h) under unchanged experimental conditions (in the mean for dolomite lattice spacing more distinct than due to anhydrite) has been detected. However, this increasing compressive strain was combined with decreased stress (from 23.8 kN to 22.6 kN - deviatoric loading). Respecting this special state of the experiment there seems to be no significant differences due to the behaviour of the treated dolomite- and anhydrite lattice spacing. Next the sample was completely unloaded. The sample remained still intact (of course still within the pressure device) and was measured again within this state of deformation during an exposition time of 24 hours (591 h). Striking are the different effects of relaxation, comparing them regarding dolomite and anhydrite: For all the five lattice spacings of dolomite we got relatively uniform values of medium intensive decompression ($\sim 0.3 \cdot 10^{-3}$). For the anhydrite (112)-lattice spacing, however, we observed relatively strong dilatation ($\sim 1.7 \cdot 10^{-3}$). Starting from this state the experiment was continued increasing stress again. Finally the sample was loaded during 10 minutes up to the maximum stress state, reached at the end of the previous load cycle (34.1 MPa at 137 h). Only due to the attempt to add a further load of about 4 MPa the sample was destroyed in a moment (at about 38 MPa). These results make us to suppose, that the interaction between residual strain and texture of the main rock components may determine the special petrophysical behaviour of "Zuckerdolomit".

References

Scheffzuek, Ch.; Walther, K.; Frischbutter, A.; Naumann, R. & I.V. Brovkin (2008): *Z. geol. Wiss.* **36:** 39-60.

Ullemeyer, K.; Spalthoff, P.; Heinitz, J.; Isakov, N.N.; Nikitin, A.N. & Weber, K. (1998): *Nucl. Instr. Meth. Phys. Res.* **A 412:** 80-88.

Walther, K. (1991): *Textures & Microstructures* **14-18**: 251-256.

Walther, K.; Scheffzuek, C. & Frischbutter, A. (2000): *Physica B, Condensed Matter*, **276-278**: 130-131.

Walther, K.; Scheffzuek, Ch.; Frischbutter, A.; Naumann, R. & Brovkin, I.V. (2008): *Z. geol. Wiss.* **36:** 123-138.

АВТОКОРРЕЛЯЦИОННАЯ МИКРОДИНАМИКА ЖИДКОГО ЛИТИЯ И РАСПЛАВА ЛИТИЙ–ВОДОРОД: ИССЛЕДОВАНИЕ МЕТОДОМ НЕУПРУГОГО РАССЕЯНИЯ НЕЙТРОНОВ

Н.М. Благовещенский, А.Г. Новиков, В.В. Савостин

Государственный научный центр РФ – Физико-знергетический институт имени А.И. Лейпунского, 249034, Обнинск, Россия

Среди различных микродинамических характеристик вещества важное место занимает *автокорреляционная скоростная функция* (АКСФ), которая описывает корреляции между скоростями частицы в два различных момента времени. АКСФ является весьма широко обсуждаемой микродинамической характеристикой вещества. Это объясняется тем, что АКСФ, с одной стороны, доступна для теоретического расчета, а с другой стороны, представляет собой прямой результат при молекулярно-динамическом (МД) моделировании. АКСФ как функция времени определяется через спектр частот колебаний атомов $g(\omega)$ вещества следующим образом [1]:

$$\Psi_{ACVF}(t) = \frac{< V(0)V(t) >}{< V^2(0) >} = \int_0^\infty g(\omega)\frac{h\omega}{kT} cth(\frac{h\omega}{2kT})\cos(\omega t)d\omega \ . \qquad (1)$$

На рис. 1 показана АКСФ атомов жидкого лития при различных температурах. Видно, что при t > 0,12 пс атом «забывает» свою начальную скорость. Положение минимума автокорреляционной функции указывает характерное время нахождения атомов в режиме «ближайших соседей», а также позволяет определить доминирующую частоту колебаний атомов в жидкости, что делает возможной оценку средней энергии колебаний атомов исследуемой жидкости. Для сравнения на рис. 2 приведены АКСФ для жидкого лития при различных температурах, полученные в настоящей работе, и с помощью МД-моделирования [2] для близких по величине температур. Из рис. 2 видны три главных отличия эксперимента и расчета: во-первых, эксперимент демонстрирует заметно более слабую зависимость АКСФ от температуры, во-вторых, положение минимума АКСФ, полученных из экспериментальных данных, соответствует более высоким энергиям колебаний атомов жидкости, и, в-третьих, экспериментальные кривые имеют более глубокий минимум. Существование этих трех различий следует понимать как некоторую неадекватность потенциала межатомного взаимодействия, использованного при МД-моделировании.

На рис. 3 и 4 демонстрируются попытки описания АКСФ с помощью сравнительно простой аналитической модели: АКСФ представляется в виде суперпозиции одной или двух гармоник колебаний по формуле [3]:

$$\Psi(t) \sim \sum_{i=1}^{2} \exp(-\frac{t}{t_0})\cos(\frac{\varepsilon_i}{\hbar}t) \qquad (2)$$

Из приведенных рисунков видно, что использование суперпозиции двух гармоник позволяет добиться лучшего описания формы АКСФ по сравнению с использованием однокомпонентной модели. Величина t_0, получаемая при таком описании АКСФ, обычно трактуется как время жизни частицы в данном окружении, что иными словами может быть названо временем жизни окружения (временем структурной релаксации).

В современной теории жидкости принято считать, что процесс релаксации флуктуаций плотности включает в себя два механизма: быстрый, связанный с бинарными соударениями, и медленный, идущий через взаимодействие движения частицы с микродинамикой окружения [2]. Соответственно, предполагается, что существуют и два различных времени структурной релаксации, относящихся к быстрому и медленному процессам.

Использованная в данной работе методика обработки экспериментальных данных включает в себя разделение спектра рассеянных нейтронов на собственно неупругую и квазиупругую составляющие и их последующий раздельный анализ. В этой связи

анализируемые АКСФ не содержат в себе диффузионных эффектов, а носят чисто колебательную природу. На основании этих соображений можно предположить, что извлекаемое из анализа АКСФ время t_0 относится к быстрому (т.е. бинарному) процессу.

Различие частотных спектров для лития и водорода в расплаве лития [4], находит свое полное отражение и в форме АКСФ, показанных на рисунке 5. Разница времен релаксации в чистом литии и расплаве литий–водород свидетельствует о том, что ближайшее окружение в литии оказывается более долгоживущим, чем это имеет место в расплаве литий-водород.

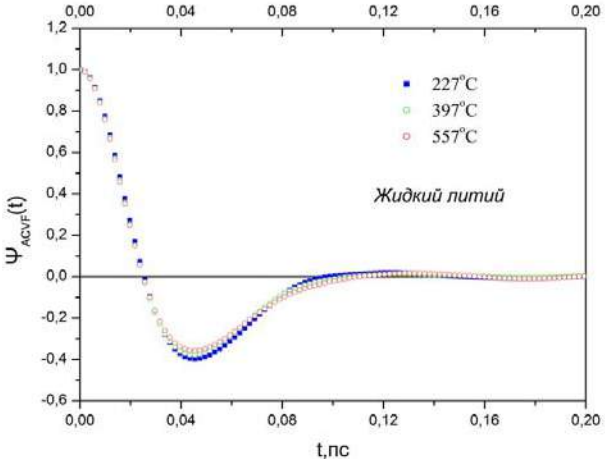

Рис. 1. АКСФ атомов жидкого лития при различных температурах.

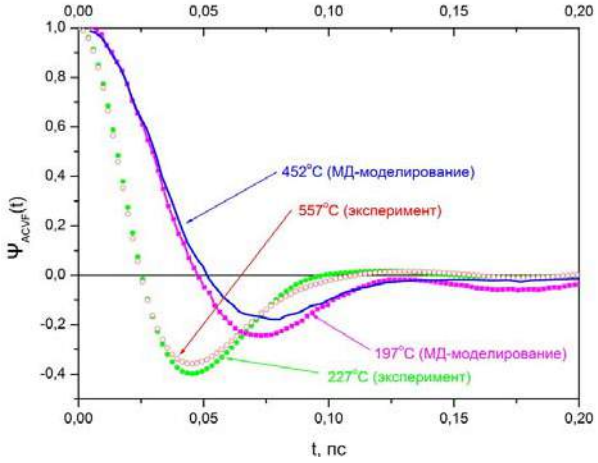

Рис. 2. АКСФ атомов жидкого лития в сравнении с результатами МД-моделирования для близких температур [2].

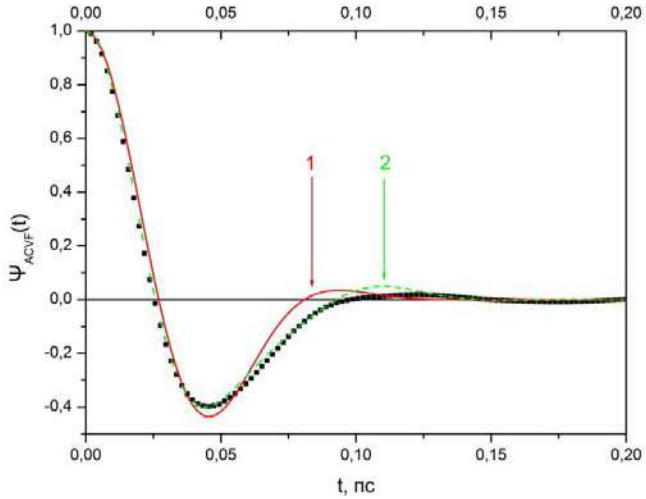

Рис. 3. Описание экспериментальной АКСФ при T = 227°C однокомпонентной моделью (2) – 1, и двухкомпонентной моделью (2) – 2: ε_1 = 35.1 мэВ, ε_2 = 66.3 мэВ, t_0 = 0.067 пс.

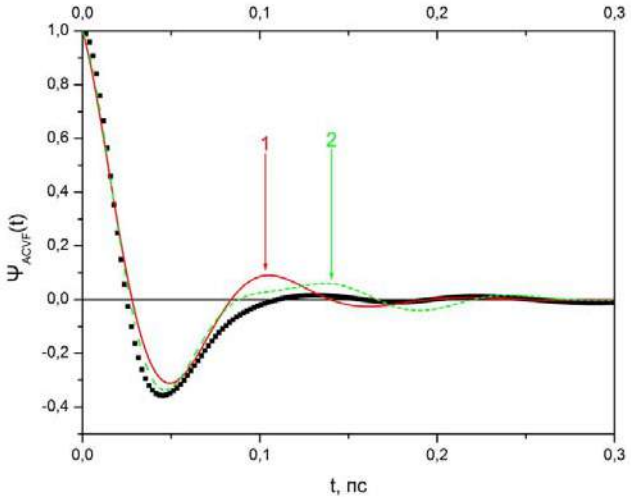

Рис. 4. Описание экспериментальной АКСФ при T = 557°C однокомпонентной моделью (2) – 1, и двухкомпонентной моделью (2) – 2: ε_1 = 32.7 мэВ, ε_2 = 52.5 мэВ, t_0 = 0.061 пс.

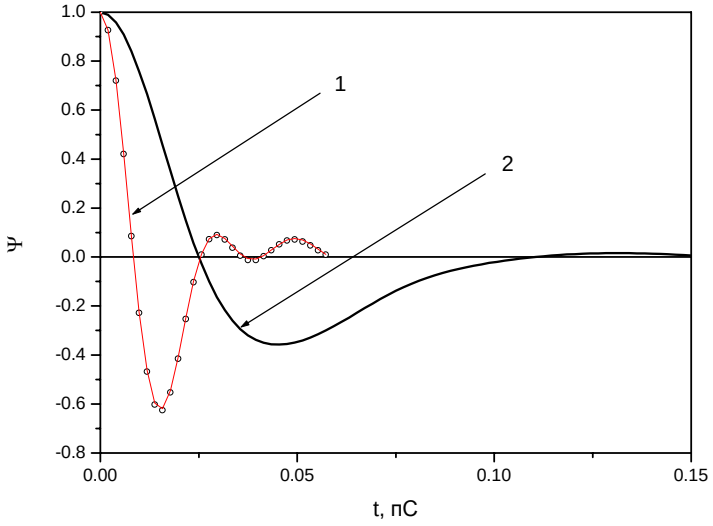

Рис. 5. Сравнение АКСФ для лития и водорода в расплаве литий–водород: 1 – водород, 2 – литий. T = 830 K.

Литература

1. Киттель Ч. Введение в физику твердого тела. М.: Наука, 1978.
2. Canales M., Gonzalez D., Gonzalez L., Alemany M., Gallego L. Density fluctuations and single-particle dynamics in liquid lithium. 2000, Phys. Rev. B, v. 62, p. 12095.
3. Sharma S.K., Tankeshwar K. Self-diffusion coefficients of expanded rubidium. J. Phys.: Condens. Matter, 1996, v. 8, p. 1089.
4. Благовещенский Н.М., Морозов В.А., Новиков А.Г., Пашнев М.А., Савостин В.В., Шимкевич А.Л. Изучение микродинамики жидкого лития и расплава литий–водород методом неупругого рассеяния нейтронов: Кристаллография.2007, т. 52(3), с. 498 – 504.

ELEMENTAL CONTENT OF INDIGENOUS BACTERIA UNDER DIFFERENT CROMIUM LOADINGS

M.V. Frontasyeva, S.F. Gundorina, T.M. Ostrovnaya, I. Zinicovscaia

FLNP JINR, e-mail: marina@nf.jinr.ru

N.Ya. Tsibakhashvili[1,2], L. Mosulishvili[1], E. Kirkesali[1], T. Kalabegishvili[1,2], S. Kerkenjia[2]

[1]*Andronikashvili Institute of Physics, Tbilisi, Georgia,*
[2]*Chavchavadze State University, Tbilisi, Georgia*

H-Y. Holman,

Lawrence Berkeley National Laboratory, Berkeley, California, USA

Introduction

Anthropogenic activity is a source of continual influx of heavy metal contamination into the environment. A complex variety of abiotic and biotic processes affects their speciation and distribution. Some of these processes can be applied to removing environmental pollutants. Indigenous bacteria can be successfully used to either detoxify or immobilize toxic heavy metals.

These bacteria are under continuous investigation, and in-depth molecular understanding has been developed for some of them. However, up to date the dependence between the ability of bacteria to reduce or immobilize metals and their elemental compositions is not clear yet.

This work is a continuation of our studies (Tsibakhashvili et al., 2004; 2006) where epithermal neutron activation analysis (ENAA) had been applied to study elemental content of Cr(VI)-reducer basalt-inhabiting bacteria.

In the present study the effect of Cr(VI) on the elemental content of these bacteria has been examined. Specifically, we tested three Gram-positive bacterial strains of *Arthrobacter* genera – *A. oxydans* (isolated in the USA from polluted Columbia basalt rocks), *Arthrobacter* sp. (61 B), and *A. globiformis* (151 B) (isolated from the most polluted regions in the Republic of Georgia).

Materials and Methods

Sample cultivation and preparation for analysis. The bacteria were grown aerobically in the following nutrient medium: 10 g of glucose, 10 g of peptone, 1 g of yeast extract, 2 g of caseic acid hydrolysate, 5 g of NaCl, and 1 liter of distilled water. To provide the chromium concentration of 35 and 200 mg/L, Cr(VI) [as K_2CrO_4] was added to the nutrient medium at an early stationary phase of growth.

After being cultivated for 4 days the cells were harvested by centrifugation (10,000 rpm, 15 min, 4 °C), rinsed twice in a 20 mM phosphate buffer and analyzed by NAA method.

To prepare bacterial samples for NAA, wet biomass was placed in an adsorption-condensation lyophilizer, dried, and pelletized to 5 mm pieces (~0.5 g) by means of titanium press form.

Instrumental Neutron Activation Analysis (INAA) at the reactor IBR-2. Bacterial samples of about 0.5 g were packed in aluminum cups for irradiation.

Samples were irradiated for 100 h and gamma-spectra of induced activity measured for 30 min – 2 hrs to provide sufficient counting statistics.

Quality assurance was achieved by relevant certified reference materials Lichen-336 and Bottom Sediments SDM-2T.

Results and discussions

The concentrations from 12 to 19 elements of the following set: Na, Al, Cl, K, Fe, Co, Zn, As, Br, Rb, Sr, Sb, Ba, Tb, Th, U was determined in the bacterial cells.

Data on chromium shows the high rate of Cr accumulation in tested bacterial cells (Fig. 1). The chromium content in the control cells was less than 10 μg/g, while the same values in the treated cells were much higher. For example, in *Arthrobacter* sp. it reached to $3 .10^3$ μg/g after exposure to 35 mg/L of Cr(VI) for 4 days. According to our recent studies (Codd et al., 2006; Tsibakhashvili, Kalabegishvili et al., 2008), reduction of Cr(VI) to Cr(III) begins at the surface of bacteria with the formation of Cr(V)-diols and the main part of reduced chromium (Cr(III hydroxide) is tightly bound to bacterial cells. Our current ENAA data provide evidence that one part of chromium penetrates inside cells as well.

Really, in bacteria treated with chromate some similarity in the behaviour of the following essential elements- potassium, sodium, chlorine was observed. First, exposure to Cr(VI) caused a lower potassium concentrations in cells and the decrease of K content was almost equal at both low (35 mg/L) and high (200 mg/L) concentrations of Cr(VI). Second, concentrations of sodium and chlorine changed in a parallel way to each other, but in an opposite way to that of potassium. Potassium is known to play an important role in maintaining cellular osmotic pressure; it is involved in nonspecific activation of many enzymes, in bacterial energy metabolism (as the coupling ion), and in the regulation of intracellular pH (Hoghes et al., 1989). Decrease of K content, in other words extrusion of K from cells to maintain the acidity of their cytosol, concomitant with increase of Na (and correspondingly Cl) content, suggests that, one part of Cr(V)-diols (as well as Cr(VI) ions (via HPO_4^{2-} channels)) were able to penetrate inside bacterial cells. NAA measurement of iron content in bacteria supports this conclusion. As is known, iron is the most important metal biologically (Hoghes et al., 1989). It is a many-functional constituent of complex molecules. Figure below demonstrates that in the tested bacteria the Fe content significantly increased in response to Cr(VI) loading, indicating that the bacterial protective system was activated significantly against chromium toxic impact.

In A. globiformis, contrary to A. oxydans and Arthrobacter sp, the content of iron increased almost linearly with increase of Cr(VI) dose. It seems that Cr(VI) transformation mechanism is rather different in *A. globiformis* than in *Arthrobacter oxydans* and *Arthrobacter* sp., that agrees with our recent data received by NAA and ESR (Tsibakhashvili N., Mosulishvili et al., 2008).

U, Rb, Nd, As were determined in all bacteria. These non-essential elements have no beneficial function and have to be considered by cells as toxins, however behaviour of some of them (for example, U) also illustrates that the permeability of bacterial cell wall changed after treatment with chromium.

References

Codd R., Lay P.A, Tsibakhashvili N.Ya., Kalabegishvili T.L., Murusidze I.G., Holman H.-Y. *J. Inorg. Biochem.*, Vol. 100, 2006, p. 1827.

Tsibakhashvili N., Mosulishvili L., Kalabegishvili T., Kirkesali E., Frontasyeva M.V., Pomjakushina E.V., Pavlov S.S., Holman H.-Y.N. *J. Radioanal. Nucl. Chem.*, Vol. 259, 2004, p. 527.

Hoghes M. N., Peele R. K. London. Metals and Microorganisms. Chapman and Hall, 1989.

Tsibakhashvili N., Frontasyeva M., Kirkesali E., Aksenova N., Kalabegishvili T., Murusidze I., Mosulishvili L., Holman H.-Y. *Analytical Chemistry*, Vol. 78, 2006, p. 6285.

Tsibakhahsvili N., Kalabegishvili T., Rcheulishvili A., Murusidze I., Kerkenjia S., Rcheulishvili O., Holman H.-Y. *Microbial Ecology* (2008) (accepted).

Tsibakhashvili N., Mosulishvili L., Kalabegishvili T., Kirkesali E., Murusidze I., Kerkenjia S., Frontasyeva M., Holman H.-Y. *J. Radioanal. Nucl. Chem.*, Vol. 278, 2008, p. 565

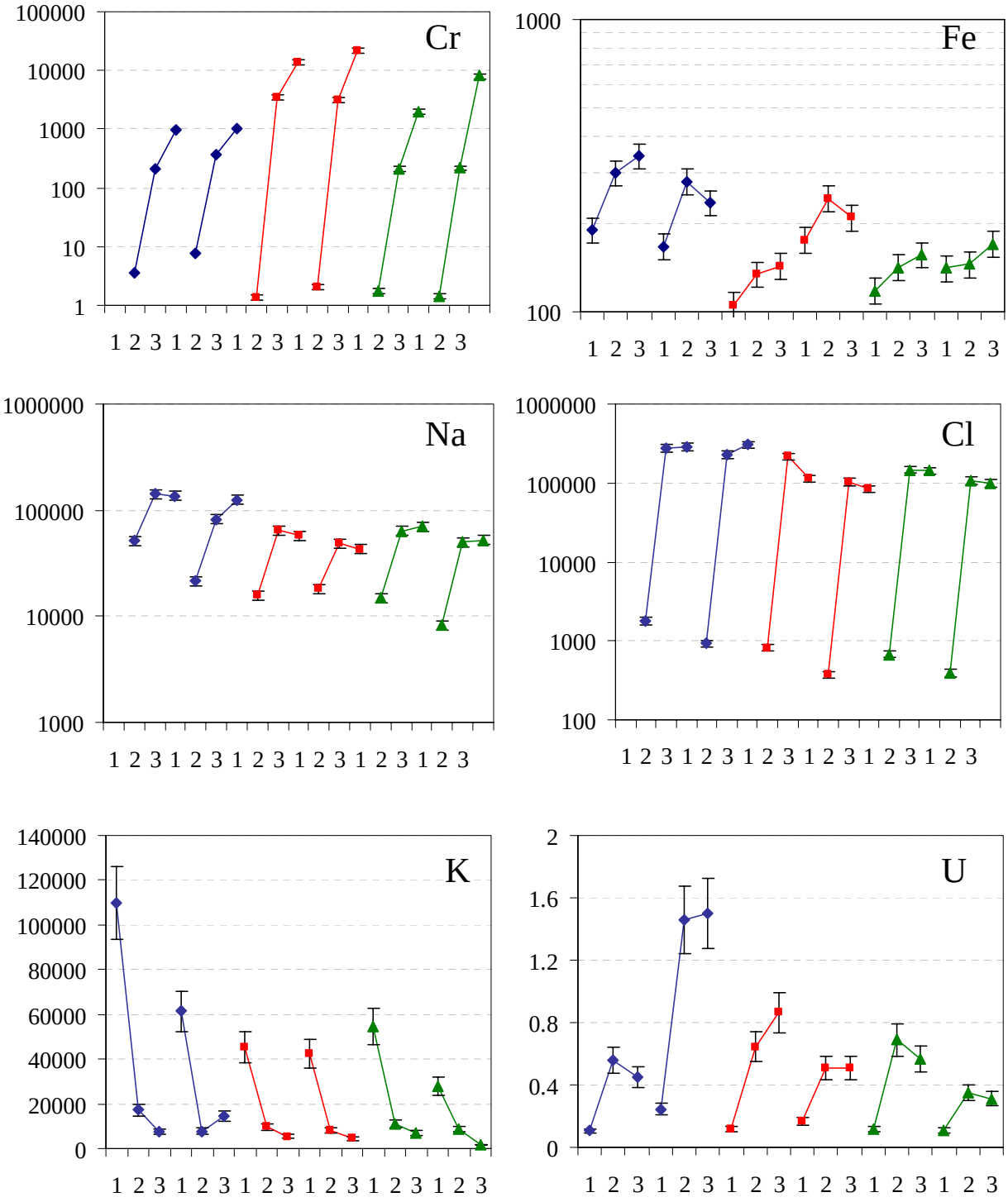

Figure: Concentration of chromium in different species of *Arthrobacter* und Cr(VI) loadings: 1 – control; 2 – 35 mg/L Cr(VI); 3 – 200 mg/L Cr(VI) and changing elemental concentrations of Fe, Na, Cl, K, and U (µg/g) in the same species as a response to Cr(VI) impact on bacterial cell wall permeability.

◆ *Arthrobacter oxydans*

■ *Artrobacter sp.* (61B)

▲ *Arthrobacter globiformis* (151B)

PRECISE APPROXIMATION OF SUMS OF EXPERIMENTAL RADIATIVE STRENGTH FUNCTIONS OF DIPOLE GAMMA-TRANSITIONS IN THE REGION $E_\gamma \approx B_n$ FOR THE ATOMIC MASSES $40 \le A \le 200$

Sukhovoj A.M., Furman W.I., Khitrov V.A.
FLNP JINR
E-mail: suchovoj@nf.jinr.ru

Introduction

It is known that the different types of nuclear excitations co-exist, interact and influence structure and parameters of a nucleus. There are quasiparticle and vibrational excitations. This is the main conclusion of models QPNM [1] and IBM [2]. But, the majority of experiments carried out by now gave direct and reliable information on structure of a nucleus only for too low excitation energy (see, for example, [3]). Strength functions of γ-transitions with energies E_γ, $k = f / A^{2/3} = \Gamma_{\lambda f} / E_\gamma^3 A^{2/3} D_\lambda$ after decay of levels $E_i < B_n$, were experimentally studied to the least degree. Main problems of experiment, which occur at determination of level density ρ and k consist in necessity to: (a) minimize the most serious systematical errors; (b) maximally exclude model notions, which are inevitable at extracting of the process parameters from registered spectra in indirect experiment. First of all, the latter refers to basic hypothesis [4] of independence of cross section of reverse reaction on excitation energy of final nucleus. According to calculation (see, for example, [5]), γ-transition probabilities below E_i ~3 MeV and experimental data [6] on cascade population of nuclear levels below $0.5B_n$, hypothesis [4] is completely inapplicable in even-even deformed nuclei.

The current status of problem

The task of experiment was first solved by registration [7] of two-step cascade intensities $I_{\gamma\gamma}$ with the summed energy 5-10 MeV proceeding between the decaying compound-state λ and a group of low-lying levels f. Analysis of two-step cascade intensities following thermal neutron capture in fixed ΔE energy intervals of their intermediate levels $E_i=B_n-E_1$ [8]:

$$I_{\gamma\gamma}(E_1) = \sum_{\lambda f} \sum_i \frac{\Gamma_{\lambda i}}{\Gamma_\lambda} \frac{\Gamma_{if}}{\Gamma_i} \qquad (1)$$

first revealed a possibility of model-free determination of ρ and k with high reliability. In variant [9] it was done at using hypothesis [4]. In the version [6] it is made without its use in region of low-lying levels ($E_i < 0.5B_n$). In order to calculate cascade intensities and compare them with the experiment, it is necessary to account for real specific of the studied process. In certain energy interval $\Delta E_j >> \rho_i^{-1}$ of excited levels there is only the value of $\Delta\Gamma_i$ (sum of partial radiative widths) available for comparison with calculation. For any interval number j of excitation energy, this sum may be always mathematically presented as a multiplication of certain average of partial width $<\Gamma_j>$ and $n_j = \rho\Delta E_j$ number of excited levels. So, equation (1) is transformed for any interval number j into:

$$I_{\gamma\gamma}(E_j) = \sum_{\lambda f} \frac{<\Gamma_j>}{\sum_k (<\Gamma_m> n_k)} n_j \frac{<\Gamma_l>}{\sum_m (<\Gamma_m> n_m)} \qquad (2)$$

Since this sum includes partial widths of γ-transitions between levels of different structure (see, for example, [5]), the average width of primary $<\Gamma_l>$ and secondary $<\Gamma_m>$ γ-transitions is an averagely weighted value for any j and i intervals in the indicated representation. It is determined by particular ratio of quasiparticle and phonon components of wave functions of the studied nucleus levels, belonging to interval ΔE_j. It is necessary to account for this at comparison of experimental and theoretical k values. System (2) includes N nonlinear

equations and ≈2N (or more) unknown parameters. So, it is impossible to determine ρ and k unambiguous values from (2) even if all available information on considered nucleus is used. However, it is possible to determine approximately or precisely interval of variation of the ρ and k values, setting given values of $I_{\gamma\gamma}$ and other parameters of given nucleus with the smallest χ^2. Corresponding experiments have been carried out at thermal neutron capture for 51 nuclei.

All practically applicable [10] models of radiative strength functions consider nucleus as a monocomponent object. Owing to the historically prevalent ideas, it is viewed as a system of Fermi-particles. Moreover, though model [11] considers nucleus only as Fermi-liquid, it reproduces a sets of parameters of the cascade gamma-decay process with better accuracy than it can be made by the simplest extrapolation [12] of cross section of reverse reaction into the region of nucleus excitation below B_n. By this reason, it is appropriate to use the notions [11] as basic in the performed analysis, because they are based on the most realistic idea about nucleus produced by theorists by now. A fraction of levels with purely dominating vibration components of wave functions (at least lower than ~$0.5B_n$) is very significant But, the existing and used [10] models of radiative strength functions do not completely account this fact. Therefore, at this stage of the analysis it is necessary to postulate the contribution of the vibrational nucleus excitations into *k(E1)+k(M1)* values in a purely phenomenological way. Below it is accepted that for a spherical nucleus fraction F_f of partial radiative width of dipole primary gamma-transitions with energy E_γ, specified by the quasiparticle excitations, is described by model [11] with two free parameters: κ and w. For the deformed one - by sum of two Lorenz curves, respectively. Fraction F_b, supposedly connected with the vibrational nucleus excitations, is approximated by peak, shape of which is preset by two exponential functions: $Pexp(\alpha\ (E-E_p))$, $Pexp(\beta\ (E_p-E))$ for its low and high energy tails:

$$k(E1,E_\gamma)+k(M1,E_\gamma)=F_f+F_b:$$
$$F_f = w\frac{1}{3\pi^2\hbar^2c^2A^{2/3}}\frac{0.7\sigma_G\Gamma_G^2(E_\gamma^2+\kappa 4\pi^2T^2)}{E_G(E_\gamma^2-E_G^2)^2} \qquad (4)$$
$$F_b = P\exp(\alpha(E_\gamma-E_p))+P\exp(\beta(E_p-E_\gamma))$$

Exponential dependence of form of its peaks F_b successfully describes all the data obtained by the present. Parameter κ in (4) accounts for possible change in nucleus thermodynamic temperature T in form $T^2=\kappa U/a$, whereas parameter w - net effect of changing in fraction ratio of quasiparticle and vibration types level density, both in the region of neutron resonances, and intermediate ($E_i<B_n$) levels of nucleus. Or it considers the fact of changing in ratio of quasiparticle and vibtation components in the normalization of wave functions of decaying and excited levels, respectively. Such conclusion follows from the strong anticorrelation of amplitudes of local peaks in the experimental data on *k(E1)+k(M1)* and their uninterrupted distribution (approximated by function F_f). In [9] *k(E1)+k(M1)* and ρ values are simultaneously determined from cascade intensities with a noticeable systematical error. First of all, the approximation of the experimental values of *k(E1)+k(M1)* sums from [6] is used in the analysis. The results are presented in figs.1-3 for the main part of the studied by the present nuclei. The value of the w parameter is to a greater or lesser extent determined by the structure of the wave function of neutron resonance. This conclusion follows from well established by theory the laws of nuclear states fragmentation which determine the type and value of compound state wave function components. This implies that the w parameter may change from resonance to resonance and, probably, correlate with values of their reduced neutron widths.

Conclusions

By the present the most reliable systematical experimental data on sums of the radiative strength functions of dipole cascade gamma-transitions following thermal neutrons capture may be approximated in the frames of the experiment uncertain in the 0.5 <E_1 <B_n-0.5 MeV region by a superposition of two components having rather different form of the dependence on energy

of gamma-transition. At the present they may be interpreted only as a contribution of fermion and boson nucleus excitations into the partial radiative width, respectively. Noticeable variation of the obtained parameters of $k(E1)+k(M1)=F(E_1)$ dependence in nuclei of different masses may be caused by strong influence of the structure of cascade initial level on the correlation of contributions of nuclear normal and superfluid states into the probability of gamma-quanta emission. This effect appears as an addition to the observed in [6] strong influence of the intermediate level structure on this value. Correspondingly, the radiative strength functions of primary gamma-transitions following decay of compound states may be determined by the structure of levels connected by them at least up to the energy of neutron binding.

References:

[1] *Soloviev V.G.* Theory of atomic Nuclei: Quasiparticles and Phonons. Bristol, 1992.
[2] *Iachello F. and Arima A.*, The Interacting Boson Model. Cambridge, 1987.
[3] *Bondarenko V.* et all, //Nucl. Phys. A762, 167. (2005).
[4] *Bohr A., Mottelson B.R*, Nuclear structure, Vol. 1 -W.A. Benjamin, Inc. New York, 1969.
[5] *Solov'ev V.G., Sushkov A.V., Shirikova N.Yu.*, Part. and Nucl., 27(6), 1661 (1996).
[6] *Sukhovoj A.M,. Khitrov V.A.*, Physics of Paricl. and Nuclei, 36(4), 359 (2005).
[7] *Boneva S.T* .et. al., Sov. J. Part. Nucl., 22(2), 232 (1991).
Boneva S.T. et al., Sov. J. Part. Nucl., 22(6), 698 (1991).
[8] *Boneva S.T., Khitrov V.A., Sukhovoj A.M.*, Nucl. Phys. A589, 293 (1995).
[9] *Vasilieva E.V., Sukhovoj A.M., Khitrov V.A.*, Phys. At. Nucl., 64(2), 153 (2001).
[10] Reference Input Parameter Library RIPL-2. http://www-nds.iaea.or.at/ripl2.
[11] *Kadmensky S.G., Markushev V.P.,.Furman W.I.*, Sov. J .Nucl. Phys., 37, 165 (1983).
[12] *Axel P.*, Phys. Rev., 126(2), 671 (1962).

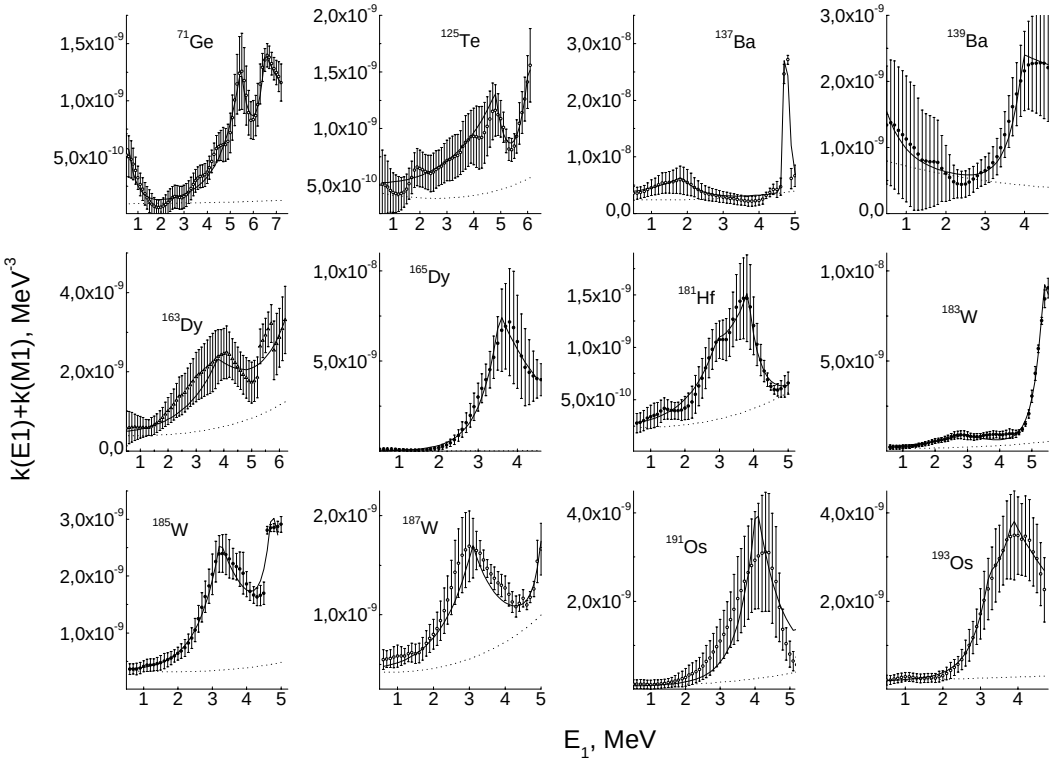

Fig. 1. Points with errors --the most probable values of sums of radiative strength functions and interval of their values, corresponding to minimum values χ^2 for even-odd compound nuclei. Open points -- data from [8], full ones – from [6]. Line -- the best fitting. Dots - component corresponding to F_f.

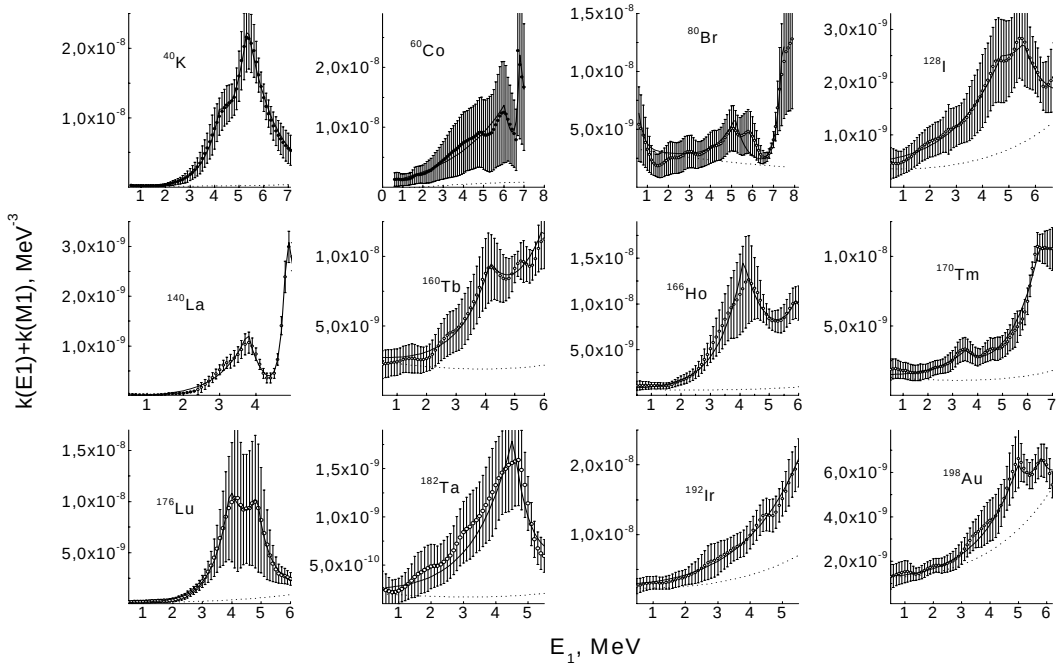

Fig. 2. The same, as in Fig.1, for odd-odd nuclei.

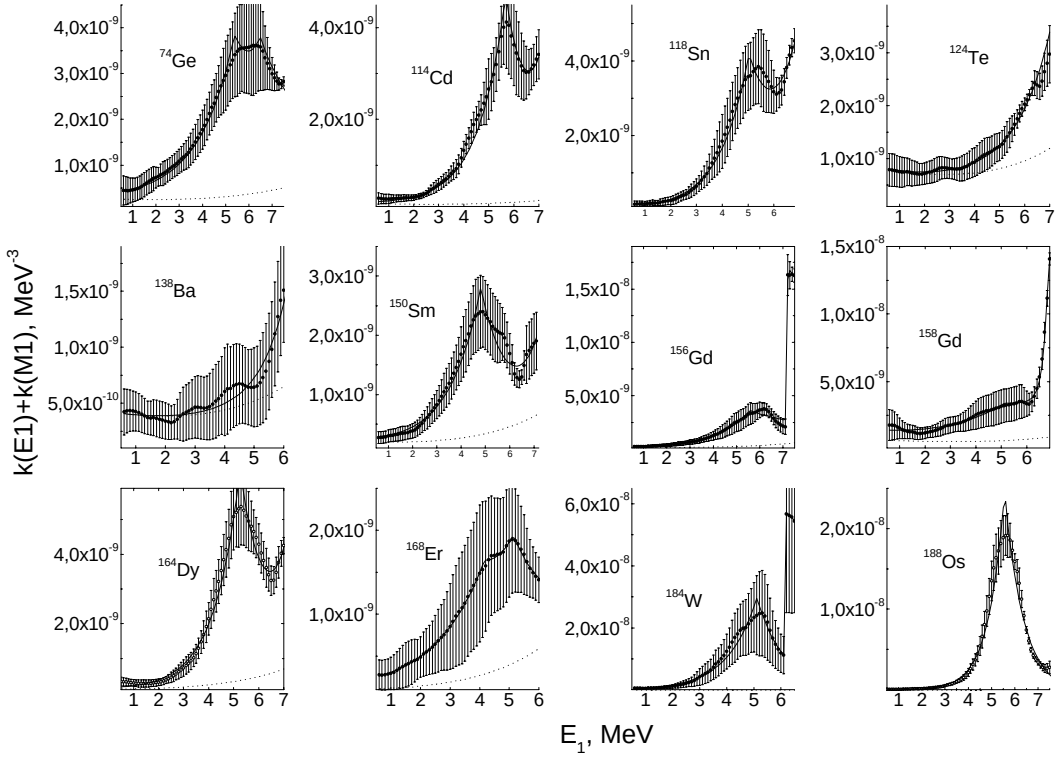

Fig. 3. The same, as in Fig.1, for even-even nuclei.

Epithermal NAA for marine geoecology

C. Cristache[a], O. Culicov[*,b], M. Toma[a], M.V. Frontasyeva[b], S.S. Pavlov[b], O.G. Duliu[c], G. Oaie[d]

[a] *Horia Hulubei National Institute for Physics and Nuclear Engineering, Magurele, Romania*
[b] *Joint Institute for Nuclear Research, Dubna, Russia*
[c] *University of Bucharest, Romania*
[d] *National Institute of Marine Geoecology and Geology, Bucharest, Romania*
[*] *National Institute for Research and Development in Electrical Engineering, Bucharest, Romania*

The Black Sea represents a remnant of the Mesozoic Tethys Ocean. A continuous layer of almost biologically dead water saturated with dissolved hydrogen sulfide is found between 180 m beyond sea level and the deepest bottom of 2,210 m. Only some anaerobic bacteria inhabit this medium, and for this reason, bottom sediments are completely voided of bioturbation that makes them ideal object for various stratigraphic investigations.

Some of the largest European rivers such as the Danube, Dnieper and Don via the Sea of Azov, flow into the Black Sea, carrying a considerable amount of pollutants, collected from industrial countries [1]. Both atmospheric nuclear weapon tests and the Chernobyl accident released into atmosphere a considerable amount of the radioactive ^{137}Cs which presence in sediments, due to its half-life of 30.4 years represents suitable marker for a recent absolute geochronology [2]. Thus the investigation of the vertical distribution of pollutants in correlation with the ^{137}Cs profile in sediments [3] could be very useful in reconstructing the history of pollution process affecting the Black Sea.

Sediments. The unconsolidated sediment core (a total length of 50 cm) has been collected from the abiotic zone of the Romanian Continental Shelf of the Black Sea, in the vicinity of the town of Constanta, at depth of 600 m below sea level. A digital radiography showed the presence of about 265 distinct layers, 1 to 3 mm thickness. For further investigations, the core was sliced into 45 fragments which thickness gradually increased from 5 mm at the surface to 4 cm at the bottom. Each section was dried at 105 ºC, ground and homogenized. The vertical distribution of five potential pollutants Zn, As, Br, Sn and Sb as well as Sc as a reference natural element in the core collected from the abiotic zone of the Black Sea was examined along with the ^{137}Cs content.

ENAA measurements. An amount of about 0.100 g of bottom sediment material was used for multi-element epithermal NAA carried out at the reactor IBR-2, FLNP, JINR, Dubna. Experimental procedure is described elsewhere [4]. Software developed at FLNP was used for acquisition and processing of gamma spectra of induced activity [5]. Quality assurance was provided by using IAEA standard reference materials SL-1, SL-3, and Sl-7.

^{137}Cs measurements. The ^{137}Cs activity of the uppermost 20 samples were measured at Horia Hulubei National Institute of Physics and Nuclear Engineering -Bucharest for 20 h, using a HPGe detector (Canberra) with a FWHM of 1.9 keV at ^{60}Co 1332 keV and a relative efficiency of 30%. Standard PC software OS2/Gennie for gamma spectra processing was used.

^{137}Cs vertical profile. Radiocesium vertical profile showed two maxima, one of them vas very sharp and localized at a depth of 1 cm and the other very broad, almost undistinguished at about 8 cm depth. As the two major radiocesium aerial pollutions took place in 1963 (atmospheric nuclear bombs tests) and 1986 (Chernobyl accident) and by taking into account

the existence of a vertical migration of Cs ions in sediments, one could conclude that the upper maximum corresponds to the 1986 Chernobyl accident. As the core has been collected in 2004, a sedimentation rate could be assessed as ~ 0.5 mm/year.

To be unambiguously considered as a pollutant, a potentially harmful compound must fulfill two criteria: (i) to exceed the legal limits, and (ii) to present an increased concentration near the sediment surface [6]. Only five of 45 determined elements follow these criteria. The results for these elements are given in the Table.

Table. Max (C_{max}), min (C_{min}), UCC (Upper Continental Crust), normal (C_{norm}); min ($C_{alert,min}$) and max ($C_{alert,max}$) alert concentrations (μg/kg)

Element	C_{max}	C_{min}	UCC [6]	C_{norm} [7]	$C_{alert,min}$ [7]	$C_{alert,\ max}$ [7]
Zn	145	53	71	100	300	700
As	16	8	1.5	5	15	25
Br	149	52	–	50	100	100
Sn	4.8	2.1	5.5	20	35	100
Sb	7.8	1.4	0.2	5	12.5	20

Heavy elements vertical profile. To exclude influence of mineral component of sediments, the concentrations of elements in question were normalized to the relevant Sc concentration considered as a naturally occurred element [8]. The distributions of these ratios along the vertical profile of the core are presented in Fig. 1.

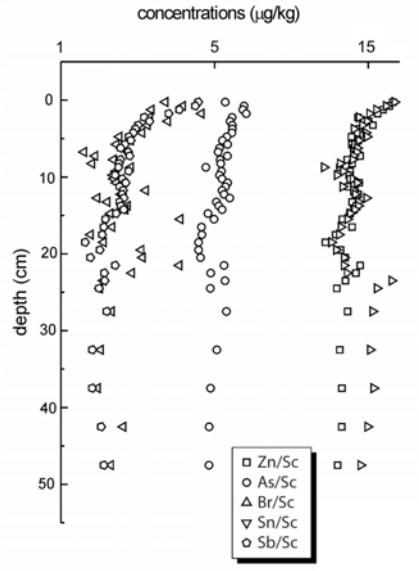

Fig. 1. The vertical distributions of concentrations of Zn, As, Br, Sn and Sb normalized to Sc

It is obviously seen that all of them demonstrate a sharp increase in the concentration range corresponding to the last 5–6 cm below the sediment surface. Taking into account the sedimentation rate discussed above, this interval could be attributed to the last 90–100 years, *i.e.* to the period of rapid industrialization of the European countries.

It should be pointed out that in case of Sn and As, their maximal concentrations are observed at 1 cm below the sediment surface that roughly corresponds to the year of 1990, while the concentrations of other three elements monotonously increases up to the sediment surface. Thus the first criterion is fulfilled for all five elements.

A box and whisker diagram for both average and extreme numerical values of the elemental concentrations is given in Fig.2. It follows from the analysis of the data collection that none of the elemental concentrations reached the intervention threshold. The normal concentrations of Zn, As, Br and Sb are slightly transcended, while the minimal alert concentrations are surpassed only in few cases by As and Br. Therefore, only As and Br satisfy the second criterion. The increased concentration of halogen Br is hardly be attributed to any pollution process, but most probably to its “marine” origin” [9].

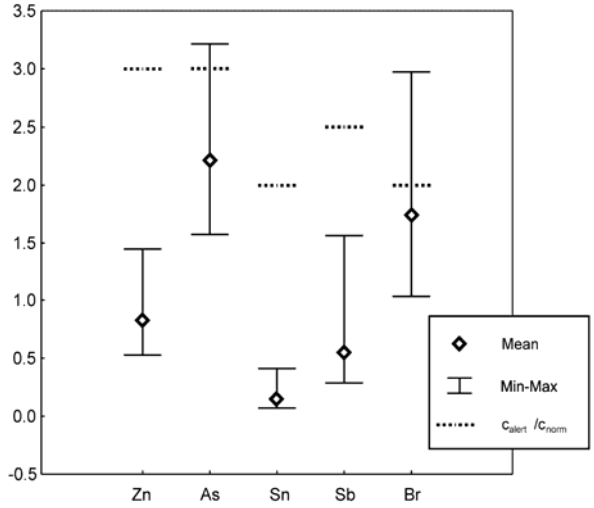

Fig. 2. Box and whiskers diagram for experimental and literature data set

This figure represents the maxim, minimum as well as the average concentrations of considered elements along the entire core. The concentrations of each element were normalized to their normal concentrations taken from [7].

The same procedure we have used for the minimum alert concentrations which positions are marked by the dashed lines.

Correlation analysis applied to the obtained experimental data set revealed strong correlation between the following elements: Zn and Sb (0.97), As and Zn (0.79) and As and Sb (0.78).

This fact could be interpreted more rather by having a common source of pollution than having similar chemical properties.

Conclusion. Epithermal Neutron activation analysis was used to investigate the vertical distribution of the concentrations of potential polluting Zn, As, Br, and Sb in the upper 50 cm of the sediments collected 600 m below sea surface from abiotic zone of the Black Sea.
All these elements presented towards superior limit of sediments increased concentration that in the case of Zn, As and Sb were, in accordance with Romanian Environment Regulations, greater than the normal ones, elements concentrations reached the intervention threshold.
By using Chernobyl ^{137}Cs as time marker it was possible to establish that the region with increased concentrations corresponds to the last 100 years. *i.e.* the period of the steadily industrialization process in Europe.

Acknowledgement. The authors acknowledge the Protocol on Scientific and Technical Cooperation between the University of Bucharest and JINR, Dubna (Reg. No. 3863-4-2008/2010) and the grant of RFBR–Romanian Academy (Project No. 07-05-91681).

References

1. S. Reschke, V. Ittekkot, N. Panin. Estuarine, *Coast. Sci*, 54 (2002) 563.
2. R. A. Ligero, M. Barrera et al. *Env. Poll*., 118, (2002), 97.
3. W. Penington, R.S. Cambray, E.M. Fisher. *Natur*e, 242 (1973) 342.
4. M.V. Frontasyeva, S.S. Pavlov. In «Problems of Modern Physics». Edts: A.N. Sissakian, D.I. Trubetskov. Dubna, JINR, 1999, p. 152-158.
5. T.M. Ostrovnaya et al. In Activation Analysis in Environment Protection, D-14-93-325, Dubna (1993) 319-326.
6. S.R. Taylor, S.M. McLennan. The Continental Crust: Its Composition and Evolution. Geoscience Texts, Blackwell, Oxford, 1985.
7. Monitorul Oficial al Romaniei 303 bis, 1997, p. 23 (in Romanian).
8. L.C. Dinescu, O.G. Duliu, M.Badea, N.G. Mihailescu, I.M. Vanghelie, *J. Radioanal. Nucl. Chem.*, 238 (1998) 75.
9. E. Steinnes, M.V. Frontasyeva. *J. Radioanal. Nucl. Chem.*, 253 (2002)173-177.

HEAVY METALS AND REE IN BOTTOM SEDIMENTS AND DREISSENIDS OF THE RYBINSK RESERVOIR

Goryaynova Z.I., Pavlov D.F.*, Frontasyeva M.V.
FLNP JINR
**Institute of Inland Water Biology, Borok, Yaroslavskay province*

Introduction

The Rybinsk Reservoir, the largest artificial water body in Europe, is the main source of drinking water for the towns located along its cost-line. The greatest potential risk of environmental contamination to this man-made lake is posed by the town of Cherepovets with its steel producing plant, largest in Europe.

Bottom sediments represent a sink for suspended matter including organic and inorganic pollutants in the freshwater ecosystem. They are frequently used for determining the contamination level of the water ecosystem as well as for assessing risk of potential remobilization of pollutants into the ecosystem.

For biomonitoring purposes in the Rybinsk reservoir two species of bivalve mollusk (*Dreissena polymorpha* and *D. Bugensis)* were used. These mollusks are characterized by their sedentary life style, good filtration capacity and resistance to acute toxicity of pollutants (Klerks et al., 1997; Pavlov, Frontasyeva, 2005).

The aim of the study is first of all to determine chemical elements, including heavy metals and rare earth elements in tissues of the dreissenids and sediments in different compartments of the reservoir. This can make it possible to assess the contamination level of the reservoir as well as to evaluate the possibility of using dreissenids for monitoring fresh water ecosystems.

Methods and materials

Sampling was carried out from research ships of the Institute of Inland Water Biology in 2005-2006 at different areas of the reservoir. Sediment samples were collected using bottom sampler and dreissenids – using bottom drag.

Mollusk samples were frozen at -18^{o}C for further sample preparation. Mollusks were dissected into a soft part and a shell being preserved separetely.

Both sediment and mollusk specimens were dried at 40 C^{0} and then homogenized with the help of mortar and pastel. The specimens were packed into aluminum cups and polyethylene bags for long and short irradiation, respectively, and analyzed for elemental composition using instrumental epithermal neutron activation analysis (ENAA) at the IBR-2 reactor (JINR, Dubna).

Results and discussions

ENAA enabled identification of 31 elements in bottom sediments and zebra mussels.

Concentrations of such elements like scandium, vanadium, manganese, barium, lanthanum, samarium, hafnium, tantalum in the soft tissues of dreissenids differ insignificantly from those in the shell. La, Sm, Hf, Ta content in the soft tissues is no more than twice as much as their shell content, while Mg and Ba concentrations are a little higher in the shell. At the same time cobalt, nickel, zinc, selenium and bromine concentrations in the soft tissues are 1-2 orders of magnitude higher than those in the shell, while strontium and calcium contents in the shell substantially exceed those in the soft tissues (Fig. 1 and 2). The last observed phenomenon is explained by the fact that calcium is a bulk material for a mineral matrix of the shell and strontium actively replaces calcium in this tissue.

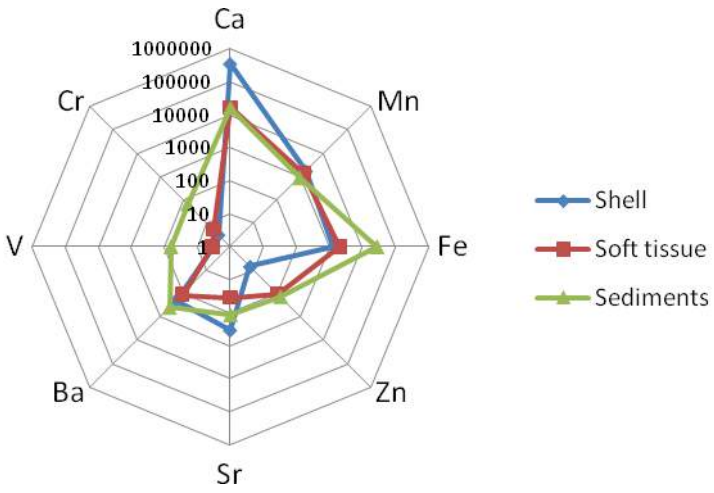

Fig. 1 Concentrations of some elements in the shell, soft tissue of the mollusks and bottom sediments

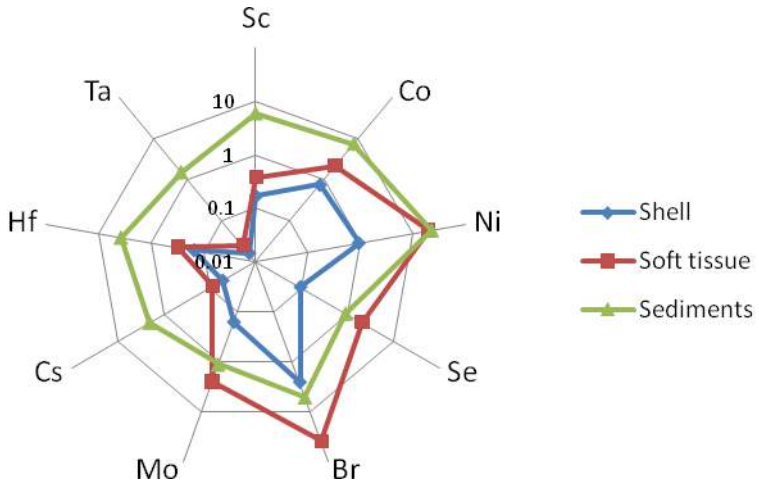

Fig. 2 Concentrations of some elements in the shell, soft tissue of the mollusks and bottom sediments

Bottom sediments concentrations for most elements are one order of magnitude higher than those in the soft tissues of the mollusks. The reverse pattern is observed for Ca, Co, Ni and Zn, whose concentrations in the soft tissues differ from those in the sediments insignificantly, while Se and Br concentrations are ten times higher in the soft tissues than in the sediments (Fig. 1 and 2). This means that most elements consumed by the mollusk are not accumulated, but cleared from its body (Wiesner et. al., 2001). Such elemental pattern also demonstrates physiological importance of the above-mentioned elements being not toxicants but essential macro and micro components for the mollusk organism. However, it is well known that under strong anthropogenic contamination microelements can accumulate in an organism in concentrations exceeding their physiological levels. In such conditions the organism cannot control the processes of element consumption and excretion. Thus it may be suggested that the high concentrations of Zn, Co, Ni in the mollusk body are explained by the influence of Cherepovets metallurgical complex.

No significant spatial differences were revealed in shell and soft tissue concentrations for the majority of heavy metals except for zinc and cobalt, whose concentrations in the shell and soft tissues sampled in close vicinity of Cherepovets exceed those from the other sampling points. Though absolute metal concentrations in soft tissues are higher than those in shells, the

latter reflects anthropogenic contamination much better. Trace metal content in the mollusk body depends very much on numerous varying extraneous and intrinsic factors. As the element turnover in the shell is much slower, the shell reflects long-term input trends.

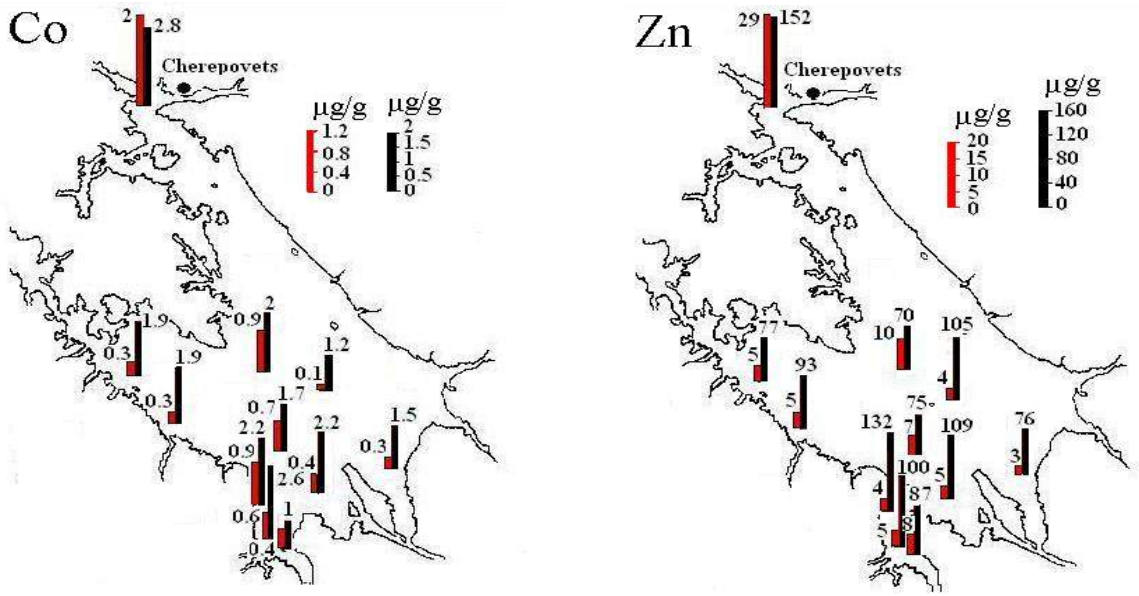

Fig 3. Spatial distribution of Co and Zn in the zebra mussel showing the element content in the soft tissue (left) and in the shell (right).

Conclusions

The results of our study confirmed that bottom sediments are reliable objects for monitoring heavy metals and rare earth elements in fresh water ecosystems. Mollusks and dreissenids, in particular, may serve as contamination indicators. Nonetheless, the shell composition reflects permanent source of anthropogenic pollution better than the soft tissue composition does. The feasibility of ENAA for freshwater monitoring has been shown.

References

Klerks, P.L., P.C Fraleigh, J.E. Lawniczak. Effects of the exotic Zebra Mussel (*Dreissena polymorpha*) on the metal cycling in Lake Erie. Can. J. Fish. Aquat. Sci. 1997, Vol. 54. P. 1630-1638.

Pavlov D. F., Frontasyeva M. V. Comparative chemical composition of two invasive dreissenids, *Dreissena polymorpha* and *D. bugensis* in the Rybinsk Reservoir (the Upper Volga basin, Russia) and assessment of invasion-related modification of exchange and balance of chemical elements in the reservoir ecosystem// Alien Species in Holarctic (Borok-2). Book of abstracts. Second Intern. Symp., Borok, Russia, 27 Sept. - 1 Oct. 2005, Rybinsk-Borok, 2005, P. 126-127.

Pavlov D. F. , Frontasyeva M. V. , Pavlov S. S., Pankratova Yu. Distribution of trace elements in freshwater ecosystem compartments of man-made Rybinsk Reservoir (Central Russia) using epithermal neutron activation analysis. Ovidius University Annals of Chemistry. 2005. 16. No 1, P. 72-75.

Wiesner L., Gŭnter B., Fenske C. Temporal and spatial variability in the heavy-metal content of *Dreissena polymorpha* (Pallas) (*Mollusca: Bivalvia*) from the Kleines Haff (northeastern Germany). Hydrobiologia, 2001, Vol. 443, No. 1-3, P. 137-145.

OPTIMIZATION OF A MODERATOR-NEUTRON GUIDE SYSTEM FOR SPECTROMETERS OF BEAM 7A OF THE IBR-2M REACTOR

Manoshin S.A.†, Belushkin A.V., Kulikov S.A., Shabalin E.P., and Zhuravlev V.V.
FLNP JINR
E-mail: † manoshin@nf.jinr.ru

Abstract

Introduction

At present, the IBR-2 reactor is shut down for modernization, which implies complete replacement of the reactor core, control and emergency units as well as the moderators. The building and biological shielding will remain unchanged. The optimization of the reactor core has been completed and the assembling is almost finished. The moderator complex has been configured and Monte Carlo simulations have been performed. Some of the spectrometers will be rebuilt and new ones will be constructed. The best utilization of neutrons provided by the complex of moderators in the existing biological shielding requires accurate simulation of all elements of the spectrometers. Two spectrometers are now situated at beam 7: SKAT (beam 7a) and NERA (beam 7b). It is shown in Fig. 1.

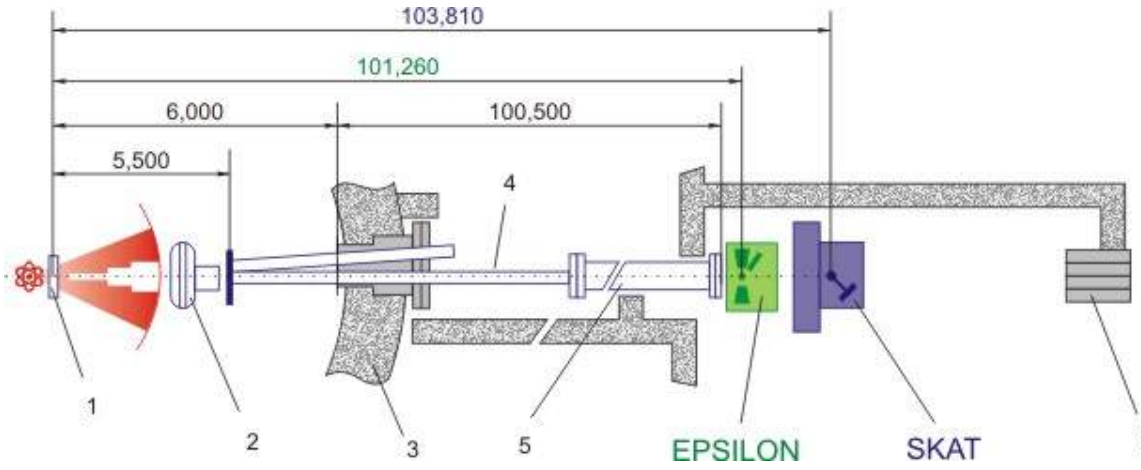

Fig. 1. Present layout of channel 7a of the IBR-2M reactor: 1 – moderator, 2 – background chopper, 3 – reactor building wall, 4 – old neutron guide (beam 7a), 5 – vacuum tube, 6 – beamstop for beam 7a.

New extraction system should be optimized according to the geometry of the ring corridor and beam hall of the IBR-2M reactor. It is planned that channel 7a will accommodate 2 neutron guides built in the separate vacuum chambers. Due to the constructive features of the ring corridor the minimal distance between the moderator and the guide entrance of channel 7 is around 6 m. Therefore, the attenuation of the neutron flux between the moderator and the guide entrance has to be minimized.

Methods and instruments

1. New moderators for beams 7, 8, 10, 11

The VITESS software package [5] has been used for simulations of channel 7a. The simulation of attenuation of the neutron beam was implemented in the VITESS software package [6, 7]. Three modules were modified: the modules “space”, “spacewindow” and “spacewindow multiple”. The detailed description of these modules can be found in the VITESS help file.

The modernized IBR-2M reactor will start its operation in 2010. At the first stage it will work with one cold moderator for beams 7, 8, 10, 11 and a common water grooved moderators for the others. The cold moderator for these beams consists of water pre-moderators, grooved water moderators and a cryogenic moderator based on a mixture of aromatic hydrocarbons (Fig.2 a,b). Optimal geometrical configuration of this complex has been chosen by the Monte Carlo simulations (MCNP code) [1]. The cold moderator (15 cm wide, 20 cm high) is situated in the bottom part of the reactor core (44 cm high) in a niche surrounded by water. Such a composition provides neutron spectrum in a wide range of energy. This gives more flexibility for optimization of instruments at neutron beams. The neutron spectrum has been calculated onto the virtual surface (Fig. 2b) situated at a distance of 15.2 cm from the point of intersection of axes of the former beams 7a and 7b of this direction. The energy distribution of neutrons at this plane is shown in Fig. 3.

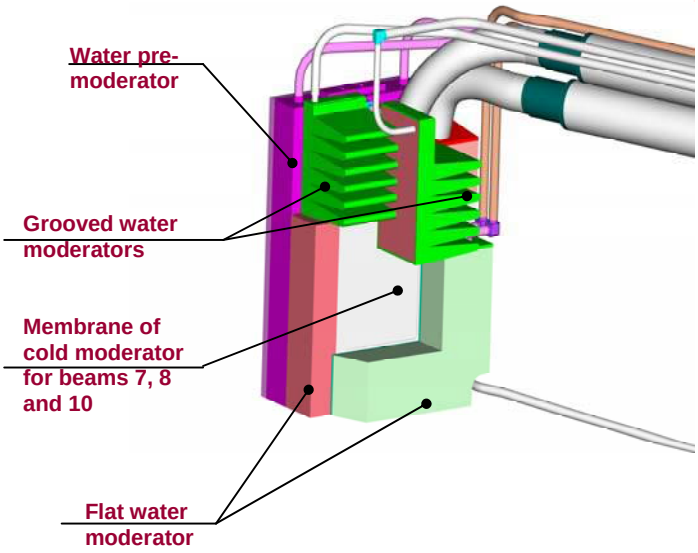

Fig 2.(a) View to the moderator from beam 7

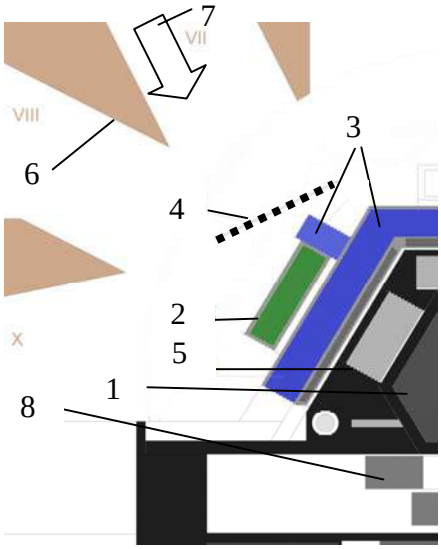

Fig 2.(b) A part of horizontal cut of the IBR-2M reactor with surroundings (1. Reactor core, 2. Cold moderator, 3. Water premoderator and grooved moderator, 4. Virtual plane for spectrum calculation, 5. Stationary reflector with control rods and emergency system, 6. Biological shielding, 7. Direction of view of beam 7, 8. Moveable reflectors)

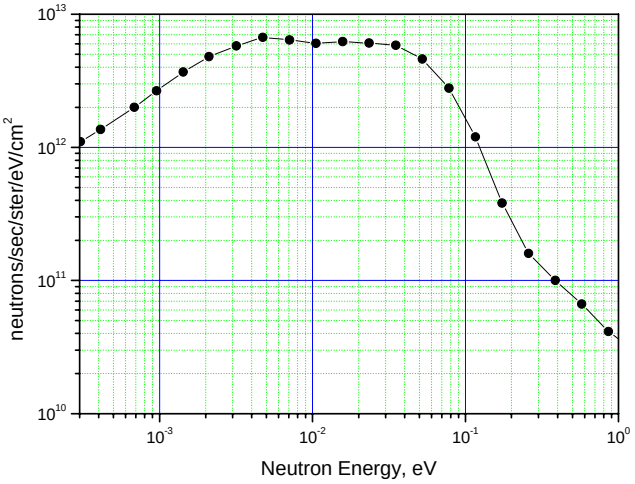

Fig. 3. The MCNP simulated spectral distribution of the neutron beam for channel 7 at the plane pos. 4 of Fig.2b at the average power of the IBR-2M reactor of 2 MW.

2. Neutron Guides of channel 7a, LAYOUT

The new channel 7a will consist of two neutron guides: 7a1 and 7a2. The first neutron guide will serve the spectrometer SKAT [2]; the second neutron guide will serve the spectrometer EPSILON [3]. The existing channel 7b serves the spectrometer NERA and is not considered in the paper. The length of each new neutron guide is about 100 m and consists of the following five parts:

1) Straight section of length 10.07 m.
2) Free space, 23.3 cm long for the second chopper.
3) Curved section of length 85 m and the radius of curvature of 13400 m
4) Straight section of length 9.61 m – for the first guide (EPSILON spectrometer) and 3.64 m – for the second guide (SKAT spectrometer).

The coating of all sections of both guides is natural nickel. The cross section of guides is rectangular and equal to 5 × 5 cm. The characteristic wavelength of the curved section is 1.6 Å for both guides and natural nickel coating. The last straight section decreases the inhomogeneity of the neutron beam at the exit of the neutron guide for neutrons with wavelengths of more than a critical wavelength of the curved section. The background chopper is installed between the moderators and the guides. The new second chopper will be installed as well. The basic configuration of the guides is presented in [4].

Another option of the geometry of the guides could be realized: the height of both guides 7a1 and 7a2 increases up to 9.5 cm to reduce the number of reflections inside the guides and makes it possible to achieve a 1.9 times increase in intensity at the guide exit.

The only difference between the new guides is the inclination angle of these guides relative to the axis of channel 7a: for the first guide, the inclination angle is 0.8°; for the second guide, the inclination angle is 1.65°. It is presented in Fig. 4.

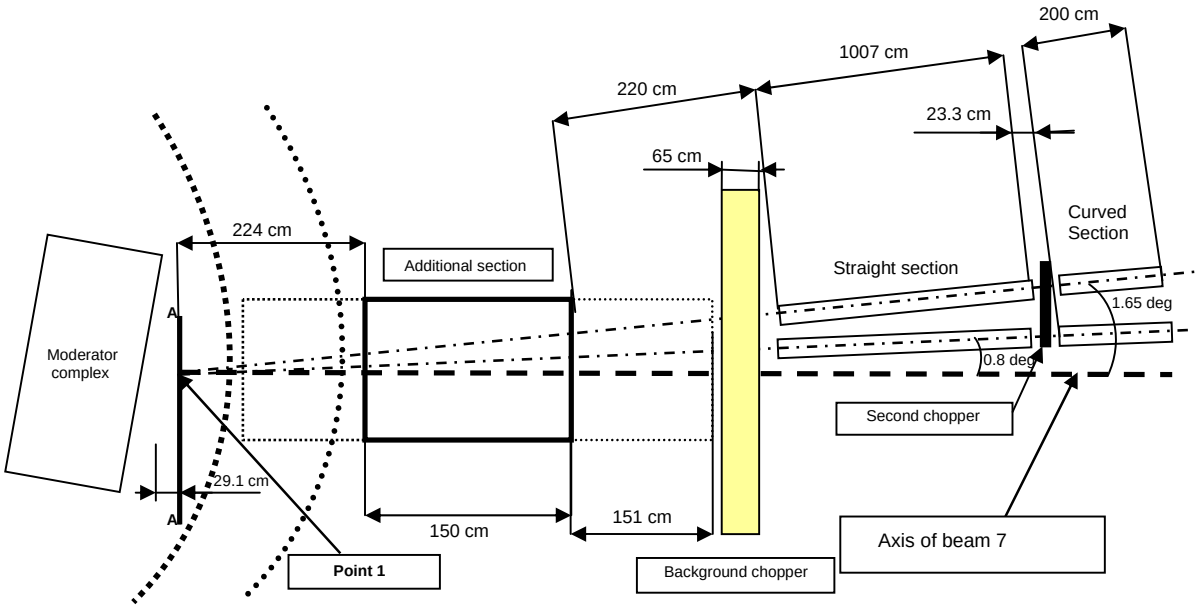

Fig. 4. Layout of the initial part of channel 7a. Point 1 is the crossing point of the axes of the **new** guides 7a1 and 7a2.

Results and discussions

1. Influences of an air gap between the moderator and the entrance of neutron guides and the extraction systems

The system with two guides described above was simulated by the VITESS software package. The count rates at the exit of the guides are presented in Figures 5 and 6. Three options were considered for channel 7a.

a) The real system, i.e. the attenuation of the neutron beam between the moderator and the entrance of neutron guides was simulated. The distance between the moderator and both neutron guides of channel 7a is 5.94 m.

b) An additional 1.5 m long section was installed between the moderator and neutron guides. This section was modeled by the polished stainless steel tube of 15 (width) × 18 (height) cm cross section. The length of the section was based on the geometry of the guide hall and the ring corridor. This section lies at a distance of 2.24 m from the crossing point of the guide central axis (see point 1 in Fig. 4). The distance between the moderator surface and point 1 is 29.1 cm.

c) Neither additional section nor an air gap was considered between the moderator and neutron guide, i.e. the idealized system.

The additional section is evacuated. Due to this, aluminum windows at the entrance and at the exit of the section were installed. The thickness of the windows was chosen to be 0.15 cm.

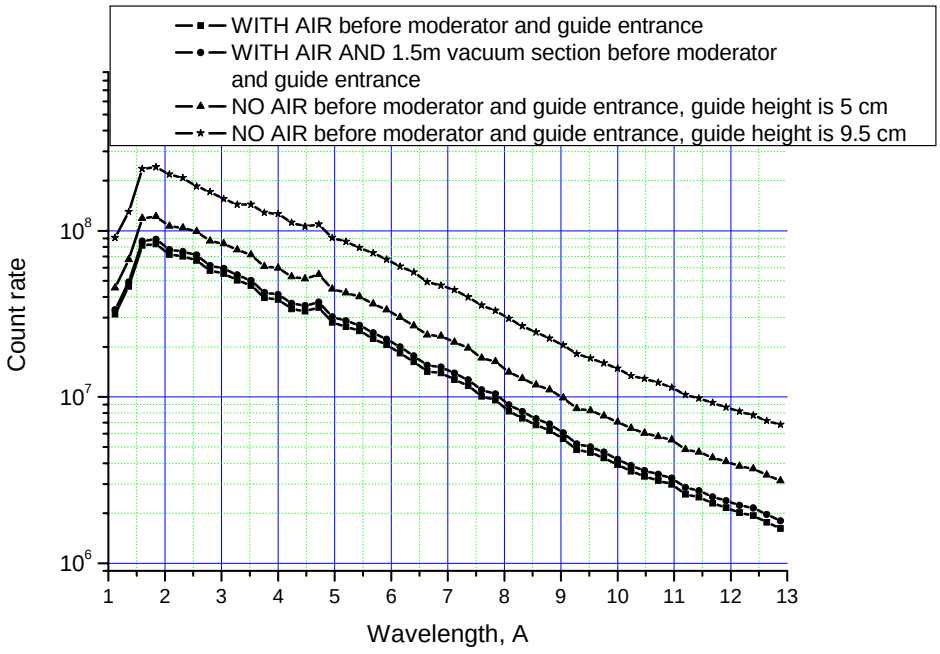

Fig. 5. Neutron count rate at the exit of the first guide for three kinds of the extraction system. If the guide height is 9.5 cm (instead of 5 cm), the shape of the curve is unchanged.

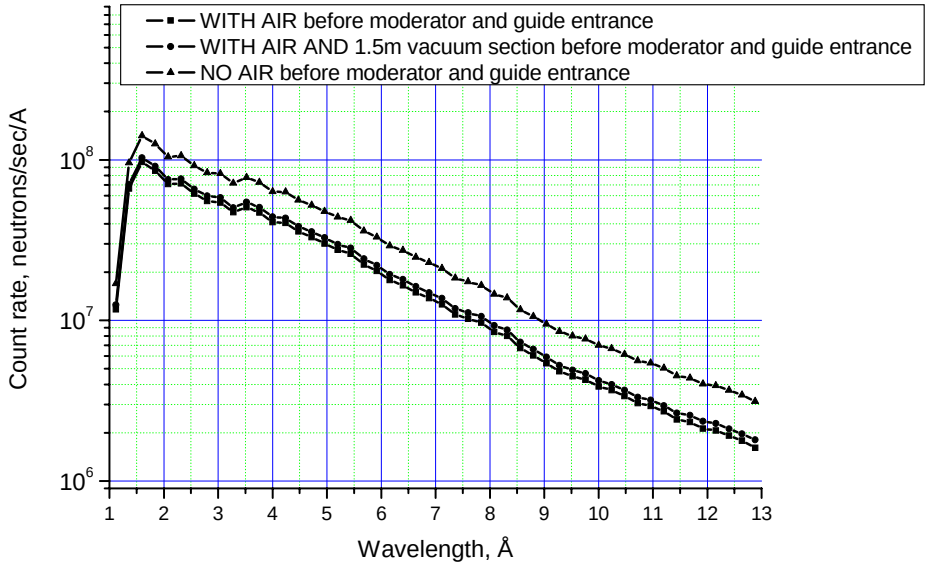

Fig. 6. Neutron count rate at the exit of the second guide for three kinds of the extraction system.

One could see that the count rate at the exit of the first guide is larger for wavelengths less than 1.25 Å. It can be explained taking into account small acceptance angles for such wavelengths despite different inclination angles of the guide axes. But a significant distance (around 6 m) between the moderator and the guides and the different inclination angle lead to the fact that for a larger inclination angle, i.e. 1.65°, the guide accepts neutrons only from a part of the moderator surface. The horizontal

size of the moderator should be increased in this case to improve the acceptance of the second neutron guide for wavelengths less than 1.25 Å.

The integrated fluxes for wavelength band of 1-13 Å at the exit of both guides are given in Table 1.

The local air conditions measured in the ring corridor and guide hall of the IBR-2M reactor (temperature is 293 K, humidity is 65 %) are used for simulations. If the local air conditions are changed: i.e. the temperature is 300 K and humidity is 85 %, the integrated flux at the guide exit would have 2.5 % additional loss. For other local air conditions: i.e. the temperature is 283 K and humidity is 45 %, the integrated flux at the guide exit would have 0.9 % gain. If the additional section (see extraction system (b)) is filled with argon, the integrated flux at the guide exit would have 1 % additional loss. If the thickness of the aluminum windows is decreased from 0.15 cm to 0.05 cm, the integrated flux at the guide exit would have 2.2 % additional gain.

Table 1. Integrated fluxes at the exit of the guides 5 cm high for different extraction systems. If the height of the guides is increased to 9.5 cm, all fluxes at the guide exit should be doubled.

Flux at the exit, neutrons/cm^2/sec	First guide (inclination angle 0.8°)	Second guide (inclination angle 1.65°)
Extraction system (a)	$1.11 \cdot 10^7$	$1.14 \cdot 10^7$
Extraction system (b)	$1.19 \cdot 10^7$	$1.22 \cdot 10^7$
Extraction system (c)	$1.72 \cdot 10^7$	$1.77 \cdot 10^7$

Figure 7 shows the gain factor of the extraction system (b) relative to the extraction system (a). The extraction system (b) gives very small gain: between 6 and 12 % for different wavelengths for both guides. So such system should be reconsidered and optimized by the Monte Carlo simulations.

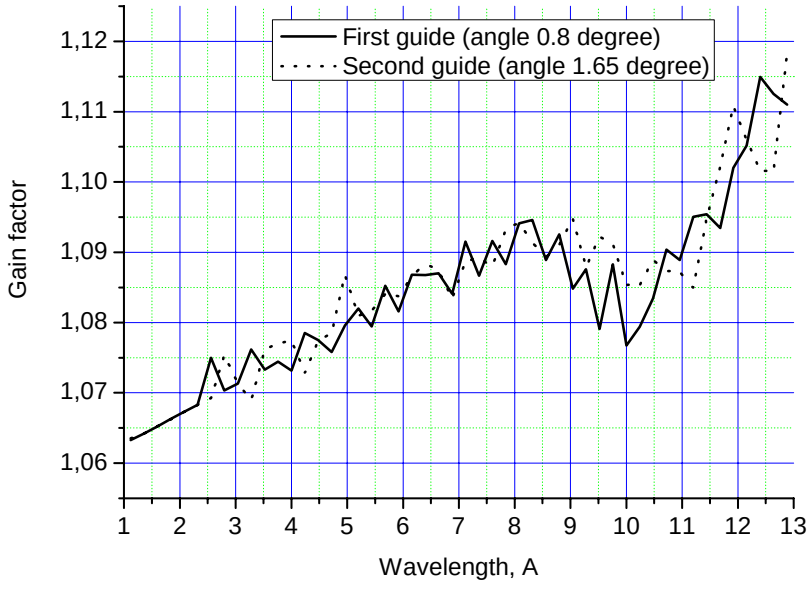

Fig. 7. The gain factor of the extraction system (b) relative to the extraction system (a) for both guides.

2. Optimization of the additional vacuum section between the moderators and the guides.

The optimization process consists of several steps:

1) Choose the shape of the cross section of the additional vacuum section.
2) Choose the coating material of the section.
3) Optimize the length of the section roughly.
4) Optimize the length of the section more carefully.

At the first step of the optimization, three variants of the section were considered with *constant height* of 18 cm at the entrance and at the exit for all cases:

Case a): entrance width is 10.5 cm; exit width is 15.5 cm, so the section has divergent geometry in the horizontal plane.
Case b): entrance width is 15 cm, exit width is 15 cm.
Case c): entrance width is 18 cm, exit width is 18 cm.

These parameters were chosen according to the design of the ring corridor and the guide hall of the IBR-2M reactor. The intensity gain factor of (b) and (c) cases relative to the case (a) for both guides are given in Fig. 8. So one can conclude that the case (a) is the worst case for wavelengths greater than 5 Å. Both (a) and (b) cases give practically the same gain for wavelengths greater than 5 Å. So, either case (b) or case (c) should be chosen, if the neutrons with wavelengths greater than 5 Å are required. Later for all simulations, the case (c) was chosen.

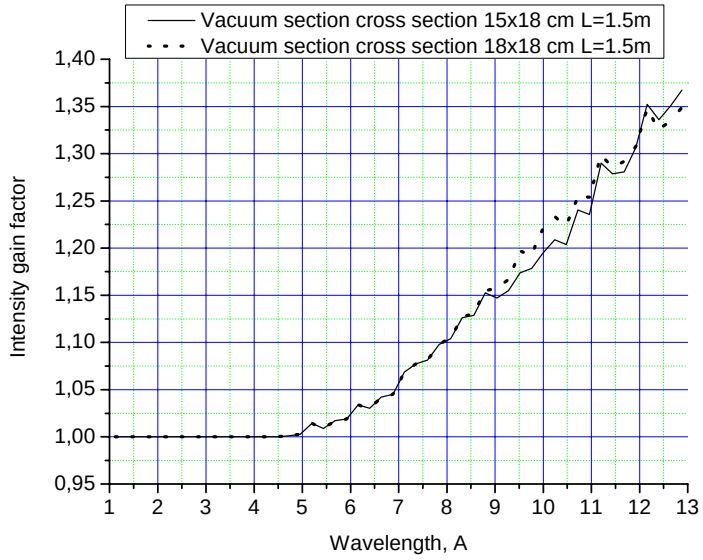

Fig. 8. The gain factor of (b) and (c) cases relative to the case (a) for the first guide.

The influence of the coating of this section should be evaluated. Three types of coatings were taken for the simulations: polished stainless steel, natural nickel and nickel-58. The relative gain factors are presented in Fig. 9. The base system is the section with polished stainless steel (m = 0.9) inside.

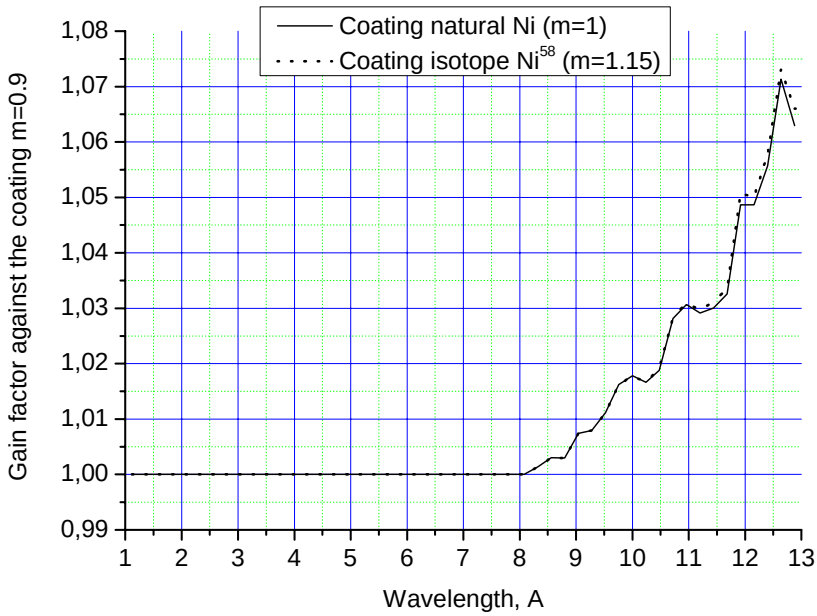

Fig. 9. The gain factor for the first guide for different coatings of the section.

So, one can see that a very small gain (several percent) factor from the wavelength of 8 Å could be explained by an increase in the effective moderator sizes. The next important step is to optimize the length of this section roughly. Three variants were considered:

1. The section becomes longer backward so that the distance between the exit of the section and the entrances of the guides becomes 1 m. The new length of the section is 2.7 m instead of 1.5 m.
2. The section becomes longer forward so that the distance between the entrance of the section and the moderators becomes 1 m. The new length of the section is 2.7 m as well.
3. The section becomes longer backward and forward, so the distance between the exit of the section and the entrances of the guides becomes 1m and the distance between the entrance of the section and the moderators becomes 1 m. The new length of the section is 3.9 m.

The gain factors relative to the system with the section 1.5 m long are presented in Fig. 10 and 11.

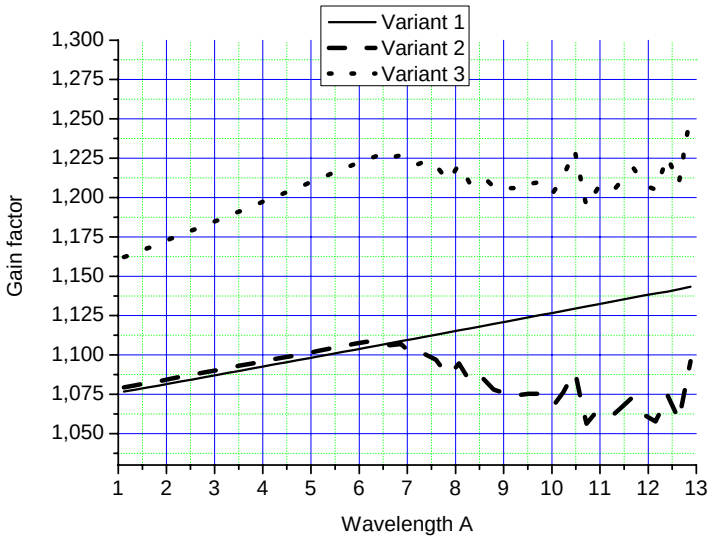

Fig. 10. The gain factor for the first guide for different lengths of the section.

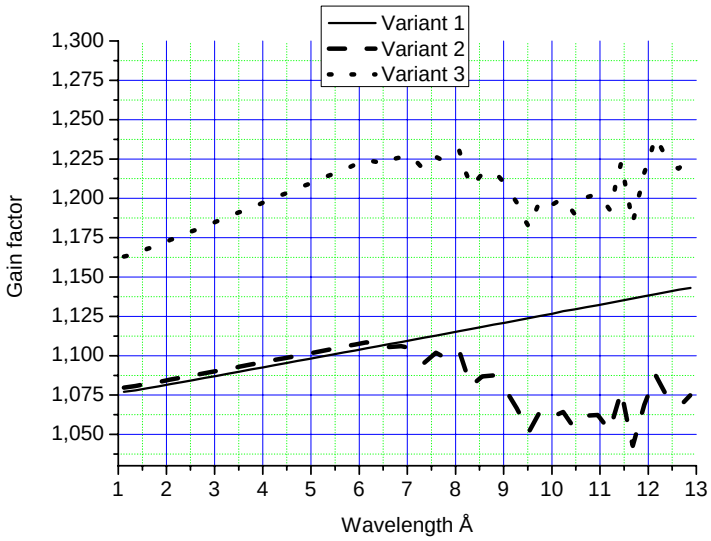

Fig. 11. The gain factor for the second guide for different lengths of the section.

The gain starts to decrease from the wavelength of 6 Å for variant 2 and variant 3 and the saturation effect is observed. It could be explained by the reduction of the effective moderator sizes: the section and neutron guide accept neutrons only from a part of the moderator. The most preferable variant is variant number 3. *But the distance between the exit of the section and the entrance of the guides should be reduced as much as possible.* The minimal distance between the section and the guides is 69 cm because the thickness of the box with the chopper is 65 cm. So the total length of the section becomes 3.9 m.

As the next step, the optimization of the coating of the section should be performed. Two coatings are considered: polished stainless steel and natural nickel. The gain factors are presented in Fig. 12. The gain factor is calculated relative to the system without the section, but the attenuation of

the flux in the air gap between the moderators and the guides was included in the simulations (guides with the extraction system (a), see Table 1).

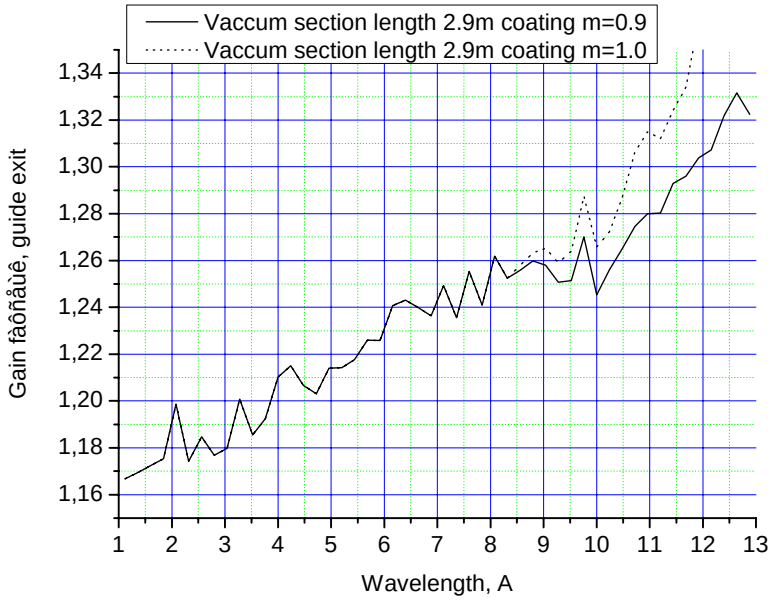

Fig. 12. The gain factor for the first guide for different coatings of the section.

So, one could see that natural nickel coating could improve the gain for wavelengths greater than 8 Å. So, the natural nickel coating is not really required for the section. No significant difference was found between the first and the second guides.

The last and important step is to optimize the length of the section more carefully. The seven variants were considered with different lengths of the section. Three effects are influenced on the gain factor: acceptance solid angle of the section (depends on the wavelength), attenuation of the neutron beam by air (depends on the wavelength as well) and effective moderator surface, which depends on:

a) the distance between the entrance of the section and surface of the moderator;
b) acceptance solid angle of the section, which depends on the wavelength.

Combination of these factors could be evaluated by Monte Carlo simulations. It is presented in Fig. 13. The saturation point is clearly seen for each line. This point indicates that the effective moderator surface (i.e. moderator surface where ALL neutron trajectories are accepted by the section) is already larger than the real moderator surface. If the length of the section increases, this point shifts to smaller wavelength values and decreases the gain factor. On the contrary, the distance, where neutrons travel through the air, decreases and the gain factor increases. The increase of the gain factor for longer wavelengths for all 7 variants could be explained by increasing acceptance solid angle of the section. There is no saturation point if the distance between the entrance of the section and the moderator surface is significant (see the gain factor for the section 301 cm long). Therefore, one can see that the optimal length is between 380-400 cm. Further increase of the length of the section does not give any extra gain factor for long wavelengths.

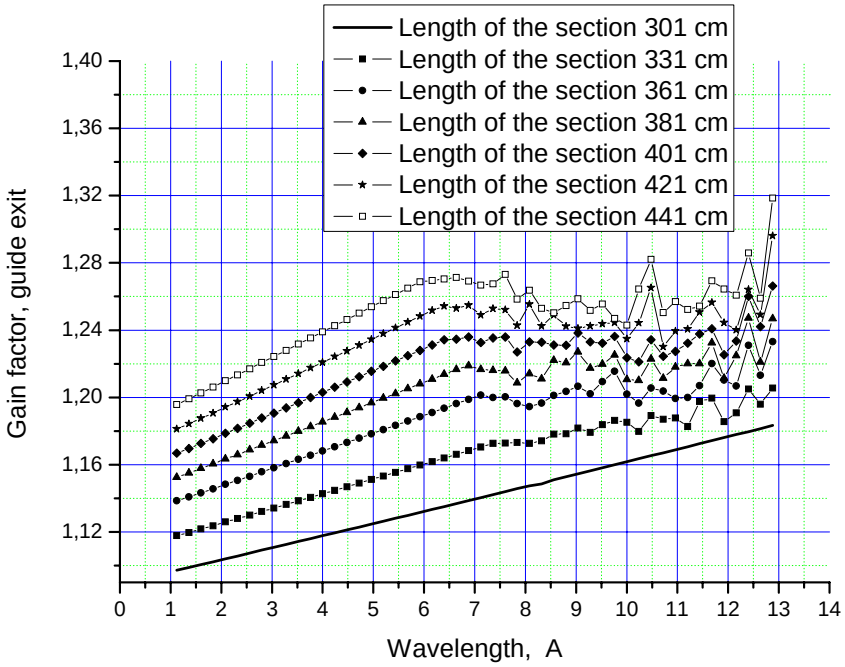

Fig. 13. Gain factors for the first guide depending on the length of the section. Similar situation takes place for the second guide. The gain factor is calculated relative to the system with the section of length 1.5 m as it is presented in Fig 4.

Conclusions

Generally, one option of the neutron extraction system optimization for the neutron guides of 7a1 and 7a2 is an additional section 270 cm long between the moderators and the guides, which improves the flux at the exit of the guides by a factor of 1.075-1.125 for different wavelengths (see Fig. 10, variant 1). This variant will be realized during the construction of the neutron guides. Additional improvement (by a factor of 1.16-1.24, see Fig. 13) could be made by increasing the length of the section towards the moderator so that the total length of the section becomes between 380-400 cm. But the last variant could not be realized technically: the present beam shutter and walls around will not be rebuilt and remain untouched. And the area has very high radiation levels. We considered it only for optimization process and academic purposes. Either polished stainless steel or natural nickel should be used as a reflecting surface for the section. Cross section of the section between the entrance and the exit of the section should be fixed and equals to 15 (width) × 18 (height) cm. Distance between the exit of the section and the entrance of the guides is 69 cm in order to install the first chopper with the thickness of the box of 65 cm. The vacuum section will be filled with argon in order to reduce the thickness of both aluminum walls (at the entrance and at the exit of the section) to 0.05 cm.

Acknowledgment

The authors are thankful to K. Walther (TU-Freiberg) and C. Scheffzuek (FU-Berlin) for useful discussions and support. This research has been supported by the European Commission under the 6th

Framework Programme through the Key Action: Strengthening the European Research Area, Research Infrastructures. Contract Number: RII3-CT-2003-505925.

References

[1] J.F.Briesmeister MCNP- A general Monte Carlo n-particle transport code: LA-12625-M, 1997

[2] K. Ullemeyer and etc. The SKAT texture diffractometer at the pulsed reactor IBR-2 at Dubna: experimental layout and first measurements Nuclear Instruments and Methods in Physics Research Section A: Accelerators, Spectrometers, Detectors and Associated Equipment Volume 412, Issue 1, 21 July 1998, Pages 80-88

[3] K. Walther and etc. Neutron time-of-flight diffractometer epsilon for strain measurements: layout and first results Physica B: Condensed Matter Volumes 276-278, March 2000, Pages 130-131

[4] K. Walther and etc. A Proposal for a Bended Neutron Guide at Beam Line 7A of the Modernized Fast Pulsed Reactor IBR-2M, Dubna, 4th EUROPEAN CONFERENCE ON NEUTRON SCATTERING 25-29 June 2007 Lund, Sweden

[5] G. Zsigmond and etc. A survey of simulations of complex neutronic systems by VITESS Nuclear Instruments and Methods in Physics Research Section A: Accelerators, Spectrometers, Detectors and Associated Equipment Volume 529, Issues 1-3, 21 August 2004, Pages 218-222

[6] http://www.helmholz-berlin.de/projects/ess/vitess

[7] See VITESS manual files included in the software

5. PUBLICATIONS

CONDENSED MATTER PHYSICS

1. Atomic and magnetic structures (diffraction)

1. Dmitriev A.I., Lashkarev G.V., Butorin P.E., Sichkovskyi V.I., Radchenko M.V., Kovalyuk Z.D., Beskrovni A.I., Aleshkevych P., Szymczak R., Dobrowolski D., Minikaev R. Neutron Diffraction Study of Magnetic Transformations in InSe Layered Semiconductor. Ukrainian Journal of Physics 2008, vol.53, N 6 , p.562-568
2. Jazdzewska M., Sliwinska-Bartkowiak M., Beskrovnyy A.I., Vasilovskiy S.G. Melting behavior of water confined in carbon nanopores; structure of the confined ice. Appl. Phys. Lett, (in press).
3. Kichanov S.E., Kozlenko D.P., Wasicki J., Nawrocik W., Czarnecki P., Savenko B.N., Glazkov V.P. and Lathe C. Structural phase transitions in pyridinium perrhenate at high pressure. Journal of Molecular Structure (2008)., v. 875, pp. 58-62.
4. Kozlenko D.P., Dubrovinsky L.S., Savenko B.N., Voronin V.I., Kiselev E.A., Proskurnina N.V.. Pressure-induced suppression of Wigner-crystal antiferromagnetic state in La0.33Ca0.67MnO3. Phys. Rev. B (2008), v. 77, pp. 104444-1-6.
5. Kozlenko D.P., Mirebeau I., Park J.-G., Goncharenko I.N., Lee S., Park J., Savenko B.N. High pressure induced spin liquid phase of multiferroic YMnO3. Phys. Rev. B (2008), v. 78, pp. 054401-1-5.
6. Nietz V.V. Precessing ball solitons in ferromagnet at the first order transition. Journal of Magnetism and Magnetic Materials, (in press).
7. Nietz V.V. Transformation of precessing ball solitons into domains of new phase during the spin-flop phase transition in antiferromagnets. Journal of Magnetism and Magnetic Materials, (in press).
8. Nietz V.V., Osipov A.A. Ball solitons and kinetics of the first order magnetic phase transition. Journal of Magnetism and Magnetic Materials, 2008, v.320, pp 1464-1471.
9. Nietz V.V., Osipov A.A. Ball solitons in kinetics of the first order magnetic phase transition. Communication JINR, E17-2007-63, Dubna, 2007.
10. Nikolaev Ivan V., D'Hondt Hans, Abakumov Artem M., Hadermann Joke, Balagurov Anatoly M., Bobrikov Ivan A., Sheptyakov Denis V., Pomjakushin Vladimir Yu., Pokholok Konstantin V., Filimonov Dmitry S., Tendeloo Gustaaf Van, Antipov Evgeny V. . Crystal structure, phase transition and magnetic ordering in the perovskitelike Pb2-xBaxFe2O5 solid solution. Phys. Rev. B, 2008, v.78, p. 024426 (1-12).

11. Trukhanov S.V., Kozlenko D.P., Trukhanov A.V. High hydrostatic pressure effect on magnetic of anion-deficient La0.7Sr0.3MnOx perovskite manganites. J. Magn. Magn. Mater. (2008), v. 320, pp. e88-91.
12. Wasicki J., Kozlenko D.P., Pankov S.E., Bilski P., Pajzderska A., Hancock B.C., Medek A., Nawrocik W., and Savenko B.N.. NMR search for polymorphic phase transformations in chlorpropamide form-A at high pressures. J. Pharm. Sci., published (2008) online DOI 10.1002/jps.21471. (что это?)
13. Балагуров А.М., Бобриков И.А., Карпинский Д.В., Троянчук И.О., Помякушин В.Ю., Шептяков Д.В.. Последовательные структурные фазовые переходы в Pr0.5Sr0.5CoO3 в диапазоне 10 – 1120 К. Письма в ЖЭТФ, 2008, т. 88(8), с. 607 - 613. (Balagurov A.M., Bobrikov I.A., Karpinsky D.V., Troyanchuk I.O., Pomjakushin V.Yu., Sheptyakov D.V.. Successive Structural Phase Transitions in Pr0.5Sr0.5CoO3 in the Range 10–1120 K. JETP Letters, 2008, Vol. 88, No. 8, pp. 531–536).
14. Балагуров А.М., Бобриков И.А., Помякушин В.Ю., Шептяков Д.В., Бабушкина Н.А., Горбенко О.Ю., Картавцева М.С., Кауль А.Р. Влияние изотопического состава и микроструктуры на кристаллическое и магнитное фазовое состояние в R0.5Sr0.5MnO3. ЖЭТФ, 2008, т.133 (3), с. 605-621. (A.M.Balagurov, I.A.Bobrikov, V.Yu.Pomjakushin, D.V.Sheptyakov, N.A.Babushkina, O.Yu.Gorbenko, M.S.Kartavtseva, A.R.Kaul “Effect of Isotopic Composition and Microstructure on the Crystalline and Magnetic Phase States in R0.5Sr0.5MnO3” JETP, 2008, Vol. 106, No. 3, pp. 528–541).
15. Благовещенский Н.М., Морозов В.А., Новиков А.Г., Савостин Д.В., Шимкевич А.Л.. Исследования микроструктуры расплава литий–азот методом дифракции нейтронов. Кристаллография, 2008, т. 53, № 1, с. 25 – 28. (Blagoveshchenskii N.M., Morozov V.A., Novikov A.G., Savostin V.V., Savostin D.V., Shimkevich A.L. Investigation of the lithium-nitrogen melt microstructure by neutron diffraction. Crystallography Reports, 2008, v. 53, № 1, pp. 14 – 17).
16. Благовещенский Н.М., Морозов В.А., Новиков А.Г., Савостин Д.В., Шимкевич А.Л.. Исследование микроструктуры расплава свинец–калий, барботированного тяжелой водой, методом дифракции нейтронов. Поверхность. Рентгеновские, синхротронные и нейтронные исследования, 2008, № 2, с. 3 – 8. (Blagoveshchenskii N.M., Morozov V.A., Novikov A.G., Savostin V.V., Savostin D.V., Shimkevich A.L. Neutron diffraction investigation of the microstructure of lead-potassium melt bubbled with heavy water. Journal of Surface Investigation. X-ray, Synchrotron and Neutron Techniques, 2008, v. 2, № 1, pp. 80 – 85).

17. Галиева Е.А., Данилова Н.А., Пряничников С.В., Титова С.Г., Титов А.Н., Бобриков И.А., Балагуров А.М. Аномалии структуры и свойств диселенида титана, интеркалированного железом. Физика твердого тела, 2008, т.50(2), с.303-306. Galieva E.A., Danilova N.A., Prayanichnikov S.V., Titova S.G., Titov A.N., Bobrikov I.A., Balagurov A.M. Anomalies in the structure and properties of titanium diselenide intercalated by iron. Physics of the Solid State, 2008, v.50(2), pp.314-317.
18. Нитц В.В. Мощные импульсные источники нейтронов для исследований с импульсным магнитным полем. Кристаллография, 2008, том 53, № 3, с.562-565; V.V.Nietz. Power pulsed neutron sources for research with a pulsed magnetic field. Crystallography Reports, 2008, v. 53, No 3, pp. 526-529.
19. Нитц В.В., Осипов А.А. Шаровые солитоны в кинетике магнитных фазовых переходов первого рода. Новый механизм фазовой перестройки. Кристаллография, 2008, том 53, № 2, с.292-296; (V.V.Nietz, A.A.Osipov Ball Solitons in the Kinetics of Magnetic First-Order Phase Transitions:A New Mechanism of Phase Reconstruction. Crystallography Reports, 2008, v. 53, No 2, pp. 266-270).

2. Soft matter (small angle scattering and diffraction)

1. D. V. Lebedev, M. V. Filatov, A. I. Kuklin, A. Kh. Islamov, J. Stellbrink, R. A. Pantina, Yu. Yu. Denisov, B. P. Toperverg, and V. V. Isaev-Ivanov. Structural Hierarchy of Chromatin in Chicken Erythrocyte Nuclei Based on Small-Angle Neutron Scattering: Fractal Nature of the Large-Scale Chromatin Organization. Crystallography Reports, 2008, Vol. 53, No. 1, pp. 110–115.
2. Gordeliy V. I. and Moiseeva E. S.. Crystallization of Membrane Proteins. In: Soft Matter: From Synthetic to Biological Materials, 2008, / ed.: J. K. G. Dhont, G. Gompper, G. Nägele, D. Richter, R. G. Winkler. – FZJ Juelich.
3. Gordeliy V. I. and E. S. Moiseeva. In meso Approaches to Membrane Protein Crystallization. In: "Molecules: Aggregation, Nucleation, Crystallization – Beyond Medical and Other Implications". WORLD SCIENTIFIC PUBLISHING CO. Singapor, 2008, New Jersey, London, In Press.
4. Karelov D. V., Lebedev D. V., Suslov A. V., Shalguev V. I., Kuklin A. I., Islamov A. Kh., Lauter H., Lanzov V. A. and Isaev-Ivanov V. V.. Large-scale structure of RecA protein from Deinococcus radiodurance and its complexes in solution. J. Phys.: Condens. Matter. Vol.20. Issue 10, 2008, p. 104215
5. Kessner D., Ruettinger A., Kiselev M.A., Wartewig S., Neubert R.H.H.. Properties of ceramides and their impact on the stratum corneum structure. A review, Part II: Stratum corneum lipid

mixtures. Skin Pharmacology and Physiology 21 (2008) 58-74.

6. Kiselev M.A., Zemlyanaya E. V., Ryabova N.Y., Hauss T., Dante S., Lombardo D.. Water distribution function across the curved lipid bilayer: SANS study. Chemical Physics 345 (2008) 185-190.
7. Moiseeva E. S., Reshetnyak A. B., Borshchevskiy V. I., Baeken C., Büldt G., Gordeliy V. I. Comparative Analysis of Quality of Membraine Protein Bacteriorhodopsin Crystals Obtained in Octylglucoside and Octylthioglucoside. Journal of Surface Investigation. X-ray, Synchrotron and Neutron Techniques, 2009, v 1, pp. 1-5 In Press.
8. Reshetnyak A.B. , Borshchevskii V.I., Klare J., Moiseeva E.S., Engelhardt M., Buldt G., Gordeliy V.I.. Comparative Analysis of Sensory Rhodopsin II Structures in Complex with a Transducer and without It. Journal of Surface Investigation. X-ray, Synchrotron and Neutron Techniques, 2008, Vol. 2, No. 6, pp. 894–899.
9. Ruettinger A., Kiselev M.A., Hauss Th., Dante S., Balagurov A.M., Neubert R.H.H. . Fatty acid interdigitation in stratum corneum model membranes: A neutron diffraction study. Eur. Biophys. J., 2008, v. 37, pp. 759-771.
10. Schroeter Annett, Kessner Doreen, Kiselev Mikhail A., Hauss Thomas, Dante Silva, Balagurov Anatoliy M., Neubert Reinhard H.H..Basic nanostructure of CER[EOS]/ CER[AP]/ CHOL/ FFA multilamellar membranes. A neutron diffraction study. Biophysical Journal, September-2008, (in press).
11. Uhríková D., Kucherka N., Teixeira J., Gordeliy V., Balgavy P. Structural changes in dipalmitoylphosphatidylcholine bilayerpromoted by Ca2+ ions: a small-angle neutron scattering study. Chemistry and Physics of Lipids , 2008, 155, pp 80–89.
12. Горшкова Ю. Е., Горделий В. И.. Исследование взаимодействия диметилсульфоксида с липидными мембранами с помощью малоуглового рассеяния нейтронов. Кристаллография, 2007, том 52, № 3, с. 584–588. (Gorshkova J. E., Gordeliy V. I. Investigation of the Interaction of Dimethyl Sulfoxide with Lipid Membranes by Small-Angle Neutron Scattering, ISSN 1063-7745, Crystallography Reports, 2007, Vol. 52, No. 3, pp. 535–539)
13. Киселев М.А., Ермакова Е.В., Филиппова С.Н., Сургучева Н.А., Данте С., Хаус Т. , Гальченко В.Ф., Структурная организация фосфолипидной компоненты клеточных мембран Streptomyces hygroscopicus по данным дифракции нейтронов, (направлено в журнал Биофизика). (название и ссылка English)
14. Лебедев Д. В., Филатов М. В., Куклин А. И., Исламов А. Х., Штеллбринк И., Пантина Р. А., Денисов Ю. Ю., Топерверг Б. П., Исаев-Иванов В. В. Структурная иерархия хроматина ядер

эритроцитов курицы по данным малоуглового рассеяния нейтронов: фрактальная природа. Кристаллография, 2008, том 53, №1, с.111-116.

15. Рябова Н.Ю., Киселев М.А., Бескровный А.И., Балагуров А.М. .Исследование структуры многослойных липидных мембран методом дифракции нейтронов в реальном времени. Физика твердого тела, ноябрь 2008, принята к печати.

3. Nanostructured materials (small-angle scattering)

1. Anitas E. M., Islamov A. Kh., Balasoiu M., Muresan C., Bica I., Kovalev Yu. S., Orelovich O. L., Kuklin A. I., Small angle neutron scattering and electron microscopy study of magnetic elastomers, Journal of Optoelectronics and Advanced Materials 2008, Vol.10, Issue 12, (to appear).
2. Avdeev M.V., Bica D., Vekas L., Aksenov V.L., Feoktystov A.V., Rosta L., Garamus V.M., Willumeit R.. Structural aspects of stabilization of magnetic fluids by mono-carboxylic acids. Advanced Materials Research, 2008, (in press).
3. Bakeeva R. F., E. M. Kosacheva, I. S. Razina, D. B. Kudryavtsev, Yu. S. Kovalev, A. I. Kuklin, L. A. Kudryavtseva, and V. F. Sopin. Influence of the Fluoride Ion on the Aggregation and Catalytic Properties of Micellar Solutions of Cetyltrimethylammonium Bromide. 2008, T.49, №5, pp.661-669.
4. Balasoiu M., Anitas E. M., Bica I., Osipov V. A., Orelovich O. L., Savu D., Savu S., Erhan R., Kuklin A. I.. SANS of interacting magnetic micro-sized Fe particles in a stomaflex creme polymer matrix, Journal of Optoelectronics and Advanced Materials Rapid Comunications, 2008, (in press).
5. Balasoiu M., Anitas E. M., Bica I., Osipov V. A., Orelovich O. L., Savu D., Savu S., Erhan R., Kuklin A. I.. SANS of interacting magnetic micro-sized Fe particles in a stomaflex creme polymer matrix. Preprint JINR E3-2008-138.
6. Balasoiu M., Barsov S. G., Bica D., Vekas L., Vorobev S. I., Gritsaj K. I., Duginov V. N., Zhukov V. A., Komarov E. N., Koptev V. P., Kotov S. A., Mamedov T. N., Petrescu K., Shcherbakov G. V., MSR Study of the Properties of Fe3O4-Based Nanostructured Magnetic Systems", Preprint JINR P14-2008-89.
7. Balasoiu M., Craus M. L., Kuklin A. I., Plestil J., Haramus V., Islamov A. Kh., Erhan R., Anitas E. M., Lozovan M., Tripadus V., Petrescu C., Savu D., Savu S., Bica I.. Microstructure of magnetite doped elastomers investigated by SAXS and SANS. JOAM, vol.10, No.11, 2008, pp.2932-2936.

8. Balasoiu M., Craus M. L., Plestil J., Haramus V., Erhan R., Anitas E. M., Lozovan M., Kuklin A. I., Bica I.. Microstructure of magnetite doped elastomers investigated by SAXS and SANS. Preprint JINR E14-2008-123.
9. Balasoiu M.,.Aksenov V.L, Bica D., Duginov D.N., Gritsaj K.I., Mamedov T.N., Tripadus V., Vekas L., Zhukov L.A.. Muon spectroscopy of a frozen ferofluid. Magnetohydrodynamics, 2008, v.44, issue 1, 61-67.
10. Balasoiu M.. Aspecte ale microstructurii lichidelor magnetice. Editura Semne, ISBN 9789736245633, 2008, p. 130. Монография.
11. Balasoiu M., Barsov S. G., Bica D., Vekas L., Vorobev S. I., Gritsaj K. I., Duginov V. N., Zhukov V. A., Komarov E. N., Koptev V. P., Kotov S. A., Mamedov T. N., Petrescu K., Shcherbakov G. V.. SR Study of the Properties of Fe3O4-Based Nanostructured Magnetic Systems. JETP Lett, Vol. 88., Issue 3 , 2008, pp. 243-247. М.Балашою, С.Г.Барсов, Д.Бика, Л.Векаш, С.И.Воробъев, К.И.Грицай, В.Н.Дугинов, В.А.Жуков, Е.Н.Коморов, В.П.Коптев, С.А.Котов, Т.Н.Мамедов, К.Петреску, Г.В.Щербаков, Исследование свойств наноструктурированных магнитных систем на основе Fe3O4 SR- методом, Письма в ЖЭТФ, Том 88, Вып.3, 2008, с.243-247.
12. Feoktystov A.V., Avdeev M.V., Aksenov V.L., Petrenko V.I., Bulavin L.A., Bica D., Vekas L., Garamus V.M., Willumeit R.. Contrast Variation in Small-Angle Neutron Scattering from Magnetic Fluids Stabilized by Different Mono-Carboxylic Acids. Advanced Materials Research, 2008, accepted.
13. Kyzyma O.A., Bulavin L.A., Aksenov V.L., Avdeev M.V., Tropin T.V., Korobov M.V., Snegir S.V., Rosta L.. Aggregation in C60/NMP, C60/NMP/water and C60/NMP/Toluene mixture.Fullerenes, Nanotubes and Carbon Nanostructures, 2008, v.16, pp 610-615.
14. Kyzyma O.A., L.A.Bulavin, V.L.Aksenov, M.V.Avdeev, T.V.Tropin, M.V.Korobov, S.V.Snegir, L.Rosta. Organization of fullerene clusters in the system C60/N-metyl-2-pyrrolidone. Materials structure, 2008, v.15, pp 17−20.
15. M. Balasoiu, V. L. Aksenov, Neutron depolarization and mSR studies of ferrofluids, Journal of Optoelectronics and Advanced Materials,Vol.10, Issue 12, 2008 (to appear).
16. Petrenko V.I., Avdeev M.V., Aksenov V.L., Bulavin L.A., Rosta L.. Effect of surfactant excess in non-polar ferrofluids probed by small-angle neutron scattering. Advanced Materials Research, 2008 (in press).

17. Petrenko V.I., Avdeev M.V., Almásy L., Bulavin L.A., Aksenov V.L., Rosta L., Garamus V.M.. Interaction of mono-carboxylic acids in benzene. Data of small-angle neutron scattering. J. Col. Surf. A, 2008, (in press).
18. Petrenko V.I., Avdeev M.V., Bulavin L.A.,.Aksenov V.L, Almasy L., Rosta L., Garamus V.. Structure features of ferrofluids stabilization. Труды VIII всероссийской научной конференция молодых ученых и специалистов, ОИЯИ Дубна Дубна, Россия, 2008. с.154-157.
19. Rajewska A. SANS study of two nonionic surfactants in water micellar solutions. Pramana J. of Physics, v.71, № 5 (2008) 15.
20. Rogachev A. V., Cherny A. Yu., Ozerin A. N., Muzafarov A. M., Tatarinova E. A., Islamov A. Kh., Gordeliy V. I., Kuklin A. I.. Revealing inner structure of the polycarbosilane dendrimers from small-angle neutron scattering data. Journal of Physics: Conference Series 129, 2008, 012041.
21. Soloviev A.G., Stadnik A. V., Islamov A. H. and Kuklin A. I.. Fitter. The package for fitting a chosen theoretical multi-parameter function through a set of data points. Application to experimental data of the YuMO spectrometer. Version 2.1.0. Long Write-Up and User's Guide. Communication of JINR E10-2008-2, Dubna.
22. Tropin T.V., Avdeev M.V., Aksenov V.L.. Small-angle Neutron Scattering Study of C60/CS2 Solutions. Fullerenes, Nanotubes and Carbon Nanostructures, 2008, v. 16, pp 616-621.
23. Vekas L., Avdeev M.V., Bica D.. Magnetic Nanofluids: Synthesis and Structure, in: Nanoscience and Its Applications in Biomedicine. Ed. Donglu Shi, Springer Verlag, 2008, Chapter 25, pp. 645-704.
24. Авдеев М.В., Боднарчук И.А., Петренко В.И., Холмуродов Х.Т., Ярадайкин С.П. Определение предельного парциального молярного объема растворов монокарбоксильных кислот в бензоле методом молекулярно-динамического моделирования. Журнал физической химии. (Принято в печать). (Avdeev M.V, Bodnarchuk I.A., Petrenko V.I., Kholmurodov Kh.T., Yradaikin S.P. Limit partial molar volume of mono-carboxylic acids in benzene by molecular dynamics simulation. Russian Journal of Physical Chemistry A. (in press).
25. Авдеев М.В., Тропин Т.В., Аксенов В.Л., Рошта Л., Холмуродов М.Т.. К вопросу об образовании кластеров фуллерена в сероуглероде. Данные малоуглового рассеяния нейтронов и молекулярной динамики. Поверхность.Рентгеновские, синхротронные и нейтронные исследования , 2008, т.12, с 5-8 (Avdeev M.V., Tropin T.V., Aksenov V.L., Rosta L., Kholmurodov M.T.. On the question of fullerene cluster formation and growth in carbon disulfide solutions. Small-angle neutron scattering and molecular dynamics data. J. Surf. Investigation. X-ray, Synchrotron and Neutron Techniques, 2008, v.2, pp 819-825.)

26. Аксенов В.Л., Тропин Т.В., Кизима Е.А., Авдеев М.В., Коробов М.В., Рошта Л..К вопросу об образовании кластеров фуллерена С60 в азот-содержащих растворителях, Физика твердого тела, (2008) Принято в печать. (Aksenov V.L., Tropin T.V., Kyzyma O.A., Avdeev M.V., Korobov M.V., L.Rosta. On fullerene cluster formation in nitrogen-containing solvents. Physics of the Solid State. 2008, (in press).)
27. Бакеева Р. Ф, Косачева Э. М., Разина И. С., Кудрявцев Д. Б., Ковалев Ю.С., Куклин А. И., Кудрявцева Л. А., Сопин В. Ф. Влияние фторид-иона на агрегационные и каталитические свойства мицеллярных растворов цетилтриметиламмоний бромида. Кинетика и катализ, 2008, Т.49, №5, с.661-669.
28. Кизима О.А., Булавін Л.А., Авдєєв М.В., Снегір С.В., Аксьонов В.Л..Ефект додавання води в систему С60/N-метил-2-пірролідон. Вісник Київ. ун-ту, серія: фіз.-мат. науки 2007, т. 4 , с 331−333. (Kyzyma O.A., Bulavin L.A., Avdeev M.V., Snegir S.V., Aksenov V.L.. Effect of water addition in the system C60/N-methyl-2- pyrrolidone. Bulletin of University of Kyiv Series: Physics & Mathematics 2007, v.4, pp 331-333, published in 2008, in Ukranian)
29. Кизима Е.А., Авдеев М.В., Аксенов В.Л., Булавин Л.А., Снегир С.В.. Реорганизация кластеров фуллерена в системе С60/N-метил-пирролидон/вода. Поверхность. Рентгеновские, синхротронные и нейтронные исследования, 2008,т. 12, с 1-4.(O.A.Kyzyma, M.V.Avdeev, V.L.Aksenov, L.A.Bulavin, S.V.Snegir. Reorganization of fullerene clusters in the system C60/N-metyl-2-pyrrolidone/water. J. Surf. Investigation. X-ray, Synchrotron and Neutron Techniques, 2008 (in press))
30. Куклин А.И.. Исследование структуры нанодисперсных пористых полимерных объектов методом малоуглового нейтронного и рентгеносвского рассеяния. Автореферат диссертации на соискание ученой степени кандидата физико-математических наук. 14-2008-151, Издательский отдел ОИЯИ, Дубна.
31. Петренко В.И., Авдеев М.В., Аксенов В.Л., Булавин Л.А., Рошта Л.. Магнитные жидкости при избытке поверхностно-активных веществ по данным малоуглового рассеяния нейтронов. Поверхность. Рентгеновские, синхротронные и нейтронные исследования, 2008. Принято в печать. (Petrenko V.I., Avdeev M.V., Aksenov V.L., Bulavin L.A., Rosta L., Magnetic fluids with the excess of surfactants. Data of small-angle neutron scattering. J. Surf. Investigation. X-ray, Synchrotron and Neutron Techniques, 2008 (in press))
32. Петренко В.И., Аксенов В.Л., Авдеев М.В., Булавин Л.А., Рошта Л., Векаш Л., Гарамус В.М., Виллумайт Р.. Анализ структуры водных феррожидкостей методом малоуглового нейтронного рассеяния. Физика твердого тела, 2008. Принято в печать. (Petrenko V.I.,

Aksenov V.L., Avdeev M.V., Bulavin L.A., Rosta L., Vekas L., Garamus V.M., Willumeit R.. Structure analysis of water-based ferrofluids by means of small-angle neutron scattering. Physics of the Solid State, 2008, (in press).)

33. Петренко В.І., Булавін Л.А., Авдєєв М.В., Аксьонов В.Л., Векаш Л., Рошта Л.. Аналіз структури магнітних рідинних систем методом нейтронного розсіяння. Вісник Київ. ун-ту, серія: фіз.-мат. науки 2007, т.4. с. 362-364 (издано в 2008); (Petrenko V.I., Bulavin L.A., Avdeev M.V., Aksenov V.L., Vekas L., Rosta L.. Analysis of the structure of ferrofluids by neutron scattering. Bulletin of University of Kyiv Series: Physics & Mathematics 2007, v.4, pp 362-364, published in 2008, in Ukranian)
34. Петренко В.І., Булавін Л.А., Авдєєв М.В., Аксьонов В.Л., Рошта Л., Нейтронні дослідження взаємодії молекул поверхнево-активних речовин в неполярному розчиннику. Укр. фіз. Журнал, 2008, т.53, с 229-234. (Petrenko V.I., Bulavin L.A., Avdeev M.V., Aksenov V.L., Rosta L.. Neutron investigations of the interaction of surfactant molecules in non-polar solvent. Ukr. J. Phys., 2008, v.53, pp 229-233)
35. Петренко В.І., Булавін Л.А.,.Авдєєв М.В, Аксьонов В.Л., Рошта Л..Нейтронні дослідження стабільності рідинної системи. Журнал фізичних досліджень, 2008, т.12, с. 3201-3205. (Petrenko V.I., Bulavin L.A., Avdeev M.V., Aksenov V.L., Rosta L.. Neutron investigations of magnetite/oleic acid/benzene ferrofluids stability with the excess of surfactant. J. Phys. Stud, 2008, v. 12, pp 3201-3205, in Ukranian)
36. Феоктистов А.В., Авдеев М.В., Аксенов В.Л., Булавин Л.А., Бика Д., Векаш Л., Гарамус В.М., Виллумайт Р.. Вариация контраста в малоугловом рассеянии нейтронов на магнитной жидкости магнетит/миристиновая кислота/бензол. Поверхность. Рентгеновские, синхротронные и нейтронные исследования,2008. Принято в печать. (Feoktystov A.V., Avdeev M.V., Aksenov V.L., Bulavin L.A., Bica D., Vekas L., Garamus V.M., Willumeit R.. Contrast variation in small-angle neutron scattering from magnetic fluid magnetite/myristic acid/benzene. J. Surf. Investigation. X-ray, Synchrotron and Neutron Techniques ,2008, (in press))
37. Феоктистов А.В., Булавін Л.А., Авдеєв М.В., Векаш Л., Гарамус В.М., Віллумайт Р.. Малокутове Розсіяння Нейтронів Магнітними Водними Системами, які Стабілізовані Монокарбоксильними Кислотами. Український Фізичний Журнал, 2008, принято в печать. Feoktystov A.V., Bulavin L.A., Avdeev M.V., Vekas L., Garamus V.M., Willumeit R.. Small-Angle Neutron Scattering on Magnetic Water Systems Stabilized by Monocarboxylic Acids. Ukr. J. Phys., 2008 (in press)

4. Thin films (reflectometry, polarized neutrons)

1. Aksenov V. L., Nikitenko Yu.V., Proglyado V.V., Khaidukov Yu.N., Gavrilov V.N., Raitman E., Bottyan L., Nagy D.L. Investigation of the Ultrasonic Wave Influence on Magnetic Ordering in a 20×[Fe(20Å)/Cr(12 Å)]/MgO Layered Structure. Crystallography Reports, 2008, vol. 53, No. 5, pp. 729-733; published in Kristallografiya, 2008, vol.53, No. 5, pp. 775-779. (русское название и журнал)
2. Bodnarchuk V.I., Kraan W.H., Rekveldt M.T., Ioffe A., Neutron spin turners with a rotating magnetic field: first experiments. Meas. Sci. Technol, 2008, v.19, p 03401.
3. Deak L., Spiering H., Bottyan L., Nagy D.L., Khaidukov Yu. N. and Yoda Y.. Perturbative Theory of Grazing-Incidence Diffuse Nuclear Resonant Scattering of Synchrotron Radiation. Phys. Rev., 2008, B 76 (22) pp.
4. Ignatovich V.K., Nikitenko Yu.V.. Experimental opportunity to investigate layered magnetic structures with the help of oscillating magnetic field. Nuclear Instruments and Methods in Physics Research, 2008, (in press).
5. Ioffe A., Bodnarchuk V., Bussmann K., Mueller R., Georgii R.. A new neutron spin–echo spectrometer with time-gradient magnetic fields: First experimental test. Nucl. Instr. Methods, 2008, A 586, pp 36–40.
6. Jernenkov M., Klimko S., Lauter-Pasyuk V., Toperverg B.P., Milyaev M., Romashev L., Ustinov V., Lauter H., Aksenov V.. Larmor precession reflectometry for magnetic film studies. Nucl. Instr. Methods,2008, A 586, pp 116-118.
7. Kozhevnikov S.V., Ott F., Paul A., Rosta L.. Resonances and off-specular scattering from neutron waveguides. European Journal of Physics Special Topics. 2008 (in press).
8. Kozhevnikov S.V., Ott F.. Data representations in off-specular neutron reflection. 2008, принято в журнал Физика Твёрдого Тела.
9. Аксенов В.Л., Никитенко Ю.В., Хайдуков Ю.Н., Вдовичев С.Н., Борисов М.М., Морковин А.Н., Мухамеджанов Э.Х.. Сосуществование сверхпроводимости и ферромагнетизма в наноструктуре Nb(500 Å)/Fe(39 Å)/[Si(34 Å)/Mo(34Å)]40/Si, 2008, направлено в Поверхность. (английское название)
10. Жерненков М.Н., Аксёнов В.Л., Климко С., Лаутер-Пасюк В.В., Лаутер Х., Топерверг Б.П., Миляев М.А., Ромашев Л.Н., Устинов В.В., Рефлектометрия с ларморовской прецессией для исследования многослойных структур. Кристаллография, 2008, т .53, с 334-341. (Zhernenkov M.N., Aksenov V.L., Klimko S., Lauter-Pasyuk V.V., Lauter H., Toperverg B.P., Milyaev M.A.,

Romashev L.N., Ustinov V.V.. Larmor procession reflectometry for studying multilayers.Crystallography Reports, 2008, v.53, pp 308-315.)

5. Atomic and magnetic dynamics (inelastic neutron scattering)

1. Blagoveshchenskii N.M., Morozov V.A., Novikov A.G., Pashnev M.A., Shimkevich A.L., Sobolev O.V.. Quasielastic neutron scattering and diffusion in liquid lithium and lithium–hydrogen melt, J. of Physics: Condens. Matter, 2008, v. 20, p. 104201 – 104204.
2. Blagoveshchenskiy N.M., Loginov N.I., Morozov V.A., Novikov A.G., Pashnev M.A., Savostin V.V. and Shimkevich A.L.. Investigations of diffusion processes in liquid lithium and lithium˜hydrogen melt by quasielastic neutron scattering. J. Phys. Conf. Series. 98, 2008, 022014.
3. Hołderna-Natkaniec K., Natkaniec I., Jakubas R., Nowak D., Medycki W.. Internal dynamics of (C3N2H5)5Bi2Cl11 studied by IINS, H1NMR and QC methods. Journal of Molecular Structure, 2008, v. 891, pp 143-150.
4. Holderna-Natkaniec K., Natkaniec I., Mikuli E., Swiergiel J., Khavryutchenko V.D., Jakubas R.. IINS, FT-IR and DFT study of the internal dynamics of [4apyH]SbCl4. Acta Physica Polonica A, 2008, v. 113, p 1117.
5. Juszynska E., Holderna-Natkaniec K., Massalska-Arodz M., Natkaniec I., Sciesinska E., Sciesinski J.. IINS, MIR and DFT investigations of vibrational spectra of 3,3-dimethyl-1-butanol and 3,3 dimethyl-2-butanol. Acta Physica Polonica A, 2008, v.113, pp 1131-1143.
6. Juszynska E., Massalska-Arodz M., Natkaniec I., Krawczyk J. Neutron scattering studies of solid-state polymorphism in dimethyl butanol glass formers. Physica B, 2008, v. 403, pp 109–114.
7. Khavryuchenko V.D., Natkaniec I., Tarasenko Yu.O., Khavryuchenko O.V., Alekseev S.A., Lisnyak V.V.. Characterization of sol-gel-derived polyhydridosiloxane pre-ceramic polymer. Materials Chemistry and Physics, 2008, v. 108, pp 24-28.
8. Majerz I., Natkaniec I.. Vibrations of the OHO hydrogen bond in t-butanol. Chemical Physics Letters, 2008, v. 465, pp 86-91.
9. Okwieka U., Szostak M.M., Misiaczek T., Turowska-Tryk I., Natkaniec I., Pavlukojc A.. Spectroscopic, structural and theoretical studies of 2-methyl-4-nitroaniline (MNA) crystal. Electronic transitions in IR. J. Raman Spectrosc., 2008, v. 39, pp 849-862.
10. Pokotilovski Yu. N., Natkaniec I., Hołderna-Natkaniec K. The experimental and calculated density of states and UCN loss coefficients of perfluoropolyether oils at low temperatures. Physica B, 403 (2008), pp 1942-1948.

11. Prager M., Grimm H., Natkaniec I., Nowak D., Unruh T. The dimensionality of ammonium reorientation in (NH4)2S2O8: the view from neutron spectroscopy. J. Phys.: Condens. Matter 20 (2008) 125218, pp11.
12. Skomorokhov A.N., Trots D.M., Sashin I.L., Fuess H., Jadrowskii E.L., Ovchinnikov S.G.. Phonon density of states in γ-, β- and α- AgCuS. Физика Твердого Тела, 50, вып.2, 2008, с.307-310. (русское название)
13. Благовещенский Н.М., Морозов В.А., Новиков А.Г., Пашнев М.А., Савостин В.В., Савостин Д.В. Исследование микродинамики жидкого лития методом неупругого рассеяния нейтронов. Труды регионального конкурса научных проектов в области естественных наук, Издательство АНО "Калужский научный центр", Вып.13, 2008, с.361.
14. Ион М., Козлов Ж.А., Матиеску Г., Падуреану И., Семенов В.А., Рапеану С.Н., Крачун Л., Морозов В.М., Опреа А.И., Опреа К., Пучков А.В., Высокотемпературный термостат для нейтронных измерений TS3000K на спектрометре ДИН-2ПИ реактора ИБР-2. Сообщение ОИЯИ Р13-2008-66, 2008, 17с.
15. Калинин И.В., Кац Е., Коза М., Лаутер В.В., Лаутер Х., Пучков А.В., Обнаружение сверхтекучей фазы в твердом гелии. Письма в ЖЭТФ, 87, вып.11, 2008, с.743-746. (английское название)
16. Калинин И.В., Лаутер-Пасюк В.В., Пучков А.В.. Нейтронография атомарных пленок жидкого гелия в терморасширенном графите. Труды регионального конкурса научных проектов в области естественных наук, Издательство АНО "Калужский научный центр", 2008, Вып.13, с.90.
17. Смирнов Л.С., Возниак К., Доминиак П., Лоозе А., Натканец И., Фронтасьева М.В., Помякушина Е.В., Баранов А.И., Долбинина В.В. Уточнение кристаллической структуры [Rbx(NH4)1-x]3H(SO4)2. I. Рентгеновская и нейтронная монокристальная дифракция фазы II с x=0.11 при 300. Кристаллография, 53(2), 2008, с. 232-241. Smirnov L.S., Wozniak K., Dominiak P., Loose A., Natkaniec I., Frontasyeva M. V., Pomyakushina E.V., Baranov A. I., Dolbinina V V. Refinement of the Crystal Structure of [Rbx(NH4)1–x]3H(SO4)2 (x = 0.11) by Single-Crystal X-ray and Neutron Diffraction: I. Phase II at 300 K. Crystallography Reports, 2008, Vol. 53, No. 3, pp. 418–427.

6. Applied studies (texture, stresses, geological materials)

1. Taran Yu.V., Balagurov A.M., Sheverev S.G., Schreiber J., Korsunsky A.M., Vorster W.J.J., Bomas H., Stoeberl C. Neutron diffraction investigation of an in-plane biaxial fatigued stainless steel sample of cruciform geometry. J. Phys.: Condens. Matter, 2008, v.20, p.104257 (6).
2. Taran Yu. V., Balagurov A. M., Schreiber J., Stuhr U.. Residual stresses in a shape welded steel tube by neutron diffraction. J. Phys.: Condens. Matter, 2008, v.20, p.104258 (4).
3. Taran Yu.V., Balagurov A.M., Schreiber J., Korsunsky A.M. .Neutron diffraction analysis of stresses in an in-plane biaxially-fatigued stainless steel sample of cruciform geometry. Materials Science Forum, 2008, v. 571-572, pp. 131-136.
4. Sheverev S.G., Markova G.V., Sumin V.V. .In Situ Neutron Diffraction Study of Internal Stresses in 60% Mn-40% Cu Alloy Introduced by Ageing. Solid State Phenomena: Interaction Between Defects and Inelastic Phenomena in Solids, 2008, v. 137, pp 163 – 168.
5. Сумин В.В., Шеверев С.Г., Ведерников П.А., Schneider R., Wimpory R., Балагуров А.М. Результаты измерения остаточных деформаций в корпусе реактора ВВЭР-1000. Физика твердого тела, ноябрь 2008, принята к печати.
6. Никишин А.В., Николаев Д.И. Анализ вычисления усредненных упругих свойств материалов, имеющих не круговой характер полюсных фигур. Кристаллография, 2008, том 53, № 3, с. 526-529. Nikishin, A.V., Nikolaev D.I. Calculation of averaged elastic properties of materials having noncircular character of pole figures. Crystallography Reports, 2008, 53 (3), pp 493-496.
7. Scheffzük Ch., Walther K., Frischbutter A., Naumann R., Brovkin, I.V. Residual strain and texture of an anhydrite-dolomite-specimen, sampled in the Piora-syncline (Central Switzerland). Z. geol. Wiss, 2008, v. 36 (1-2), pp 39-60.
8. Siegesmund S., Mosch S., Scheffzük Ch. , Nikolayev D.I... The bowing potential of granitic rocks: Rock fabrics, thermal properties and residual strain. Environ. Geol. 2008, v. 55, pp 1437-1448.
9. Walther K., Scheffzük Ch., Frischbutter A., Naumann R., Brovkin I.V. A “Zuckerdolomit”-sample from the Piora Mulde (Switzerland), studied by an in situ applied load experiment using neutron time-of-flight diffraction. Z. geol. Wiss, 2008, v. 36 (3), pp 123-138.
10. Никитин А.Н., Иванкина Т.И., Уллемайер К., Васин Р.Н. Аналогичные кристаллографические текстуры кварца в горных породах континентальной земной коры по данным нейтронографии. Часть I. Типизация текстур в мономинеральных горных породах. Кристаллография, 2008, т. 53, № 5, с 902-909. Nikitin A.N., Ivankina T.I., Ullemeyer K., Vasin

R.N. Similar quartz crystallographic textures in rocks of continental Earth's crust (by neutron diffraction data): I. Quartz textures in monomineral rocks. Crystallography Reports, 2008, Vol.53, № 5, pp 812-818.

11. Никитин А.Н., Иванкина Т.И., Уллемайер К., Васин Р.Н. Аналогичные кристаллографические текстуры кварца в горных породах континентальной земной коры по данным нейтронографии. Часть II. Типизация текстур в многофазных горных породах. Кристаллография. 2008, т. 53, № 5, с 910-918. Nikitin A.N., Ivankina T.I., Ullemeyer K., Vasin R.N. Similar quartz crystallographic textures in rocks of continental Earth's crust (by neutron diffraction data): II. Quartz textures in multiphase rocks. Crystallography Reports, 2008, Vol.53, № 5, pp 819-827.
12. Никитин А.Н., Иванкина Т.И., Уллемайер К., Васин Р.Н. Аналогичные кристаллографические текстуры кварца в горных породах континентальной земной коры по данным нейтронографии. Часть III. Связь типов текстур кварца с механизмами и условиями текстурообразования. Кристаллография. 2008, т. 53, № 5, с 919-928. Nikitin A.N., Ivankina T.I., Ullemeyer K., Vasin R.N. Similar quartz crystallographic textures in rocks of continental Earth's crust (by neutron diffraction data): III. Relation of quartz texture types with means and conditions of texture formation. Crystallography Reports, 2008, Vol.53, № 5, pp 828-836.
13. Kern H., Ivankina T.I., Nikitin A.N., Lokajicek T., Pros Z. The effect of oriented microcracks and crystallographic and shape preferred orientation on bulk elastic anisotropy of a strongly foliated biotite gneiss. Tectonophysics. 2008, Vol.457, № 3-4, pp 143-149.
14. Родкин М.В., Никитин А.Н., Васин Р.Н. Сейсмотектонические эффекты твердотельных превращений в геоматериалах. М.: Геос, 2008, 220 с. (Монография, поддержана грантом РФФИ, № 08-05-07049).
15. Базалеев Н.И., Бандурян Б.Б., Воробьев И.Б., Иванкина Т.И., Клепиков В.Ф., Литвиненко В.В., Лонин Ю.Ф., Никитин А.Н. и др. Радиационные методы оценки рисков захоронения радиоактивных отходов в горных породах. Енергетика, економіка, технології, екологія. Науковый журнал. Національный технічний університет України. 2008, № 2 (21), с.78-84.
16. Никитин А.Н., Иванкина Т.И., Игнатович В.К. Особенности распространения продольных и поперечных упругих волн в текстурированных горных породах. Физика Земли, 2008, принято к печати. Сообщения ОИЯИ, 2008, Р18-2008-50.
17. Никитин А.Н., Васин Р.Н., Родкин М.В. Возможное влияние полиморфных переходов в минералах (на примере кварца) на сейсмотектонические процессы в литосфере. Физика Земли, 2008, принято к печати.

18. Kern H., Mengel K., Strauss K.W., Ivankina T.I., Nikitin A.N., Kukkonen I.T. 2008: Elastic wave velocities, chemistry and modal mineralogy of crustal rocks sampled by the Outokumpu Scientific Drill Hole: evidence from lab measurements and modeling. Physics of the Earth and Planetary Interiors (in press).
19. Rudaev V., Locajicek T., Vasin R.V., Nikitin A.N. Application of acoustic emission and ultrasonic sounding for assessment of heating influence to rock samples fracturing. International Journal of Rock Mechanics and Mining Sciences. 2008 (in press).

7. Reports at Schools and Conferences

1. Anitas E, Islamov A.Kh, Erhan R. Balasoiu M., Bica I, Osipov V.A., Kuklin A.I.. SANS of interacting microsized particles in a polymer matrix., Moscow International Symposium on Magnetism (MISM'08), June 20-25 2008, Book of Abstracts, p. 462, 23 PO-3-17.
2. Avdeev M.V. Introduction to small-angle neutron scattering. Lecture, 2008 Summer Student Practice in JINR Fields of Research, 29.06.-20.07.2008, Dubna, Russia.
3. Avdeev M.V. Structure research of magnetic colloidal systems for biomedical applications, JINR days in Hungary, December 3-7, Budapest, Hungary.
4. Avdeev M.V., Bica D., Vekas L., Aksenov V.L., Feoktystov A.V., Rosta L., Garamus V.M., Willumeit R. Structural aspects of ferrofluids stabilization with mono-carboxylic acids, 4th International Conference «Physics of Liquid Matter: Modern Problems (PLMMP-2008)», May 23-26, Kyiv, Ukraine.
5. Avdeev M.V., Bica D., Vekas L., Aksenov V.L., Feoktystov A.V., Rosta L., Garamus V.M., Willumeit R. Structural aspects of stabilization of magnetic fluids by monocarboxylic acids, Moscow International Symposium on Magnetism 2008 (MISM-2008), June 20-25, Moscow, Russia.
6. Avdeev M.V., Feoktystov A.V., Aksenov V.L., Vekas L., Garamus V.M., Willumeit R. Structural Aspects of Stabilization of Ferrofluids by Small-Angle Neutron Scattering, Deutsche Neutronenstreutagung 2008, September 15-17, Garching, Germany.
7. Avdeev M.V., Petrenko V.I., Feoktystov A.V., Bodnarchuk V.I., Tropin T.V., Willumeit R., Garamus V.M., Schuster A., Mucha B., Aksenov V.L., Porokhova A.V., Lamszus L. Structural aspects of biocompatible ferrofluids by scattering methods: stabilization, properties control and applications, Workshop Helmholtz-JINR, June 24, 2008, Dubna, Russia.
8. Avdeev M.V., Rozhkova N.N., Aksenov V.L., Garamus V.M., Willumeit R., Ōsawa E. Aggregate Structure in Concentrated Liquid Dispersions of Ultrananocrystalline Diamond by Small-Angle

Neutron Scattering, 3rd International Symposium on Detonation Nanodiamonds: Technology, Properties and Applications, July 1–4, 2008, St Petersburg, Russia.

9. Balagurov A.M. ADVANCED NEUTRON DIFFRACTION AT PULSED SOURCES: NEW IDEAS, NEW TECHNIQUE, NEW SCIENCE. 13th International Seminar on "Neutron Scattering Investigation in Condensed Matter", Adam Mickiewicz University, May 8 –10, 2008, Poznan, Poland.
10. Balagurov A.M. NEUTRON DIFFRACTION AT PULSED SOURCES. 53rd Annual Conference of the South African Institute of Physics (SAIP), 8 – 11 July 2008, University of Limpopo, Polokwane, SA.
11. Balasoiu M, Aksenov V.L., Bica D., Vekas L., Barsov S.G., Vorobev S.I., Gritsaj K.I., Duginov V.N., Komarov E.N., Koptev V.P., Kotov S.A., Mamedov T.N., Mikirtychyants C.M., Shcherbakov G.V., Tripadus V.Muon and muopnium fractions behavior in ferrofluids. Moscow International Symposium on Magnetism (MISM'08), June 20-25 2008, Book of Abstracts, pag.401, 23RP-F-4
12. Balasoiu M, Craus M.L., Anitas E.M, Erhan R., Kuklin A.I., Islamov A.Kh, Kovalev Yu.S., Ivankov A.I., Lozovan M., Muresan C.,Tripadus, Savu D., Savu S., Bica I. Physical modifications induced in elastomers by Fe particles doping. Moscow International Symposium on Magnetism (MISM'08) June 20-25 2008, Book of Abstracts, pag.454, 23 PO-3-9
13. Balasoiu M, Craus M.L., Haramus V, Plestil J., Kuklin A.I., Erhan R., Anitas E.M, Lozovan M., Schreyer A., Tripadus V., Bica I. Magnetic microstructure of magnetite doped elastomers investigated by SANS and SAXS. Moscow International Symposium on Magnetism (MISM'08), June 20-25 2008, Book of Abstracts, pag.234, 22RP-E-7
14. Balasoiu M. Magnetic fluids and their applications. Invited lecture, 13 International Seminar on Neutron Scattering 8-10 May , Poznan, Poland.
15. Balasoiu M., Aksenov V.L., Bica D., Vekas L., Barsov S.G., Vorobev S.I., Gritsaj K.I., Duginov V.N., Zhukov V.A., Komarov E.N., Koptev V.P., Kotov S.A., Mamedov T.N., Shcherbakov G.V., Petrescu C. Investigationn of magnetite ferrofluid by means of positive polarized muons. IBWAP2008, Constanta 7-9 July 2008.
16. Balasoiu M., Anitas E., Bica I., Erhan R., Orelovich O.L., Osipov V., Kuklin. A.I. SANS of interacting magnetic micro-sized Fe particles in a stomaflex creme polymer matrix. ERMR08 Dresden, 25-29 August 2008.
17. Balasoiu M., Bica I., anitas E.M., Islamov A.Kh., Erhan R., Osipov V.A., Kuklin A.I. SANS of interacting magnetic micro-sized Fe particles in a stomaflex creme polymer matrix. CNF 2008 Bucuresti, September

18. Balasoiu M., Craus M.L., Kuklin A.I., Plestil J., Haramus V., Islamov A.H., Erhan R., Anitas E.M., Lozovan M., Tripadus V., Petrescu C., Savu D., Savu S., Bica I. Physical modifications induced in elastomers by magnetic particles doping. IBWAP2008, Constanta 7-9,July 2008.
19. Budziak A., Krawczyk J., Natkaniec I., Zielinski P. Sieverts apparatus at the IFJ, Krakow. HyCones (Hydrogen Storage in Carbon Cones), SINTEF/NTNU – Technical University ,24-Month Meeting, 12-13 November 2008, , Trondheim, Norway.
20. Bulkin A.P., Schebetov A.F., Kudryashev V.A., Pleschanov N.K., Zhuravlov V.V., Frischbutter A. , Walther K. Проект нейтроноводной системы 7 канала реактора ИБР-2М. Abstract at the XX. Conference for using neutron diffraction for investigations of condensed states. PIKS-2008, Gatchina (Russia), October 13-19, 2008 Met-22, p. 152.
21. Craus M.L., Cornei N., Lozovan M., Balasoiu M. Magnetoresistance of La0.54Ho0.11(Sr/Ca)0.35-x(K/Na)xMnO3 manganites. Moscow International Symposium on Magnetism (MISM'08), June 20-25 2008, Book of Abstracts, pag.642, 24PO-7-28
22. Feoktystov A., Avdeev M., Aksenov V., Bulavin L., Bica D., Vekas L., Garamus V., Willumeit R. Contrast variation in small-angle neutron scattering from magnetic fluids as polydisperse superparamagnetic systems, Deutsche Neutronenstreutagung 2008, September 15-17, Garching, Germany.
23. Feoktystov A.V., Avdeev M.V., Aksenov V.L., Bulavin L.A., Bica D., Vekas L., Garamus V.M., Willumeit R. Small-angle neutron scattering contrast variation on polydisperse superparamagnetic systems, 4th International Conference «Physics of Liquid Matter: Modern Problems (PLMMP-2008)», May 23-26, Kyiv, Ukraine.
24. Feoktystov A.V., Avdeev M.V., Aksenov V.L., Bulavin L.A., Bica D., Vekas L., Garamus V.M., Willumeit R. Contrast variation in small-angle neutron scattering from magnetic fluids as polydisperse and superparamagnetic systems, Moscow International Symposium on Magnetism 2008 (MISM-2008), June 20-25, Moscow, Russia.
25. Internal dynamics study of ethisterone by IINS, QC and 1H NMR methods.13th International Seminar on Neutron Scattering Investigations in Condensed Matter, UAM, 8 -10 May, 2008 Poznań, Poland.
26. K. Hołderna-Natkaniec, I. Natkaniec, R. Jakubas, E. Grech, E. Mikuli, J. Swiergiel, Dynamics of hydrogen bonds of 4-aminopiridinium with different anions studied by IINS, IR, NMR and QC methods. Polish conference on molecular crystals (KM2008), Poznań-Błażejewko, 8 – 12 September 2008.
27. Kern H., Mengel K., Strauss K.W., Ivankina T.I., Nikitin A.N., I.T. Kukkonen. Elastic wave velocities, chemistry and modal mineralogy of crustal rocks sampled by the Outokumpu Scientific

Drill Hole: evidence from lab measurements and modeling. IX международная конференция "Физико-химические и петрофизические исследования в науках о Земле", 9-11 октября, 2008, Москва.

28. Kozhevnikov S.V., Ott F. Data representations in off-specular neutron reflection. РНИКС-2008, 13-19 октября 2008, г. Гатчина, Россия. Стендовый доклад.
29. Kozhevnikov S.V., Ott F., Paul A., Rosta L. Resonances and off-specular scattering from neutron waveguides. International Conference on Surface X-Ray and Neutron Scattering (SXNS-10), 2-5 July 2008, Paris, France, poster
30. Kyzyma O.A., Avdeev M.V., Bulavin L.A., Aksenov V.L., Tropin T.V., Snegir S.V., Korobov M.V., Rosta L. Reorganization of fullerene clusters in the system C60/NMP after addition of water, 4th International Conference «Physics of Liquid Matter: Modern Problems (PLMMP-2008)», May 23-26, Kyiv, Ukraine.
31. Kyzyma O.A., Avdeev M.V., Bulavin L.A., Aksenov V.L., Tropin T.V., Snegir S.V., Korobov M.V., Rosta L. Reorganization of fullerene clusters in the system C60/NMP/water after addition of water, Joint International Summer School-Conference "Advanced Materials and Technologies", August 27-31, 2008, Palanga, Lithuania.
32. Murugova T.N., Gordeliy V.I., Kuklin A.I., Ivankov A.I., Solodovnikova I.M., Yurkov V.I., Yaguzhinsky L.S. Study of mitochondrial membrane structure by small angle neutron scattering. The 28th meeting of PAC for Condensed Matter Physics, 16–17 June 2008, Dubna, Russia.
33. Natkaniec I. Development of inelastic neutron scattering methods for research of molecular dynamics of condensed matter. Programme Advisory Committee for Condensed Matter Physics, 28th meeting, June 16-17, 2008, Dubna, Russia.
34. Natkaniec I., Hołderna-Natkaniec K. Quantum chemistry modeling of the INS and IR spectra of carbon cone clusters. HyCones Meeting (Hydrogen Storage in Carbon Cones), Institute of Nuclear Physics, Polish Academy of Sciences, May 27-28, 2008, Kraków, Poland.
35. Natkaniec I., Hołderna-Natkaniec K., Juszyńska E., Massalska-Arodź M., Ściesińska E., Ściesiński J., Hydrogen bonds and molecular dynamics of dimethyl-butanols. Polish conference on molecular crystals (KM2008), Poznań-Błażejewko, 8 – 12 September 2008.
36. Natkaniec I., Hołderna-Natkaniec K., Rachwalska M., Urbanek Z., Zborowski K. The structure and molecular dynamics of bioactive (E)-2-hydroxyimino-2-cyanoacetic acid ethyl ester as seen by NPD and IINS neutron scattering methods. 13th International Seminar on Neutron Scattering Investigations in Condensed Matter, UAM, 8 -10 May, 2008, Poznań, Poland.

37. Natkaniec I., Hołderna-Natkaniec K., Rachwalska M., Urbanek Z., Zborowski K. The structure and molecular dynamics of bioactive (E)-2-hydroxyimino-2-cyanoacetic acid ethyl ester as seen by NPD and IINS neutron scattering methods. 13th International Seminar on Neutron Scattering Investigations in Condensed Matter, UAM, 8 -10 May, 2008, Poznań, Poland.
38. Nowak D., Hołderna-Natkaniec K., Natkaniec I., Jurga K., Peplińska B., Internal dynamics study of ethisterone by IINS, QC and 1H NMR methods.13th International Seminar on Neutron Scattering Investigations in Condensed Matter, UAM, 8 -10 May, 2008 Poznań, Poland.
39. Petrenko V.I., Avdeev M.V., Aksenov V.L., Bulavin L.A., Rosta L. Effect of surfactant excess in non-polar ferrofluids by small-angle neutron scattering, Moscow International Symposium on Magnetism 2008 (MISM-2008), June 20-25, Moscow, Russia.
40. Petrenko V.I., Avdeev M.V., Bulavin L.A., Aksenov V.L., Rosta L. Behavior of mono-carboxylic acids in non-polar organic solvent by small-angle neutron scattering, Joint International Summer School-Conference "Advanced Materials and Technologies", August 27-31, 2008, Palanga, Lithuania.
41. Petrenko V.I., Avdeev M.V., Bulavin L.A., Rosta L. Solutions of dodecylbenzene sulfonic acid in polar carrier studied by small-angle neutron scattering, 4th International Conference «Physics of Liquid Matter: Modern Problems (PLMMP-2008)», May 23-26, Kyiv, Ukraine.
42. Ryabova N.Yu., Kiselev M.A., Dante S., Hauß Th., Balagurov A.M. Investigation of stratum corneum lipid model membranes with free fatty acids composition by neutron diffraction. 6th Euro Fed Lipid Congress, 07-11 September, 2008, Athens, Greece.
43. Scheffzük Ch., Walther K., Frischbutter A., Bulkin A.P. , Schilling F. The new neutron guide system for the time-of-flight diffractometers at the beamline 7 of the pulsed neutron source IBR-2M Dubna. German Neutron Scattering Conference, september 15-17, 2008, Garching, Germany.
44. Авдеев М.А., Мартынов П.Н., Мельников В.П., Новиков А.Г., Пучков А.В. Исследование микроструктуры активированных углей методом малоуглового рассеяния медленных нейтронов. РНИКС-2008, 13-19 октября 2008, Гатчина, Россия.
45. Авдеев М.В. Нейтронография магнитных жидкостей для биомедицинских приложений. Лекция, Высшие курсы стран СНГ «Синхротронные и нейтронные исследования наносистем (СИН-нано)», 7-26 июля, 2008, Москва-Дубна, Россия.
46. Авдеев М.В. Нейтронография магнитных жидкостей. VIII научная конференция молодых ученых и специалистов ОИЯИ. Лекция, 4−8 февраля, 2008 г, Дубна, Россия.
47. Авдеев М.В., Аксенов В.Л., Векаш Л., Феоктистов А.В., Петренко В.И., Рошта Л., Гарамус В.М., Виллумайт Р. Структурные аспекты стабилизации магнитных жидкостей моно-карбоксильными кислотами по данным малоуглового рассеяния нейтронов, Российское

Совещание по Использованию Рассеяния Нейтронов в Исследованиях Конденсированных Сред (РНИКС-2008), 13-19 октября, Гатчина, Россия.

48. Аксенов В.Л., Тропин Т.В., Кизима О.А., Авдеев М.В., Коробов М.В., Рошта Л. К вопросу об образовании кластеров фуллерена С60 в азот-содержащих растворителях, Российское Совещание по Использованию Рассеяния Нейтронов в Исследованиях Конденсированных Сред (РНИКС-2008), 13-19 октября, Гатчина, Россия.
49. Балагуров А.М. Мезоскопическое фазовое расслоение в сложных магнитных оксидах марганца. XI МЕЖДУНАРОДНЫЙ, МЕЖДИСЦИПЛИНАРНЫЙ СИМПОЗИУМ «ПОРЯДОК, БЕСПОРЯДОК И СВОЙСТВА ОКСИДОВ" (ODPO-11), 16-21 сентября 2008 г, Ростов-на-Дону, Россия.
50. Балагуров А.М. Нейтронные исследования мезоскопического фазового расслоения в сложных оксидах переходных металлов. Международная школа-семинар «Современные импульсные источники нейтронов (PANS III)», 29.01-4.02.2008, Дубна, Россия.
51. Балагуров А.М. Спектрометры на реакторе ИБР-2М: статус и перспективы . XX совещание по использованию рассеяния нейтронов в исследованиях конденсирован-ного состояния (РНИКС-2008), 13 – 19 октября 2008, Гатчина, Россия.
52. Балашою М., Краус М.Л., Гарамус В., Плештил Ж., Исламов А.Х., Куклин А.И., Ерхан Р., Анитас Е.М., Осипов В.А., Бика И., Аксенов В.Л. Исследование магнитных эластомеров методами МУРН и МУРР, XX совещание по использованию рассеяния нейтронов в исследованиях конденсированного состояния (РНИКС-2008), 13 – 19 октября 2008, Гатчина, Россия., Тезисы, ISBN 978-5-86763-212-0, PNPI (2008) p.38
53. Балашою М., Куклин А.И., Грабчев Б., Ионита И., Ука О., Охмс К., Юцос Г. Наблюдение нанофазных структур в бинарных сталях МУРН методом, XX совещание по использованию рассеяния нейтронов в исследованиях конденсирован-ного состояния (РНИКС-2008), 13 – 19 октября 2008, Гатчина, Россия., Тезисы, ISBN 978-5-86763-212-0, PNPI (2008) p.127
54. Балашою М., Санду В., Горделий В.И., Петренко А.В., Куклин А.И. Исследование магнитных структур в YBa2Cu3O7-d. XX совещание по использованию рассеяния нейтронов в исследованиях конденсирован-ного состояния (РНИКС-2008), 13 – 19 октября 2008, Гатчина, Россия., Тезисы, ISBN 978-5-86763-212-0, PNPI (2008) p.122
55. Благовещенский Н.М., Новиков А.Г., Осава Е., Рожкова Н.Н. Квазиупругое рассеяние нейтронов водной дисперсией наноалмазов. РНИКС-2008, 13-19 октября 2008, Гатчина, Россия.
56. Благовещенский Н.М., Новиков А.Г., Савостин В.В. Коллективные моды в жидком литии:

исследование методом неупругого рассеяния нейтронов. РНИКС-2008, 13-19 октября 2008, Гатчина, Россия.

57. Благовещенский Н.М., Новиков А.Г., Савостин В.В., Шимкевич А.Л..Структурные и микродинамические особенности жидких металлов из экспериментов по рассеянию нейтронов. X11 Российская конференция по теплофизическим свойствам веществ (РКТС-12), октябрь 2008, Москва, Россия.
58. Василовский С. Г., Бескровный А. И., Симкин В. Г., Кодесс Б. Н.. Особенности водородной связи в кристаллах твердых растворов КДП-ДКДП. XX совещание по использованию рассеяния нейтронов в исследованиях конденсированного состояния (РНИКС 2008), 13-19 октября 2008, Гатчина, Россия.
59. Васин Р.Н., Никитин А.Н. Нейтронографические исследования кристаллографических текстур кварца в горных породах континентальной коры Земли. «XX совещание по использованию рассеяния нейтронов в исследованиях конденсированного состояния (РНИКС-2008)», 13-19 октября 2008 г, Гатчина, Россия.
60. Васин Р.Н., Никитин А.Н., Локаичек Т. Деформации и акустическая эмиссия в моно- и поликристаллическом кварце при температурах 20-600°С и одноосных нагрузках до 120 МПа. IX международная конференция “Физико-химические и петрофизические исследования в науках о Земле”, 7-10 октября, 2008, Москва.
61. Дубовский О.А., Орлов А.В. Излучение пучков сверхзвуковых и дозвуковых солитонных волн – генераторов реструктуризации нанокристаллов при бомбардировке атомами. Российский Семинар ТММ – 2008 (Теория и многоуровневое моделирование дефектов, явлений и свойств материалов ядерной техники), ВНИИМ, июнь 2008 ,Москва, Россия.
62. Дубовский О.А., Орлов А.В. Излучение пучков сверхзвуковых солитонных волн - генераторов реструктуризации нанокристаллов при бомбардировке атомами и самоорганизация динамической суперрешетки комплексов солитонных колебаний атомов. РНИКС-2008, 13-19 октября 2008, Гатчина, Россия.
63. Иваньков О. И., Горделий В. И., Мачулин А. В., Соловьев Д. В., Утробин П. К., Куклин А.И. Исследование липидных мембран под высоким гидростатическим давлением. Тезисы докладов XX совещания по использованию рассеяния нейтронов в исследованиях конденсированного состояния. РНИКС-2008, 13-19 окт. 2008г. Гатчина, Россия, с.173.
64. Калинин И.В., Кац Е., Коза М., Лаутер В.В., Лаутер Х., Пучков А.В. Сверхтекучесть в твердом гелии. РНИКС-2008, 13-19 октября 2008, Гатчина, Россия.
65. Кизима А.А. Организация кластеров фуллерена в системе С60/N-метил-2-пирролидон. VIII

научная конференция молодых ученых и специалистов ОИЯИ, 4−8 февраля, 2008 г, Дубна, Россия.

66. Киселев М.А. Наноструктура однослойных фосфолипидных везикул и четырехкомпонентных липидных мембран на основе церамида 6. XX совещание по использованию рассеяния нейтронов в исследованиях конденсированного состояния (РНИКС 2008), 13-19 октября 2008, Гатчина, Россия.
67. Киселев М.А., Ермакова Е.В., Данте С., Хаус Т., Балагуров А.М.. Исследования наноструктуры бислоя фосфолипид/лизофосфолипид методом дифракции нейтронов. XX Совещание по использованию рассеяния нейтронов в исследованиях конденсированного состояния (РНИКС 2008), 13-19 октября 2008, Гатчина, Россия.
68. Киселев М.А., Ермакова Е.В., Филиппова С.Н., Сургучева Н.А., Данте С., Хаус Т., Гальченко В.Ф.. Структурная организация липидных мембран, построенных на основе фосфолипидной фракции клеточных мембран Streptomyces hygroscopicus. IV Молодежная школа-конференция с международным участием «Актуальные аспекты современной микробиологии», 20-22 октября, 2008, ИНМИ им. С.Н. Виноградского, Москва.
69. Кичанов С.Е. Исследование структуры молекулярных кристаллов солей пиридина PyHNO3 и PyHReO4 при высоких давлениях. РНИКС-2008, 13-19 октября, 2008,Гатчина,Россия.
70. Козленко Д.П. Подавление антиферромагнитного состояния и спиновый переход в Y0.3Sr0.7CoOO2.62 . РНИКС-2008, 13-19 октября,2008, Гатчина, Россия.
71. Козленко Д.П.Структурные исследования с использованием нейтронографии, лекция. Высшие курсы для стран СНГ Син-Нано, 7-25 июля, 2008, Дубна, Россия.
72. Куклин А. И., Исламов А. Х., Ковалев Ю. С., Муругова Т. Н., Рогачев А.В., Иваньков А. И., Горшкова Ю. Е., Балашою М., Соловьев Д. В., Кутузов С. А., Соловьев А. Г., Сиротин А. П., Кирилов А. С., Горделий В. И. Исследование структуры и свойств наноматериалов с помощью малоуглового рассеяния нейтронов. Роснанофорум, 3-5 декабря 2008 г. Москва т.1.стр.257-258.
73. Куклин А. И., Исламов А. Х., Утробин П. К., Кутузов С. А., Ковалев Ю. С., Рогачев А. В., Иваньков О. И., Горделий В. И. Позиционно-чувствительный детектор в двухдетекторной системе регистрации нейтронов на малоугловом спектрометре ЮМО. Тезисы докладов XX совещания по использованию рассеяния нейтронов в исследованиях конденсированного состояния. РНИКС-2008, 13-19 окт. 2008г. Гатчина, Россия, с.135-136.
74. Куклин А. И., Пепи Ж., Костромин С., Шван Д., Черезов В. Г., Рогачев А. В., Шибаев В.П.. Прецизионное определение параметров гребнеобразного жидкокристаллического полимера.

Тезисы докладов XX совещания по использованию рассеяния нейтронов в исследованиях конденсированного состояния РНИКС-2008, 13-19 окт. 2008г, Гатчина, Россия, с.71.

75. Лашкарёв Г.В., Дмитриев А.И. Буторин П. Е., Бескровный А. И., Миникаев Р.. Исследование магнитных превращений в слоистом полупроводнике InSe<Mn> методами нейтронной дифракции. XX совещание по использованию рассеяния нейтронов в исследованиях конденсированного состояния (РНИКС 2008), 13-19 октября 2008, Гатчина, Россия.
76. Лохматов В.И., Новиков А.Г., Пучков А.В., Сиротин А.П. Механический монохроматор для малоуглового спектрометра на реакторе SAFARI-1 (NECSA, Южная Африка). РНИКС-2008, 13-19 октября 2008, Гатчина, Россия.
77. Лукин Е.В. Влияние высокого давления на кристаллические и магнитные свойства манганита La0.55Ca0.45MnO3. РНИКС-2008, 13-19 октября, 2008, Гатчина, Россия.
78. Муругова Т. Н., Иваньков О. И., Исламов А. Х., Дроздов А. В., Горделий В. И., Куклин А. И. Восстановление структуры белков из данных МУРН, полученных на модернизированном спектрометре ЮМО. Тезисы докладов XX совещания по использованию рассеяния нейтронов в исследованиях конденсированного состояния. РНИКС-2008, 13-19 окт. 2008г. Гатчина, Россия, с.160.
79. Муругова Т.Н., Горделий В.И., Исламов А.Х., Куклин А.И., Солодовникова И.М., Юрков В.И., Ягужинский Л.С. Изучение структуры сердечных митохондрий с помощью метода малоуглового рассеяния нейтронов. XLII Зимняя школа ПИЯФ, 25 февраля-1 марта 2008, Репино, Россия.
80. Муругова Т.Н., Иваньков О.И., Исламов А.Х., Дроздов А.В., Горделий В.И., Куклин А.И. Восстановление структуры белков из данных МУРН, полученных на модернизированном спектрометре ЮМО. XX совещание по использованию рассеяния нейтронов в исследованиях конденсированного состояния (РНИКС-2008), 13 – 19 октября 2008, Гатчина, Россия.
81. Натканец И., Холдерна-Натканец К., Новак Д. Нейтронные исследования конденсированных фаз и квантово-химическое моделирование структуры и динамики изомеров гексана – C6H14, XX Совещание по использованию рассеяния нейтронов в исследованиях конденсированного состояния (РНИКС–2008), 13–19 октября, 2008, Гатчина, Россия.
82. Никитенко Ю.В. Зимняя школа ПИЯФ, март 2008, Санкт-Петербург, Репино.
83. Никитенко Ю.В. Нейтронная рефлектометрия слоистых структур с использованием стоячих волн поляризованных нейтронов. XII Международный Симпозиум, 10-14 марта 2008, Нижний Новгород, Россия, устный доклад.

84. Никитин А.Н., Иванкина Т.И., Игнатович В.К. Квазипродольные и квазипоперечные упругие волны в текстурированных горных породах. IX международная конференция “Физико-химические и петрофизические исследования в науках о Земле”, 7-10 октября, 2008, Москва.
85. Папушкин И.В., Попа Н., Сумин В.В., Шеверёв С.Г., Вимпори Р., Балагуров А.М. Новый метод определения остаточных деформаций в сильно - текстурированных образцах. XX совещание по использованию рассеяния нейтронов в исследованиях конденсирован-ного состояния (РНИКС-2008), 13 – 19 октября 2008, Гатчина, Россия.
86. Петренко В.И. Структурные особенности стабилизации магнитных жидкостей. VIII научная конференция молодых ученых и специалистов ОИЯИ, 4−8 февраля, 2008 г, Дубна, Россия.
87. Петренко В.И., Аксенов В.Л., Авдеев М.В., Булавин Л.А., Рошта Л., Векаш Л., Гарамус В.М., Виллумайт Р. Нейтронные исследования влияния структуры магнитных жидкостей на их стабильность, Российское Совещание по Использованию Рассеяния Нейтронов в Исследованиях Конденсированных Сред (РНИКС-2008), 13-19 октября, Гатчина, Россия.
88. Рогачев А. В., Черный А. Ю., Озерин А. Н., Музафаров А. М., Татаринова Е. А., Исламов А. Х., Горделий В. И., Куклин А. И. Внутренняя структура поликарбосилановых дендримеров. Тезисы докладов XX совещания по использованию рассеяния нейтронов в исследованиях конденсированного состояния. РНИКС-2008, 13-19 окт. 2008г, Гатчина, Россия, с.75.
89. Рябова Н.Ю., Киселев М.А., Бескровный А.И., Балагуров А.М. Исследование липидных мультислоев методом нейтронной дифракции в реальном времени. XX совещание по использованию рассеяния нейтронов в исследованиях конденсированного состояния (РНИКС 2008), 13-19 октября 2008, Гатчина, Россия.
90. Семенов В.А., Козлов Ж.А., Крачун Л., Матееску Г., Морозов В.М., Опреа А.И., Опреа К., Пучков А.В. Спектр частот тантала при температурах 293-2300К. РНИКС-2008, 13-19 октября 2008, Гатчина, Россия.
91. Хайдуков Ю.Н. Исследование магнетизма сверхпроводящих и магнитных наноструктур методом рефлектометрии поляризованных нейтронов. XII Международный Симпозиум, 10-14 марта 2008, Нижний Новгород, Россия, стендовый доклад.
92. Холдерна-Натканец К., Юшиньска Е., Массальска-Ародзь М., Натканец И., Сцесиньска Е., Сцесиньски Я. Нейтронная спектроскопия и квантово-химические расчеты водородных связи и вибрационных спектров молекулярных кластеров изомеров диметил-бутанола – C6H13OH. Совещание по использованию рассеяния нейтронов в исследованиях конденсированного состояния (РНИКС–2008), 13–19 октября, 2008, Гатчина, Россия.
93. Шеверев С.Г., Сумин В.В., Ведерников П.А., Schneider R., Wimpory R.C., Балагуров А.М. Результаты измерения остаточных деформаций в корпусе реактора ВВЭР-1000. XX

совещание по использованию рассеяния нейтронов в исследованиях конденсирован-ного состояния (РНИКС-2008), 13 – 19 октября 2008, Гатчина, Россия.

NEUTRON NUCLEAR PHYSICS

1. Experimental investigations

1. Andrianov V. R., Druzhinin A. A., Furman V. I., Gundorin N. A., Lihachev A. N., Pikelner L. B., Rebrova N. V., Salamatin I. M., Vyachin V. N., Zhdanova K. V., «Yield of delayed neutrons in the reaction 245Cm(n,f) on thermal neutrons», Physics of atomic nuclei, 2008, V.71, No.10, pp.1-9.
2. Bondarenko V., Tomandl I., Wirth H.-F., Honzatko J., Sukhovoj A.M., Malov L.A., Simonova L.I., Hertenberger R., T. von Egidy, Berzics J. Nuclear structure of 187W studied with (n,gamma) and (d,p) reactions, Nucl. Phys. A, 811 (2008) p. 28-76.
3. Guohui Zhang, Jiaguo Zhang, Rongtai Cao, Li'an Guo, Jinxiang Chen, Gledenov Yu. M., Sedysheva M. V., Khuukhenkhuu G., Szalanski P. J.. Measurement of Differential Cross Section for the 64Zn(n,a) 61Ni Reaction at 2.54, 4.00, and 5.50 MeV. NUCLEAR SCIENCE AND ENGINEERING: 160, 123–128 (2008).
4. Lee Y.S., Kim G.N., Ko I. S., Cho M. H., Namkung W., Gledenov Yu.M.. Development of a Plate-Parallel Gridded Ionization Chamber with Gaseous Samples for Fusion Neutronics. Journal of the Korean Physical Society, v.53 (4), p. 1848-1853 (2008).
5. Mutterer M., Kopatch Yu. N., Yamaledtinov S. R., Lyapin V. G., J. von Kalben, Khlebnikov S. V., Sillanpaa M., Tyurin G. P., Trzaska W. H. Energy distribution of ternary α particles in spontaneous fission of 252Cf, Physical Review C, 788, 6, 064616 (2008).
6. Pokotilovski Yu. N., Natkaniec I., Holderna-Natkaniec K. „The experimental and calculated density of states and UCN loss coefficient of perfluoropolyether oils at low temperature", Physica B409 (2008) 1942-1948.
7. Pokotilovski Yu. N., Novopoltsev M. I., Geltenbort P. „Test of the fast thin-film ferromagnetic shutters for ultracold neutrons", JINR Comm. P3-2008-139.
8. Pokotilovski Yu. N., Novopoltsev M. I., Geltenbort P. "A study of the ultracold neutron upscattering at reflection from solid surfaces", Eur. Phys. Journ. AP, accepted.
9. Nesvizhevsky V.V. , Lychagin E.V., Musychka A.Yu., Strelkov A.V., Pignol G. , Protasov K.V. "The reflection of very cold neutrons from diamond powder nanoparticles" // NIM A 595, (2008) 631-636.

10. Serebrov K., Varlamov V. E., Kharitonov A. G., Fomin A. K., Pokotilovski Yu. N., Geltenbort P., Krasnoschekova I. A., Lasakov M. S., Taldaev R. R., Vassiliev A. V., Zherebtsov O. M. “Neutron lifetime measurement using gravitationally trapped ultracold neutrons”, Phys. Rev. C78 (2008) 035505.
11. Sheets S.A., Agvaanluvsan U., Becker J.A., Becvar F., Bredeweg T.A., Haight R.C., Jandel M., Krticka M., Mitchell G.E., O'Donnell J.M., Parker W., Reifarth R., Rundberg R.S., Sharapov E.I., Ullmann J.L., Vieira D.J., Wilhelmy J.B., Wouters J.M., Wu C.Y.. “Test of the statistical model in 96Mo with the DANCE array”. Submitted to Phys. Rev. C (2008).
12. Sukhovoj A. M. Main parameters of the gamma-decay process and the property of nucleus174Yb,, which are manifested in the radiative capture of resonance and thermal neutrons.Physics of atomic nuclei, 2008, V.71, pp.1907-1917.
13. Sukhovoj A.M., Furman W.I., Khitrov V.A. Semiphenomenological approximation of the sums of experimental radiative strength functions for dipole gamma transitions in the region around Eγ~ Bn for masses number in the range 40 ≤A ≤ 200, Physics of atomic nuclei, 2008, V.71(6), pp.982-997
14. Vesna V. A., Gledenov Yu. M., Nesvizhevsky V. V., Petoukhov A. K., Sedyshev P. V., Soldner T., Zimmer O., Shulgina E. V.. *Measurement of the parity-violating triton emission asymmetry in the reaction 6Li(n, α)3H with polarized cold neutrons.* Phys. Rev., 2008, v. 77, p. 035501.
15. Анджеевски Ю., Гледенов Ю. М., Попова В. М., Суховой А.М., Хуухэнхуу Г.. Юрий Павлович Попов (к 80-летию со дня рождения). ЭЧАЯ, 2008, т. 39, вып.4, с. 1215-1232.
16. Андрианов В. Р., Вячин В.Н., Гундорин Н. А., Дружинин А. А., Жданова К. В., Лихачёв А. Н., Пикельнер Л. Б., Реброва Н. В., Саламатин, Фурман В. И. «Выход запаздывающих нейтронов в реакции 245 Cm (n,f) на тепловых нейтронах», Ядерная Физика, 2008, том 71, №10, с.1-9.
17. Гундорин Н.А., Дикусар Н.Д., Мазный Н.Г., Пикельнер Л.Б., Саламатин И.М., Цулаиа М.И. «Экспресс-анализ спектров в прецизионных экспериментах» Подписано к печати в Известия АН, сер. Физическая, №2, 2009.
18. Петров Г.А., Гагарский А.М., Гусева И.С., Копач Ю.Н., Генненвайн Ф., Муттерер М. О перспективах дальнейших исследований эффектов Т-нечетной асимметрии эмиссии легких частиц в тройном делении тяжелых ядер поляризованными нейтронами, Ядерная Физика , 71, 7, 1149-1155 (2008).
19. Суховой А. М. Основные параметры процесса гамма-распада и свойства ядра 174Yb, проявляющиеся при радиационном захвате резонансных и тепловых нейтронов, ЯФ, 2008, 71, с. 1937-1947.

20. Суховой А.М., Хитров В.А., Каскадный гамма-распад компаунд-состояния 191Os. Известия РАН, серия физическая, 2008, т.72, N 3, с. 392-401. A.M.Sukhovoi, V.A.Khitrov, Cascade γ decay of the 191Os compound state. Bull.Rus.Acad.Sci.Phys. 72, 366 (2008)ю
21. Суховой А.М., Фурман В.И., Хитров В.А. Полуфеноменологическая аппроксимация сумм экспериментальных радиационных силовых функций дипольных гамма-переходов в диапазоне Eγ~ Bn для области масс 40 ≤A ≤ 200, ЯФ, 2008, 71(6), 1009-1024.
22. Тюкавкин А.Н., Пятков Ю.В., Каманин Д.В., Копач Ю.Н., Александров А.А., Александрова И.А., Борзаков С.Б., Воронов Ю.Н., Денисов С.В., Ефимов Г.Л., Жучко В.Е., Кондратьев Н.А., Кузнецова Е.А., Лаврова Ю.Е., Митрофанов С.В., Пантелеев Ц., Саламатин В.С. Измерение ядерного заряда осколков деления большой ионизационной камерой в составе двухплечевого времяпролетного спектрометра, JINR Preprint, P15-2008-88, 17(2008).
23. Франк А.И., Гелтенборт П., Жентшель М., Кустов Д.В., Кулин Г.В., Носов В.Г., Стрепетов А.Н.. Эффект ускоряющегося вещества в нейтронной оптике. Ядерная Физика, 71 (2008),1686- 1704. Frank A.I., Geltenbort P., Jentschel M., Kustov D.V., Kulin G.V., Nosov V.G., Strepetov A.N.. Effect of Accelerated Matter in Neutron Optics. Physics of Atomic Nuclei, 71 (2009). 1656-1654.
24. Франк А.И., Кулин Г.В., Кустов Д.В., Гелтенборт П., Жентшел М., Носов В.Г., Стрепетов А.Н.. Первое наблюдение нового оптического эффекта с ультрахолодными нейтронами. Новости ОИЯИ, 2008, №1 С.17-19

2. Theoretical investigations

1. Bunatian G.G. «The Ward-Takahashi identities to describe nucleon and pion electroweak transitions». Preprint of JINR E2-2008-36, 2008.
2. Lyuboshitz V.L., Lyuboshitz V.V. “On the pair correlations of nuclear fission neutrons with small relative momenta” . Ядерная физика, т. 71 (3), 2008 , сс. 478-483 [Physics of Atomic Nuclei , v. 71, No. 3, 2008 , pp. 454-459].
3. Бунатян Г.Г. «Тождества Уорда-Такахаши в описании электрослабых переходов нуклонов и пионов». Журнал Экспериментальной и Теоретической Физики, том 134, вып.4(10), 2008 г., стр. 660-679.
4. Игнатович В.К. По поводу парадокса ЭПР , неравенств Белла и экспериментов, которые ничего не доказывают. Concepts of Physics, the old and new, v. 5, No 2, pp. 227-272, 2008.
5. Игнатович В.К. Фаза Берри. Простейший вывод и значение фазы Берри для поиска ЭДМ нейтрона с помощью УХН. Am.J.Phys. v.76, No 3, pp. 258-264, 2008.

6. Игнатович В. К. Одномерный периодический потенциал в квантовой механике. Вестник Новосибирского государственного университета. Серия: Физика, Т. 3, № 2, С. 99-107, 2008.
7. Игнатович В.К. О нейтронных поверхностных волнах. ОИЯИ Р4-2008-48.
8. Игнатович В.К. Аналитические расчеты нейтронных спектров для прямого измерения n-n рассеяния на импульсном реакторе ЯГУАР. ОИЯИ Е4-2008-49.
9. Игнатович В. К., Раду Ф. Отражение нейтронов от магнитных систем с веероподобной намагниченностью. Оияи р4-2008-63.
10. Никитин А.Н., Иванкина Т.И., Игнатович В.К. Особенности распространения продольных и поперечных упругих волн в текстурированных горных породах. Сообщение ОИЯИ Р4-2008-50.

3. Applied research

1. Aničić M., Tasić M., Frontasyeva M.V., Tomašević M., Rajšić S., Strelkova L.P., Steinnes E.. Active biomonitoring with wet and dry moss: a case study in an urban area. Accepted by *Environmental Chemistry Letters,* http://dx.doi.org/10.1007/s10311-008-0135-4, 2008.
2. Baljinnyam N., Belov A.G., Ganbold G., Gerbish Sh., Maslov O.D., Shvetsov V.N. Possibility of some radionuclides production using high energy electron Bremsstrahlung. Book of Abstracts, ISINN-16, 10-14 June, 2008, JINR Preprint, E18-2008-119, Dubna, 2008**,** pp. 11.
3. Barandovski L., Cekova M., Frontasyeva M.V., Pavlov S.S., Stafilov T., Steinnes E., Urumov V. Atmospheric deposition of trace element pollutants in Macedonia studied by the moss biomonitoring technique. Environmental Monitoring and Assessment, Vol. 138, 2008, p. 107-118, http://dx.doi.org/10.1007/s10661-007-9747-6.
4. Boháček P., Huran J., Kobzev A.P., Balalykin N.I., and Petzold J. PECVD silicon carbon nitrid thin films: properties. In: ASDAM 2008. The 7th Inter. Conf. Advanced Semicond. Devices Microsyst. Eds. Š. Haščík and J.Osvald. Piscataway: IEEE 2008. ISBN: 978-1-4244-2325-5. P. 291-294.
5. Budzynski P., Polanski K., Kobzev A.P. Changes in Surface Properties of Nitrogen-Implanted AISI316L Stainless Steel. Journal of Surface Investigations. X – ray, Synchrotron and Neutron Techniques, 2008, Vol. 2, No. pp. 657 – 662. Pleiades Publishing, Ltd., 2008.
6. Gerbish Sh., Baljinnyam N., Ganbold G., Ganchimeg G. Determination major and minor elements in sediments of central and northern Mongolian some rivers using INAA. Book of Abstracts, ISINN-16, 10-14 June, 2008, JINR Preprint, E18-2008-120, Dubna, 2008, pp. 9.
7. Harmens H., Norris D., Frontasyeva M.V., Vergel K.N., Pankratova Yu.S. et al. European Atlas: Spartial and temporal trends in heavy metal accumulation in mosses in Europe (1990-2005),

UNECE ICP Vegetation. Centre for Ecology & Hydrology, University of Wales Bangor, United Kingdom, July 2008, pp. 51, ISBN: 978-1-85531-239-5.

8. Huran J., Kobzev A.P., Balalykin N.I. and Petzold J. Hydrogenated amorphous carbon films prepared by plasma-enhanced chemical vapor deposition. In: ASDAM 2008. The 7th Inter. Conf. Advanced Semicond. Devices Microsyst. Eds. Š. Haščík and J.Osvald. Piscataway: IEEE 2008. ISBN: 978-1-4244-2325-5. P.127-130.
9. Klos A., Rajfur M., Waclawek M., Waclawek W., Frontasyeva M.V., Pankratova Ju.S. The influence of unidentified pollution sources on the irregularity of biomonitoring test results. Water, Air, and Soil pollution, Vol. 191, No. 1-4, June, 2008, p. 345-352, http://dx.doi.org/10.1007/s11270-008-9629-8.
10. Krzyzanowska H., Kobzev A.P., Zuk J., Kulik M. Hydrogen and oxygen concentration analysis of porous silicon. Journal of Non – Crystalline Solids, Vol. 354, 2008, pp. 4367 – 4374.
11. Meresova J., Florek M., Holy K., Ješkovský M., Sýkora I., Frontasyeva M.V., Pavlov S.S., Bujdoš M. Evaluation of elemental content in airborne particulate matter in low-level atmosphere of Bratislava. JINR Preprint, E18-24-2008, Dubna, 2008, pp. 18. Accepted by Atmospheric Environment, ATMENV-D-08-00266R1.
12. Bystritsky V.M., Gerasimov V.V., Kadyshevsky V.G., Kobzev A.P., Nozdrin A.A.. Rogov Yu.N., Rapatsky V.L., Sadovsky A.B., Salamatin A.V., Sapozhnikov M.G., Sissakian A.N., Slepnev I.V., Slepnev V.M., Utkin V.A., Zamyatin N.I., Peredery A.N., Likhachev N.P., Romanov I.V., Safonov M.V., .Sedin A.N. and Scherbakov A.G. DViN – STATIONARY SETUP FOR IDENTIFICATION OF EXPLOSIVES. Physics of Particles and Nuclei Letters. Vol. 5, No. 5, pp. 441 – 446, (2008).
13. Dutov A.G., Komar V.A., Shipilo N.V., Azarko I.I., Frontasyeva M.V., Pavlov S.S. Synthesis of fine crystalline diamonds. Chapter in the Book “Diamond and Related Materials”. Editor Frank Columbus, Nova Science Publishers, Inc., USA, 2008 (in print).
14. Frontasyeva M.V. Radioanalytical investigations at FLNP JINR for Life Sciences. Workshop Proceedings “Nuclear Physics and Society”, (Plovdiv, Bulgaria, September 9-11, 2007), Plovdiv, 2008, p.117-125. ISBN 978-954-423-467-6.
15. Mosulishvili L.M., Tsibakhashvili N.Ya., Kirkesali E.I., Tsertsvadze L.A., Frontasyeva M.V., Pavlov S.S. Biotechnology in Georgia for various applications. Bulletin of the Georgian National Academy of Sciences, Vol. 2, No. 3, 2008 (in English).
16. Mosulishvili L.M., Belokobylsky A.I., Kirkesali E.I., Khizanishvili A.I., Ginturi E.N., Kuchava N.E., Frontasyeva M.V., Pavlov S.S., Aksenova N.G. Development of pharmaceutical substances based on blue-green alga Spirulina platensis. JINR Preprint, E18-2008-8, 2008, pp.13.

17. Popovic D., Todorovic D., Frontasyeva M., Ajtic J., Tasic M., Rajsic S. Radionuclides and heavy metals in Borovac, Southern Serbia. Environmental Science and Pollution Research – International (ESPR – Environ Sci Pollut Res), Vol. 15, No. 6, September. 2008, p. 509-520. http://dx.doi.org/10.1007/s11356-008-0003-6
18. Stafilov T., Šajn R., Pančevski Z., Boev B., Frontasyeva M.V., Strelkova L.P.. Geochemical Atlas of Veles and Environs. Submitted to "2nd August", Stip, Macedonia, 2008, pp. 130.
19. Steinnes E., Frontasyeva M.V., Gundorina S.F., Pankratova Y.S. Identification of metal emissions from closely located sources using moss biomonitoring and factor analysis. JINR Preprint, E18-2008-4, 2008, pp. 8; Accepted by Chemia Analityczna/Chemical Analysis (Warsaw), 2008
20. Tsibakhashvili N., Mosulishvili L., Kalabegishvili T., Kirkesali E., Murusidze I., Kerkenjia S., Frontasyeva M.,. Holman H.-Y. Biotechnology of Cr(VI) transformation into Cr(III) complexes. Journal of Radioanalytical and Nuclear Chemistry, Vol. 278, No. 3, 2008, p. 357-370.
21. Будзински П., Полянски К., Кобзев А.П. Изменение свойств поверхности нержавеющей стали марки AISI316L, имплантированной азотом. ПОВЕРХНОСТЬ. Рентгеновские, синхротронные и нейтронные исследования. 2008, № 8, с. 80-85.
22. Ильченко И.Н., Былова Н.А., Фронтасьева М.В., Ляпунов С.М., Окина О.И., Горбунов А.В., Павлов С.С., Куликов О., Арутюнов Г.П. Концентрации тяжелых металлов в крови московских женщин и риск развития низкой массы тела. Общественное здоровье и профилактика заболеваний. 2008, № 2, стр. 8-11.
23. Ион М., Козлов Ж.А., Матиеску Г., Падуреану И., Семенов В.А., Кречун Л., Рыпеану С., Морозов В.М., Опреа А.И., Опреа К., Пучков А.В. Высокотемпературный термостат для нейтронных измерений TS-3000k на спектрометре ДИН-2ПИ реактора ИБР-2, Preprint JINR, P13-2008-66, Дубна, 2008, сс. 11.
24. Панкратова Ю.С., Зельниченко Н.И., Фронтасьева М.В., Павлов С.С. Атмосферные загрязнения на территории Удмуртской Республики – оценки на основе анализа мхов-биомониторов. Препринт ОИЯИ, Р18-2008-96, Дубна, 2008, сс 8. Принято в печать общественно-научным журналом «Проблемы региональной экологии».
25. Семенов В.А., Козлов Ж.А., Кречун Л., Матиеску Г., Морозов В.М., Опреа А.И., Опреа К., Пучков А.В. Спектр частот тантала при температурах 293 – 2300 К ФААЭ ГНЦ РФ – ФЭИ, Препринт ФЭИ, Обнинск, Россия, 2008 г.
26. Смирнов Л.С., Возниак К., Доминиак П., Лозе А., Натканец И., Фронтасьева М.В., Помякушина Е.В., Баранов А.И., Долбинина В.В.. Уточнение кристаллической структуры [Rbx(NH4)1-x]3H(SO4)2. I. Рентгеновская и нейтронная монокристальная дифракция фазы II с x=0.11 при 300 К. Кристаллография, том 53, № 2, 2008, с. 232-241.

27. Фронтасьева М. В. Эпитепловой нейтронный активационный анализ на реакторе ИБР-2 ЛНФ ОИЯИ. Ядерная физика, том. 71, вып. 10, 2008, с. 1714-1725.

4. Reports at Schools and Conferences

1. Alexandrov A.A., Alexandrova I.A., Borzakov S.B., Efimov G.L., Kamanin D.V., Kopatch Yu.N., Kuznetsova E.A., Panteleev Ts., Pyatkov Yu.V., Tyukavkin A.N., Voronov Yu.N., Zhuchko V.E. Experimental setup and data processing in studying of the reaction 235U(nth, f) at the IBR-2 beam, Proceedings of 15th International Seminar on Interaction of Neutrons with Nuclei: "Neutron Spectroscopy, Nuclear Structure, Related Topics"., p. 248-255, (2008).
2. Alexandrov Yu. A., Oprea C., Oprea I.A. Determination of n-e scattering length from neutron diffraction on a tungsten isotopic mixture in magnetic field. Proceedings of the ISINN-16, May 11-16, Dubna, 2008 (in press).
3. Aničić Mira, Tasić Mirjana, Tomašević Milica, Frontasyeva Marina, Rajšić Slavica, Popović Aleksandar (2008): Active biomonitoring of heavy metal and other elements atmospheric deposition with moss Sphagnum girgensohnii in urban area of Belgrade and industrial zones (Obrenovac, Pancevo), Book of Abstracts of the 5th Symposium Chemistry and Environmental Protection (May 27-30, 2008, Tara, Ireland), pp. 98-99.
4. Crawford B.E., Sharapov E.I., Stephenson S.L. “On the coincidence measurement in the YAGUAR nn-experiment”. XVI International Seminar on Interactions of Neutrons with Nuclei, ISINN-XVI Abstracts, 2008-47, p.19, Joint Institute for Nuclear Research, Dubna, 2008.
5. Cristach C. I., Duliu O. G., Culicov O. A., Frontasyeva M. V., Ricman C., Toma M. Epithermal neutron activation, radiometric, correlation and principal component analysis applied to the distribution of major and trace elements in some igneous and metamorphic rocks from Romania. Submitted to Proceedings of 5th International Conference on Radionuclide Metrology Low-Level-Radioactivity Measurement Techniques ICRM-LLRMT'08, September 22 - 26, 2008, Braunschweig, Germany, to be published in Applied Radiation and Isotopes 2008.
6. Culicov O.A., Frontasyeva M.V., Pantelica A., Badita C.R., Szoke R., Laszlo I., Baranyai R. Instrumental neutron activation analysis interlaboratory comparison based on short-lived isotopes. Book of Abstracts, ISINN-16, 10-14 June, 2008, Dubna.
7. Duliu O.G., Culicov O., Olteanu C., Ricman C., Mihailescu N., Frontasieva M.V., Dinescu L., Oaie G. Instrumental neutron activation analysis applications to environmental and geological studies. Book of Abstracts, ISINN-16, 10-14 June, 2008, Dubna.

8. Duliu O.G., Culicov O.A., Frontasyeva M.V., Ricman C., Szobotca S. and Cristache C.I., Toma M. ENAA of ocean sediments and volcanic rocks. Submitted to FLNP Annual Report, 2008.
9. Florek M., Meresova J., Holy K., Sykora I., Frontasyeva M.V., Pavlov S.S. Application of NAA and AAS in environmental research in Slovakia. Book of Abstracts of the 16th Conference of Czech and Slovak Physicists (September 8-11, 2008, Hradec Králové, University of Hradec Králové), p 19-20.
10. Florek M., Merešová J., Holý K., Ješkovský M., Sýkora I., Burda C., Melicherová T., Frontasyeva M.V., Pavlov S.S.. Comparison of elemental cncentrations in the atmosphere in Bratislava with other Slovakian and European sites. Proceedings of International Conference "Contaminated sites - Bratislava 2008" (Bratislava, Slovakia, June 16-18, 2008). The conference is organized under the auspices of the Ministry of the Environment of the Slovak Republic and Ministry of the Environment of the Czech Republic.
11. Frank, Geltenbort P., Kulin G. V., Kustov D. V., Nosov V. G. and Strepetov A. N. First Observation of the Acceleration Matter Effect in Neutron Optics. Доклад на международном семинаре «Физика частиц с медленными нейтронаvи», Гренобль, май 2008г. Направлено в печать в журнал Nuclear Instrument and methods.
12. Frank A.I., Geltenbort P., Jentschel M., Kulin G. V., Kustov D.V., Nosov V. G. and Strepetov A.N. New Test of the Weak Equivalence Principle for Neutron. Доклад на международном семинаре «Физика частиц с медленными нейтронаvи», Гренобль, май 2008г. Направлено в печать в журнал Nuclear Instrument and methods.
13. Frank A.I. and Kozlov A.V. Dynamic reflection and diffraction of neutrons. Доклад на международной конференции «Polarized Neutrons for Condensed Matter Investigations, PNCMI 2008, Tokai, Japan», сентябрь 2008г. Будет опубликовано в трудах конференции.
14. Frontasyeva M.V., Aleksiayenak Yu.V., Faanhof A., Florek M. Moss biomonitoring of long-lived radionuclides in Belarus: 20 years after Chernobyl. Book of Abstracts of The 22nd Task Force Meeting UNECE ICP Vegetation (February 2-5, 2009, Braunschweig, Germany).
15. Frontasyeva M.V. Current status and future needs of nuclear analytical techniques and their applications. The 4th National Conference on Applied Physcis (September 25-26, 2008, Galati, Romania) (Invited talk).
16. Frontasyeva M.V., Lodoysamba S., Baljinnyam N., Ganbold G., Kobzev A.P., Pavlov S.S., Shovoodoi G. A system of complex monitoring heavy metals and radionuclides in Mongolia based on nuclear and related analytical techniques. Book of Abstracts of the 4th National Conference on Applied Physcis (September 25-26, 2008, Galati, Romania), p. 37-38.

17. Frontasyeva M.V., Bylova N.A., Ilchenko I.N., Lyapunov S.M., Okina O.I., Gorbunov A.V., Pavlov S.S., Aroutiounov G.P. Assessment of exposure to toxic elements in women of fertile age with different nutritional status in Russia using nuclear and related analytical techniques. 9-th International Conference on Nuclear Analytical Methods in the Life Sciences (NAMLS-9), Book of Abstracts, p. A-11, Lisbon, Portugal, 7-12 September, 2008.
18. Frontasyeva M.V. Trace element atmospheric pollution in the Balkans studied by the moss technique, ENAA and AAS. Book of Abstracts 21st Task Force Meeting of the ICP Vegetation (Oulu, Finland, February 26-29, 2008), p. 12.
19. Furman W.I., Lychagin E.V., Muzichka A.Yu., Nekhaev G.V., Strelkov A.V., Sharapov E.I., Shvetsov V.N., Chernukhin Yu.I. , Kandiev Ya.Z., Litvin V.I, Lyzhin A.E., Howell C.R., Mitchell G.E., Tornow W., Crawford B.E., Stephenson S.L. and Bowman C.D. "Status of the experiment on direct measurement of neutron-neutron scattering." // Neutron Spectroscopy, Nuclear Structure, Related Topics; ISINN-16 June 11-14, (to be published).
20. Gheboianu A., Popescu I.V., Stihi C., Belc M., Bancuta I., Vlaicu Gh., Frontasyeva M., Culicov O. Atomic Absorption Spectrometry And Neutron Activation Analysis Methods Applied In Environmental Studies Using Mosses As Bioindicators, 9th International Balkan Workshop On Applied Physics, July, 7-9, 2008, Constanta, Romania.
21. Gledenov Yu. M., Sedysheva M.V., Khuukhenkhuu G., Jiaguo Zhang, Rongtai Cao, Li-an Guo, Jinxiang Chen, Jianyong Wang, Guohui Zhang. Differential and Angle-Integrated Cross-Section Measurement for the 64Zn(n,α)61Ni Reaction at 2.5, 4.0 and 5.5 MeV. In: Proc. of the "Neutron Spectroscopy, Nuclear Structure, Related Topics". XV International Seminar on Interaction of Neutrons with Nuclei, Dubna, 2008, p.147-150.
22. Goryaynova Z.I., Pavlov D.F., Frontasyeva M.V. Heavy metals and ree in bottom sediments and dreissenids of the Rybinsk reservoir. Submitted to FLNP Annual Report, 2008.
23. Ilchenko, Bylova N., Frontasyeva M., Lyapunov S., Okina O., Gorbunov A., Pavlov S., Aroutiounov G., Gorobech P. Blood Concentrations of selected heavy metals in blood of Moscow women with different nutritional status. In the Book of Abstracts of the XVIII IEA World Congress of Epidemiology, (September 20-24, 2008, Porto Alegre-RS, Brazil), p. 2662.
24. Kamanin D.V., Kopach Yu.N., Pyatkov Yu.V., Alexandrov A.A., Borzakov S.B., Lavrova J.E., Panteleev Ts., Tyukavkin A.N. Study of the multy-cluster decays in the neutron induced fission of 235U, p. 274-280, Proceedings of 15th International Seminar on Interaction of Neutrons with Nuclei: "Neutron Spectroscopy, Nuclear Structure, Related Topics"., (2008).
25. Kamanin D.V., Pyatkov Yu.V., Tyukavkin A.N., Kopatch Yu.N. Experimental evidences of clustering in low excited heavy nuclear systems, 2250-2254, Int. Journal of Modern Physics E.

Proceedings of the First Workshop on State of the Art in Nuclear Cluster Physics "SOTANCP2008", France, Strasbourg, 13-16 May, 2008, 17, 10 (2008),

26. Khuukhenkhuu G., Odsuren M., Munkhbat B., Gledenov Yu.M., Sedysheva M.V.. Nuclear reaction models for systematic analysis of the fast neutron induced (n,p) reaction cross sections. In: Proc. of the International Conference on Nuclear Data for Science and Technology (ND2007), Nice, France, 2007, p. 215-218.
27. Khuukhenkhuu G., Bayarbadrakh B., Odsuren M., Gledenov Yu.M., Sedysheva M.V. Statistical Model Analysis for (n,α) Reaction Cross Sections. In: Proc. of the "Neutron Spectroscopy, Nuclear Structure, Related Topics". XV International Seminar on Interaction of Neutrons with Nuclei, Dubna, 2008, p.157-162.
28. Kobzev A.P., Huran J., Maczka D., Turek M. Investigation of light element contents in subsurface layers of silicon. ION2008. VII – th International Conference "Ion Implantation and other Applications of Ions and Electrons". Kazimierz Dolny, Poland June 16 – 19, 2008. Submitted to Vacuum.
29. Lychagin E., Musychka A.Yu., Nesvizhevsky V.V. , Pignol G. , Protasov K.V., Strelkov A.V. "Storage of Very Cold Neutrons in bottles. First experimental results." // Neutron Spectroscopy, Nuclear Structure, Related Topics; ISINN-16 June 11-14 (to be published).
30. Lyuboshitz V.L., Lyuboshitz V.V. "Low-energy scattering of a polarized neutron on a polarized proton". Proceedings of the XVI International Seminar on Interaction of Neutrons with Nuclei – ISINN-16 (Dubna, June 11 – 14, 2008).
31. Lyuboshitz V.L., Lyuboshitz V.V. "Sign of the singlet length of neutron scattering on the proton, neutron radiative capture by the proton and problem of the virtual level of the (np) system". Proceedings of the XV International Seminar on Interaction of Neutrons with Nuclei – ISINN-15 (Dubna, May 16 – 19, 2007), JINR E3-2008-26, Dubna, 2008, pp. 37-43 .
32. Lyuboshitz V.L., Lyuboshitz V.V. "The coherent inelastic processes on nuclei at ultrarelativistic energies" . Proceedings of the XII International Conference on Elastic and Diffractive Scattering ("Forward Physics and QCD") – EDS'07 (DESY, Hamburg, Germany, May 21 – 25, 2007) , DESY-PROC-2007-02 (Hamburg , December 2007) , pp. 336-341, 2008. .
33. Lyuboshitz V.L., Lyuboshitz V.V. "Spin structure of the "forward" charge-ex-change reaction $n + p \rightarrow p + n$ and the deuteron charge-exchange breakup $d + p \rightarrow (pp) + n$ ". Proceedings of the XII Advanced Research Workshop on High Energy Spin Physics – DUBNA-SPIN-07 (Dubna, September 3 – 7, 2007) , JINR E1,2-2008-57 , Dubna, 2008, pp. 106-111 .
34. Lyuboshitz V.L., Lyuboshitz V.V. "The coherent inelastic processes on nuclei at ultrarelativistic energies". Proceedings of the XVIII International Baldin Seminar on High Energy Physics

Problems – ISHEPP-18 (Dubna, September 25 – 30, 2006), JINR E1,2-2008-113 , vol. II , Dubna, 2008, pp. 60-68 .

35. Lyuboshitz V.L., Lyuboshitz V.V. "The coherent inelastic processes in collisions of particles and nuclei at ultrarelativistic energies" . In Proceedings of the VII International Workshop "Very High Multiplicity Physics" – VHMP'07 (Dubna, September 17 – 19, 2007) , Dubna, 2008
36. Lyuboshitz V.L., Lyuboshitz V.V. "The coherent inelastic processes in collisions of particles and nuclei at ultrarelativistic energies" .Talk at the 6-th International Conference on Perspectives in Hadronic Physics – Hadron'08 (ICTP, Trieste, Italy, May 12 – 16, 2008) ; allocated on the Hadron'08 website http://www.pg.infn.it/hadronic08.
37. Lyuboshitz V.L., Lyuboshitz V.V. "Low-energy scattering of a polarized neutron on a polarized proton". Talk at the XVI International Seminar on Interaction of Neutrons with Nuclei – ISINN-16 (Dubna, June 11 – 14, 2008) .
38. Lyuboshitz V.L., Lyuboshitz V.V. "Angular correlations in the decays of $\Lambda\Lambda$ and $\Lambda\overline{\Lambda}$ pairs produced in relativistic heavy ion collisions". Talk at the XIII International Conference on Selected Problems of Modern Theoretical Physics, dedicated to the 100-th anniversary of the birth of D.I.Blokhintsev – SPMTP-2008 (Dubna, June 23–27, 2008).
39. Lyuboshitz V.L., Lyuboshitz V.V. "Spin correlations in the $\Lambda\Lambda$ and $\Lambda\overline{\Lambda}$ systems generated in relativistic heavy ion collisions" Talk at the Helmholtz International Summer School "Dense Matter in Heavy Ion Collisions and Astrophysics" – Dense Matter 2008 (Dubna, July 14 – 26, 2008) ; allocated on the Dense Matter 2008 website http://theor.jinr.ru/~dm2008.
40. Lyuboshitz V.L., Lyuboshitz V.V. "Pair correlations of neutral K, D, B and Bsmesons with close momenta generated in inclusive multiparticle processes". Talk at the Helmholtz International Summer School "Heavy Quark Physics" – HQ-2008 (Dubna, August 11 – 21, 2008) ; allocated on the HQ-2008 website http://theor.jinr.ru/~hq2008.
41. Lyuboshitz V.L., Lyuboshitz V.V. "Angular correlations in the decays of $\Lambda\Lambda$ and $\Lambda\overline{\Lambda}$ pairs produced in relativistic heavy ion collisions" . Poster presentation at the International Conference "Strong and ElectroWeak Matter 2008" – SEWM-2008 (Amsterdam, the Netherlands, August 26 – 29, 2008) ; allocated on the SEWM-2008 website http://staff.science.uva.nl/~sewm08.
42. Lyuboshitz V.L., Lyuboshitz V.V. "Strangeness conservation and pair correlations of neutral kaons with close momenta produced in inclusive multiparticle processes". Poster presentation at the International Conference "Strong and ElectroWeak Matter 2008" – SEWM-2008 (Amsterdam, the Netherlands, August 26–29, 2008); allocated on the SEWM-2008, http://staff.science.uva.nl/~sewm08.

43. Lyuboshitz V.L., Lyuboshitz V.V. "The coherent inelastic processes in collisions of particles and nuclei at ultrarelativistic energies". Poster presentation at the International Conference "Strong and ElectroWeak Matter 2008" – SEWM-2008 (Amsterdam, the Netherlands, August 26 – 29, 2008) ; allocated on the SEWM-2008 website http://staff.science.uva.nl/~sewm08.
44. Lyuboshitz V.L., Lyuboshitz V.V. " Spin correlations of muons produced in the annihilation process $e^+ e^- \to \mu^+ \mu^-$ ". Talk at the XIX International Baldin Seminar on High Energy Physics Problems – ISHEPP-19 (Dubna, September 29 – October 4, 2008); allocated on the ISHEPP-19 website http://relnp.jinr.ru/ishepp.
45. Lyuboshitz V.L., Lyuboshitz V.V. "Spin correlations of muons generated in the process of electron-positron pair annihilation". Poster presentation at the 18-th Interna-tional Conference on Particles and Nuclei – PANIC-08 (Eilat, Israel, November 9–14, 2008) .
46. Lyuboshitz V.L., Lyuboshitz V.V. "Strangeness conservation and pair correlations of neutral kaons with close momenta produced in inclusive multiparticle processes".
47. Poster presentation at the 18-th International Conference on Particles and Nuclei – PANIC-08 (Eilat, Israel, November 9 – 14, 2008).
48. Lyuboshitz V.L., Lyuboshitz V.V. "The coherent inelastic processes in collisions of particles and nuclei at ultrarelativistic energies". Poster presentation at the 18-th International Conference on Particles and Nuclei – PANIC-08 (Eilat, Israel, November 9 – 14, 2008) .
49. Lyuboshitz V.L., Lyuboshitz V.V. "Spin structure of the nucleon charge-exchange reaction at zero angle and the deuteron charge-exchange breakup". Poster presentation at the 18-th International Conference on Particles and Nuclei – PANIC-08 (Eilat, Israel, November 9 – 14, 2008).
50. Lyuboshitz V.L., Lyuboshitz V.V. "The process of Coulomb dissociation of weakly bound relativistic hypernuclei within the two-cluster model" . Poster presentation at the 18-th International Conference on Particles and Nuclei – PANIC-08 (Eilat, Israel, November 9 – 14, 2008) .
51. Lyuboshitz V.L., Lyuboshitz V.V. "The coherent inelastic processes in collisions of particles and nuclei at ultrarelativistic energies" . Sixth International Conference on Perspectives in Hadronic Physics (ICTP, Trieste, Italy, May 12 – 16, 2008) . Abstracts of Talks. Trieste, 2008, p. 13 ; also online on the Conference website: http://www.pg.infn.it/hadronic08/abstracts/pdfs/Lyuboshitz-1.pdf .
52. Lyuboshitz V.L., Lyuboshitz V.V. "Low-energy scattering of a polarized neutron on a polarized proton" . Abstracts of the XVI International Seminar on Interaction of Neutrons with Nuclei – ISINN-16 (Dubna, June 11 – 14, 2008) , JINR E3-2008-47, Dubna, 2008 , p. 34.
53. Lyuboshitz V.L., Lyuboshitz V.V. " Spin correlations of muons produced in the annihilation process $e^+ e^- \to \mu^+ \mu^-$ " . Book of Abstracts of the XIX International Baldin Seminar on High

Energy Physics Problems – ISHEPP-19 (Dubna, September 29 – October 4, 2008) , JINR E1,2-2008-128 , Dubna, 2008 , p.77 .

54. Mankovska B., Oszlányi J., Florek M., Frontasyeva M.V., Pavlov S.S. Neutron activation analysis as method for critical evaluation of pollution of ecosystem. International Conference "Contaminated sites - Bratislava 2008" (Bratislava, Slovakia, June 16-18, 2008). The conference is organized under the auspices of the Ministry of the Environment of the Slovak Republic and Ministry of the Environment of the Czech Republic.
55. Mitsyna L.V., Nikolenko V.G., Parzhitski S.S., Popov A.B., Samosvat G.S. "Neutron-electron scattering length extraction from the neutron diffraction data measured on noble gases", report on ISINN-16 (2008): Nucl.Phys.A (in print).
56. Mosulishvili L., Tsibakhashvili N., Kalabegishvili T., Kirkesali E., Frontasyeva M., Pavlov S. Neutron Activation Analysis in Biotechnology. Book of Abstracts of the International Scientific Conference – Actual Problems of Experimental and Theoretical Biolog (Tbilisi, Georgia, October 3-4, 2008), p. 71-72.
57. Mutterer M., Kopatch Yu. N., Yamaledtinov S. R., Lyapin V. G., J. von Kalben, Khlebnikov S. V., Sillanpaa M., Tyurin G. P., Trzaska W. H. On the Ternary a Spectrum in 252Cf(sf), World Scientific, Seminar in Fission Corsendonk Priory, Belgium 18 - 21 September 2007 edited by Cyriel Wagemans (University of Gent, Belgium), Jan Wagemans & Pierre D`hondt (SCK•CEN, Mol, Belgium), p. 89-98, (2008).
58. Oprea A. I., Oprea C., Gledenov Yu. M., Sedyshev P. V. Multilevel Approach in the Evaluation of the Asymmetry Effects on (n,p) Reaction for 35Cl and 14N Nuclei. In: Proc. of the "Neutron Spectroscopy, Nuclear Structure, Related Topics". XV International Seminar on Interaction of Neutrons with Nuclei, Dubna, 2008, p.296-303.
59. Oprea, Oprea. C., Gledenov Yu. M., Sedyshev P.V. A Monte Carlo Simulation of the Asymmtry Coefficients Measurements in the (n,p) reaction. Proceedings of the ISINN-16, May 11-16, Dubna, 2008 (in press).
60. Oprea, C. Oprea, Gledenov Yu. M., Sedyshev P.V., Sedysheva M. V., Szalansky P. J. Statistical Model Evaluation of the Cross-section in (n,□) reaction on 64Zn. Proceedings of the ISINN-16, May 11-16, Dubna, 2008 (in press).
61. Oprea C., Maslov O. D., Gustova M. V.,. Belov A. G, Oprea I.A., Mihul A., Loghin V., Nicolescu C., Gorghiu G. Impact evaluation of the toxic and biologic active elements consumed through food crops on the consumer`s health using nuclear methods and neural network technique. Proceedings of the ISINN-16, May 11-16, Dubna, 2008 (in press).

62. Oprea C., Velichkov A., Oprea I.A., Filosofov D. V. The perturbation angular correlations for HFI and biological researches. Proceedings of the ISINN-16, May 11-16, Dubna, 2008 (in press).
63. Oprea, Oprea C., Sedyshev P.V., Szalansky P. J. Asymmetry effects. Proceedings of the ISINN-16, May 11-16, Dubna, 2008 (in press).
64. Oprea C., Gustova M. V., Maslov O. D.,. Belov A. G, Oprea I.A., Szalansky P. J. IGAA and XRF analysis of Sea lettuce algae samples. Proceedings of the ISINN-16, May 11-16, Dubna, 2008 (in press).
65. Oprea C., Gustova M. V., Maslov O. D., Oprea I.A., Belov A. G. Comparison of inorganic chemical constituents of different herbal medicines. Proceedings of the ISINN-16, May 11-16, Dubna, 2008 (in press).
66. Oprea C., Gustova M. V., Maslov O. D., Oprea I.A., Belov A. G., Szalansky P. J. A statistical analysis of regional oil impacts on environment. Proceedings of the ISINN-16, May 11-16, Dubna, 2008 (in press).
67. Oszlanyi J., Mankovska B., Frontasyeva M.. Use of mosses as biomonitors of heavy metal deposition in the Carpathians Mountains (Slovak Part). Book of Abstracts 21st Task Force Meeting of the ICP Vegetation (Oulu, Finland, February 26-29, 2008), p. 41.
68. Pankratova Yu.S., Frontasyeva M.V., Pavlov S.S.. Air pollution studies in the republic of udmurtia (rf) using the moss biomonitoring techique and NAA. Submitted to FLNP Annual Report, 2008.
69. Pantelica A., Badita C.R., Culicov O., Frontasyeva M., Companis I., Ciortea C.. PIXE and INAA analytical sensitivity of edible vegetal samples. The 4th National Conference on Applied Physics (September 25-26, 2008, Galati, Romania).
70. Pantelica A., Frontasyeva M.V., Oprea C., Ammerlaan A., Bode P., Georgescu I.I., Pincovschi E.. Investigation of the working place atmosphere in a Romanian fertilizer plant by neutron activation analysis. Book of Abstracts, NRC7, Hungary, August, 2008.
71. Pantelica A., Culicov O.A., Frontasyeva M.V., Oprea C., Georgescu R., Georgescu I.I., Pincovschi E.. Investigation of the occupational exposure in a fertilizer plant by instrumental neutron activation analysis of hair and nail samples. Book of Abstracts, NRC7, Hungary, August, 2008.
72. Pantelica A.I., Badita C.R., Frontasyeva M.V., Culicov O.A. A retrospective review of JINR – IFIN-HH collaborative projects based on NAA. Book of Abstracts, ISINN-16, 10-14 June, 2008, Dubna.
73. Pantelică A., Bădiţa C.R., Culicov O., Frontasyeva M., Companiş I., Gugiu M., Popescu I.V. Determination by nuclear techniques of the elemental concentrations in vegetables from industrial zone Targoviste. The Scientific Session “Sciences Applied in Environmental and Materials Study” (in Romanian), 5-6 June 2008, Târgovişte, Romania.

74. Pokotilovski Yu. N. “On the prospects for the neutron lifetime measurements in material traps”, Poster at the Intern. Workshop on Particle Physics with Slow Neutrons, Grenoble, 29-31 May, 2008.
75. Pokotilovski Yu. N., Novopoltsev M. I., Geltenbort P., Brenner Th. “A differential time of flight spectrometer for very low energy neutrons”, Poster at the Intern. Workshop on Particle Physics with Slow Neutrons, Grenoble, 29-31 May, 2008.
76. Shovoodoi G., Shvetsov V.N., Gerbish G., Nyamsuren B., Belov A.G. Application a Linac of the IREN Facility for production some radionuclides and multielemental activation analysis. Book of Abstracts of the Ulaanbaatar Conference on Nuclear Physics and Applications. (September 8-11, 2008, Ulaanbaatar, Mongolia), p. 56.
77. Spiric Z., Frontasyeva M.V., Stafilov T., Enimiteva V., Bukovec D., Mesic Z.. Environmental and health consequences of mercury air pollution. Cell Biology and Toxicology (Springer, Netherlands. ISSN: 0742-2091), P12 The Environmental and health consequences of mercury air pollution, pp. S104-S105, DOI: 10.1007/s10565-007-9052-8, Vol. 24, Supple 1, 2008, p. 104-105, 2008 http://www.springerlink.com/content/r708830518116g80/
78. Spiric Z., Frontasyeva M.V., Bukovec D., Stafilov T.. Remote sensing and biomonitoring techniques as health and environmental risks early warning tools. Book of Abstracts of the First International Conference: Disaster Management and Emergency Response in the Mediterranean Region (Zadar, Croatia, 22–24 September 2008), p. 140.
79. Spiric Z., Frontasyeva M., Stafilov T., Enimiteva V., Barandovski L., Urumov V.. Atmospheric deposition of Cd, Hg, and Pb in Croatia and neighbouring countries: assessment based on moss analysis. Book of Abstracts 21st Task Force Meeting of the ICP Vegetation (Oulu, Finland, February 26-29, 2008), p. 44.
80. Stafilov T., Pančevski Z., Frontasyeva M., Strelkova L., Šajn R. Distribution of heavy metals in surface soil due to industrial pollution. (Pleanry lecture by Prof. T.Stafilov) VII. 6th Aegean Analytical Chemistry Days (AACD-2008), 9-12 October 2008, Pamukkale, Denizli, Turkey.
81. Stafilov T., Frontasyeva M.V., Barandovski L., Enimiteva V., Pavlov S.S., Urumov V.. Biomonitoring air pollution using AAS and NAA: the Republic of Macedonia case study. Cairo University Biannual International Conference on Analytical Chemistry. Green and Sustainable Chemistry in Developing Countries. Book of Abstracts, p. 19, Cairo, Egypt, 3-6 March, 2008.
82. Steinnes E., Frontasyeva M.V., Gundorina S.F., Pankratova Y.S.. Identification of metal emissions from closely located sources using moss biomonitoring and factor analysis. Book of Abstracts 21st Task Force Meeting of the ICP Vegetation (Oulu, Finland, February 26-29, 2008), p.45.

83. Sukhovoj A.M., Furman W.I., Khitrov V.A. Approximation of sums of experimental radiative strength functions of dipole gamma-transitions in the region Eγ~ Bn for the atomic masses 40 ≤A ≤ 200, In: XV International Seminar on Interaction of Neutrons with Nuclei, Dubna, May 2007, E3-2008-26, Dubna, 2008, pp. 92-107.
84. Sukhovoj A.M., Khitrov V.A., Problems of the experimental determination of parameters of nucleus and applicability of the Bohr-Mottelson hypothesis , In: XV International Seminar on Interaction of Neutrons with Nuclei, Dubna, May 2007, E3-2008-26, Dubna, 2008, pp. 108-112.
85. Sukhovoj A.M., Khitrov V.A., Gamma decay of the compound state and change of structure of the 124Te excited levels, In: XV International Seminar on Interaction of Neutrons with Nuclei, Dubna, May 2007, E3-2008-26, Dubna, 2008, pp. 113-125.
86. Sukhovoj A.M., Khitrov V.A., Calculation of the total gamma-spectra of the fast neutrons capture in the isotopes 117,119Sn for the different parameters of cascade gamma-decay, In: XV International Seminar on Interaction of Neutrons with Nuclei, Dubna, May 2007, E3-2008-26, Dubna, 2008, pp. 126-133.
87. Sukhovoj A.M., Khitrov V.A., Crawford B.E., Stephenson S.L. Reanalysis of the process of the cascade gamma decay of 198Au compound state, In: XV International Seminar on Interaction of Neutrons with Nuclei, Dubna, May 2007, E3-2008-26, Dubna, 2008, pp. 134-146.
88. Sukhovoj A.M., Khitrov V., Maslov V.. Completely model-free determination of the level density, radiative strength functions and their main peculiarities. In International Conference on nuclear data for science and technology 2007, Nice, 2007, p. 175-178.
89. Sukhovoj A.M., Furman W.I., Khitrov V.A. Status and problems of experimental study of excited nucleus superfluidity. The 2-nd international conference "Current problems in nuclear physics and atomic energy", Book of abstracts, Kyiv, 2008, p. 27.
90. Sukhovoj A.M., Khitrov V.A. About nucleus "superfluid-normal" state transition dynamics, The 2-nd international conference "Current problems in nuclear physics and atomic energy", Book of abstracts, Kyiv, 2008, p. 27.
91. Sukhovoj A.M., Khitrov V.A. Main parameters of the gamma-decay process and the properties of nucleus 174Yb, which are manifisted in radiative cvapture of resonancee and thermal neutrons, The 2-nd international conference "Current problems in nuclear physics and atomic energy", Book of abstracts, Kyiv, 2008, p.65.
92. Sukhovoj A.M., Furman W.I., Khitrov V.A. Precise approximation of sums of experimental radiative strength functions of dipole gamma-transition, The 2-nd international conference "Current problems in nuclear physics and atomic energy", Book of abstracts, Kyiv, 2008, p.65.

93. Vesna V.A., Gledenov Yu. M., Nesvizhevsky V.V., Petukhov A.K., Sedyshev P.V., Soldner T., Shulgina E.V., Zimmer O.. “Zero” Experiment and Final Result of the Measurements of the P-odd Asymmetry in the 6Li(n,α)3H Reaction. In: Proc. of the "Neutron Spectroscopy, Nuclear Structure, Related Topics". XV International Seminar on Interaction of Neutrons with Nuclei, Dubna, 2008, p.332-338.
94. Гледенов Ю.М. Исследование реакций (n,p), (n,t), (n,α) на быстрых нейтронах. В сб.: «Ядрена физика и общество» (Материалы рабочего совещания 9-11 сентября 2007 г., Пловдив). Издательство университета Паисий Хилендарский, 2008, с. 74-90.
95. Гледенов Ю.М. О сотрудничестве между сектором редких реакций ЛНФ ОИЯИ и кафедрой атомной физики Пловдивского университета. В сб.: «Ядрена физика и общество» (Материалы рабочего совещания 9-11 сентября 2007 г., Пловдив). Издательство университета Паисий Хилендарский, 2008, с. 136-141.
96. Горяйнова З. И., Павлов Д.Ф., Фронтасьева М.В. Тяжелые металлы и редкоземельные элементы в донных отложениях и дрейссенидах Рыбинского водохранилища. Тезисы доклада на конференции «Антропогенное воздействие...» (11-16 ноября 2008, Борок, Ярославская область, РФ).
97. Динг Я., Гундорин Н.А., Жанг Ж., Немченок И.Б., Пикельнер Л.Б. Жидкий сцинтиллятор для регистрации тепловых нейтронов, Международная конференция «Инженерия сцинтилляционных материалов и радиационные технологии», Сборник аннотаций, Харьков, 2008, стр. 71.
98. Кобзев А.П. Аналитические исследования наноструктур на ускорителе ЭГ-5 ОИЯИ. XVII Международная конференция по электростатическим ускорителям и пучковым технологиям. 21 – 23 октября, 2008 года.
99. Кобзев А.П. Элементный анализ наноструктур на пучках заряженных частиц. В сборнике «Ядерная физика и нанотехнологии: ядерно-физические аспекты формирования, изучения и применения наноструктур». Дубна, 2008, стр. 142 – 154.
100. Франк А.И.. Спектрометрия УХН с интерферометрами Фабри-Перо. В сб: Рентгеновская оптика – 2008. Материалы совещания. г. Черноголовка, 6-9 октября 2008г. С.133-135.

DEVELOPMENT AND CONSTRUCTION OF ELEMENTS OF NEUTRON SPECTROMETERS FOR CONDENSED MATTER INVESTIGATIONS

1. Belushkin A.V., et al. 2D position-sensitive monitor for thermal neutrons. Technical Physics, 2008, v.78, №.1 pp. 121 - 125.

2. Belushkin A.V.. Modern trends in position-sensitive neutron detectors development for condensed matter research (Invited talk at the International Symposium on Neutron Scattering, ISNS 2008, 15-18 January 2008, Mumbai, India), JINR Preprint E13-2007-184, Dubna, 2007.
3. .Kirilov A.S, et al. Organization of remote control of the spectrometers at the IBR-2M reactor. JINR Preprint P10-2008-23, Dubna, 2008 (submitted to Instruments and Experimental Techniques).
4. Belushkin A.V., et al. 2D position-sensitive detector for thermal neutrons. Proc. of XXI International Symposium on Nuclear Electronics & Computing, JINR E10,11-2008-37, Dubna, 2008, pp. 116-120.
5. Manoshin S., Ioffe A.. New modules for the VITESS software package: Time-gradient magnetic fields and neutron refractive lenses. Nuclear Instruments and Methods in Physics Research, Section A, v.586, №1, pp. 81-85.
6. Miron N.F., Kirilov A.S., et al. Modernization and creation of new measuring modes for the MOND facility. XX International Workshop on Neutron Scattering in Condensed Matter Investigations (NSCMI-2008), Gatchina, October 13-19, 2008, Abstracts, p.150.
7. Novikov A.G., Sirotin A.P., et al. Mechanical monochromator for small-angle spectrometer at the SAFARI-1 reactor. Ibid, p.151.
8. Churakov A.V.. Developments of gas PSD for thermal neutrons in FLNP JINR. Ibid, p.156.
9. Budagov J., Chernikov A., Sabirov B., Sissakian A., Shirkov G., Sukhanova A., Malkov I., Perevozchikov V., Rybakov V.,.Zhigalov V, Basti A., Bedeschi F., Frasconi F., Linari S., Kephart R., Nagaaitsev S.. Leak rate measurements on bimetallic transition samples for ILC cryomodules. JINR Communications, E13-2008-110, Dubna, 2008.
10. Kuzmin E.S., Drozdov V.A., Zhuk V.V., et al. Multichannel modular scintillation detector for thermal neutrons. Instruments and Experimental Techniques, 2008, №5, pp. 5-13.

6. PRIZES

JINR Prizes:

Experimental Physics Research:

First Prize:
A.I. Frank, P. Geltenbort, M. Jentschel, D.V. Kustov, G.V. Kulin, V.G. Nosov, A.N. Strepetov. "Prediction and experimental observation of effect of accelerated matter in neutron optics".

Second Prize:
S.P.Avdeyev, A.Budzanowski, V.A.Karnaukhov, W.Karcz, V.V.Kirakosyan, V.K.Rodionov, H.Oeschler, I.Skwirczynska. "Experimental investigation of spinodal state of nuclear matter".

Applied Physics Research:

Second Prize:
Yu.V.Taran, J.Schreiber."Neutron diffraction studies of martensitic transformation and fatigue properties of austenitic stainless steels".

JINR Prizes for young scientists and specialists:

Experimental Physics Research:

First Prize:
S.E.Kichanov. "Study of the structure and dynamics of pyridine salts PyHNO3 and PyHReO4 at high pressures".

Applied Physics Research:

Encouraging Prize:
O.A.Kyzyma. "Organization of fullerene clusters in the system C_{60}/N-methyl-2-pyrrolidone".

7. SEMINARS

Date	Authors	Title
05.02.08	Rolando Granada	Pulsed Neutrons in Bariloche: Past Activities and Ideas for the Future
13.03.08	S.M.Ignatov, M.G.Mitel'man	Scintillation Solid-State Detectors
02.04.08	A.B.Popov, A.V.Strelkov, Ye.P.Shabalin	"Vladislav Ivanovich Lushikov – Half a Century in Service of Science"
18.09.08	S.G.Yavshitz	Models and codes for description of characteristics of nuclear fission in the reactions with nucleons of medium and intermediate energies
17.10.08	V.N.Shvetsov, Yu.M.Chuvil'skii A.L.Barabanov A.A.Goverdovskii V.L.Aksenov	Seminar dedicated to the 70-th anniversary of V.I.Furman
13.11.08	B.N.Zakhariev	Extraction of the quantum ABC from the problem of finding physical essence of new non-Cooper particle pairing.

8. ORGANIZATION AND USER INTERACTION
8.1. STRUCTURE OF LABORATORY AND SCIENTIFIC DEPARTMENTS

Directorate:
Director: A.V.Belushkin Deputy Director: V.N.Shvetsov Scientific Secretary: O.A.Culicov

Reactor and Technical Departments
Chief engineer: A.V.Vinogradov **IBR-2 reactor** Chief engineer: A.V.Dolgikh **Department of IREN** Head: V.G.Pyataev **Mechanical maintenance division** Head: A.A.Belyakov **Electrical engineering department** Head: V.A.Trepalin **Design bureau** Head: A.A.Kustov **Experimental workshops** Head: A.N.Kuznetsov

Scientific Departments and Sectors
Condensed matter department Head: D.P.Kozlenko **Nuclear physics department** Head: Yu.N.Kopatch **Department of IBR-2 spectrometers complex** Head: S.A.Kulikov

Administrative Services
Deputy Director: S.V.Kozenkov Secretariat Finances Personnel

Scientific Secretary Group
Translation Graphics Photography Artwork

NEUTRON INVESTIGATIONS OF CONDENSED MATTER

Sub-Division	Title	Head
Sector 1: Neutron Diffraction. Head: A.M.Balagurov		
Group No.1	HRFD	A.M.Balagurov
Group No.2	DN-2	A.I.Beskrovnyi
Group No.3	DN-12	B.N.Savenko
Group No.4	Geomaterials	A.N.Nikitin
Group No.5	SKAT	Ch.Scheffzük
Sector 2: Neutron Optics. Head: M.V. Avdeev		
Group No.1	Surfaces	Yu.V.Nikitenko
Group No.2	Nanostructures	M.V.Avdeev
Small angle scattering group.		**Head: V.I.Gordeliy**
Inelastic scattering group.		**Head: I.Natkaniec**

NUCLEAR PHYSICS DEPARTMENT

Sub-Division	Title	Head
Sector 1. Correlation γ-spectroscopy and development of experimental installations.		**Head: N.A.Gundorin**
Sector 2. Investigation of neutron properties.		**Head: Ye.V.Lychagin**
Sector 3. Neutron activation analysis.		**Head: M.V.Frontasyeva**
Group No.1	Analytical	M.V.Frontasyeva
Group No.2	Experimental	S.S.Pavlov
Group No.4	Fission	Yu.N.Kopatch
Group No.5	Proton and α-decay	Yu.M.Gledenov
Group No.6	Polarized neutrons and nuclei	V.P.Skoy

DEPARTMENT OF IBR-2 SPECTROMETERS COMPLEX

Sub-Division	Title	Head
Group No.1	Detectors	A.V.Churakov
Group No.2	Electronics	A.A.Bogdzel
Group No.3	Information technologies	A.S.Kirilov
Group No.4	Sample environment and choppers	A.P.Sirotin
Group No.5	Cryogenic investigations	A.N.Chernikov
Group No.6	Methodical developments	S.G.Vasilovskii
Group No.7	Cold moderators	S.A.Kulikov

8.2. MEETINGS AND CONFERENCES

In 2008, FLNP organized the following meetings:

1. International Seminar-School “Pulsed Advanced Neutron Sources” PANS-III dedicated to the centenary of the birth of D.I.Blokhinzev, Dubna, January 29 – February 4.
2. IAEA TC 2nd Workhop “Harmonization of QA/QC Systems According to ISO and International Standards in Nuclear Analytical Laboratories of the Russian Federation”, Dubna, May 26-30.
3. XVI International Seminar on Interaction of Neutrons with Nuclei ISINN-16, Dubna, June 11-14.
4. IAEA TC 3nd Workhop “Harmonization of QA/QC Systems According to ISO and International Standards in Nuclear Analytical Laboratories of the Russian Federation”, Dubna, October 27-31.
5. International Seminar Dedicated to the centenary of the birth of I.M. Frank, Dubna, October 23-24.

In the year 2009, FLNP will organize:

XVII International Seminar on Interaction of Neutrons with Nuclei ISINN-17, Dubna, May 27-30.

8.3. COOPERATION

List of Visitors from Non-Member States of JINR in 2008

Name	Organization	Country	Dates
L. Cser	KFKI RIPNP, Budapest	Hungary	21.10-26.10.
K. Dufren	IAEA	Austria	19.09-20.09.
A. Faigel	IAEA	Austria	14.01.-18.01.
			28.10.-31.10.
P. Vermerke	NRC, Mol	Belgium	08.06.-14.06.
K. Walther	Potsdam Geol. Res. Centr.	Germany	22.06.-27.06. 28.10.-07.11.
			19.05.-30.05.
K. Ullemeyer	University of Kiel	Germany	09.07.-15.07. 07.09.-11.09. 17.04.-25.04. 08.10.-22.10. 16.11.-29.11. 25.05.-30.05.
K. Hoppstock	Research Centre Julich	Germany	26.10.-02.11.
A. Frischbutter	Potsdam Geol. Res. Centr.	Germany	05.02.-09.02. 20.06.-29.06. 04.11.-08.11. 26.05.- 30.05.
H. Hemmpel	University of Freiburg	Germany	05.02.-10.02.

F. Shilling	Potsdam Geol. Res. Centr.	Germany	22.06.-24.06.
R. Lieckefett	Potsdam Geol. Res. Centr	Germany	26.05.-29.05.
G. Spikermann	Potsdam Geol. Res. Centr	Germany	19.11.-20.11.
K. Feldmann	Research Centre Julich	Germany	25.05.-29.05.
G. Zhang	Ints. of Heavy Ion Physics, Beijing	China	09.06.-21.06.
G. Tan	Ints. of Heavy Ion Physics, Beijing	China	09.06.-21.06.
P. Bode	TU, Delft	Netherlands	25.05.-01.06.
P. Bode	TU, Delft	Netherlands	09.03.-14.03.
M. Anicic	VINCA Inst, Belgrade	Serbia	07.06.-18.06.
H. J. Lauter	ILL, Grenoble	France	14.06.-19.06.
H. J. Lauter	ILL, Grenoble	France	19.01.02.02
V. Lauter	ILL, Grenoble	France	19.01.02.02
A. Faanhof	NECSA, Pretoria	South Africa Rep.	26.10.-02.11.
H. Boshoff	NECSA, Pretoria	South Africa Rep.	09.02.-23.02.

8.4. EDUCATION

The objective of the FLNP educational program is the training of specialists in the field of neutron methods for condensed matter and nuclear physics research. The students of the Neutron Diffraction Department of MSU, of the Interfaculty Center «Structure of Matter and New Materials» and of the Electronics and Automatics Department of MIREA (Moscow State Institute of Radioengineering, Electronics and Automatics) perform their term and diploma works in FLNP. At the University Centre of JINR the students from Tula State University, Belgorod State University, Tver State University and other universities of Russia and JINR Member States write their term papers and do summer and winter practical works in FLNP.

On January 29 to February 4, 2008 the International Seminar-School on Pulsed Advanced Neutron Sources (PANS-III) was organized. In addition to scientific aspects, this Seminar was at the same time a School for training young scientists in the advancement of various types of neutron sources. The course attracted more than 40 students from Russian, Romanian and Vietnamese universities. During the guided excursion to the IBR-2 high-flux pulsed reactor, the participants became familiar with this unique facility and the variety of neutron-scattering investigations carried out at FLNP. On June 29 – July 20, 2008 Summer Student Practice in JINR Fields of Research was organized. The main purpose of the Practice was to allow its participants to learn about the JINR research programme and facilities. On September 11-27, 2008 the same Student Practice was organized for polish students, and on September 22 – October 10, 2008 for the south african students.

8.5. PERSONNEL

Distribution of the Personnel per Department as of 01.01.2009

Theme	Departments	Main staff
-1036-	Nuclear Physics Department	46
-1069-	Condensed Matter Physics Department	41
-1052-	IBR-2 Spectrometers Complex Department	43
-0993-	IREN Department	10
-0851-	IBR-2 Department	42
	Mechanical and Technical Department	43
	Electric and Technical Department	30
	Central Experimental Workshops	40
	Nuclear Safety Group	4
	Design Bureau	7
	FLNP infrastructure:	
	Directorate	9
	Services and Management Department	22
	Scientific Secretary Group	5
	Supplies Group	4
Total		**346**

Personnel of the Directorate as of 01.01.2009

Country	People
Moldavia	1
Bulgaria	2
Vietnam	1
Germany	2
Georgia	2
KPDR	5
Kazakstan	1
Mongolia	3
Poland	2
Romania	6
Russia	23
Ukraine	9
TOTAL	**57**

8.6. FINANCE

Financing of the FLNP Scientific Research Plan in 2008 (th. USD)

No.	Theme	Financing plan, $ th.	Expenditures For 12 months, $ th.	In % of FLNP Budget
I	**Condensed matter physics**	5984,4	6619,3	110,6
	-1069-	1463,4	1761,0	120,3
	-0851-	3484,3	3792,6	108,8
	-1052-	1036,7	1065,7	102,8
II	**Neutron nuclear physics**	1523,7	1750,3	114,9
	-1036-	1077,3	1169,6	108,5
	-0993-	446,4	580,7	130,1
III	**Elementary particle physics**	6,3	6,4	101,6
	-1007-			
	TOTAL:	**7514,4**	**8376,0**	**111,5**